A 3D ribbon diagram of a protein structure, likely a lipid transport protein, rendered in various colors (green, blue, yellow, orange, red) to highlight different regions or domains. The protein is shown in a complex, folded conformation with multiple alpha-helices and beta-strands. The background is white with a light blue horizontal band across the middle.

**Investigation of the Antimicrobial Properties
of Lipid Transport Proteins from
Members of the Brassicaceae Family**

**Katrine Bugge
Master's Thesis
AAU, 2012**

Title: *Investigation of the Antimicrobial Properties of Lipid Transport Proteins from Members of the Brassicaceae Family*

Theme: Master's Thesis

Project period: 5th of January 2012 to the 13th of June 2012

Supervisor: Associate Professor Evamaria Petersen

Author:

Katrine Østergaard Bugge

Print run: 4

Report page count: 120

Appendix page count: 19

Total page count: 139

Date finished: 13th of June 2012

Front page: 3D models of LTP5 and LTP8

The content of the report is public available, but any publication requires approval from the author.

Abstract:

The overall subject of this study is LTPs from members of the Brassicaceae family. The project can be divided in two parts.

The first part revolves around LTP5 and LTP8 from *A. thaliana*, which have unusual LTP pIs of 11 and 5, respectively. 3D models of these two proteins were created by use of homology modeling, and calculation and visualization of their electrostatic potentials were performed. Significant differences were revealed from these, which suggested that these two proteins with very similar folds have different modes of action. LTP5 and LTP8 were attempted to be produced in different strains of *P. pastoris*. Low amounts of putative LTP5 were detected in concentrated supernatant from one expression study, and was found to have antimicrobial activity against *B. subtilis*. In general, accumulation of LTP5 and LTP8 was not detectable following the expression studies conducted under different conditions, and characterizations of these proteins were therefore not possible within the time frame.

In the second part, selective protocols for extraction and isolation of putative LTPs from cabbage were developed. The developed protocols were considered well-suitable for isolation of LTPs, but needs improvements in terms of yield and through-put. It was concluded that 3 distinct members of the LTP family 1 with different tissue specificities were identified and partly isolated by use of the protocols. Lipid transfer activity assays were performed to verify that the proteins were true LTPs, however, the results remained inconclusive. No antimicrobial activity on four tested microbes could be detected with low concentrations of the putative LTP-fractions.

Dansk Resumé

Det overordnede tema for dette studie er lipid transport-proteiner (LTP'er) fra planter tilhørende Brassicaceae familien. Projektet består af to dele.

Den første del af projektet omhandler LTP5 og LTP8 fra *A. thaliana*, som har usædvanlige LTP pl'er på henholdsvis 11 og 5. 3D modeller af disse proteiner blev konstrueret vha. homologi modellering, og beregning og visualisering af deres elektrostatiske potentialer blev udført. Betydelige forskelle mellem disse blev observeret, hvilket antyder at de to proteiner med meget ens foldninger har forskellige virkningsmekanismer. LTP5 og LTP8 blev forsøgt produceret i forskellige stammer af *P. pastoris*. En meget lille mængde LTP5 blev detekteret i koncentreret overskydende kultur medie fra et af protein-udtrykningerne, og dette blev vist at det formodede LTP5 havde antimikrobiel aktivitet imod *B. subtilis*. Generelt var ophobningen af LTP5 og LTP8 i protein-udtrykningerne, som blev udført under forskellige eksperimentelle betingelser, ikke i en detekterbar mængde, og karakterisering af de to proteiner var derfor ikke mulig indenfor tidsrammen.

I den anden del af projektet blev protokoller for udtrækning og isolering af formodede LTP'er fra kål udviklet. De udviklede protokoller er anset som anvendelige til isolering af LTP'er fra kål, men betydelige forbedringer mht. udbytte og produktionsmængde blev fundet nødvendige. Det blev konkluderet at tre forskellige medlemmer af LTP 1 familien med forskellig vævsspecificitet blev identificeret og delvist isoleret vha. de udviklede protokoller. Lipid transfer aktivitetssassay blev udført for at bekræfte at proteinerne var ægte LTP'er, men resultaterne heraf forblev tvetydige pga. eksperimentelle usikkerheder. Ingen antimikrobiel aktivitet kunne detekteres imod fire testede mikrober vha. assays med lave koncentrationer af de formodede LTP-fraktioner.

Preface

The work of the following project was conducted in the 10th semester period of Nanobiotechnology at the Department of Physics and Nanotechnology, Aalborg University, from the 5th of January 2012 to the 13th of June 2012. It considers Lipid Transport Proteins (LTPs) from the Brassicaceae family, and was written under the supervision of Evamaria Petersen (Associate Professor, Aalborg University). Experimental work has been carried out at Aalborg University, Department of Physics and Nanotechnology, and Department of Biotechnology, Chemistry and Environmental Engineering.

The first part of the report gives relevant knowledge about plant LTPs, especially with focus on the possible biological roles of these. Furthermore, *P. pastoris* as expression system is reviewed, followed by a description of the aim and experimental strategy of the present study. In the following part, the biological materials and methods used in the study are described. A list of the chemicals used is found in Appendix B. In the following chapter the results of the theoretical and experimental part are presented, and in the last part a discussion of the results and experiments will lead to a conclusion and perspectives. In Appendix, a theoretical description of the chromatographic methods used are found, along with supplementary figures.

The references are presented and sorted by appearances in the bibliography at the end of the report. When a reference is placed after a paragraph it applies to the entire paragraph and when placed after a sentence it refers to the sentence itself. In the main text other references are also used to represent figures, tables, and sections which are referred to as Fig., Tab., and Sec., respectively. Data and a PDF version of the report are found on the DVD placed on the inside of the back page.

I would like to thank Aida Droce (PhD fellow, AAU) for providing *Fusarium graminearum* spores. Furthermore I would like to thank Peter Fojan (Associate professor, AAU) for advice on lipid transfer assays, and Christian Skjødt Hansen (stud.polyt, AAU) for borrowing his fermentation setup.

Contents

1	Introduction	1
2	Lipid Transport Proteins	3
2.1	Plant Lipid Transport Proteins	3
2.2	Structure of LTPs	4
2.3	Mode of Lipid Exchange by LTPs	10
2.4	Gene Expression Patterns	11
2.5	Biological Roles of Plant LTPs	12
2.6	LTPs from the Brassicaceae Family	19
3	The <i>P. pastoris</i>	
	Expression System	23
3.1	<i>Pichia pastoris</i>	23
3.2	Fermentation of <i>P. pastoris</i>	26
3.3	Known Production Barriers	28
3.4	The pPICZ α Expression System	31
4	Project Description	33
4.1	Review of Previous Work	33
4.2	Aim of Present Study	38
4.3	Experimental Strategy	39
5	Materials and Methods	41
5.1	Biological Materials and Primers	41
5.2	Theoretical Characterizations	42
5.3	Recombinant Expression of LTPs in <i>P. pastoris</i>	43
5.4	Isolation of putative LTPs from Cabbage	46
5.5	Assays	48
5.6	Protocols and Recipes	49
6	Results	55
6.1	Theoretical Characterizations	55
6.2	Recombinant Expression of LTPs in <i>P. pastoris</i>	64
6.3	Isolation and Characterization of Putative LTPs from <i>B. oleracea</i>	79
7	Discussion	95
7.1	Theoretical Characterizations of LTP5 and LTP8	95
7.2	Recombinant Expression of LTPs in <i>P. pastoris</i>	98
7.3	Isolation and Characterization of LTPs from Cabbage	103

8 Conclusion	109
8.1 Perspectives	110
Bibliography	113
A Appendix	121
A.1 Chromatography	121
B Appendix	127
B.1 Chemicals	127
C Appendix	129
C.1 Supplementary Figures for Theoretical Characterizations	129
C.2 Supplementary SDS-PAGEs	130
C.3 Supplementary Chromatograms	134
C.4 Supplementary Time Resolved Fluorescence Plot	136
D Appendix	137
D.1 Expression Constructs	137

Introduction

1

The dramatic growth of the human population has made preservation of the world's food supplies one of the major challenges of the future. Moreover, considerable financial gains in the field of agriculture could be obtained by enhancing harvest yields and reducing pre-harvest and post-harvest losses. It has been estimated that 20-40 % of the agricultural production worldwide is lost to pests and diseases [1]. Strategies addressing this issue commonly taken in modern agriculture include classical and molecular marker-based resistance breeding, genetic engineering of plant immunity, and chemicals functioning as fertilizers or pesticides. However, many of these strategies result in undesired side effects or are simply insufficient. Breeding strategies are time-consuming and struggle with problems caused by linkage drag (co-transfer of undesirable traits). [1], [2] The long use of chemical pesticides has led to the development of resistance among pathogens and imposes environmental problems and health risks to consumers. [3] Genetic engineering however represents a strategy that is reasonably fast and predictable in its consequences; by use of this method, targeted introduction of individual traits into specific crop lines can be achieved. [1] One approach to plant improvement through genetic engineering is the introduction of novel genes into agricultural plants. Genes encoding antimicrobial proteins can e.g. be introduced to boost their resistance against phytopathogens, and it has been shown that transgenic plants expressing antimicrobial proteins are more robust. Different organisms often produce different antimicrobial proteins for defense against pathogens, and therefore a diversity of antimicrobial proteins are available in nature. [4]

Plants have the innate ability to combat microbial invasions, and most plants are resistant to most plant pathogens. [5] They have this ability in spite of the fact that they lack specialized defense cells and a somatic adoptive immune system, as found in mammals. Instead, plants have to rely on the innate immunity of each cell, and systemic signals emerging from infected sites. This innate, non-specific immune system has two main components: an outer barrier consisting of a waxy cuticular skin layer, and preformed antimicrobial compounds. Some of the non-specific resistance compounds are constitutively expressed, while the expression of others is induced by the attack of pathogens. [5], [6] The apparent efficiency of this innate immune system have fostered the idea that the template for the ultimate weapon against phytopathogens should be found in the plants themselves. A high amount of research has focused on antimicrobial proteins (AMPs) as templates for engineering durable, broad-spectrum plant disease resistance, which at the same time does not harm the environment or product consumers. [1] AMPs are usually composed of less than 200 amino acids, and most commonly less than 50 amino acids (antimicrobial peptides). They are as a group known for their immediate and non-specific activity against Gram-negative and Gram-positive bacteria, fungi, viruses and parasites, without any damage to the host. They have been isolated from a wide range of organisms and show great molecular diversity, but can be grouped based on specific structural folds. Often, AMPs possess a variable number of cysteine residues that helps stabilize their structure through the formation of disulphide bridges. AMPs belonging to different classes have been found to exert synergistic effects against pathogens, which is probably the rationale behind their molecular diversity. [3], [7]

Besides their potential as transgenes in elite crop lines, AMPs are also considered promising as food preservatives, in antimicrobial surfaces and in medicine. As the natural purpose of plant-derived AMPs is to protect plants from their natural pathogens, their activity is often directed against phytopathogens. However, several studies have shown that they can be effective against animal microbial predators, which is also supported by the typical broad-spectrum activity of AMPs. Such clues extend interest in their properties from use in agriculture and food industry to possible pharmaceutical applications. Because of the development of microbial resistance and the untoward side reactions of current antibiotics, it is of great interest to develop new antimicrobial therapeutics. It though still remains to be conclusively proven that AMPs represents a new class of therapeutic drugs. [7], [3], [8], [4]

Before e.g. laborious and expensive generation of transgenic crop lines with specific AMP-expression genes are initiated, *in vitro* bioactivity assays are an essential tool for selecting suitable candidates. Furthermore, complete elucidation of the mode of action and which factors determines the potency and selectivity of certain AMPs are essential for engineering optimized derivatives of natural AMPs, or completely artificial AMPs. [3] One promising lead in the search for antimicrobial candidates for improvement of crop resistance and medicine is the plant Lipid Transport Proteins (LTPs). LTPs are small secreted proteins that are often cationic. They display an α -helical fold stabilized by four disulfide bridges in which a large hydrophobic cavity allows the binding of different types of lipids. [9] The *in vivo* role of LTPs has not yet been determined, but substantial evidence has been presented suggesting that LTPs are active defense proteins. The structure/function relationship and mode of action of their antimicrobial activity is however unknown. The puzzles of these needs to be solved before LTPs truly can be utilized in agriculture or medicine. [10]

Lipid Transport Proteins 2

2.1 Plant Lipid Transport Proteins

In plant cells, lipids in the plasma membrane and membrane of organelles are build up and renewed by lipids imported from the endoplasmatic reticulum (ER), which is the main site of lipid biosynthesis. For this to be possible, a transport system for the intracellular movement of lipids is necessary, as lipids have poor solubility inside the aqueous milieu of the cell cytoplasm. The search for a lipid carrier protein to fulfill this task led to the discovery of non-specific lipid transport proteins (LTPs) approximately 30 years ago by Kader et al. [11]. These proteins are characterized by their ability to facilitate the transfer of phospholipids between a donor and an acceptor membrane, and bind fatty acids *in vitro* (hence the name). LTPs have a broad specificity for phospholipids and are able to transfer phosphatidylcholine (PC), phosphatidylinositol (PI), phosphatidylethanolamine (PE), galactolipids and sulfolipids between various membranes. [12], [13] Even though studies have confirmed that LTPs are well suited for transporting various lipids, the involvement of these proteins in the intracellular flux of lipids have not been confirmed. Furthermore, it has been observed that LTPs are extracellularly located and are secreted, and therefore the possible role of these proteins in intracellular lipid transfer seems unlikely. Thus, LTPs have yet to be assigned a biological role. [14], [12], [13]

Generally, plant LTPs are small proteins that are found in numerous monocotyledons and dicotyledons. It has been demonstrated that they are relatively stable, resisting thermal and chemical denaturation and enzymatic digestion. [14] They comprise two families. The first family to be discovered and characterized was the LTP family 1. Members of this family have molecular masses of approximately 10 kDa and posses 90-95 amino acid residues in their mature form. Of these amino acids, eight are cysteines, which are conserved in similar positions in the primary structure of the members of LTP family 1. The eight cysteines form four disulfide bridges that helps stabilize their tertiary structure. Later, the LTP family 2 was discovered, and members of this family have molecular masses of approximately 7 kDa and possess on average 70 amino acids in their mature form. The pattern of four conserved disulfide bridges is shared with the LTP family 1.

The two LTP families both mainly consist of basic proteins with isoelectric points (pI) of 9-10 and a signal peptide at the N-terminal region. However, the amino acid sequences of the members in general show low similarity. Almost all known LTP coding genes have an intron placed in the region corresponding to the C-terminus of the protein, often two codons before the stop codon. The length of the intron varies from one gene to another: 89 bp in a rice LTP, 114 bp in one of the two *Sorghum* LTP genes, 115 bp in an *A. thaliana* LTP, 133 bp in a barley LTP, 271 bp in a broccoli LTP and 980 bp in a tobacco LTP. [13] The size of their signal peptide also varies, and is between 21 and 27 amino acids for the LTP family 1 and between 27 and 35 amino acids for the LTP family 2. This signal peptide targets the LTPs to the cell secretory pathway where they are exported to the apoplast. In agreement with this, members of LTP family 1 of various plant species have been found to be localized in the cell wall, which has been demonstrated

in e.g. *Arabidopsis thaliana*, *Brassica oleracea var. italica* leaves and in *Ricinus communis* and *Vigna unguiculata* seeds. [14], [15], [16], [13] Though it is well established that LTPs are extracellular proteins, a few exceptions has been found. For example has an LTP isoform from *R. communis* seeds been found inside an organelle, which was characterized as the glyoxosome, and in *T. aestivum* seeds an LTP has been found inside the alleurone granules. [14], [13]

The finding of an extracellular location along with other observations has led to different suggestions of putative biological roles of LTPs, such as: cutin biosynthesis, surface wax formation, plant adaption to environmental changes and plant defense against phytopathogens. These different suggestions will be described in detail later in this report. [14], [12]

Another important aspect of plant LTPs is their involvement in food allergies. Several studies have suggested that the major allergens of diverse plant food species are protein members of the LTP family 1. The most well studied allergenic LTP is Pru p 3, which originates from peach (*Prunus persica*). Closely related allergens (above 80% of sequence identity) have been found in apple, apricot, cherry and plum. Moreover, allergenic LTPs have also been identified in other fruits, such as grape, nuts, and hazelnuts, in products derived from cereal seeds, such as maize (*Z. mays*) and barley (*H. vulgare*), and in vegetables, such as asparagus, lettuce, carrot and onion. Some pollen allergens are also LTPs, and allergens belonging to the LTP family have also been identified in non-food related plants. [17]

The high resistance of LTPs to proteolytic digestion and heat treatment points to these allergens as primary sensitizers by ingestion, as these stable physical-chemical features allow the proteins to reach the intestine of mammals with their immunogenic and allergenic motifs intact. The ability of LTPs to sensitize via the gastrointestinal tract is not fully understood, but it is believed that once they are present in the gastrointestinal tract in an immunogenic form they are free to interact with the intestinal immune system, thereby inducing both sensitization and systemic symptoms. [14], [17] A characteristic that is shared by allgergenic proteins is the ability to bind ligands, which seems to make them more stable. In the case of LTPs, proteins bind to phosphatidylcholine, a physiological surfactant that is secreted by gastric mucosa and also occurs in bile. It has been shown that this binding results in an additional enzymatic protection, slowing down the breakdown of a grape LTP. [14], [18]

2.2 Structure of LTPs

As mentioned, the primary structure of members of the LTP family 1 and 2 comprise a unique polypeptide chain containing 90-95 amino acids and approximately 70 amino acids, respectively. Among these amino acids, eight strictly conserved cysteine residues are found, which form four intrachain disulfide bridges (Fig. 2.1 and 2.2). These eight cysteine residues are conserved among the two families, but differences is found in the cysteine paring motif. In the LTP family 1 the Cys₃ pares with Cys₅₀, and Cys₄₈ pares with Cys₈₇. In LTP family 2 the Cys₃ pares with Cys₃₅, and Cys₃₇ pares with Cys₆₈. In members of LTP family 1, the cysteine residues are located at conserved positions according to the pattern 2/3-C-8-C-12/15-CC-19-C-1-C-21/23-C-13-C-4/8. Still, great divergence can be observed between different LTP sequences, even from the same species. In castor bean seeds for example, the degree of sequence identity of the LTPs varies from 34-97 % [12]. In spite of the low homology of the resulting proteins, they all

display characteristic LTP structure features. [12], [13], [19]

Most known LTPs are abundant in charged residues. Often, 11-12 charged residues are found in members of the LTP family 1, and the presence of these gives the members a high pI varying between 9 and 10. Of these residues, Asp₄₃, Arg₄₄ and Lys₅₂ (numbering according to maize LTP [14]) are conserved among the members of the LTP family 1 that has been characterized so far. Furthermore Val₆, Gly₃₀, Ala₆₆, Val₇₂, Ile₈₁ and Ser₈₂ are often conserved in members of LTP family 1. In the LTP family 2 the number of charged residues is found to vary more, but they have in the range of 6-10 charged residues and a pI around 9. [14], [12] Concerning aromatic amino acids, no tryptophan residues are found in known LTP type 1 sequences, and phenylalanine is rare. However, two relatively conserved tyrosine residues are often located towards the N- and C-termini of the LTP type 1 polypeptide. [19], [20]

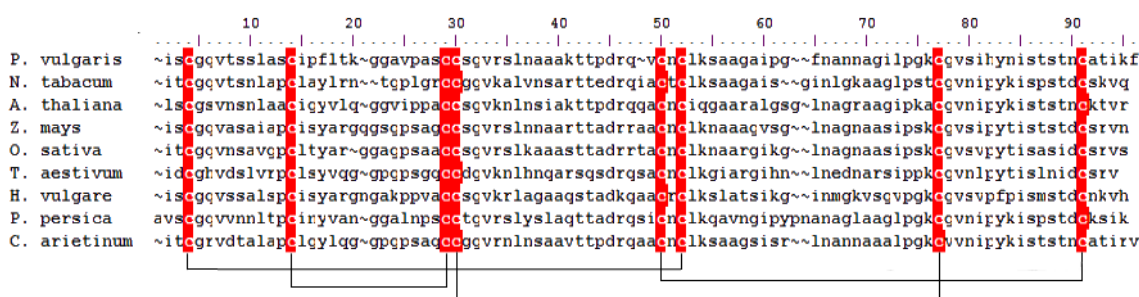


Figure 2.1: Alignment of the complete mature amino acid sequence of various plant LTPs from LTP family 1. Gaps are indicated by the sign ~ and are included to optimize alignment. The numbers at the top of the sequences gives amino acid residue number relative to the *Z. mays* LTP sequence. The lines below the sequences indicate the pattern of the disulfide bond connectivity. Cysteine residues are highlighted with a red background. The species the aligned LTPs originates from and data bank accession numbers of the LTPs are (from the top): *Phaseolus vulgaris* (O24440), *Nicotiana tabacum* (Q42952), *Arabidopsis thaliana* (Q42589), *Zea mays* (P19656), *Oryza sativa* (P23096), *Triticum aestivum* (Q8GZB0), *Hordeum vulgare* (Q43766), *Prunus persica* (Q8H2B3), *Cicer arietinum* (O23758). Created in Bioedit.



Figure 2.2: Alignment of the complete mature amino acid sequence of various plant LTPs from LTP family 2. Gaps are indicated by the sign ~ and are included to optimize alignment. The numbers at the top of the sequences gives amino acid residue number relative to the *Z. mays* LTP sequence. The lines below the sequences indicate the pattern of the disulfide bond connectivity. Cysteine residues are highlighted with a red background. The species the aligned LTPs originates from and data bank accession numbers of the LTPs are (from the top): *Triticum aestivum* (P82900 and P82901), *Hordeum vulgare* (P20145), *Oryza sativa* (P83210), *Zea mays* (P83506) and *Prunus armeniaca* (P82353). Created in Bioedit.

Different members of the LTP family 1 has been examined with NMR, CD, infrared, and Raman spectroscopy. These experiments have revealed that the polypeptide chain is mainly organized as helical segments, which are stabilized by four disulfide bridges. [14], [13], [19] The first 3D structure of an LTP was presented by Shin et al. [21] in 1995. They used X-ray crystallography to determine the 3D-structure of a type 1 LTP from maize seedlings (Fig. 2.5). This study for the first time revealed the now well-established all- α -type structure of members of LTP family 1. Following, numerous studies on the 3D structure of LTPs have shown that the all- α -type structure of LTP family 1 is composed of a single compact domain with four α -helices and a long C-terminal tail, through which a hydrophobic tunnel run (Fig. 2.3). The four α -helices that make up most of the secondary structure of the members of LTP family 1 is helices H₁ (Cys₃ to Ala₁₇), H₂ (Ala₂₅ to Ala₃₇), H₃ (Thr₄₁ to Ala₅₆) and H₄ (Ala₆₃ to Cys₇₃). The first three α -helices are amphiphilic and parallel to the central tunnel. In all structures solved till now, the first helix has a pronounced kink near the second cysteine that often corresponds with a conserved proline. Three short loops connects the α -helices. The long C-terminal tail lacks a defined secondary structure, except for the presence of one turn of the 3_{10} -helix. The structure lacks any β -structure and nearly two-thirds of its residues are found in α -helices. The secondary structure elements of members of LTP family 1 are interconnected with four disulfide bridges which are formed by the Cys₃ from the H₁ with the Cys₅₀ from H₃, Cys₁₃ from H₁ and Cys₂₇ from H₂, Cys₂₈ from H₂ and Cys₇₃ from H₄ and by the Cys₄₈ from H₃ and Cys₈₇ from the C-terminal region. These disulfide bridges are found in two clusters on opposite sides of the 3D structure. [22], [21], [20], [19], [13], [14], [23], [24]

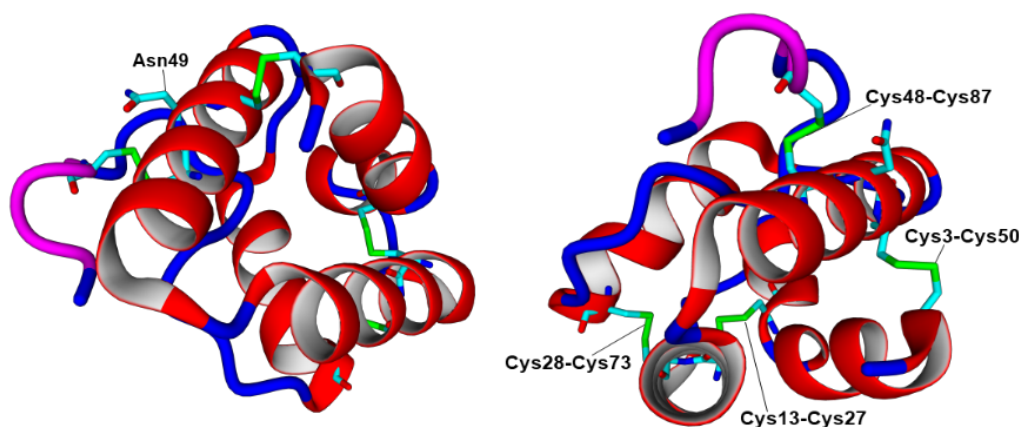


Figure 2.3: 3D structure of a type 1 LTP from rice seeds (1RZL.pdb) in the unliganded state as determined by Lee et al. [25], shown from two different angles. The central residue of the -C-1-C- motif (Asn49) is seen to be located at the surface. α -helices are shown in red, coils are shown in blue, 3_{10} -helix is shown in magenta, selected residues are shown in light blue and disulfide bridges are shown in green. Molecular graphics were created by YASARA and PovRay.

Hoh et al. [22] were the first to determine the 3D structure of a member of the LTP family 2 by X-ray crystallography, which they performed on a type 2 LTP from wheat (Fig. 2.4). This study showed that the secondary and tertiary structure of LTPs from family 1 and 2 are analogue. Though, a major difference is that the structure of type 2 LTPs contains five α -helices and that the hydrophobic cavity is split in two separate cavities ending with a common wall. [22] The secondary structure of type 2 LTPs follows the same pattern as the other family, and is besides the five α -helices composed of an N-terminal 3_{10} -helix and a short polyproline type II C-terminal

helical segment¹. The core of the structure is organized as a helical bundle stabilized by four disulfide bridges (Fig. 2.4). The N-terminal segment containing the 3_{10} -helix (Ala4-Cys10) is anchored to this bundle by two disulfide bridges (Cys2-Cys34 and Cys10-Cys24). The helices 3_{10} , H₁ (Ala₁₁ to Ser₁₆), H₂ (Gly₂₂ to Gln₃₁), H₃ (Phe₃₅ to Tyr₃₈), H₄ (Gly₄₅ to Ile₄₈) and H₅ (Pro₅₁ to Ser₅₉) pack into a globular structure and delineate a deep hydrophobic cavity. A type I β -turn is observed between helices H₂ and H₃, and helices H₃ and H₄ are connected by an α -turn. [22]

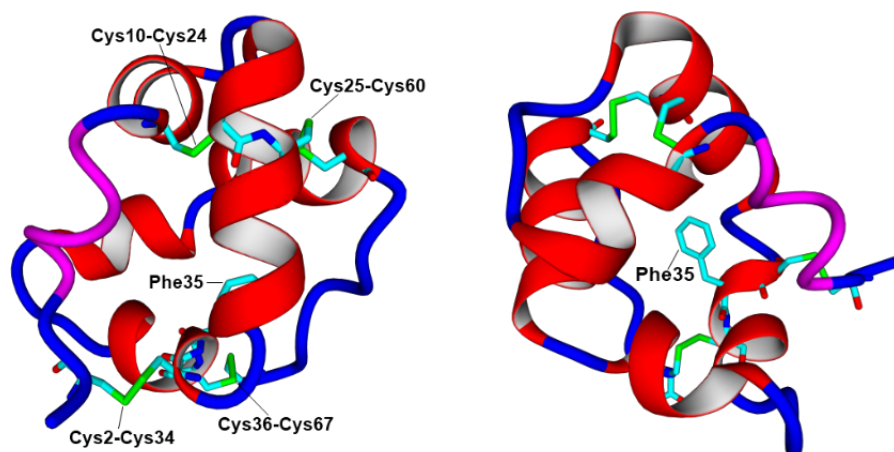


Figure 2.4: 3D structure of a type 2 LTP from wheat (1TUK.pdb) in the unliganded state as determined by Hoh et al. [22], shown from two different angles. The central residue of the -C-1-C- motif (Phe35) is seen to be buried inside the structure. α -helices are shown in red, coils are shown in blue, 3_{10} -helix is shown in magenta, selected residues are shown in light blue and disulfide bridges are shown in green. Molecular graphics were created by YASARA and PovRay.

The positions of cysteines, hydrophobic amino acids and positively charged residues are well conserved between members of LTP family 1 and 2. Differences are however found in e.g. the -C-1-C- cysteine motif. For example, the asparagine in this cysteine motif in a type 1 LTP from rice is replaced by a hydrophobic amino acid, phenylalanine, in a type 2 LTP from wheat. As mentioned, the disulfide bond pattern in members of LTP family 2 differs from members of LTP family 1 at the -C-1-C- motif (Fig. 2.1 and 2.2). The hydrophobic residue in the -C-1-C- motif of type 2 LTPs is buried inside the protein (Fig. 2.4), whereas the hydrophilic residue of type 1 LTPs is at the surface (Fig. 2.3). These observations suggest that the central residue of the -C-1-C- motif may govern the cysteine pairing and influence the overall fold of the proteins. [26]

2.2.1 The Hydrophobic Cavity

One of the most important structural features of LTPs is their flexible hydrophobic cavity in form of a tunnel that runs through the axis of the protein. This tunnel is especially well studied in members of LTP family 1. In members of LTP family 1 the tunnel-like cavity is lined with amino acids such as Ala, Arg, Ile, Leu, Lys, Pro, Ser, Thr, Tyr and Val. These amino acids provide the cavity with a hydrophobic character, and this way offers a potential binding site for hydrophobic or amphiphilic ligands. The cavity has one small and one large entrance, and two charged amino acids (Arg₄₄ and Lys₃₅) are often strategically localized at the larger entrance.

¹left-handed helix with three residues per turn.

The placement of these charged amino acids indicates a possible role of these in the interactions with lipids. The lipid molecules interact with amino acids at the larger entrance and the hydrophobic portions of the lipid stay buried inside the cavity, while the carboxylate portion remains turned towards or exposed to the solvent. [14], [19]

The volume of the tunnel-like hydrophobic cavity of LTPs is variable for lipid-free proteins, and is able to increase when large lipids are bound. The capability of high volume increase upon lipid binding shows that the cavity has a high plasticity, which is believed to be responsible for the lack of specificity in the transport ability. However, this also indicates that it is impossible to predict the binding properties of LTPs on basis of the tunnel volume of a free protein. The hydrophobic cavity is able to bind different types of monoacylated and diacylated lipid molecules, such as fatty acids, fatty acyl CoA, lyso-phosphatidylcholine and phosphatidylglycerol. Other hydrophobic molecules, such as e.g. organic solvents, can also be bound in the cavity. Carvolin et al. [27] was the first to show that LTPs are capable of binding two monoacylated lipids. The two lipids were shown to be inserted head to tail in the hydrophobic tunnel, crossing the protein axis, and with their polar head groups exposed to solvent in opposite ends. They found that this was possible due to the existence of two lipid binding sites (site 1 and 2), each with a different affinity for lipids. Site 2 has lower affinity for lipids than site 1, and a large excess of lipids are necessary to saturate site 2. The head group of the lipid bound in site 1 is located between the beginning of H₃ and the C-terminal loop, whereas the head group of the lipid bound in site 2 are located between the end of H₁ and the loop connecting H₃ and H₄. [27], [19], [14]

In a study of a maize LTP (member of the LTP family 1) by Shin et al. [21], the crystal structure of maize LTP in complex with the ligand palmitate (C16:0) was determined (Fig. 2.5 C). This study revealed that the overall fold of the LTP-palmitate complex is almost identical to that of the uncomplexed LTP, with only minor differences between the structures. A slight swelling of the tunnel-like cavity is found in the complexed structure, and the side-chain atoms of three isoleucine residues (Ile11, Ile79 and Ile83) are displaced from the cavity so that the acyl chain of palmitate fits comfortably inside it. The carboxylate group of the bound palmitate is exposed to the solvent, whereas approximately 12 carbon atoms in the tail of the palmitate chain is buried inside the hydrophobic cavity (Fig. 2.5, B and C). Oxygen atoms of the carboxylate group form hydrogen bonds with the hydroxyl group of Tyr₈₁ and two bound water molecules, which stabilizes the complex. The tunnel is roughly formed by placing part of the long C-terminal region over the hydrophobic channel, whose hydrophobic surface is provided by the buried side-chain atoms of the four amphipathic α -helices. The C-terminal region does not cover the hydrophobic channel completely, yielding a small gap (approximately 2 Å wide and 12 Å long), in which five water molecules are bound to the backbone atoms by a network of hydrogen bonds. Hence, the maize LTP structure does not have a tightly packed hydrophobic core, like typically found in globular, water-soluble proteins. The disulfide bridges and charge interactions (including hydrogen bonds) seem to have an important role in maintaining the 3D structure of LTPs in the absence of a bound ligand. [21]

Another study with a maize LTP showed that saturated molecules of 16-18 carbons have the best interactions with this LTP. Saturated molecules of 12-14 carbons are not able to compete with lipids that contain fatty acids of 16-18 carbons, due to the low level of interaction they have with the LTP. Similarly, lipids of 20-22 carbons also do not efficiently compete with lipids

that contain fatty acids of 16-18 carbons, due to their long chains not being properly accommodated for by the hydrophobic cavity of the members of LTP family 1. [28] As mentioned, the primary sequence of type 1 LTPs contains some amino acids that are relatively conserved. Of these an aromatic residue at the carboxyl terminal region at approximately position 79 is of particular interest (Fig. 2.3). This residue is positioned at the larger entrance of the hydrophobic cavity and as shown in the study of complexed maize LTP and palmitate, the aromatic residue interacts with the fatty acids. This stabilizes the binding between the LTP and the hydrophobic molecule by a hydrogen bond formed between the hydroxyl group of the aromatic residue and the carboxyl group of the polar head of the lipid. The fatty acids must have between 16 and 18 carbons to reach the aromatic residue, and this is likely to explain the preference of binding in relation to stability of the molecules of such size. If the fatty acid chain is below 16 carbons it does not reach the aromatic residue and therefore does not form the stabilizing hydrogen bond. If the fatty acid is above 20 carbons it is also unable to form the stabilizing hydrogen bond. When the C-terminal aromatic residue is absent, the conserved Arg residue could be an alternative for binding of anionic lipids. [14], [19]

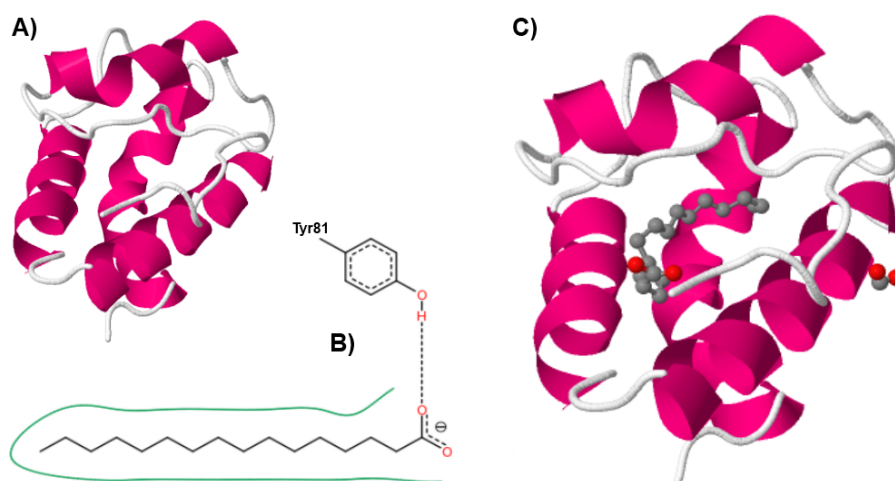


Figure 2.5: Crystal structures solved by Shin *et al.* A) 3D structure of an LTP from maize seedlings (1MZL.pdb), showing an all- α -type structure. α -helices are shown in pink and other secondary structures are shown in white. B) Palmitate (1MZM:PLM:A:201). The black dashed lines represent hydrogen bonds and green solid lines indicate hydrophobic interactions in the LTP cavity. C) 3D structure of an LTP from maize seedlings complexed with palmitate (1MZM.pdb). α -helices are shown in pink, other secondary structures are shown in white, carbon atoms are shown in grey and oxygen are shown in red. In the complex structure most of the acyl chain of palmitate is buried inside the hydrophobic cavity. [21] Visualized with Jmol.

In the LTP family 2, the larger of its two cavities is formed like a triangular hollow box instead of a tunnel, and is lined with amino acids such as Ala, Cys, Ile, Leu, Phe and Val. Computational modeling has shown that this box is more flexible than the tunnel cavities of the LTP family 1. This is supported by the observation that members of the LTP family 2 are capable of binding sterols, which is not possible for members of the LTP family 1. [14]

2.3 Mode of Lipid Exchange by LTPs

One of the defining characteristics of LTPs is their ability to mediate the transfer of lipids between membranes. The way in which LTPs transfers lipids has however not been completely elucidated. It has been suggested that LTPs facilitate the transfer by acting as carriers capable of extracting one lipid molecule from a membrane and transferring it to another (Fig. 2.6). This implies the formation of a reversible lipid-protein complex in agreement with structural analysis performed with lysophospholipid-protein complexes. The complex then interacts with the membrane and exchanges its bound phospholipid with a phospholipid molecule from the membrane. A similar mechanism has been suggested for LTPs purified from mammalian cells and yeasts. Despite their apparently similar mode of action, no sequence homology has been found between LTPs from mammalian, plant and yeast sources. [13], [12]

Two important interactions are likely to be important for the transfer mechanism: adsorption of the protein to the membrane interface (probably through electrostatic or polar interactions) and the binding of lipids by the protein. For the intermembrane transfer to occur, the strength of these interactions has to be in an order such that the reverse process is possible. [13], [12], [19]

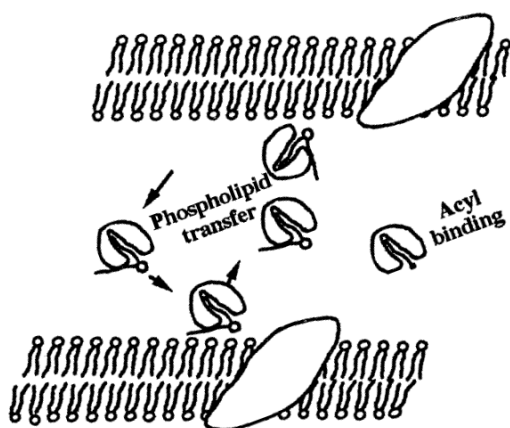


Figure 2.6: Proposed mode of action in lipid exchange by LTPs. A reversible complex between the LTP and phospholipid is formed. It is believed that the hydrophobic tunnel of the LTP is involved in this process. The binding and release of phospholipid molecules, facilitated by polar domains situated around the opening of the cavity, leads to their exchange with phospholipids of the membranes. Adapted from [13].

2.3.1 Lipid Transfer Activity Assays

The use of proper assays is an important tool for identification of true LTPs. The standard method to determine LTP activity involves two types of membranes (donor and acceptor) and a reporter system. The methods used can be classified into two main groups: radiochemical techniques and fluorimetric techniques. The former was used in the early assays for detection of lipid transfer activity, and involves many steps compared to the fluorimetric techniques. In these methods, the donor membranes are often liposomes prepared by ultrasonication using a radioactive phospholipid. Acceptor membranes are either natural membranes such as mitochondria or plasma membranes, or artificial membranes (or any other subcellular fraction that can be separated from liposomes by centrifugation). When the donor and acceptor mem-

branes are incubated in presence of an LTP and then separated, radioactive phospholipid is detected in the acceptor membrane. This indicates transfer from the donor membranes, as spontaneous movement of phospholipids is very slow. [12], [13]

In the fluorimetric assays, the donor membranes are self-quenching vesicles containing fluorescent lipids. In this method, separation of acceptor and donor membranes are not required, as direct measurements of fluorescence is used to detect LTP activity. When the fluorescent lipids leave the donor vesicles to reach the acceptor vesicles, the fluorescence increases because of a release in the self-quenching occurring in the donor membrane. [12], [13], [29]

The lipid transfer assays can be performed with either crude extracts or with purified LTPs, and have been able to detect LTP activity of 50 nM solutions. [12], [13], [29]

2.4 Gene Expression Patterns

It has been demonstrated that in e.g. the genome of *O. sativa* and *A. thaliana* several genes code for different LTPs, and it is well established that LTPs exist in multigene families in plants. It may be that these different genes codify LTPs with different tissue specificity and functions, which coexists in the same plant. To understand the *in vivo* role of plant LTPs, it is important to determine when and where the LTP genes are expressed. [14], [13], [30]

The expression patterns reported for different plant LTPs are complex and characterized by strong developmental and tissue specificity, with distinct patterns of expression for different genes. Studies made primarily with Northern blot analysis have shown that when the vegetative organs were considered, no LTP gene transcript was detected in the roots of various plants. However, an LTP gene has been found to be expressed in rice seedlings. The expression of LTP genes has been observed to be active in above ground portions of the plants (e.g. leaves or stems). It has been found that in a given plant, each LTP gene displays its own peculiar pattern of expression. E.g. in barley, one of two seedling-specific LTP genes is more expressed in leaves than in coleoptiles² of seedlings, whereas the reverse is true for the other gene. It has also been observed that the expression of LTP genes seems to be higher in young tissues than in old, e.g. in tobacco leaves. This is supported by the finding of high LTP expression levels early in the development of embryo cotyledons³ and leaf primordia⁴ of *A. thaliana* and in somatic embryos of carrot. Furthermore, it has been found that in the tobacco plant the expression of an LTP gene is highest in the upper part of the tobacco plant and that it declines toward the base, indicating that the LTP gene is expressed in a developmental gradient. [12],[13]

Studies using *in situ* hybridization revealed that LTP gene expression is mainly restricted to defined cell layers, which in general are situated peripherally. It has in general been found in e.g. maize seedlings, carrot, *A. thaliana*, tobacco and cotton that LTP gene expression takes place

²Coleoptile is the pointed protective sheath covering the emerging shoot in monocotyledons.

³A cotyledon is a significant part of the embryo within the seed of a plant. Upon germination, the cotyledon may become the embryonic first leaves of a seedling.

⁴Primordia is defined as an organ or tissue in its earliest recognizable stage of development.

in precursors of epidermis and in the shoot apical meristem⁵. E.g. in *A. thaliana* the LTP gene transcripts were detected first in the protoderm⁶ cells of the embryo cotyledons, then in the leaf primordia in young seedlings, and at a later stage of development in the epidermal cells of meristem and leaves. [13], [31].

Another example of cell specificity of LTP gene expression is found in floral organs. It has been observed that an LTP gene is specifically expressed in the tapetum⁷ layer of the tobacco anther⁸. Furthermore it was shown that another LTP was only present in the outermost cell layer in floral apical meristem at the stage of transition to floral development. In *B. napus* an LTP was likewise found to be exclusively expressed in the tapetal cells of *B. napus* anthers. Furthermore, LTP gene expression has been detected in the epidermal cells of several floral organs, including *A. thaliana* and *G. hybrida*. [13]

To validate these observations, studies with transgenic plants containing a fusion of a promoter region of the LTP genes to the reporter gene β -glucuronidase (GUS) has been performed. Such experiments were carried out with the *ltp1* in barley, the LTP1 gene from *A. thaliana* and in *B. oleracea* using the wax 9D gene. The resulting data was overall consistent with the above described *in situ* hybridization experiments, and showed that LTP expression was dependent on the stage of development. [31], [13], [14]

A complete understanding of the expression pattern of LTPs may give clues about their biological role and perhaps make it possible to utilize their promoters to express genes of interest in specific tissues or developmental stages of transgenic plants. [16]

2.5 Biological Roles of Plant LTPs

As mentioned, it was initially believed that LTPs take part in membrane biogenesis by facilitating intracellular lipid transfer. Though, as it became clear that LTPs are extracellular located and are secreted, a role of these proteins in intracellular lipid transfer seems unlikely. Following this discovery, several hypothesis for the *in vivo* role of LTPs have been postulated. Despite numerous studies on plant LTPs, no direct evidence has been demonstrated for most of their suggested functions, and they are yet to be assigned a biological role. As different patterns of expression have been described for LTP genes, it seems possible that different gene families account for the observed diversity in patterns of expression, each one perhaps performing a different function. A systematic study of all LTPs from one plant species, e.g. *A. thaliana*, has been suggested to provide a clear picture of their functionality. [16], [20] Following is a review of the most supported putative biological roles of LTPs proposed till now.

⁵Meristem is a specialized section of plant tissue characterized by cell division and growth. Meristems are classified by location as apical, or primary (at root and shoot tips), lateral, or secondary (in the vascular cambium and cork cambium), or intercalary (at internodes, stem regions between the places at which leaves attach, and at leaf bases). Apical meristems give rise to the primary plant body.

⁶Protoderm is one out of three differentiations of the meristem. The protoderm lies around the outside of the stem and develops into the epidermis.

⁷Tapetum is a layer of nutritive cells in the sporangia of ferns and anthers of flowering plants that surrounds developing spore cells.

⁸Anther is the pollen-bearing structure in the stamen (male organ) of the flower usually located on top of the filament of the stamen.

2.5.1 Cutin Formation

The surface of plants is covered by the cuticular wax that protects them from water loss and environmental stresses. The wax composition of a large number of plants is known, as well as the biosynthetic pathway of the major types of cuticular components. It has been shown that wax components are synthesized in the epidermal tissue and that key steps in the synthesis are catalyzed by enzymes. However, it remains unknown how the wax components and cutin monomers are transported to the cuticle. [32] The extracellular location of LTPs gave rise to the hypothesis that they may be involved in the secretion or deposition of extracellular lipophilic material, including cutin. It has been suggested that LTPs participate in the biosynthesis of the cutin layer and surface wax by carrying acyl monomers. This is supported by the ability of LTPs to bind acyl chains, that they are mainly located in the cell wall and that they are secreted. Moreover, LTP gene expression and LTP gene product accumulation was detected in high levels in peripheral cell layers, including epidermis. It has also been found that LTPs, particularly in young leaves where cutin deposition is active, are mainly concentrated in the surface wax. [13], [12] The cutin formation hypothesis is also supported by studies on LTP expression in *B. oleracea* var. *italica* by Pyee et al. [32]. In this plant, LTPs were found to be associated with the waxy surface of the leaves. It was demonstrated that LTPs are expressed at high levels in young leaves, and as the leaves become older, the expression level drops significantly. As mentioned earlier, LTP expression has also shown to diminish in older tissue of e.g. *A. thaliana*. [32], [14]

In spite of the circumstantial evidence for the involvement of LTPs in cutin formation, it remains to be validated by e.g. an antisense approach or by studying *A. thaliana* mutants. [12], [13]

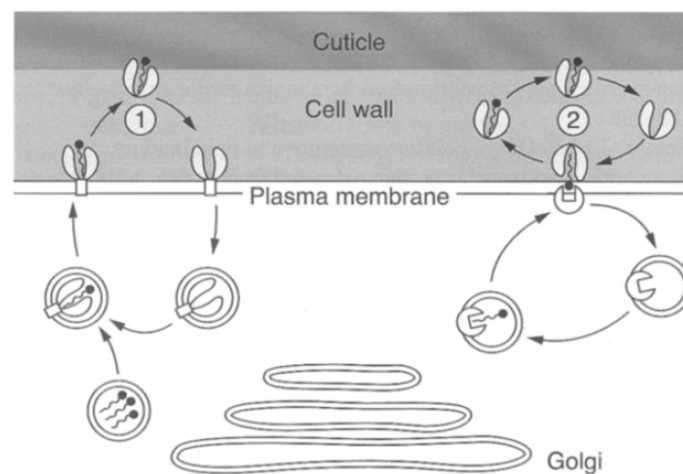


Figure 2.7: Processes proposed for the shuttle function of LTPs in cutin formation. 1) LTPs are taken up by receptor-mediated endocytosis and loaded by the fusion of endocytotic vesicles with cutin monomer-containing vesicles derived from the Golgi apparatus. 2) LTPs remain outside the cell and are loaded by a membrane-bound cutin monomer carrier. Adapted from [12].

Hendricks et al. has proposed that the function of LTPs in the cutin formation is that of a shuttle for cutin monomers from their site of synthesis towards the cuticle. They have presented two possible processes (Fig. 2.7). In the process first proposed (Fig. 2.7, 1), LTPs are taken up by receptor-mediated endocytosis and loaded by the fusion of endocytotic vesicles with cutin monomer-containing vesicles derived from the Golgi apparatus. In the other proposed process

(Fig. 2.7, 2), LTPs remain outside the cell and are loaded by a membrane-bound cutin monomer carrier. [12]

2.5.2 Plant Signaling

The hypothesis that LTPs could be involved in plant defense signaling emerged recently. In plants, a localized attack by a pathogen induces systemic acquired resistance (SAR). SAR is a distinct signal transduction pathway, which trigger a whole-plant resistance. This systemic resistance is effective against a wide range of pathogens. Accumulation of salicylic acid is required for activation of local defenses at the initial site of attack, and for subsequent expression of SAR upon a secondary, distant challenge. [33] Maldonado et al. [34] investigated the plant signaling by screening *Agrobacterium tumefaciens* transfer DNA (tDNA) tagged lines of *A. thaliana* for mutants specifically compromised in SAR. They screened an especially compromised mutant for the development of SAR for defection in induced resistance (missing *dir1-1* gene). This mutant showed unaffected local resistance against virulent or avirulent strains of *Pseudomonas syringae*, but pathogenesis-related gene expression ceased in uninfected, distant leaves. Furthermore this mutant was unable to develop SAR against virulent *P. syringae* and *Perenospora parasitica*. Further experiments indicated that the *A. thaliana* mutant was defective in the production or transmission from the affected leaf of an essential mobile signal. Super-expression of the missing *dir1-1* gene did not induce SAR (exposure to pathogens required), which implies that this gene is probably not the mobile signal itself. The *dir1-1* gene was found to encode a sequence of 102 amino acids with a molecular weight of app. 10 kDa, which shows 30-75 % similarity to members of the *A. thaliana* LTP family. The sequence contains the eight cysteines conserved in all LTPs and a signal sequence. As certain lipid molecules are released from membranes upon pathogen or insect attack, Maldonado et al. proposed that the putative LTP interacts with one of these lipid molecules to function as a long distance signal complex. [14], [34]

In support of this hypothesis, it has been shown that an LTP from *T. aestivum* is capable of binding with high affinity rate to a binding site on the tobacco plasma membrane. Through binding and *in vivo* competition experiments it has been demonstrated by Buhot et al. [35] that the binding site is the same as that used by elicitors. Elicitors are proteins with a molecular weight of approximately 10 kDa, which are secreted by fungal pathogens from the *Phytophthora* or *Pythium* genera. These peptides induce disease resistance responses and SAR in tobacco plants, and sterol binding is required for induction of these responses. Elicitors resemble plant LTPs; they are small in size (98 amino acids and 10 kDa), basic, possess three disulfide bonds and have an α -helix secondary structure. Furthermore they also have a hydrophobic pocket that gives them the capacity to bind hydrophobic molecules. They mainly bind sterols, but are also capable of binding phospholipids and fatty acids. Despite the similarities, the primary structure homology is low between the two types of proteins, but at the tertiary level there are superimpositions of some helices. [14], [34], [35]

Elicitor receptors and LTPs have been found in many plants, although many of them do not develop a hypersensitive reaction after elicitor treatment. This, along with the above indications, made Buhot et al. suggest that these receptors are associated with a general mechanism involving LTPs in a warning system able to detect exogenous organisms. The LTPs may be involved in the plant defense signaling pathway by binding a lipid molecule, and it is suggested

that a plasma membrane receptor may also play a role in LTP-mediated long distance signaling during SAR. Furthermore, elicitors trigger a hypersensitive reaction leading to the release of different mediators and molecules from cells, which are comparable with that observed in severe allergy. Therefore, the question arises if panallergen LTPs of plant-derived foods may interact with animal specific receptors and if these receptors belong to the same family as those found in plants. Recognition by such receptors could be the start of a cascade of metabolic pathways originating the allergenic response to some plant LTPs. [35]

2.5.3 Adaption of Plants to Environmental Changes

Several studies suggest that the expression of LTP genes can be induced by environmental factors such as extreme temperatures and salt or drought stresses. An example is a low-temperature response study in barley, in which it was found that several genes induced by cold treatment code for LTP-like proteins. These genes are also induced by treatment with abscisic acid (ABA), which is common for genes induced by low temperature or drought. Even though these genes are induced by cold temperatures, there are varietal differences in the response of the barley LTP gene family to low temperature. E.g. one gene is upregulated by low temperature in the winter cultivars but not in spring cultivars. In other barley types, no induction was observed for the expression of three LTP genes because of cold temperatures or other factors. These findings led to a study of regulatory elements in the genes from barley. A putative ABA-responsive element and a low-temperature responsive element were found in the barley LTP genes. Other examples of LTPs that are induced by environmental factors are LTPs from *Z. elegans*, LTPs from the stems of tomato plants and LTP1 from rice. Yubero-Serrano et al. [16] have demonstrated that an LTP gene from strawberry is induced by ABA, wounding and cold stress. Furthermore the promoter region of the LTP1 gene from *A. thaliana* contains sequences homologous to putative regulatory elements of genes in the phenylpropanoid biosynthetic pathway and sequence elements that have been found in the promoters of stress-induced genes. [12], [13], [16]

The response of LTP genes to developmental and environmental signals is complex, and additional studies are needed to determine the involvement of these proteins in adaption of plants to several stresses. However, drought, cold and salt stresses are related to water stress. If LTPs are involved in cutin deposition, the induction of LTP genes by conditions leading to desiccation seems logical. Furthermore a relationship between the putative protective role of LTPs and their differential expression under various stress conditions may exist. [12], [13]

2.5.4 Plant Defense against Phytopathogens

The unexpected antimicrobial activity of LTPs was initially discovered when proteic extracts of plants were screened for proteins that inhibit the growth of phytopathogens *in vivo*. Both bacteria and fungi were found to be inhibited by LTPs, but the activity was stronger against fungi. [14], [13] Since then, many studies have found antimicrobial activity of different LTPs against several phytopathogens. However, the mechanism of action has not yet been elucidated. [4]

In a study by Molina et al. [36] four LTPs from barley leaves and one from *Z. mays* leaves were isolated and all shown to possess antimicrobial activity against the bacteria *Clavibacter*

michiganensis subsp. *sepedonicus* and *Rhizoctonia (Pseudomonas) sonanacearum*, and the fungus *Fusarium solani*. [36] In another study by Segura et al. [37] the antimicrobial activity of two LTPs isolated from *A. thaliana* leaves and two LTPs isolated from *Spinacia oleracea* leaves was examined. It was found that these proteins also displayed antimicrobial activity against the aforementioned pathogens. Furthermore Carvalho et al. [38] found that an LTP from *Vigna unguiculata* was active against different fungi. The only Gram negative bacterium which has been proven inhibited by LTPs is *Pseudomonas aeruginosa*, which was inhibited by two LTPs isolated from *Pandanus amaryllifolius*. These two LTPs were however found not to have activity against the other tested Gram negative bacteria. An LTP isolated from the leaves of *O. sativa* have been found to present activity against the fungi *Pyricularia oryzae* and *Pseudomonas syringae*. Wang et al. [39] has examined the antimicrobial activity of an LTP isolated from mung bean seeds. This LTP was found to have activity against the fungi *F. solani*, *F. oxysporum*, *Pythium aphanidermathum* and *Sclerotium rolfsii*, and also against the Gram positive bacteria *S. aureus* but not the Gram negative *Salmonella typhimurium*. [39]

Hence, antimicrobial activity has been proven to be a property of many LTPs. The LTPs seem to have some degree of selectivity and it seems that they are most often active against fungi and sometimes Gram positive bacteria, and that they, with one exception, does not have activity against Gram negative bacteria. Though, it has been reported that some LTPs have low or no antifungal activity, e.g. LTPs isolated from *T. aestivum* and *Z. mays*. [14]

Further circumstantial evidence for the defense role of LTPs was added when it was discovered that some LTP genes respond to infection by pathogens in a way that is consistent with their products having a defensive role. It has e.g. been found that LTP genes in barley are upregulated when the barley leaves were inoculated with different fungi. In a study by Blilou et al. [40] it was shown that the expression of an LTP-coding gene in *O. sativa* is upregulated in response to infection with the fungus *Glomus mosseae*. [10], [13], [40] Because of their antimicrobial activity, sequence similarities and induction upon pathogen attack, LTPs have been included in the family of pathogenesis-related (PR) proteins that compose family 14. [14], [41]

It has been speculated that the ability of LTPs to inhibit certain microbes could result from electrostatic interactions of LTPs with biological membranes. Such interactions could possibly lead to permeabilization due to loss of membrane integrity. LTPs have further been shown to interact with model membranes such as monolayers composed of dipalmitoylphosphatidylglycerol. [14] It should however be noted that as LTPs have the ability to transfer lipids between model membranes, the evidence of interactions with lipid membranes is not enough to hypothesize their putative mode of antimicrobial action. [42] Diz et al. [43] have shown that LTPs from chili pepper seeds were able to inhibit the growth of *S. cerevisiae*, *C. albicans* and *Schizosaccharomyces pombe* at concentrations of 9-150 $\mu\text{g}/\text{mL}$. By use of confocal laser microscopy (DIC and fluorescence) they further showed that the chili LTP is capable of permeabilizing yeast plasma membranes and allow the entrance of the small dye SYTOX Green (Molecular Probes). This high affinity nucleic acid stain fluoresces upon binding to nucleic acids and only penetrates cells with compromised plasma membranes. [43], [14] An LTP from *Helianthus annuus* has also been subjected to the SYTOX Green permeabilization assay, and were found to be able to permeabilize the membranes of *F. solani* spores. [14] Another study by Caaveiro et al. [44] LTP2 from barley were shown to interact with large unilamellar negatively charged vesicles filled with fluorescent dyes. The LTP showed modest vesicle aggregation and leakage-inducing ac-

tivity, but only at low ionic strength. It is commonly accepted that protein-induced leakage requires hydrophobic interaction of the protein with the membrane phospholipid matrix [44]. Therefore the authors suggest that the barley LTP perhaps get inserted in the bilayer matrix in a way that resembles the integral membrane proteins. As no effect of this LTP was observed with electrically neutral bilayers it seems likely that this LTP interacts electrostatically with the phospholipid headgroups before proper insertion occurs. This interaction could perhaps neutralize some LTP cationic residues. [44]

Wang et al. [39] investigated *S. aureus* subjected to an LTP in a scanning electron microscope (SEM). This investigation revealed a difference in bacterial structure between cells with and without LTP, which demonstrated a possible antipathogenic mechanism due to destruction of bacterial cell wall. In ultrastructural and cytochemical studies Wang et al. observed wall disruption, release of cell sap from cell wall, and cytoplasmic leakage from the *S. aureus* cells. [39]

Studies by Regente et al. have also provided clues to the elucidation of the antimicrobial mode of action of LTPs. They isolated a potent LTP from sunflower seeds (Ha-AP10), showing fungicidal activity against *F. solani*. By use of SYTOX green experiments, they were capable of demonstrating that Ha-AP10 not only induces liposome leakage but also modifies the permeability of fungal cells. Furthermore, they found a cause-effect relationship between the pattern of permeabilization and the lethal effect, indicating that this permeabilization is part of the mechanism of action of this LTP. In their studies they furthermore showed that the LTP displayed no toxicity towards phytocells, illustrating its ability to discriminate between cell types. The authors speculated that the LTP selectivity may be linked to electrostatic interactions with anionic membrane phospholipids. As only a moderate release of fluorescent probes encapsulated in the model membranes were observed, it was further postulated that the electrostatic interaction with phospholipids is required but not sufficient to produce the full antimicrobial effect. [45], [42] Furthermore, as the LTPs seems to have some degree of specificity towards certain pathogens, it cannot exclusively be electrostatic interactions with the membranes that cause the inhibitory effect of LTPs. [10] It has by others been suggested that the central hydrophobic cavity of LTPs forms a pore upon membrane permeabilization by protein insertion, permitting outflow of intracellular ions and thus leading to cell death. [4] It however remains speculative along with the factors providing the ability to discriminate between cell types.

Plant LTPs have the necessary inhibitory properties, the appropriate distribution (cell-wall location), concentration and correct patterns of gene expression under pathogen attack to be considered active defense proteins. [10] Still, the mechanism of action, their structure/function relationship and their ability to discriminate between cell types remains a mystery. A synergistic effect against fungi has been observed when LTPs are combined with thionins, and it is suggested that they together form a general barrier against pathogens. It has also been demonstrated that LTPs are found in concentrations much higher than those required to inhibit many pathogens. Thus, LTPs appear to provide the plant with a defensive protein shield. [13], [10] That not all LTPs possess antimicrobial properties, whereas others show strong activity, suggests that different LTPs have different biological roles. Perhaps some LTP types take part in defense reactions, whereas others fulfill a role in the deposition of extracellular lipids such as cutin monomers. Moreover, these functions are not mutually exclusive. Another suggestion is that the antimicrobial properties of some LTPs should be regarded as an acquired secondary

function. [46], [37]

Ace-AMP1

The most potent antimicrobial protein belonging to the LTP class discovered till now is the Ace-AMP1, extracted from onion seeds by Cammue et al. [46]. Cammue et al. found that Ace-AMP1 inhibited all 12 tested plant pathogenic fungi at concentrations below 10 $\mu\text{g}/\text{mL}$. This strong antifungal activity was either not at all or weakly affected by the presence of different cations. Ace-AMP1 was also proven active against two Gram positive bacteria (*Bacillus megaterium* and *Sarcine lutea*) but showed no activity against Gram negative bacteria and cultured human cells. In comparison, LTPs isolated from wheat and maize seeds showed little or no antimicrobial activity against the 12 fungi, whereas a radish LTP only displayed antifungal activity in media with low cation concentration. The underlying mechanism of action of the potent activity of Ace-AMP1 is still unknown. In the LTP-characteristic *in vitro* lipid transfer assay, Ace-AMP1 however failed in transferring either phosphatidylcholine or phosphatidylinositol from liposomes to mitochondria. [46] Still, Ace-AMP1 has been classified as a member of the LTP type 1 family on basis of sequence similarities. The missing lipid transfer ability of Ace-AMP1 indicates that the binding and transport activities of lipids may not be directly associated or correlated with the ability of interaction with membranes and with the antimicrobial activity in this case. [14], [30] Ace-AMP1 has already shown its potential as antimicrobial agent in e.g. transgenic wheat and rose lines, which both showed improved resistance to pathogens. [47], [48]

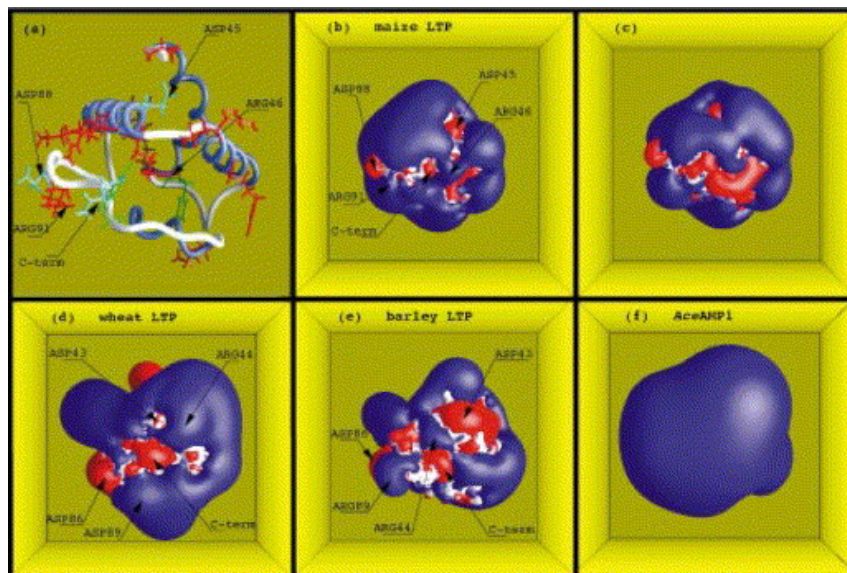


Figure 2.8: Electrostatic potential contours as calculated by Gomar et al [30]. The molecular surface is shown in white. The isopotential surfaces for values of $0.5 k_B T/e$ and $-0.5 k_B T/e$ are colored in blue and red, respectively. a) Orientation of the molecules. b) Maize LTP. c) Maize LTP complexed with a palmitate molecule. d) Wheat LTP. e) Barley LTP. f) Ace-AMP1. Adapted from [30].

By use of homology modeling, Gomar et al. [30] created a 3D structure model of Ace-AMP1 with the purpose of comparing the structure and molecular properties of Ace-AMP1 with con-

ventional LTPs. They found that the global fold of Ace-AMP1 is similar to that of other LTPs. However, the hydrophobic cavity in Ace-AMP1 was found to be blocked by a number of bulky residues, which is likely to explain the inability of Ace-AMP1 to bind lipids. Another interesting finding from this study arose from investigations and comparisons of the electrostatic potentials. Isopotential contours were drawn at $\pm 0.5 k_B T/e$ at pH 7 with the GRASP program on a maize LTP (pI of 9), a wheat LTP (pI of 10), a barley LTP (pI of 8), and Ace-AMP1 (pI of 11.8) (Fig. 2.8). It was found that the electrostatic contours of conventional LTPs compared to Ace-AMP1 showed differences that may suggest a different mode of interaction with membranes. Globally all the proteins except barley LTP were surrounded by a positive potential. However, the shape of the positive contours and the distribution of negative surface contours differed significantly. The electrostatic potential of the three conventional LTPs showed common features, which do not appear on the contour of Ace-AMP1. These similarities were discovered in the region between the second loop and the C-terminus, which is located at one extremity of the hydrophobic cavity. It therefore may be that this region is the interaction site of LTPs with lipids, perhaps explaining the conservation of the shape and location of these positive patches. Ace-AMP1 is only surrounded by a positive electrostatic potential, because the two aspartic acid residues are not capable of compensating for the effect of the 19 arginines. Only two negative spots on one side of the molecule were discovered. Together, these findings suggest that conventional LTPs and Ace-AMP1 interacts differently with membranes. [30]

2.6 LTPs from the Brassicaceae Family

The presence of LTPs in a variety of higher plants has currently been reported. These include well known plants such as *Triticum* spp. (wheat) [49], [50], [51], *Prunus persica* (peach) [52], *Hordeum vulgare* (barley) [53], [54], *Oryza sativa* (Asian rice) [55], *Zea mays* (maize) [56], *Nicotiana tabacum* (tobacco) [57], [58], *Ricinus communis* (castor oil) [59], *Allium cepa* (onion) [46], *Spinacia oleracea* (spinach) [37], *Fragaria x ananassa* (garden strawberry) [16], and many more. Several confirmed LTP expressing plants are members of the Brassicaceae family such as *Arabidopsis thaliana* [60], *Raphanus sativus* (radish) [61], and members of the Brassicaceae tribe [62], [29]. The Brassicaceae family (informally known as the mustard family) is a large plant family currently estimated to consist of 338 genera and 3700 species. The phylogeny of this family is illustrated in Fig. 2.9. This large family is considered to have major scientific and economic importance; scientific importance because the genera *Arabidopsis* and *Brassica* are important model organisms in plant sciences, and economic importance because of the nutritional value of many of its members. [63], [64]

2.6.1 LTPs Found in Members of the Brassicaceae tribe

The Brassicaceae tribe is one of 26 tribes belonging to the Brassicaceae family, and it consists of approximately 50 genera and 240 species. Members of this tribe are distinguished from the rest of the Brassicaceae family by the presence of conduplicate cotyledons and/or transversely segmented fruits. The tribe include the species *Brassica oleracea*, which have well known cultivar groups such as *capitata* (cabbage), *acephala* (kale, collard greens), *gemmifera* (brussels sprout),

and *italica* (broccoli). [64], [65]

The presence of LTPs have been reported in several members of the Brassicaceae tribe, such as *Brassica napus* [66], [62] and *B. oleracea* (var. *italica* [32], var. *capitata* [29]), and putative LTP encoding genes have been identified in the members *Brassica rapa*, *Brassica juncea*, *Brassica campestris*, and *Sinapis alba* (*Brassica hirta*) [67].

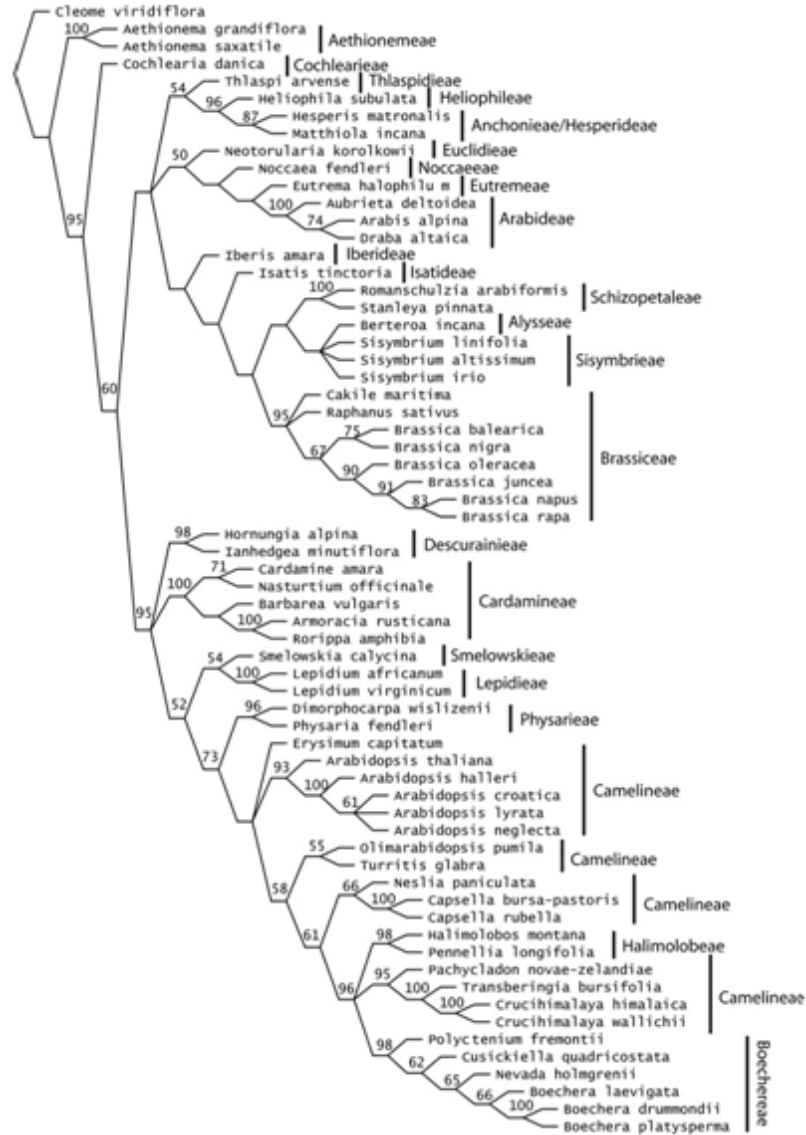


Figure 2.9: Phylogenetic tree of the Brassicaceae family displayed as cladogram. Bootstrap values are given above each node, and the vertical black lines outlines members of the same tribe. Adopted from [64].

2.6.2 LTPs from *A. thaliana*

The model plant *A. thaliana* is one of the most suitable organism for obtaining an exhaustive collection of LTP isoforms, as it has a relatively small genome where an important part has been sequenced. By obtaining the complete collection of *A. thaliana* LTPs it may be possible to get closer to determining the *in vivo* functions of these proteins. [60]

Arondel et al. [60] in 2000 reported that the LTP gene family in *A. thaliana* contains at least 15 genes, which they named LTP1-15. All the sequences of these genes were found to exhibit the typical features of plant LTPs; their molecular weight is around 9 kDa, the isoelectric point is near 9 and typical amino acid residues such as cysteines are conserved. However, Arondel et al. discovered three acidic LTPs (LTP8, LTP9 and LTP14) with isoelectric points around 4-5 and a LTP with a high isoelectric point of 11.4 (LTP5). All the deduced proteins share a similar hydrophobic profile and contain a typical signal sequence. The number of amino acids ranges from 89-98 when the signal sequence is excluded. [60]

Segura et al. [37] isolated two LTPs from the leaves of *A. thaliana* in 1993, which showed antimicrobial activity against the bacterial phytopathogens *Clavibacter michiganensis* subsp. *sepedonicus* and *Pseudomonas solanacearum* (0.1 μ M range), and against the fungal phytopathogen *Fusarium solani* (10 μ M range). It is however unknown which of these LTPs were isolated in this study. [37]

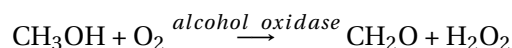
The *P. pastoris* Expression System

3

3.1 *Pichia pastoris*

The yeast *P. pastoris* is a highly successful expression system for the production of a variety of heterologous proteins [68]. The yield of a given recombinant protein has been increased from only a few micrograms to more than 15 g/L of *P. pastoris* culture [69], [70]. *P. pastoris* is a single-celled microorganism and is therefore, like bacteria, relatively fast growing and relatively easy to genetically manipulate. However, unlike bacteria, yeasts are eukaryotes and their intracellular environment therefore allows them to perform many eukaryote-specific post-translational protein modifications such as proteolytic processing, disulfide bridge formation and glycosylation. Thus, many proteins that end up as inactive inclusion bodies in bacterial systems are produced as biological active molecules in *P. pastoris*. Several additional features makes *P. pastoris* a popular system: its ability to produce foreign proteins either intracellular or extracellular at high levels, easy scale up from shake-flasks to high density fermentor cultures and growth to extremely high concentrations under fermentor conditions. [69], [71], [72], [73], [74]

P. pastoris is one of approximately 30 yeast species from four different genera (*Pichia*, *Candida*, *Hansenula* and *Torulopsis*) capable of metabolizing methanol as its only carbon and energy source. The methanol metabolic pathway appears to be shared by these species and involves a unique set of enzymes. The first step in the metabolism of methanol is an oxidation of methanol to formaldehyde using molecular oxygen. This reaction also generates hydrogen peroxide and is catalyzed by the enzyme alcohol oxidase (AOX) [75], [72], [73], [74]:



A consequence of this is that when *P. pastoris* is grown on methanol, molecular oxygen is not only used for respiration, but also consumed to perform the initial oxidation of methanol. The generated formaldehyde and hydrogen peroxide is toxic to the cell, so the process takes place within the peroxisomes. AOX has a poor affinity for O₂, which it seems *P. pastoris* compensate for by generating large amounts of the enzyme. [75], [73], [70]

Two genes in *P. pastoris* codes for AOX, namely AOX1 and AOX2. Although both genes encode equally functional AOX enzymes and are more than 90% identical, AOX1 account for the majority of the AOX produced, because the AOX1 gene has a very strong promoter. [75], [72] Expression of the AOX1 gene is controlled at transcriptional level, tightly regulated and induced by methanol to very high levels. When methanol is present in the growth medium of shake-flask cultures, approximately 5% of the total cell protein is AOX, whereas AOX is undetectable when no methanol is present. In cells fed methanol at growth limiting rates in fermentor cultures, up to 30% of the protein is AOX. [68], [69], [75], [73]

The strong, highly-inducible AOX1 promoter (P_{AOX1}) can be utilized for recombinant expression of a protein of interest. The gene of the protein of interest has to be successfully cloned downstream of the P_{AOX1} in a vector, and then the construct has to be transformed into the chromosome of the chosen *P. pastoris* strain. Linear vector DNA can via homologous recombination between sequences shared by the vector and host genome generate stable transformants of *P. pastoris*. These integrants show strong stability in the absence of selective pressure even when present as multiple copies. The insertion also occurs with non-linearized plasmids and plasmids that religates, though at a lower frequency. All *P. pastoris* expression vectors carry at least one *P. pastoris* DNA segment that can be used to direct the vector to integrate into the host genome by a single crossover event (insertion). Expression vectors containing 3' AOX1 sequences can be integrated into the genome of *P. pastoris* by a single crossover event (Fig. 3.1) or by a double crossover event (replacement) at AOX1. The latter scenario arises from crossovers at both the AOX1 promoter and 3' AOX1 regions of the vector and genome, and results in the deletion of the AOX1 coding region and no Zeocin resistance in X-33. Single crossover events are much more likely to happen than double crossover events, and multiple insertion events occur spontaneously at about 1-10 % of the single insertion events. [73], [75]

The productivity of most proteins produced in the AOX1-promoter system is relatively low, but this is compensated for by production over many days and the fact that *P. pastoris* can grow on methanol to very high cell densities in bioreactors. [76]

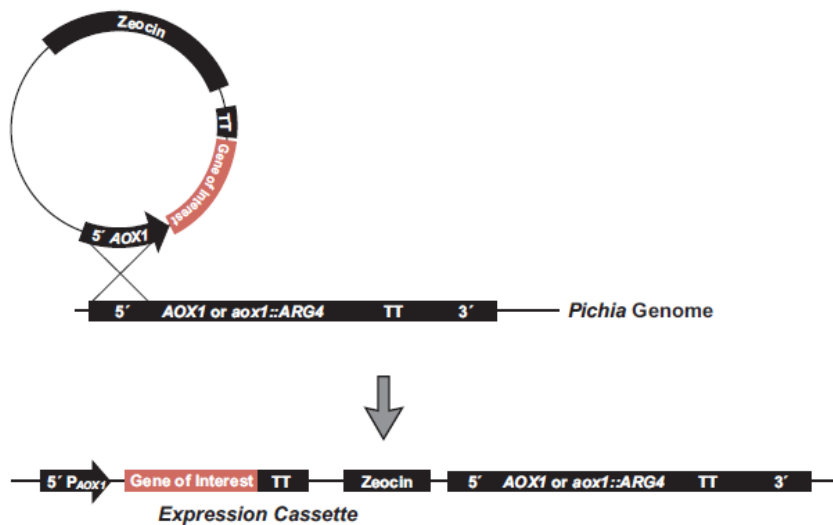


Figure 3.1: Result of an insertion of a construct harboring a gene of interest 5' to the intact AOX1 locus (resulting in a phenotype Mut^+ transformant) and the gain of P_{AOX1} , the gene of interest and the Zeocin resistance gene. Adopted from [75].

Three phenotypes of *P. pastoris* host strains with regard to methanol utilization exist, which vary in their ability to utilize methanol due to deletions in one or both AOX genes. These three phenotypes are denoted Mut^S , Mut^+ and Mut^- . Mut^S refers to the "Methanol utilization slow" phenotype, and this type is characterized by the loss of the AOX activity encoded by the AOX1 gene. They still harbor the wild type AOX2 gene and are therefore capable of slow growth on methanol, due to the cells' reduced ability to metabolize methanol. Mut^+ refers to "Methanol utilization plus" and this type is characterized by having the wild type ability to metabolize methanol as the sole carbon source. In the Mut^- , or the "Methanol utilization minus", both

AOX genes are deleted, and this type is therefore completely incapable of growing on methanol. Transformation of the wild type X-33 strain with plasmid DNA linearized in the 5' AOX1 region will yield Mut⁺ transformants, while use of the KM71¹ strain will yield Mut^S transformants. Both Mut⁺ and Mut^S recombinants are useful because one phenotype may favor the expression of a protein of interest compared to the other. [75], [73], [74]

3.1.1 Protein Secretion

Heterologous protein expression in *P. pastoris* can either be intracellular or secreted. In order for secretion from the cells to occur, the expressed protein must contain a signal sequence. This sequence targets the protein to the secretory pathway. [75]

The secretory pathway of all eukaryotes is essentially the same and the basic mechanism involves three steps: (1) protein synthesis and translocation across the rER membrane, (2) protein folding and modification inside the rER lumen, and (3) protein transport to the Golgi complex and then further to its final destination. [77]

Several different signal sequences have been used successfully in *P. pastoris*, including native secretion signal sequences on heterologous proteins. However, the signal sequence α -factor pre-propeptide from *Saccharomyces cerevisiae* is the most commonly used. The α -factor signal sequence consists of a 19 amino acid signal pre-sequence followed by a 66-residue pro-sequence. The signal sequence contains three N-linked glycosylation sites and a dibasic Kex2 endopeptidase processing site. The processing of the signal sequence involves three steps: (1) removal of the pre signal by a signal peptidase in the ER, (2) Kex2 endopeptidase cleavage between Arg-Glu of the pro-sequence, and (3) cleavage of Glu-Ala repeats by the Ste13 enzyme. [68], [75]

The major advantage of protein secretion in *P. pastoris* is that it only secretes a very low amount of native proteins and its medium contains no added proteins. This implies that the protein of interest often is the majority of the total protein in the growth medium, and therefore secretion serves as the first step in purification of the protein. [75], [73]

3.1.2 Glycosylation

Protein glycosylation is one of the post-translational modifications carried out in yeast on secreted proteins, and *P. pastoris* is capable of adding both N- and O- linked carbohydrates. Yeast in general carries out glycosylation on asparagine residues, which is called N-glycosylation, and on threonine and serine residues, which is called O-glycosylation. The details of the glycosylation pathways have been derived from *S. cerevisiae*. [71], [69]

N-type glycosylation is a well-established mechanism which occurs on amide nitrogen on the side chain of asparagine residues that are located in the recognition sequence Asn-X-Ser/Thr, where X is any amino acid, except proline. The N-glycosylations begin in the rER where

¹KM71 is a strain that have a mutation in the histidinol dehydrogenase gene (*HIS4*) to allow selection for vectors harboring *HIS4*.

a lipid-linked oligosaccharide unit is transferred to the asparagine residue. This unit is further modified to its final structure, Man₈GlcNAc₂ (Man: mannose; GlcNAc: N-acetylglucosamine) as the glycoprotein proceeds to the Golgi complex. Beyond this point, lower and higher eukaryotic glycosylation patterns differ significantly. [71], [72]

O-glycosylation occurs on the hydroxyl group of serine and threonine. In mammals, O-linked oligosaccharides are composed of many different sugars, whereas lower eukaryotes like *P. pastoris* add O-oligosaccharides composed of solely mannose residues. [71], [72]

P. pastoris as expression system has the advantage in comparison to *S. cerevisiae* that it does not hyperglycosylate secreted proteins. N-glycosylation occurs more frequently than O-glycosylation in both *P. pastoris* and *S. cerevisiae*, and is of the high-mannose type. The oligosaccharides added post-translationally to the proteins are of different length; in *P. pastoris* the chains are on average 8 to 14 mannose residues per side chain and in *S. cerevisiae* they are between 50 and 100 mannose residues. [75] In mammals the mannose chains are significantly shorter, because the process involves removal of mannose followed by the addition of other sugars. [78]

The N-linked high-mannose oligosaccharides added in yeast is problematic for the use of recombinantly expressed proteins in the pharmaceutical industry. These N-linked high-mannose oligosaccharides can be antigenic and the difference in length may interfere with the folding or function of the mammalian foreign proteins. [68] Recently, advances in humanizing yeast N-glycosylation have been made, resulting in yeast strains that can perform hybrid N-glycosylation at high uniformity and complexity. [78] In near future it will be possible to produce recombinant glycoproteins with uniform carbohydrates of known structure that is similar to those produced in mammals. [68]

3.2 Fermentation of *P. pastoris*

Successful expressions of foreign proteins in *P. pastoris* shake-flask cultures at reasonable levels have been reported, however, the expression levels are often low. In the controlled environment of fermentor cultures it is possible to grow *P. pastoris* to high cell densities (up to 130 g/L dry cell weight [70]) by controlling parameters such as oxygen level, carbon source feed, temperature and pH. As the concentration of especially secreted product is roughly proportional to cell concentration, fermentation often improves the product yield significantly. Furthermore, different continuous and fed-batch culture techniques can be utilized, which have been optimized to increase yields. [71] These include methanol limited fed-batch (MLFB) [71], temperature limited fed-batch (TLFB) [79], and oxygen limited fed-batch (OLFB) [70]. Fortunately, one of the forces of *P. pastoris* as expression system is the ease in scale up from shake-flask to high density fermentor cultures. Adding the economical and well defined mineral media, *P. pastoris* is nearly ideal for large-scale fermentation. [71], [80]

P. pastoris fermentation schemes often involve three general phases (Fig. 3.2). In the first phase the strain is grown in glycerol batch, which serves to generate cell mass. When the glycerol is depleted, a second phase is often initiated in which glycerol is fed to the culture at growth-limiting rate. This second phase ensures a smoother transition between glycerol and methanol growth. In the third phase a mixture of methanol and glycerol, or just methanol, is fed to the culture to induce expression. The mixed feeding strategy offers improved cell-culture

viability and possibly higher recombinant protein production rate due to a smoother transition to methanol as sole carbon source. The danger of this approach is however that excess glycerol (or other carbon sources) is a strong repressor of the AOX1 promoter, and therefore may result in lower yields. A low but increasing methanol feed is applied in this phase, which should match the increasing AOX activity caused by the induction. As a result, the oxygen uptake rate increases. When the dissolved oxygen tension (DOT) is around 25%, the methanol feed rate is kept constant. Through these conditions the methanol concentration becomes the growth-rate limiting factor. The fermentation should be ended at peak concentration of the foreign protein, but this time point varies with the specific protein produced. [71], [80]

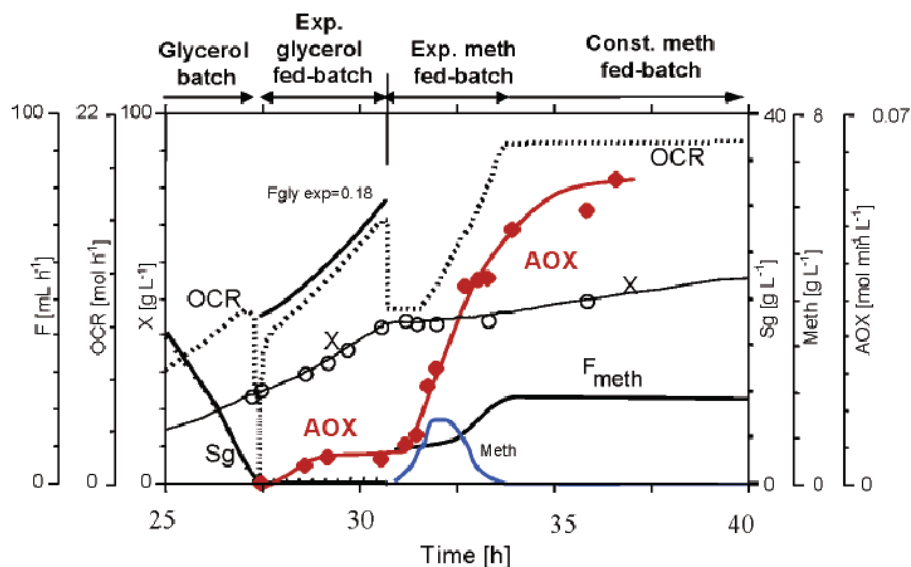


Figure 3.2: *P. pastoris* methanol-limited fed-batch (MLFB) process. Biomass concentration (solid line, open circles, cross); glycerol concentration (solid line, Sg); methanol concentration (solid blue line, Meth); alcohol oxidase activity (solid red line, filled diamonds, AOX); oxygen consumption rate (dotted line, OCR); glycerol feed rate (solid line, Fgly); methanol feed rate (solid line, Fmeth) is plotted against batch time. Adapted from [76].

Different bioreactor culture techniques may be most suitable for production of a specific foreign protein in *P. pastoris*. In the traditional MLFB technique, the methanol concentration is as mentioned the growth-rate limiting factor. [70], [76] In the TLFB technique, temperature is utilized as the limiting factor instead of methanol to prevent oxygen limitation at high cell density. The temperature controller is set to maintain a specific DOT; when DOT is below the set point the temperature is decreased, and when DOT is above set point, the temperature is increased. This technique has been shown to result in higher cell density, lower cell death, higher concentration of product and lower proteolytic degradation compared to MLFB. [79], [76]

In OLFB, the oxygen level is utilized as the growth limiting factor. OLFB is an advantages technique in combination with *P. pastoris*, because this yeast is an obligately aerobic organism when grown on methanol. Thus, it does not produce alternative, inhibiting products of fermentative metabolism, which is the case with facultative organisms such as *S. cerevisiae* and *E. coli*. Due to the requirement of oxygen in methanol metabolism, it was initially believed that oxygen limitation would affect expression of foreign genes negatively. This has however not been confirmed, as slightly higher cell densities, higher product concentration, and a similar viability has been found in these fermentations when compared with MLFB. The oxygen lim-

itation has been reported to increase cell maintenance demand, and reduce the total amount of proteins released into the medium, decreasing the amount of down-stream product purification. The advantages obtained with OLFB is caused by the batch being run with at DOT of approximately zero, which results in a higher oxygen transfer rate, leading to comparatively increased cell productivity due to an increased rate of methanol consumption. [76], [70]

Each of these techniques have been found advantages for the production of different proteins in *P. pastoris*. Currently, empirical approaches are the only way of determining the most suitable conditions for production of a protein of interest. [71], [76], [70]

3.3 Known Production Barriers

Like any other expression system, the *P. pastoris* expression system have drawbacks and unresolved issues. Cases of low yields or failure of expression are numerous, but often remain unpublished [80]. Factors believed to drastically influence protein production in *P. pastoris* include the copy number of the expression cassette, site of chromosomal integration of the expression cassette, mRNA 5'- and 3'-untranslated regions (UTR), translational start codon context, A+T composition of cDNA, transcriptional and translational blocks, host strain physiology, media and growth conditions, and fermentation parameters. [81], [82], [80] The expression of smaller proteins (below 10 kDa) has furthermore often been low or missing, often due to RNA instability [83]. The most common problem encountered is however believed to be that of proteolytic degradation of secreted proteins. [80] In the following, some of these factors will be described in more detail.

Proteolytic degradation is in general a well known issue in the field of recombinant protein expression, and often an important factor, since many proteins are susceptible to degradation by proteases. Proteolytic degradation does not only have the potential to dramatically reduce the product yield, but also complicates the downstream purification of the product. [71], [79] The proteases in *P. pastoris* are not well characterized, even though their influence on the production yield of specific recombinant proteins are well documented in literature [84], [85], [86]. Especially in high density cell cultures the proportional higher release of proteases to the cell medium imposes a significant problem. It however appears that the proteases in *P. pastoris* are very similar to those of the well characterized yeast *S. cerevisiae*. The presence of extracellular proteases in yeasts have not been reported, however their vacuoles contain various proteases that may be released upon cell lysis. In *S. cerevisiae* the major vacuolar proteases are proteinase A (PrA), proteinase B (PrB), carboxypeptidases, and aminopeptidases. [86], [79], [87], [71]

It is known that the use of methanol as sole carbon source results in higher levels of vacuolar proteases in the culture medium, and that these levels increase with induction time. This may be due to a lower cell viability when *P. pastoris* is grown on methanol compared to glycerol, even though only a small fraction of cells lyse due to nonviability. It has been speculated that the formation of hydrogen peroxide and formaldehyde as a by-product of the methanol metabolism may cause leaky membranes, and this way be partly responsible for the higher protease release. Furthermore, it is likely that growth on methanol causes stress on the cell machinery, which elicits higher protease production. It is speculated that these different effects of growth on methanol together is responsible for the increased proteolytic activity in culture

supernatant. [86]

Different measures can be taken to reduce or eliminate proteolytic degradation of the product. One approach is to add casamino acids or peptone, which is reported to reduce product degradation by acting as excess substrates. [71], [86], [79], [76] An expression variable that can be manipulated to reduce proteolytic activity is e.g. the cultivation temperature. *P. pastoris* is a psychrotrophic organism that can grow at a temperature as low as 12 °C, with the result of a lowered specific growth rate. Lowering of the cultivation temperature has a negative effect on the protease activity in the culture supernatant for two reasons; pure thermodynamic reasons and a reduced amount of nonviable cells lysing, resulting in lower vacuolar protease levels in the supernatant. [79] Another advantages approach is to change the pH of the culture to one that is not optimal for problematic proteases. This is durable because *P. pastoris* is capable of growing at pH values ranging from 3 to 7. As an example, aspartyl proteases (such as PrA) are generally active at pH 3, and therefore do not cause significant problems at physiological pH. [71], [86]

Another measure taken to circumvent the negative effects of proteases is the addition of protease inhibitors. In a study by Sinha et al. [86] it was found that post-harvest addition of 1 mM phenyl methyl sulfonyl fluoride (PMSF) (serine protease inhibitor) reduced the total protease activity on the casein substrate by 78%, and that addition of 1 mM ethylenediaminetetraacetic acid (EDTA) (metalloprotease inhibitor) reduced it by 45%. By adding a combination of these, a total reduction of 94% of the protease activity was achieved. It was found that PMSF almost completely inhibits PrB and carboxypeptidases, while EDTA inhibits aminopeptidases. However, a variety of proteases have been reported to be present in *P. pastoris* supernatant, which have different specific activities against different proteins. Therefore the suitability of different protease inhibitor cocktails in preventing proteolytic degradation of specific heterologous proteins has to be evaluated independently. [86] Another disadvantage of this measure is that the addition of protease inhibitors in large scale fermentations are rather costly, and that for example PMSF is toxic and have a half-life of 110 min in aqueous solutions. Therefore protease inhibitor cocktails are often not added until the fermentation has ended. [88], [89]

Protease-deficient strains have been found to represent an alternative and efficient solution to increase product stability in culture supernatant. The protease deficient *P. pastoris* SMD series (Invitrogen) contains strains which have had the *PEP4* gene knocked out. This gene encodes PrA, which is a vacuolar aspartyl protease required for the activation of other vacuolar proteases, such as carboxypeptidase Y and PrB. This however comes at the cost of a lower growth rate. [71]

At DNA level, several factors are suspected to influence the production of foreign proteins in *P. pastoris*. The nucleotide sequence and the length of the 5'UTR may e.g. negatively influence expression. For optimal synthesis of foreign proteins it seems essential to maintain the 5'-UTR as identical as possible to that of the natural AOX1-mRNA. [82] The production level of human serum albumin has been shown to be increased over 50-fold by adjusting the 5'-UTR [90]. Further, it seems important to avoid AUG sequences in the 5'-UTR to ensure translation of the mRNA from the actual translation initiation site. [82] Often, a single copy of the expression cassette is sufficient for optimal production in *P. pastoris*, and multiple copies have in rare cases even been found to decrease production. However, sometimes multiple copies are necessary for high expression, revealing that the effect of gene copy number on expression is

unpredictable. [82]

The AT content in the gene of interest has also been found to be important, as genes with high A+T content have been reported to be transcribed inefficiently because of premature termination. An example of a nucleotide sequence blocking transcription in *P. pastoris* is 5'-ATTATTTTATAAA. By decreasing the AT content of this particular sequence stretch, Scorer et al. [91] were capable of eliminating premature termination. As it is unknown which AT-rich stretches that act as transcriptional terminators, problematic genes should in general be redesigned to have an A+T content in the range of 30-55%. [91], [82] It is furthermore recommended to consider the codon bias of *P. pastoris*. [82]

Boettner et al. [92] investigated sequence-based factors influencing intracellular expression of heterologous genes in *P. pastoris* by making a comparative study of the expression of 79 human genes. They divided the resulting clones into four groups based on expression level: no detectable expression, low expression level, medium expression level, and high expression level. 44 of 79 clones ended up in the category with no detectable expression, while only six clones were characterized as having high expression levels. In this study, three factors proved to have statistically significant association with the expression level: i) rare occurrence of AT-clusters in the cDNA was associated with a high expression level; ii) a high pI was associated with no detectable protein expression; iii) the presence of a homologous protein in yeast was associated with general success of the expression. Factors not showing statistically significant association with the expression level in this study were amongst others the codon bias, GC content, and protein size. [92]

The protein of interest is often secreted when produced in *P. pastoris*, and many foreign proteins have been secreted with success in this system. However, some proteins have been reported not to be secreted properly or were found to be secreted, but with improperly processed signal sequence. Examples exist where the same strain, vector and methodology were used, but the expression level of different secreted proteins varied from 1 mg/L to above 10 g/L. It has been found that the secretion efficiency is not only dependent on the signal sequence, but also partly on the structure of the foreign protein. A change in signal sequence can change the secretion efficiency dramatically, and it seems that a match between *cis*-acting information in the signal sequence and partner protein are crucial for success. Unfortunately there is currently no way of predicting which signal sequence will give the desired successful secretion in *P. pastoris* for a protein of interest - trial and error experiments is the only mean of finding the optimum secretion signal for a specific protein. [80]

From the above, it is evident that there is still some issues that needs to be resolved and questions that needs to be answered before the full potential of this promising expression system can be realized. Currently, only few reliable criteria for predicting the success of expression of a particular protein exist. The right combination of expression system and protein, and the optimization of protein yield is for now only achievable through "trial and error" approaches. [92]

3.4 The pPICZ α Expression System

The expression vector used to harbor the gene constructs in present study is the pPICZ α A vector (Fig. 3.3), which was chosen because it is specialized for secreted expression. The pPICZ α A vector is a 3.6 kb *E. coli*/*P. pastoris* shuttle vector which contains an origin of replication for plasmid maintenance in *E. coli* and is designed for protein expression in *P. pastoris*. [71] It is based on the AOX1 promoter which allows methanol-inducible high-level expression. Furthermore, it contains the α -factor secretion signal, and a multiple cloning site with 10 unique restriction sites, which permits the insertion of a gene of interest. A C-terminal myc epitope tag and a C-terminal polyhistidine tag provides means of detection and purification of an expressed protein, respectively. Furthermore, it contains the *Sh ble* gene from *Streptoalloteichus hindustanus*. This is a small gene of 375 bp which confers resistance to the drug Zeocin in *E. coli*, yeast (including *P. pastoris*) and other eukaryotes. Because this gene serves as selection marker in both *E. coli* and *P. pastoris*, Zeo^R vectors are much smaller and easier to manipulate than other *P. pastoris* expression vectors. [75], [73]

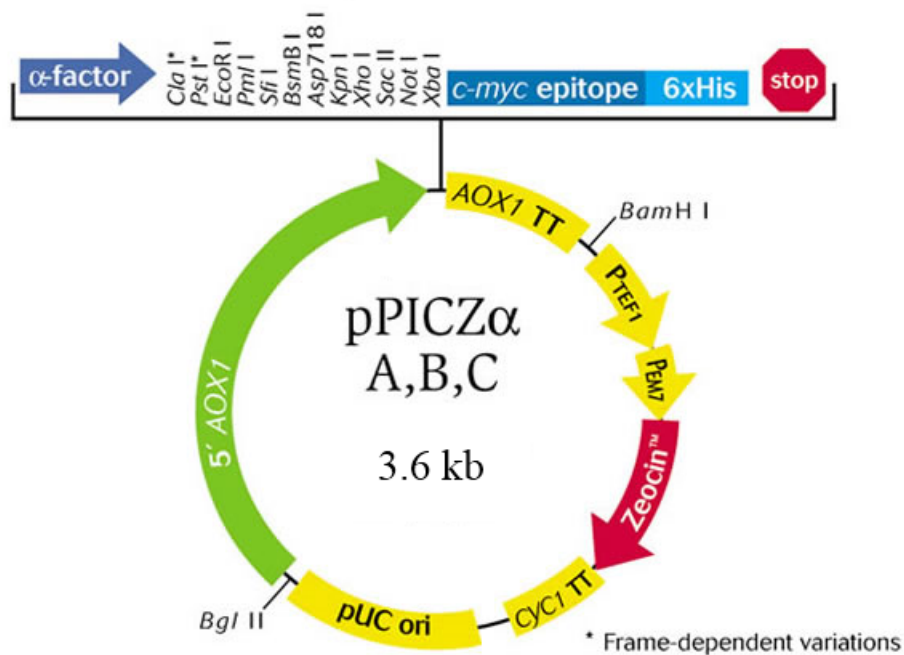


Figure 3.3: Schematic drawing of the 3.6 kb *E. coli*/*P. pastoris* shuttle vector pPICZ α A. The AOX1 promoter allows methanol-inducible high-level expression. It contains the α -factor secretion signal and a multiple cloning site with 10 unique restriction sites. A C-terminal myc epitope tag and a C-terminal polyhistidine tag permits detection and purification of an expressed protein, respectively. Furthermore, it contains a Zeocin resistance gene. Adopted from [75].

Project Description

4

4.1 Review of Previous Work

In a previous study [93] the putative lipid transport proteins LTP5 and LTP8 from *Arabidopsis thaliana* were chosen for recombinant expression and characterizations. LTP5 was chosen due to an unusual high predicted pI of 11.4, and sequence similarities to the highly potent Ace-AMP1. LTP8 was chosen because of its unusual low predicted pI of 4.9. Following are a review of this work and most important findings of the previous study.

4.1.1 Sequence Characterizations

The nucleotide sequence of the full-length cDNA encoding LTP5 was found to comprise 357 bp and encode a protein of 118 amino acids with a molecular weight of 12.50 kDa. The prediction of the original N-terminal signal peptide using SignalP 3.0, revealed that the most likely signal sequence of LTP5 is amino acid 1 to 25. Hence, the signal sequence cleavage site is between Ala25 and Ala26. Removal of the predicted signal sequence yields a theoretical proLTP5 with a molecular weight of 9.89 kDa.

The nucleotide sequence of the full-length cDNA encoding LTP8 was found to comprise 351 bp and encode a protein of 115 amino acids with a molecular weight of 11.79 kDa. The most likely signal sequence of LTP8 was predicted to be amino acid 1 to 24, which yields a cleavage site between Ser24 and Ala25. Removal of the predicted signal sequence yields a theoretical proLTP8 with a molecular weight of 9.09 kDa.

A BLAST search was performed on each of the LTPs, and the highest identities was found with LTPs originating from members of the same plant family as *A. thaliana* (Brassicaceae). In a phylogenetic analysis, LTP5 was found to be closets related to LTPs originating from members of the Brassicaceae family, whereas LTP8 appeared to be closets related to LTPs from members of more diverse plant families.

The mature amino acid sequences of LTP5, LTP8 and Ace-AMP1 (AAB60896) were aligned in BioEdit for comparison purposes (Fig. 4.1). The identity of LTP5 and LTP8 were found to be 32% by use of the pairwise alignment feature (BLOSUM62 matrix). The identity of Ace-AMP1 to LTP5 was found to be 19% and the identity of Ace-AMP1 to LTP8 was found to be 17%. In spite of their low sequence identity, it is seen that the sequences share the LTP family 1 characteristic cysteine position motif and other typically conserved amino acids.

The LTP5 primary sequence contains 16 charged residues, which is more than the 11-12 charged residues usually found in the members of the LTP family 1. Of these 16 residues, 15 are arginines (positively charged) and one is aspartic acid (negatively charged). This is consistent with the high pI of 11.4 of LTP5. According to literature, Val₆, Gly₃₀, Asp₄₃, Arg₄₄, Lys₅₂, Ala₆₆, Val₇₂, Ile₈₁

and Ser₈₂ (numbering according to maize LTP [14]) are often conserved in members of LTP family 1. All of these amino acids are found in conserved positions in the LTP5 sequence, except lysine which is replaced by glutamine (position 54). This is a non-conservative change, as lysine is a positive charged amino acid while glutamine is neutral. With numbering according to the alignment in Fig. 4.1 the conserved LTP family 1 amino acids are: Val₇, Gly₃₂, Asp₄₅, Arg₄₆, Ala₆₉, Val₇₈, Ile₈₄ and Ser₈₅. Positions 35 and 44 (numbering relative to maize LTP) are of special interest, as they are found in the larger entrance of the hydrophobic cavity. As earlier stated, it is believed that charged amino acids at this position plays a role in the interaction with the lipids. In LTP5 the neutral leucine and the positively charged arginine (position 36 and 46) are found in these positions. Furthermore an aromatic residue at approximately position 79 is speculated to stabilize the binding between the LTP and the lipid molecule. In LTP5, the aromatic tyrosine is found in position 82.

As earlier stated, it is speculated that the central residue of the -C-1-C- cysteine motif may govern the cysteine pairing and influence the overall fold of the protein. In LTP5 the hydrophilic, positively charged arginine is found in this position. This supports the notion that LTP5 holds the LTP family 1 characteristic fold.

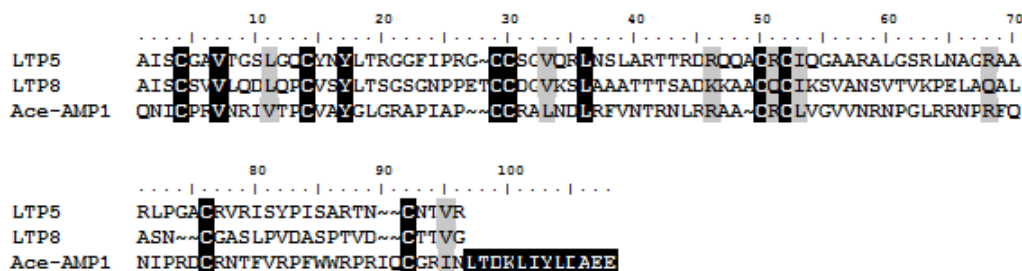


Figure 4.1: Alignment of mature amino acid sequences of LTP5, LTP8 and Ace-AMP1 (AAB60896). Gaps are included to optimize alignment and are indicated by the sign ~. The black shading highlights identical residues whereas the gray shading highlights conservatively exchanged residues. Furthermore, the 12 amino acid extension of the Ace-AMP1 sequence are highlighted with black shading. Created in BioEdit.

The LTP8 primary sequence contains 12 charged residues, which is consistent with the 11-12 charged residues usually found in the members of LTP family 1. Of these residues 5, are lysines (positively charged), 5 are aspartic acids (negatively charged), and 2 are glutamic acids (negatively charged). This is consistent with the slightly anionic pI of 4.9 of LTP8. Like LTP5, most of the LTP family 1 conserved amino acids are also found in conserved positions in LTP8. Exceptions are though arginine, valine and isoleucine (position 46, 78 and 84, respectively). Valine and isoleucine are both replaced by alanine, which are conservative changes, likewise is the change from arginine to lysine. With numbering according to the alignment in Fig. 4.1 the conserved LTP family 1 amino acids are: Val₇, Gly₃₂, Asp₄₅, Lys₅₄, Ala₆₉, and Ser₈₅. In position 35 and 44 (numbering relative to maize LTP), which are located in the larger entrance of the hydrophobic cavity, the neutral leucine is found in position 36, while the positively charged lysine is found position 46 in LTP8. No aromatic residue is found around position 79 in the sequence of LTP8.

The central residue of the -C-1-C- cysteine motif is in the LTP8 sequence a glutamine. Glutamine is polar and uncharged, which is consistent with the typical hydrophilic residue found in this position in LTP family 1. Therefore it is also believed that LTP8 holds the family 1 char-

acteristic fold.

The above described characterizations of length, size, cysteine motif, and conserved amino acids indicated that both LTP5 and LTP8 belong to the LTP family 1.

Ace-AMP1 is as earlier stated the most potent antimicrobial protein belonging to the LTP class discovered till now, but has been found to be unable to transport lipids *in vitro*. It is seen in the alignment with LTP5 and LTP8 (Fig. 4.1) that it holds the characteristic eight conserved cysteines, and that many of the other conserved amino acids also are present in its sequence. The amino acid sequence of Ace-AMP1 contains 26 charged amino acids, which is an unusually high amount for LTPs. Of these, one is lysine (positively charged), four are aspartic acids (negatively charged), two are glutamic acids (negatively charged) and 19 are arginines (positively charged). Ace-AMP1 and LTP5 share this arginine-rich primary structure, like they also share a high pI (above 11). One major difference is though that the mature Ace-AMP1 has a C-terminal extension of 12 amino acids, and a molecular weight of 12.2 kDa. Ace-AMP1 furthermore have one of the conserved positively charged amino acids (position 36 and 46) at the larger entrance of the hydrophobic cavity, and aromatic residues are found in position 80, 84, 85 and 86.

Based on these characterizations and comparisons, it was in the preliminary work speculated that LTP5 may have potent antimicrobial activity comparable to that of Ace-AMP1, and that LTP5 has a defense role in *A. thaliana*. The geometry, charge distribution and ability to form multiple hydrogen bonds make arginines ideal for binding negatively charged groups. For this reason, arginines prefer to be on the outside of proteins where it can interact with the polar environment. It was therefore speculated that the putative antimicrobial activity of LTP5 may be initiated by an electrostatic interaction between the relatively many arginines of LTP5 and the negatively charged head groups of membrane phospholipids. This may either directly lead to membrane permeabilization or that the LTP gets inserted into the membrane so the central hydrophobic cavity forms a pore, which permits outflow of intracellular ions, thus leading to cell death. In opposition to Ace-AMP1, the characteristics of the LTP5 sequence also indicate that this LTP should be capable of transporting lipids *in vitro*. Experimental studies are however vital to establish if LTP5 and Ace-AMP1 indeed have similar antimicrobial activity, how potent this activity possibly is and if LTP5 in opposition to Ace-AMP1 is capable of transporting lipids *in vitro*.

LTP8 was found interesting because of its unusual low pI of 4.9, as most type 1 LTPs have a pI of 9-10. This leaves LTP8 slightly anionic in opposition to the cationic nature of most LTPs. If the antimicrobial activity of LTPs involves an electrostatic interaction with the negatively charged head groups of phospholipids, LTP8 most likely does not have antimicrobial activity. It seems highly interesting to investigate the activities of this unusual LTP compared to e.g. Ace-AMP1 and LTP5.

4.1.2 Construction of Expression Plasmids

LTP5 and LTP8 were in the preliminary work attempted to be obtained through recombinant expressions. Due to the absolute requirement of disulfide bridges, recombinant expression of LTPs in *E. coli* has been found to be laborious, give low yields and require either a complex re-folding procedure or fusion protein strategy [9]. *P. pastoris* was therefore chosen as expression host, because heterologous expression of LTPs in *P. pastoris* has been shown to be efficient, and result in correct folding of the proteins [94], [9], [49], [95].

The previously described *E. coli/P. pastoris* shuttle vector pPICZ α A was chosen to harbor the LTP genes. This vector has an origin of replication for plasmid maintenance in *E. coli* and is designed for protein secretion in *P. pastoris*. The coding regions of the LTPs were prepared for vector insertion by use of PCRs. The LTP5 and LTP8 sequences was in PCRs amplified from RAFL06-12-D06 and RAFL17-50-B02, respectively, while the appropriate restriction sites were simultaneously introduced at the 5'- and 3'-ends of the genes. It is important that the ORF of the genes are cloned in frame and downstream of the α -factor signal sequence. As it for the purpose of the study was important to have no additional amino acids that may alter the properties of the expressed proteins, the *Xho*I site was chosen. This site allowed cloning of the genes directly downstream of the Kex2 cleavage site and leaves the expressed protein with its native N-terminus [75]. For the same reason two stop codons were introduced at the end of the sequences, so the C-terminal tag were not included in the expressed proteins. At the end of the sequences, *Xba*I was used to introduce the sequences into the vector. The primers for constructing pPICZ α -LTP5 and pPICZ α -LTP8 are given in Tab. D.1 found in the appendix. The forward primers contain a *Xho*I restriction site, the Kex2 signal cleavage site and a region for annealing with the beginning of the mature LTP5 or LTP8 sequence. The reverse primers (in 5'-3' direction) contain a *Xba*I restriction site followed by two stop codons and a region for annealing with the end of the mature LTP5 or LTP8 sequence. For each construct, an additional primer was designed that anneals approximately in the middle of each of the coding regions to be used for screening of *E. coli* and *P. pastoris* transformants.

The resulting pPIC-LTP5 construct and the pPIC-LTP8 construct are illustrated in Fig. D.1 and D.2 (found in appendix), respectively.

The constructed plasmids were transformed into *E. coli* DH5 α . Positive clones were identified by use of DNA based screenings, and DNA sequencing was conducted to confirm that correct pPIC-LTP5 and pPIC-LTP8 constructs had been obtained.

4.1.3 Transformations into *P. pastoris* X-33 and Expression Studies

The correct pPIC-LTP5 and pPIC-LTP8 constructs were propagated in their respective *E. coli* transformants, and the plasmid DNA isolated. Following, the plasmids were linearized, and introduced into *P. pastoris* X-33 cells by use of electroporation. Approximately three days after transformation, around 100 colonies appeared on each YPDSZ plate. No growth was observed on the reference YPDSZ plate. Three potential PIC-LTP5 transformants and three potential PIC-LTP8 transformants were randomly selected, and subjected to DNA based screenings.

The first PCR was performed with the primers α -factor and 3'AOX1. This PCR should yield a single DNA fragment of 507 bp for PIC-LTP5 harboring transformants and 504 bp for

LTP8 harboring transformants. The PCR of potential PIC-LTP5 transformants yielded a single DNA fragments just above 500 bp for all samples (Fig. 4.2, A, lane 2, 3 and 4). This is consistent with the expected 507 bp. The screening of potential PIC-LTP8 transformants also yielded a single DNA fragment just above 500 bp for all samples (Fig. 4.2, A, lane 5, 6 and 7), which is consistent with the expected 504 bp. On basis of these PCRs it seemed likely that all 6 colonies either harbored PIC-LTP5 or PIC-LTP8, and a second PCR were conducted.

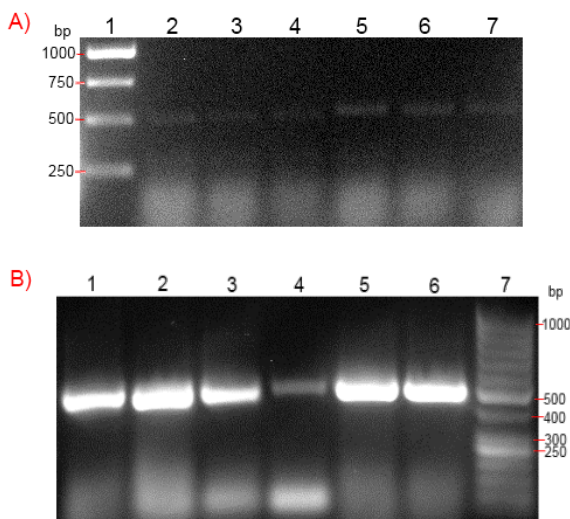


Figure 4.2: **A)** 1% agarose gel of products from PCR 1 with chromosomal DNA isolated from 6 randomly selected *P. pastoris* colonies potentially harboring PIC-LTP5 or PIC-LTP8 as template, with the primers α -factor and 3'AOX1. 1) 6 μ L 1 kb ladder (Fermentas). 2) 10 μ L DNA sample from PCR 1 on DNA isolated from potential PIC-LTP5 *P. pastoris* colony 1. 3) 10 μ L DNA sample from PCR 1 on DNA isolated from potential PIC-LTP5 *P. pastoris* colony 2. 4) 10 μ L DNA sample from PCR 1 on DNA isolated from potential PIC-LTP5 *P. pastoris* colony 3. 5) 10 μ L DNA sample from PCR 1 on DNA isolated from potential pPIC-LTP8 *P. pastoris* colony 1. 6) 10 μ L DNA sample from PCR 1 on DNA isolated from potential PIC-LTP8 *P. pastoris* colony 2. 7) 10 μ L DNA sample from PCR 1 on DNA isolated from potential pPIC-LTP8 *P. pastoris* colony 3. 8) 6 μ L 50 bp ladder (Fermentas). **B)** 1% agarose gel of products from PCR 2 on chromosomal DNA isolated from 3 *P. pastoris* colonies potentially harboring pPIC-LTP5 with the primers LTP51for and 3'AOX1 and 3 *P. pastoris* colonies potentially harboring pPIC-LTP8, with the primers LTP81for and 3'AOX1. 1) 10 μ L DNA sample from PCR 2 on DNA isolated from potential PIC-LTP5 *P. pastoris* colony 1. 2) 10 μ L DNA sample from PCR 2 on DNA isolated from potential PIC-LTP5 *P. pastoris* colony 2. 3) 10 μ L DNA sample from PCR 2 on DNA isolated from potential PIC-LTP5 *P. pastoris* colony 3. 4) 10 μ L DNA sample from PCR 2 on DNA isolated from potential pPIC-LTP8 *P. pastoris* colony 1. 5) 10 μ L DNA sample from PCR 2 on DNA isolated from potential pPIC-LTP5 *P. pastoris* colony 2. 6) 10 μ L DNA sample from PCR 2 on DNA isolated from potential PIC-LTP5 *P. pastoris* colony 3. 7) 6 μ L 50 bp ladder (Fermentas).

The second PCR was performed on chromosomal DNA from colonies potentially harboring PIC-LTP5 with the primers LTP51for and 3'AOX1, which was expected to yield a single DNA fragment with size of 469 bp. An electrophoresis gel revealed that all the PCRs yielded a single DNA fragment around 500 bp (Fig. 4.2, B, lane 1, 2 and 3), which is consistent with the expected. A second PCR was also performed on chromosomal DNA from colonies potentially harboring PIC-LTP8 with the primers LTP81for and 3'AOX1, which should yield a single DNA fragment with a size of 466 bp. All the PCRs yielded a single DNA fragment around 500 bp (Fig. 4.2, B, lane 1, 2 and 3), which was consistent with the expected.

Both PCRs on all the six randomly selected *P. pastoris* colonies yielded the expected DNA

fragment sizes, which indicates that a successful integration of the linearized constructs into the chromosomal DNA of the *P. pastoris* X-33 cells had taken place. Two of the screened colonies were chosen for expression studies.

One expression study was performed with a PIC-LTP5 *P. pastoris* X-33 transformant and one was performed with a PIC-LTP8 *P. pastoris* X-33 transformant. Expression was attempted in shake-flask cultures at 28 °C and pH 6 for 64 hours, with induction of the P_{AOX1} by addition of methanol every 24th hour. An X-33 wild type *P. pastoris* culture was treated in the same way as reference. After isolation and lyophilization of the culture supernatant, SDS-PAGEs were performed on all culture supernatants. No bands or smeared, distorted bands were seen for culture supernatants from both transformants as well as the background culture. As mentioned, LTPs have in other studies been shown to be efficiently expressed in *P. pastoris*. Because of this fact, it was believed that it is possible to efficiently produce LTP5 and LTP8 in *P. pastoris*. Furthermore, it was supported by the similar results obtained with the background *P. pastoris* X-33 culture supernatant that the SDS-PAGE distortions did not arise from the specific expression of these LTPs. It was speculated that the distortions could be due to some kind of mistake in the execution of the expression studies, either in the media mixing, during the expression or in the following handling of the culture supernatants. It was therefore concluded that the best way to proceed was to conduct new expression studies with the LTP5 and LTP8 transformants, as it was believed that correctly folded versions of the proteins were obtainable with these. Due to time limitations, new expression studies were not attempted in the previous study.

4.2 Aim of Present Study

LTPs have not yet been assigned a biological role, even though substantial evidence has been found for different theories. It seems likely that no single function can be assigned to LTPs as a group, with individual LTPs perhaps playing specific or multiple biological roles. One especially interesting theory is that of a possible defense role of LTPs. The already established antimicrobial properties of many of these proteins can perhaps be utilized in agriculture, medicine, or in the design of optimized antimicrobial proteins. The ability of antimicrobial LTPs to discriminate between cell types is furthermore highly relevant for these applications. The structure/function relationship, selectivity, and mode of action of the LTP antimicrobial activity however remain largely unknown. To reach the full potential of these proteins, it is crucial that these characteristics are elucidated.

In present study it is suspected that the LTP antimicrobial activity depends on electrostatic surface characteristics, and that electrostatic interactions are part of both their mode of action and ability to discriminate between cell types. The validity of these speculations is approached with theoretical and experimental investigations. The objects of these investigations will be different LTPs from the Brassicaceae family, and the characteristics of their putative antimicrobial activities. The study can be divided into two parts, each taking different approaches to obtaining the LTPs to be characterized.

The first part of the present study revolves around LTP5 and LTP8 from *A. thaliana*, which also was the main focus of the preliminary work. LTP5 is found interesting because of its characteristic LTP features combined with a high predicted pI of 11.4 (cationic) [60], and its se-

quence similarities with Ace-AMP1. LTP8 also have characteristic LTP features, but at the same time has an interestingly low predicted pI of 4.9 (anionic) [60]. The 3D structures of these two LTPs have not yet been solved, and it will therefore be attempted to produce reliable 3D homology models of these. Subsequent, these 3D structure models will be used for theoretical characterizations of their electrostatic potential surfaces. In addition to this, correctly folded versions of LTP5 and LTP8 will be attempted to be obtained through recombinant expressions in the yeast *P. pastoris*. If successful production is achieved, the proteins should following be purified and subjected to characterizations with special regard to antimicrobial activities. It is hoped that the combination of theoretical and experimental characterizations of these two unusual LTPs will result in clues about structure/function relationships, mode of action and specificity of the LTP antimicrobial activity.

In the second part of the study it will be attempted to develop extraction and isolation protocols for identification and purification of putative LTPs from plants of the Brassicaceae family. Following, the obtained LTP(s) should be subjected to characterizations, and screened for antimicrobial activity. An efficient extraction and isolation protocol may be applicable for large-scale screening of different plants for interesting LTPs with potent antimicrobial activity.

4.3 Experimental Strategy

The electrostatic characteristics of LTP5 and LTP8 will be investigated using computational tools. 3D models are built by use of homology modeling, with the assumption that LTP5 and LTP8 are members of the LTP family 1. Homology modeling is currently the most reliable way of constructing 3D structure models, and in principle simply requires the primary sequences and suitable template structures. As the 3D structure is highly conserved among members of the LTP family 1, it is believed that homology modeling of these two proteins applying solved 3D structures of LTP family 1 members are relatively straight forward. The automated protein homology-modeling server "SWISS-MODEL" [96], [97], [98], [99], [100] is therefore utilized for the purpose. SWISS-MODEL is the most widely used public available modeling server, and its reliability and accuracy is continuously evaluated by the Continuous Automated Model Evaluation (CAMEO) project. [98] When reliable 3D models have been obtained, their electrostatic potentials will be calculated, visualized and compared to that of the potent Ace-AMP1 and other LTPs.

Correctly folded versions of LTP5 and LTP8 will be attempted to be obtained through expression studies with the *P. pastoris* X-33 transformants constructed in the previous study. *P. pastoris* was chosen as expression host because of the absolute requirement of disulfide bridges imposed by the LTP fold. For this reason, recombinant expression of LTPs in *E. coli* has been found to be laborious, give low yields and require either a complex refolding procedure or fusion protein strategy [9]. Heterologous expression of LTPs in *P. pastoris* has however been shown to be efficient, giving a high yield and correct folding of LTPs. [94], [9] Different expression yield optimization strategies will be applied, especially with the purpose of reducing protease activity, to ensure an adequate amount of protein for subsequent experiments. Following successful expression, LTP5 and LTP8 should be purified, and subjected to characterization studies and antimicrobial activity assays.

Protocols for extraction and isolation of putative LTPs from plants of the Brassicaceae family will be developed. Tissue from the plant *Brassica oleracea* var. *capitata* (cabbage) is chosen as extraction material because this plant belongs to the Brassicaceae family, and LTPs have been isolated from different cultivars of this species. The above ground parts of cabbage consist of wrapper leaves, head, and stem [101]. In this study, focus is on the head and stem part, as these are easy and cheap to acquire from local stores. The term "leaves" therefore refer to "head leaves" throughout this study. The head grows inside-out, and leaves closest to the stem are therefore the youngest. [101] As different LTPs are often found in different plant tissues, it is speculated that the putative LTP content varies in different parts of the cabbage. Furthermore, it has often been found that LTP genes are expressed in a developmental gradient, with higher expression in younger tissue. The cabbage head is therefore divided into three groups: younger leaves (inner leaves), older leaves (outer leaves) and stem.

The selective extraction protocol will be designed based on current literature. To reduce the workload of the isolation process, it will be attempted to sort out the high amount of proteins by utilizing LTP-characteristic properties as selection criteria. Cation-exchange chromatography will be utilized for purification of putative LTPs, as one of the selection criteria are a pI above 9. Following isolation, putative LTPs should be subjected to a lipid transfer activity assay to verify that they are true LTPs, followed by characterization, identification and antimicrobial activity assays. Furthermore, the efficiency of the developed protocols should be evaluated with the purpose of optimizing the selectivity and yield.

5.1 Biological Materials and Primers

Biologicals	Description/Genotype	Manufacturer
Microbial Strains		
<i>Bacillus subtilis</i>		DSMZ 2109
<i>Escherichia coli</i> DH5 α	fhuA2delta(argF-lacZ)U169 phoA glnV44 sigma80 delta(lacZ)M15 gyrA96 recA1 relA1 endA1 thi-1 hsdR17	NEB
<i>Fusarium graminearum</i>		
<i>Micrococcus luteus</i>		ATCC 4698
<i>Pichia pastoris</i> X-33	Wild-type	Invitrogen
<i>Pichia pastoris</i> SMD1168H	<i>pep4</i>	Invitrogen
<i>Saccharomyces cerevisiae</i>		Baker's yeast
Plasmids		
Pda03097	cDNA clone name RAFL06-12-D06	RIKEN
Pda20133	cDNA clone name RAFL17-50-B02	RIKEN
pPICZ α A		Invitrogen
Lipids		
1-palmitoyl-2-12-[7-nitro-2-1,3-benzoxadiazol-4-yl)amino]dodecanoyl- <i>sn</i> -glycero-3-phosphocholine (C ₁₂ -NBD PC)	810131P	Avanti polar lipids
L- α -phosphatidyl-DL-glycerol (egg, chicken) (EPG)	841138P	Avanti polar lipids
L- α -phosphatidyl-gholine (egg yolk) (EPC)	Lot: 33H7230	Sigma
Enzymes		
DreamTaq TM DNA Polymerase	Lot: 00061554	Fermentas
<i>PmeI</i>	Lot: 0161009	NEB
<i>XbaI</i>	Lot: 0401101	NEB
<i>XhoI</i>	Lot: 0581008	NEB

Table 5.1: Biologicals used in this project.

Primers	Sequence	Manufacturer
α -factor	5'-TACTATTGCCAGCATTGCTGC-3'	Invitrogen
α -factor2	5'-ACAACAGAAGATGAAACGGCAC-3'	Invitrogen
3'AOX1	5'-GCAAATGGCATTCTGACATCC-3'	Invitrogen
LTP51for	5'-CTACTCGAGAAAAGAGCAATCTCGTGCG-3'	Tag Copenhagen
LTP52rev	5'-ACGTCTAGATCATCACCTGACGGTGTAC-3'	Tag Copenhagen
LTP53for	5'-G TTCAGAGGCTCAACACTTGG-3'	Tag Copenhagen
LTP81for	5'-TACTCGAGAAAAGAGCTATATCTTGCAGTGTG-3'	Tag Copenhagen
LTP82rev	5'-CTGCGGTCTAGATCATCAACCAACAG-3'	Tag Copenhagen
LTP83for	5'-TGCGACGGAGTTAAGAGTTTACG-3'	Tag Copenhagen

Table 5.2: Primers used in this project. In the primer sequences restriction sites are marked in bold face.

A list of chemicals used in this project is found in Appendix B.

5.2 Theoretical Characterizations

5.2.1 Homology Modeling

With the assumption that LTP5 and LTP8 are members of the LTP family 1, their 3D structures can be predicted by use of homology modeling. The 3D structures of LTP5 and LTP8 were predicted by feeding their primary sequence to the template identification tool on the automated protein homology-modeling server "SWISS-MODEL" [96], [97], [98], [99], [100]. The template suggestion resulting in the best validation scores was chosen for the model construction. The homology models are build through four main steps performed on the SWISS-MODEL server: 1) Identification of suitable template structures. BLAST is used to find homologous sequences, and if no suitable templates are found, HHsearch is used for detection of remotely related sequences. This step was not performed in the modeling, as the template structure was preselected. 2) Alignment of target sequence with the selected template structure. 3) Model building, starting from the generation of the core of the model, and moving through loop building and side chain modeling. The last step of the modeling process is an energy minimization, performed with the steepest descent energy minimization using the GROMOS96 force field. 4) Structure validation. [98] In the case of LTP5, 1fk5.pdb was used for automated homology modeling, while 1bwo.pdb was used for homology modeling of LTP8.

5.2.2 3D Model Validation

Structure validation of the two homology models were mainly performed with the structure assessment tools available on the SWISS-MODEL server, by uploading the pdb-file of the models to the server. Root mean square deviation (RMSD) between the models and their templates was calculated and visualized in YASARA by use of the MUSTANG alignment tool.

5.2.3 Electrostatic Potentials

The electrostatic potential of the LTP5 model, the LTP8 model and 1MZL.pdb was calculated by use of PyMol [102], PDB2PQR [103] and the Adaptive Poisson–Boltzmann Solver (APBS) [104]. Prior to the calculations, the 3D coordinates for the pdb-files were converted from PDB format to PQR format, which was performed by use of PDB2PQR. The generated PQR files incorporates van der Waals radii and partial charges obtained from the PARSE forcefield [105]. The non-linearized Poisson–Boltzmann equation was solved in a suitable grid. Water molecules were represented by spheres of 1.4 Å and were used to determine the protein molecular surface. Monovalent counter-ions in a concentration of 0.15 M and with a sphere radius of 2.0 Å, were used to determine the ion accessible surface. The temperature was set to 298 K and the pH to 7, and an internal protein dielectric constant of 2 and a solvent dielectric constant of 80 were used.

The strength and spatial distribution of the electrostatic potential generated by the proteins were visualized in PyMol. The electrostatic potential was mapped onto the solvent accessible surface in an interval from -5 to 5 $k_B T/e$. Spatial distributions of the electrostatic potential were displayed in the form of isopotential contours, and were plotted at $\pm 0.5 k_B T/e$.

5.3 Recombinant Expression of LTPs in *P. pastoris*

5.3.1 Screening of *P. pastoris* X-33 Transformants

Four *P. pastoris* X-33 transformants harboring PIC-LTP5 or PIC-LTP8 was thawed from -80 °C on ice, and plated on YPD plates containing 300 $\mu\text{g}/\text{mL}$ Zeocin. Chromosomal DNA was isolated from resulting colonies by the protocol described in Sec. 5.6.1. The isolated DNA was subjected to PCRs, performed according to the protocol in Sec. 5.6.2. The first PCR was performed on 1 μL of the chromosomal DNA isolate from all transformants with the primers α -factor and 3'AOX1. The second PCR was performed on 1 μL of the chromosomal DNA isolate from two PIC-LTP5 transformants with the primers LTP53for and 3'AOX1, and on 1 μL of the chromosomal DNA isolate from two PIC-LTP8 transformants with the primers LTP83for and 3'AOX1. The results were analyzed with DNA gel electrophoresis in accordance with Sec. 5.6.3.

A reference batch of *P. pastoris* X-33 cells were also plated on a YPD plate containing 300 $\mu\text{g}/\text{mL}$ zeocin to confirm the effectiveness of the compound.

5.3.2 Transformation of *P. pastoris* SMD1168H

Plasmid DNA constructs were linearized with *PmeI* under optimal conditions and introduced into *P. pastoris* SMD1168H host cells by electroporation using a MicroPulser TM (Bio-Rad). Electrocompetent cells were prepared as follows: *P. pastoris* SMD1168H cells were grown overnight in 5 mL YPD medium at 30 °C, and 250 rpm. 100 mL YPD medium was inoculated with 0.5 mL of the preculture and grown overnight at 30 °C and 250 rpm. The cells were harvested by centrifugation at 1500 g for 5 min at 4 °C, and the pellet was resuspended in 100 mL ice-cold sterile Milli-Q water. This centrifugation step was repeated and the cells were resuspended first in 50 mL ice-cold sterile Milli-Q water, next in 20 mL ice-cold 1M sorbitol and finally in 1 mL

ice-cold 1 M sorbitol.

80 μ L electrocompetent cells were mixed with approximately 10 μ g linearized pPIC-LTP5 or pPIC-LTP8, which had been heated to 60 °C and then kept on ice. The mixture was transferred to an ice-cold 0.2 cm electroporation cuvette and incubated on ice for 5 min. Then it was pulsed once at 2.0 kV for 5 ms, immediately added 1 mL 1 M ice-cold sorbitol and incubated for 1-2 hours at 30 °C. The cells were plated in volumes of 50, 100 and 200 μ L on separate YPDS plates containing 300 μ g/mL Zeocin and incubated at 30 °C until colonies emerged.

A reference batch of electrocompetent cells were treated in the same way as the above, except that no DNA was added prior to the pulsing. These cells were also spread on a YPDS plate containing 300 μ g/mL zeocin.

5.3.3 Screening of *P. pastoris* SMD1168H Transformants

One putative PIC-LTP5 *P. pastoris* SMD1168H transformant and one putative PIC-LTP8 *P. pastoris* SMD1168H transformant was plated on YPD plates containing 300 μ g/mL Zeocin. Chromosomal DNA was isolated from resulting colonies by the protocol described in Sec. 5.6.1. The isolated DNA was subjected to PCRs, performed according to the protocol in Sec. 5.6.2. The first PCR was performed on 1 μ L of the chromosomal DNA isolate from the putative PIC-LTP5 transformant with the primers LTP53for and 3'AOX1, and on 1 μ L of the chromosomal DNA isolate from the putative PIC-LTP8 transformant with the primers LTP83for and 3'AOX1. The second PCR was performed on 1 μ L of the chromosomal DNA isolate from both transformants with the primers α -factor2 and 3'AOX1. The third PCR was performed as a negative control. This PCR was performed on 1 μ L of the chromosomal DNA isolate from the putative PIC-LTP5 transformant with the primers LTP83for and 3'AOX1, and on 1 μ L of the chromosomal DNA isolate from the putative PIC-LTP8 transformant with the primers LTP53for and 3'AOX1. The results were analyzed with DNA gel electrophoresis in accordance with Sec. 5.6.3.

5.3.4 Expression studies in Shake-Flaks of *P. pastoris* Transformants

For the first expression studies (E1) of PIC-LTP5 or PIC-LTP8 *P. pastoris* X-33 transformants, 25 mL BMGY medium was inoculated with the *P. pastoris* transformants in a 250 mL wide-mouth flask and grown overnight at 28 °C and 250 rpm. The cells from these cultures were harvested by centrifugation at 1500 g for 5 min, resuspended in 100 mL BMMY medium and grown at 28 °C and 250 rpm in a 2 L baffled flask. Methanol was added to a final concentration of 0.5% every 24 hour to maintain induction. OD₆₀₀ and pH were monitored every 24th hour. An X-33 wild type *P. pastoris* reference culture was treated in the same way for determination of background expression. After 96 hours of incubation the supernatants were isolated by centrifugation at 1500 g for 5 min and shock-frozen in liquid nitrogen.

Different variations to the above procedure were used in subsequent expression studies. In the second expression study (E2), care was taken that the expression start optical density at 600 nm (OD₆₀₀) was 1 (which was continued for all subsequent expression studies). Furthermore the temperature was lowered to 23 °C, and the expression time reduced to 72 hours. In the expression study with the *P. pastoris* SMD1168H transformants, the temperature was also lowered to

23 °C but the expression time was kept at 96 hours. In the expression studies with addition of protease inhibitors conducted on all transformants, the temperature was also lowered to 23 °C and the methanol induction frequency was increased by addition of methanol to a final concentration of 0.25% every 12th hour. Furthermore, the protease inhibitors EDTA and PMSF were added every 12th hour and after ended expression to a final concentration of 1 mM and 1 mM, respectively.

Optical density was measured with a spectrophotometer at 600 nm, and a cuvette with suitable medium was used as reference. Concentration by lyophilization was performed in a Christ alpha 1-4 LSC freeze dryer.

5.3.5 Fermentation Study of PIC-LTP5 *P. pastoris* SMD1168H Transformant

Fermentation of PIC-LTP5 *P. pastoris* SMD1168H was performed with an initial volume of 1 L in a BIOSTAT Aplus bioreactor (Sartorius), and consisted of both batch and fed-batch culture procedures. 100 mL BMGY medium was inoculated with the PIC-LTP5 *P. pastoris* SMD1168H transformant in a 2 L baffled flask and grown overnight at 28 °C and 250 rpm. The cells from this culture were harvested by centrifugation at 1500 g for 5 min, and resuspended in 1 L BMGY medium (containing 2% glycerol). This inoculated BMMY medium was placed in the bioreactor. The fermentation was performed at 25 °C and pH 6, while stirring at 1093 rpm. Filter sterilized 2 M NaOH and 2 M H₃PO₄ was used for pH-adjustments. OD₆₀₀ was measured approximately every 24th hour, and antifoam was added whenever it seemed necessary. After 41 hours the induction phase was initiated. The induction phase was conducted as a methanol fed-batch procedure, with addition of 2.4 mL filter sterilized 50 % methanol pr. hour. The methanol fed-batch culture was continued for 109 hours, after which the culture supernatant were isolated, added protease inhibitors to a final concentration of 1 mM and frozen.

5.3.6 Analysis of Expression Supernatants

Isolated supernatants were subjected to SDS-PAGEs under reducing conditions and in accordance with Lammeli, as described in Sec. 5.6.6. The SDS-PAGEs were either stained with Coomassie Brilliant Blue dye in accordance with Sec. 5.6.6, or silver stained in accordance with Sec. 5.6.6.

Chromatographic analysis was either performed with Reversed-Phase High Performance Liquid Chromatography (RP-HPLC) or ion-exchange chromatography on a FPLC system.

RP-HPLC was performed on lyophilized supernatant from expression studies of the PIC-LTP5 *P. pastoris* SMD1168H transformant, the PIC-LTP8 *P. pastoris* SMD1168H transformant, and *P. pastoris* SMD1168H background, and in accordance with Sec. 5.4.4 with a few alterations: a linear gradient of 2-60% acetonitrile in acidified water was applied over a period of 35 min, followed by a 5 min period in isocratic mode at 80% acetonitrile. The flow rate of all scans were 3.5 mL/min.

Cation-exchange chromatography on culture supernatant was in general performed in

accordance with Sec. 5.4.3. Elution was performed with a buffer containing 10 mM Tris-HCl and 10 mM NaCl (pH 4) (buffer A), and retained material was eluted with 1 M NaCl (buffer B) in the same buffer (4 mL/min).

5.4 Isolation of putative LTPs from Cabbage

5.4.1 Wax Protein Extraction

Approximately 400 g of intact leaves from *Brassica oleracea* var. *capitata* were dipped for ~10 s in 500 mL of a 2/1 (v/v) mixture of chloroform and methanol. Following, the chloroform/methanol mixture was completely evaporated in a water bath at 55 °C under reduced pressure in a rotary evaporator. The remaining residue was dissolved in 60 mL chloroform, transferred to a separatory funnel, shaken with 30 mL dH₂O, and the aqueous phase separated from the organic phase after 1 hour. [32] The aqueous phase was dialyzed in accordance with Sec. 5.6.5, and concentrated by lyophilization.

The extraction was attempted with a mixture of old and young leaves, and with exclusively young leaves.

5.4.2 Protein Extraction from Plant Tissue

A flowchart of the following method is presented in Fig. 6.25. The cabbage head was divided into three groups: stem (S), young leaves (YL), and older leaves (OL). Material from each group was frozen in liquid nitrogen, sliced and grounded to powder using a mortar and pestle. The powder was added ice-cold acetone in a 1:5 (wt/vol) relation, and left for 1 hour at 4 °C. Following, centrifugation at 11000 g for 10 min was performed, and the supernatant was discarded. The acetone defatting step was then repeated, followed by drying of the pellet for approximately 40 min. It should be noted that the pellet should not be allowed to over dry, as it then will be hard to dissolve. Extraction was performed by addition of 0.5 M NaCl in a 1:5 (wt/vol) relation, and the solution was left for 1 hour at 4 °C. Following, centrifugation at 9000 g for 30 min was performed, and the supernatant was saved. The extraction protocol was then repeated with the pellet, after which the extraction supernatants were pooled, while the pellet was discarded. To get rid of clumps, the extraction solution was filtrated. The filtrated extraction solution was concentrated by 0-90% ammonium sulfate precipitation. The solution was left for 1 hour at 4 °C while stirred, followed by centrifugation at 10.000 g for 30 min. The supernatant was discarded, and the pellet redissolved in a suitable amount of 0.2 M NaCl (resulting in F0-90). The F0-90 solution was then subjected to a 80 °C water bath for 15 min followed by centrifugation at 8000 rpm for 10 min. The supernatant was saved, and filtrated to get rid of precipitated proteins. Prior to further fractionation, the obtained heat-resistant fraction was dialyzed and lyophilized.

The above method are mainly build on two studies by Palacin et al. [50] and [106], and a study by Terras et al. [61]

5.4.3 Ion-exchange Chromatography

Cation-exchange chromatography was conducted on a ÄKTA purifier FPLC system (Amersham Biosciences) with a Source 15S PE 4.6/100 column (Amersham Biosciences). The FPLC system consists of a program controller, four P-900 pumps (two each for buffers A and B), a M-925 mixer, a prefilter, a seven-port M-7 valve, a 1 mL loading loop, a pH/c-900 monitor (containing a flow cell for conductivity measurement), a UV-900 UV monitor, a flow restrictor, and a Frac-900 fraction collector. Elution was performed with a buffer containing 10 mM Tris-HCl and 10 mM NaCl (pH 4) (buffer A), and retained material was eluted with 1 M NaCl in the same buffer (buffer B). A flow rate of 4 mL/min was used in all runs. A linear gradient ranging from 0-80% buffer B over a period of 25 min was applied, followed by isocratic mode at 100% buffer B over 5 min. A focused gradient were applied for chromatography on FS, with a linear gradient from 0-20% buffer B over 1.5 min, a shallower linear gradient from 20-60% buffer B over 17 min, and a steep linear gradient from 60-100% buffer B for 2 min. Column effluent was monitored by UV absorbance at 214 nm and 280 nm, and the corresponding peak fractions were collected.

The collected peak fractions were dialyzed, lyophilized, and subjected to SDS-PAGEs under reducing conditions and in accordance with Lammeli, as described in Sec. 5.6.6. Fractions containing proteins with a size around 10 kDa was selected, and subjected to further fractionation.

5.4.4 RP-HPLC

Fractionation by differences in hydrophobicity was performed on a HPLC system from Dionex composed of an Ultimate 3000 pump system, an Ultimate 3000 Diode array detector, and a Manual Injection Valve from IDEX Health and Science. Column effluent was monitored by UV absorbance at 214 nm and 280 nm, and the corresponding peak fractions were collected by an automated Ultimate 3000 Fraction Collector. The RP-HPLC was performed on a semi-preparative Gemini-NX C18 reverse-phase column (250 mm x 10.00 mm, 110 Å pore size, 5 µm particle size, Phenomenex) equilibrated with 1% isopropanol or 2% acetonitrile and acidic water (0.1% TFA). The separation was performed with either a linear gradient of isopropanol in acidified water ranging from 1 to 55 % at a flow rate of 1.25 mL/min, or a linear gradient of acetonitrile in acidified water ranging from 2 to 60 % at a flow rate of 4 mL/min. Two isopropanol gradient profiles were used. The first was performed with a linear gradient from 1-55 % over a period of 40 min. The second profile consisted of a steep gradient from 1-16% isopropanol over 15 min, a shallower gradient from 16-40% over 40 min, a steep gradient from 40-55% over 15 min, and isocratic mode at 55% over 10 min. The acetonitrile gradient from 2-60% was performed over a period of 40 min.

The collected peak fractions were lyophilized, and subjected to SDS-PAGEs under reducing conditions and in accordance with Lammeli, as described in Sec. 5.6.6. Fractions containing proteins with a size around 10 kDa was selected, and subjected to further analysis.

5.5 Assays

5.5.1 Bradford Protein Assay

Dye reagent was prepared by diluting one part Dye Reagent Concentrate (Biorad) with four parts demineralized water. The solution was filtered to remove particulates. Five dilutions (1 $\mu\text{g}/\text{mL}$ to 10 $\mu\text{g}/\text{mL}$) of the protein standard (BSA) was prepared in 0.15 M NaCl for the creation of a standard curve. 800 μL of each standard was placed in a test tube, 200 μL of diluted dye reagent was added, and the solution was vortexed. The solutions were then incubated for precisely 10 min. in the dark, followed by OD₅₉₅ measurements. All the standards were performed in triplicates, and linear regression was performed to find the relationship between the OD₅₉₅ measurements and protein concentration.

The sample to be assayed were treated in the same way. Dilutions were performed until the OD₅₉₅ measurement of the sample fitted into the linear range of the standard curve. Subsequent, the concentration was calculated using the equation for the standard linear regression line.

5.5.2 Lipid Transfer Activity Assay

Lipid transfer activity assays was essentially performed in accordance with a study by Hinch et al. [29] and a study by Bourgis et al. [107]. Donor vesicles were composed of 50 mol% C₁₂-NBD PC (Avanti polar lipids), 40 mol% egg phosphatidylcholine (EPC), and 10 mol% egg phosphatidylglycerol (EPG) (total weight of 1 mg pr. batch). Acceptor vesicles consisted of 90 mol% EPC and 10 mol% EPG (total weight of 9 mg pr. batch). Each of the lipid mixtures were dissolved in 2 mL chloroform, and thoroughly mixed on a rotary evaporator at 60 °C (temperature above phase transition temperature for all the used lipids) for at least 30 min. Following, vacuum were applied to the rotary evaporator until the solution had completely dried. The lipid film was stored under vacuum overnight to remove traces of solvent completely.

The lipid films were hydrated each with 1 mL 10 mM HEPES buffer (pH 7.3) on a rotary evaporator at 60 °C for at least 1 hour. Unilaminar vesicles were obtained by extrusion, performed with an Avanti Mini-Extruder with heating block (Avanti Polar lipids) through a Whatman filter with a pore size of 100 nm (minimum of 10 passings), and at a temperature of 60 °C. Donor vesicles were applied to a Econo-Pac 10DG desalting column (BioRad), which are packed with a matrix that excludes solutes greater than 6 kDa, allowing them to elute in the void volume. Seven individual fractions were eluted with 10 mM HEPES buffer (pH 7.3), and subjected to fluorescence spectroscopy on a PTI spectrofluorometer in a 10 mm Hellma Precision cell made of Quartz SUPRASIL. Fluorescence was excited at 475 nm and measured at 530 nm by two channels, at a constant temperature of 25 °C. Background fluorescence was monitored, and 100 μL 10% SDS was added to measure fluorescence when all fluorophores were de-quenched. A donor vesicle fraction showing low background fluorescence, but high fluorescence increase upon addition of SDS, was chosen for the following assay.

The lipid transfer activity assay were performed with 2 mL 10 mM HEPES buffer (pH 7.3), 20 μL acceptor vesicles and 30 μL diluted donor vesicles, which was estimated to ensure over representation of acceptor vesicles. The fluorescence measurement was allowed to run for some

time before addition of pLTP fractions, and total measurement time varied between 600-900 s. Addition of tested fractions was performed by applying an approximate 10-15 s pause of the measurements. Between 15-50 μL solutions of varying pLTP concentration was added.

5.5.3 Antimicrobial Activity Assays

Radial diffusion assays (RDAs) were performed on 0.8% agarose plates with four different microbes: *Micrococcus luteus*, *Bacillus subtilis*, and *S. cerevisiae*. The bacteria were thawed on ice from $-80\text{ }^{\circ}\text{C}$ and transferred to suitable agar plates (suitable media found in Tab. 5.3). Precultures with 25 mL of suitable media were inoculated with the bacteria or *S. cerevisiae*, and incubated overnight at suitable temperatures (Tab. 5.3). To make the agarose plates, 13 g/L agarose was added to 20 mL suitable media pr. plate, and the mixtures were heated until the agarose was completely dissolved. After cooling, 200-300 μL of either *M. luteus* or *B. subtilis* preculture was added to the agarose media and a plate was poured. For the yeast *S. cerevisiae*, 1.8 mL of the preculture was used. After the plate had solidified, a pipette tip was used for making wells in the gel. The test samples were placed in the wells, and the plates were incubated at suitable temperatures until colonies emerged.

Microorganism	Applied growth temperature	Medium
<i>M. luteus</i>	30 $^{\circ}\text{C}$	LB
<i>B. subtilis</i>	37 $^{\circ}\text{C}$	Peptone
<i>S. cerevisiae</i>	30 $^{\circ}\text{C}$	YPD
<i>F. graminearum</i>	25 $^{\circ}\text{C}$	PDA

Table 5.3: Overview of the microbes, media and temperatures used for antimicrobial activity assays. Media recipes are found in Sec. 5.6.7 and Sec. 5.6.4.

Because of the hyphal growth of *Fusarium graminearum*, a different approach was required for the antifungal assays with this phytopathogen. In these assays, the liquid sample was placed on top of a Whatman no. 1 filter paper, while 3 μL spores were placed in the center of the plate, resulting in radial extension of hyphae after germination. The assays were conducted on PDA-plates, and incubated for up to five days at 25 $^{\circ}\text{C}$. Assays with placement of samples adjacent to non-germinated and germinating spores were performed.

5.6 Protocols and Recipes

5.6.1 Extraction of Genomic DNA from Yeast

Extraction of genomic DNA from *P. pastoris* transformants were performed in accordance with the procedure developed by Løoke et al. [108]. A *P. pastoris* colony was picked and suspended in 100 μL of 200 mM LiOAc, 1 % SDS solution. The mixture was incubated at 70 $^{\circ}\text{C}$ for 5 minutes. Following, 300 μL of 96 % ethanol was added, and the solution was vortexed. The solution

was centrifuged for 3 minutes at 15000 g, and the supernatant discarded. Then, the pellet was washed with 70 % ethanol. The resulting pellet was dissolved in 100 μL DNA water, and subjected to centrifugation for 15 seconds at 15000 g. 1 μL of the supernatant was used for PCR analysis.

5.6.2 Polymerase Chain Reactions

PCRs were performed in a total volume of 100 μL with 200 μM dNTPs, 10x Dream Taq buffer (including 2 mM MgCl_2), 1 μM of each primer, 0.5 μL Dream Taq polymerase and approximately 10-20 ng template DNA. The PCR program was set up as stated in Tab. 5.4 with an annealing temperature in accordance with Tab. 5.5.

PCR	Time	Temperature	Cycles
Initial denaturation	2 min	94 °C	
Denaturation	30 sec	94 °C	x35
Annealing	30 sec	X °C	
Extension	1 min	72 °C	
Additional extension	10 min	72 °C	
Product storage		4 °C	

Table 5.4: General PCR program used for the PCRs in this project. The annealing temperature for each PCR (X) can be found in Tab. 5.5.

Primer	α -factor	LTP51for	LTP53for	LTP81for	LTP83for
3'AOX1	55 °C	56 °C	56 °C	56 °C	55 °C
LTP52rev	56 °C	63 °C	59 °C	-	-
LTP82rev	56 °C	-	-	62 °C	58 °C

Table 5.5: Annealing temperatures (X in Tab. 5.4) used with the different primer pairs in PCRs.

5.6.3 DNA Gel Electrophoresis

10 g/L agarose was added to 1xTAE buffer and the solution was heated until it was completely clear. 30 mL of this agarose gel solution was mixed with approximately 0.5 μL EtBr. The DNA sample was mixed with 6x loading dye (Fermentas) in a 5:1 ratio, and loaded into the slots along with 1 kb or 50 bp DNA ladder (Fermentas). Analytic electrophoresis was performed at 70 V (DC) for 70 minutes. Afterwards the gel was analyzed by illumination with high intensity UV-light.

5.6.4 *P. pastoris* Media and Agar plates

Following are recipes for media and agar plates used in connection with expression of recombinant proteins in *P. pastoris* in this project. Tab. 5.6 gives an overview of their different use.

Medium	Description	Application
YPD (+ agar)	Rich, complex broth	General growth and storage
YPDS + Zeocin	YPD with sorbitol and Zeocin	Selection of <i>P. pastoris</i> Zeo ^R transformants
BMGY	Buffered complex medium containing glycerol	Used to control the pH of the medium, decrease protease activity and generate biomass when using secreted expression
BMMY	Buffered complex medium containing methanol	Used to control the pH of the medium, decrease protease activity and induce expression when using secreted expression

Table 5.6: Overview of the *P. pastoris* media used in this project. [75]

Yeast Extract Peptone Dextrose (YPD) Medium and Agar Plates

20 g/L peptone and 10 g/L yeast extract were added to deionized water and sterilized by autoclavation. Afterwards, when the solution had cooled to 60 °C, 20 g/L separately autoclaved dextrose was added to the solution and if required, zeocin was added to a final concentration of 25 µg/L. Agar plates were made by adding 20 g/L of agar to the solution before autoclavation. [75]

Yeast Extract Peptone Dextrose Sorbitol (YPDS) Agar Plates

20 g/L peptone, 182,2 g/L sorbitol, 10 g/L yeast extract and 20 g/L agar were added to deionized water and sterilized by autoclavation. Afterwards, when the solution had cooled to 60 °C, 20 g/L separately autoclaved dextrose was added to the solution and if required, zeocin was added to a final concentration of 300 µg/L. [75]

Buffered Glycerol-complex Medium (BMGY) and Buffered Methanol-complex Medium (BMMY)

The recipe with the final concentrations:

1% yeast extract

2% peptone

100 mM potassium phosphate, pH 6.0

1.34% YNB

$4 \cdot 10^{-5}$ % biotin

1% glycerol or 0.5% methanol

10 g yeast extract and 20 g peptone were dissolved in 700 mL Milli-Q water and autoclaved. When cooled down, 100 mL 1 M potassium phosphate buffer (pH 6.0), 100 mL 13.4% YNB and 2 mL 0.02% biotin were added. For BMGY, 100 mL 10% glycerol was further added and for BMMY, 100 mL 5% methanol was added instead. The mixture was mixed completely. All the solutions were sterilized before they were added to the mixture, either by autoclavation or filtration (biotin). [75]

5.6.5 Dialysis

Different protein solutions were dialyzed against dH₂O in a 1:100 (v/v) relation while stirring at 4 °C in a Spectra/Por 7 dialysis membrane (Spectrum) with a MWCO of 1.000 or 3.500. Three changes of dH₂O with a minimum of 4 hours separation were performed before the dialysis was ended.

Following dialysis, samples were concentration by lyophilization in a Christ alpha 1-4 LSC freeze dryer.

5.6.6 SDS-PAGEs

SDS-PAGEs were performed with either a BioRad Tris/Glycine/SDS or a BioRad Tris/Tricine/SDS buffer system. A PageRuler Unstained protein ladder or PageRuler Low Range Unstained protein ladder (Fermentas) was used for molecular weight estimations.

Tris/Glycine/SDS buffer system

10%, 12% or 15% (w/v) acrylamide separation gels with a 4% (w/v) acrylamide stacking gel was casted, used with a BioRad Tris/Glycine/SDS buffer system, and performed according to Lammeli [109]. Samples were mixed in a 1:1 relation with Sample Buffer containing 2-mercaptoethanol (Laemmli 2×Concentrate (Sigma-Aldrich)) and heated for 3 minutes at 95 °C to obtain reducing conditions. Samples were stored at -20 °C until loading. The SDS gel electrophoresis was performed at 130 V for approximately 90 minutes.

Tris/Tricine/SDS buffer system

Tris-Tricine precast gels (Bio-Rad) with 10-20% (w/v) acrylamide gradient or 16.5% (w/v) acrylamide separation gels was used with a BioRad Tris/Glycine/SDS buffer system, and performed according to Lammeli [109]. Samples were mixed in a 1:1 relation with Sample Buffer containing 2-mercaptoethanol (Laemmli 2×Concentrate (Sigma-Aldrich)) and heated for 3 minutes at 95 °C to obtain reducing conditions. Samples were stored at -20 °C until loading. The SDS gel electrophoresis was conducted at 200 V for 30 min. (in accordance with instructions

provided by the manufacturer).

Coomassie Brilliant Blue Stain and Destain

One tablet of PhastGel Blue R (Coomassie brilliant blue R-350) was dissolved in 80 mL distilled water and stirred for 5 to 10 min. Following, 120 mL ethanol was added and the solution was stirred until the dye was completely dissolved. The solution was then filtrated. This stock solution (0.2%) is stable for one to three weeks at 4 °C. For the final 0.1% solution, filtrated stock solution was mixed with 20% acetic acid in distilled water, in a 1:1 ratio.

The destain solution was made by mixing 100 mL acetic acid, 300 mL ethanol and 1 L distilled water. SDS-PAGEs were stained for at least one hour using Coomassie brilliant blue R-350 based Page-blue protein staining solution, and then destained overnight while shaking.

Silver Staining

The following steps were performed in a glass tray under rigorous shaking. The SDS-PAGE was soaked in 7% acetic acid for 7 min., followed by two times 20 min. soaking in 50% ethanol. The SDS-PAGE was then rinsed with demineralized water for two times 10 min. Meanwhile, the staining solution was prepared: 250 μ L 30% NaOH and 1.4 mL 14.8 M ammonium hydroxide was added to 21 mL demineralized water. 0.8 g silver nitrate dissolved in 4 mL demineralized water was added to the above solution dropwise while stirring, followed by addition of 76 mL demineralized water. The gel was soaked in the staining solution for 25 min. while kept in the dark. After staining, the gel was rinsed in demineralized water for two times 5 min. Finally, the SDS-PAGE was soaked in developing solution (200 mL demineralized water, 1 mL 1% citric acid, 100 μ L 37% formaldehyde) until sufficient contrast was obtained. Development was stopped by rinsing three times with demineralized water.

5.6.7 Other Media and Agar plates

Low Salt Luria-Bertani (LB) medium was made by adding 10 g/L tryptone, 5 g/L yeast extract and 5 g/L sodium chloride to deionized water, and sterilizing the solution by autoclavation. LB-agar plates were prepared by further addition of 15 g/L agar to the above described medium before autoclavation.

Peptone medium as made by adding 5 g/L peptone and 5 g/L yeast extract to deionized water, and sterilizing the solution by autoclavation. Peptone-agar plates were prepared by further addition of 15 g/L agar to the above described medium before autoclavation.

Potato-dextrose-agar (PDA) plates were made by adding 200 g/L potato extract and 15 g/L agar to deionized water, and sterilizing the solution by autoclavation. Afterwards, when the solution had cooled to 60 °C, 10 g/L separately autoclaved dextrose was added to the solution.

6.1 Theoretical Characterizations

6.1.1 Homology Modeling

The 3D structures of LTP5 and LTP8 were predicted by use of the automated protein homology-modeling server "SWISS-MODEL" [96], [97], [98], [99], [100].

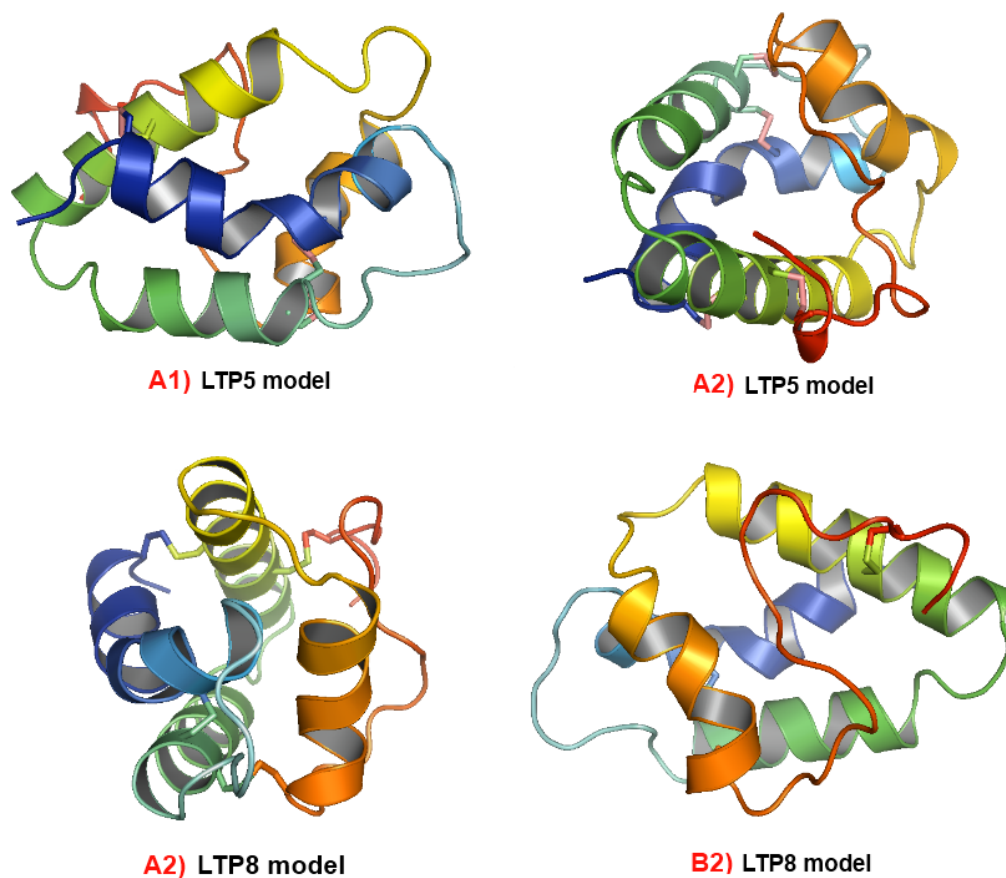


Figure 6.1: 3D structure of homology models visualized in PyMol. **A1 and A2)** The LTP5-1fk5 model. **B1 and B2)** The LTP8-1bwo model.

For homology modeling of LTP5, 1fk5.pdb (resolution of 1.30 Å) was estimated as the best template by SWISS-MODEL. This structure of a maize LTP (UniProtKB P19656) was solved by X-ray crystallography in 2001 by Han et al. [110], is 93 amino acids long in its mature form and shares 49% sequence identity with LTP5. Automated homology modeling was also tested with the two next best template suggestions, but they showed poorer validation scores (data not shown). Modeling in automated mode by SWISS-MODEL resulted in the LTP5-1fk5 model (Fig. 6.1, A1 and A2), which from this point on is referred to as the LTP5 model.

A secondary structure summary by PROMOTIF [111] reveals that the LTP5 model is com-

posed of no strands, one C-terminal 3_{10} -helix, and that 53% of its amino acids are found in α -helices. Helix H_1 runs from Cys₄ to Leu₁₈, with three amino acids (Gly₁₂, Gln₁₃, and Cys₁₄) being in a conserved 3_{10} -helix conformation. These three amino acids make up a pronounced kink of the helix, which is found in all H_1 's of LTPs solved so far. H_2 runs from Cys₂₃-Leu₂₈, H_3 runs from Thr₄₂-Arg₅₇, and H_4 runs from Ala₆₅-Ala₇₄. A slight curvature of H_4 is observed, which is also a common LTP type 1 structure element. The above observations are consistent with the known secondary structure positions in type 1 LTPs. The LTP5 model contains four disulphide bridges: Cys₄ pares with Cys₅₁, Cys₄₉ pares with Cys₈₉, Cys₁₄ pares with Cys₂₈, and Cys₂₉ pares with Cys₇₅. This disulfide bonding pattern is also consistent with that of LTP family 1 (Fig. 2.1).

A cavity runs through the axis of the LTP5 model, which is delineated with hydrophobic amino acids found in conserved positions (numbering relative to Fig. 6.2): Val₇, Leu₁₁, Leu₁₈, Val₃₃, Leu₃₅, Ala₄₀, Ala₄₉, Ile₅₃, Ala₅₆, Ala₅₇, Leu₆₀, Leu₆₄, Ala₆₉, Leu₇₂, Val₇₈, Ile₈₀, and Ile₈₄. A conserved tyrosine (position 82) is found at the larger entrance of the LTP5 model, and all charged amino acids are located at the surface of the 3D structure.

```

          10          20          30          40          50
LTP5  .....|.....| .....|.....| .....|.....| .....|.....| .....|.....|
1fk5  AISCQAVTGS LGQCYNLTR GGFIPR~GCC SGVQRLNSLA RTTRDRQQAC
          60          70          80          90
RCIQGAARAL GSRLNAGRAA RLPGACRVRI SYPISARTNC NTVR
NCLKNAAAGV S~GLNAGNAA SIPSKCGVSI PYTISTSTDC SRVN

          10          20          30          40          50
LTP8  .....|.....| .....|.....| .....|.....| .....|.....| .....|.....|
1bwo  ~IDCGHVDSL VRPCLSYVQG G~PGPSGQCC DGVKSLAAAT TTSADKKAAC
          60          70          80          90
QCICKSVANSV T~VKPELAQA LASNCGASLP VDasPTVDCT TVG
NCLKGIARGI HNLNEDNARS IPPKCGVNLP YTISLNIDCS RV

```

Figure 6.2: Alignment of LTP5 and LTP8 with their modeling templates, created by SWISS-MODEL and visualized in BioEdit.

For homology modeling of LTP8, 1fk5.pdb was also suggested as the best template. However, after automated modeling was performed with the two next best template suggestions (not all data shown), it was found that the best validation scores were obtained with 1bwo.pdb as template. This structure of a wheat LTP (UniProtKB P24296) was solved by X-ray crystallography in 1999 by Charvolin et al. [27], is 90 amino acids long in its mature form, and share 34% sequence identity with LTP8. Modeling in automated mode with this template by SWISS-MODEL resulted in the LTP8-1bwo model (Fig. 6.1, B1 and B2), which from this point on is referred to as the LTP8 model. Following optimal alignment of LTP8 and the template, an additional amino acid was present at the beginning and end of the LTP8 primary sequence (Ala₁ and Gly₉₂). These amino acids are therefore not included in the LTP8 3D model.

A secondary structure summary by PROMOTIF [111] reveals that the LTP8 model is composed of no strands, one C-terminal 3_{10} -helix, and that 57% of its amino acids are found in α -helices. Helix H_1 runs from Cys₄ to Leu₁₈, with three amino acids (Glu₁₂, Pro₁₃, and Cys₁₄) being in the conserved 3_{10} -helix conformation. Like in the LTP5 model, these three amino acids also compose a pronounced kink of the helix. H_2 runs from Glu₂₇-Ala₃₉, H_3 runs from Ser₄₃-

Ala₅₇, and H₄ runs from Pro₆₄-Cys₇₄. A slight curvature of H₄ is also observed in this model. These characteristics are consistent with the known secondary structure positions of type 1 LTPs. The LTP8 model contains four disulphide bridges: Cys₄ pares with Cys₅₂, Cys₅₀ pares with Cys₈₈, Cys₁₄ pares with Cys₂₉, and Cys₃₀ pares with Cys₇₄. This disulfide bonding pattern is also consistent with that of LTP family 1 (Fig. 2.1).

A cavity runs through the axis of the LTP8 model, which is delineated with hydrophobic amino acids found in conserved positions (numbering relative to Fig. 6.2): Val₇, Leu₁₁, Leu₁₈, Val₃₃, Leu₃₆, Ala₃₇, Ala₄₉, Ile₅₃, Val₅₆, Ala₅₇, Val₆₀, Ala₆₇, Leu₇₁, Leu₇₉, Val₈₁, and Ala₈₃. All charged amino acids are located at the surface of the 3D structure.

Both 3D structure models display characteristic LTP type 1 features, such as an all- α -type structure, a long C-terminal tail, a hydrophobic cavity in their core and the expected disulfide bonding pattern.

6.1.2 Structure Validation

Root mean square deviation (RMSD) between the optimal superimposition of the models and their templates was calculated in YASARA by use of the MUSTANG alignment tool [112]. The alignment of the LTP5 model and ifk5.pdb revealed that they have a backbone ($C\alpha$) RMSD of 0.648 Å. A RMSD of less than 0.75 Å is considered good [113]. By visualizing the optimal superimposition of the LTP5 model and 1fk5.pdb (Fig. 6.3) structural deviations become apparent. For the LTP5 model, deviations are especially observed in the loop connecting H₃ and H₄ (Leu₆₀-Asp₆₅).

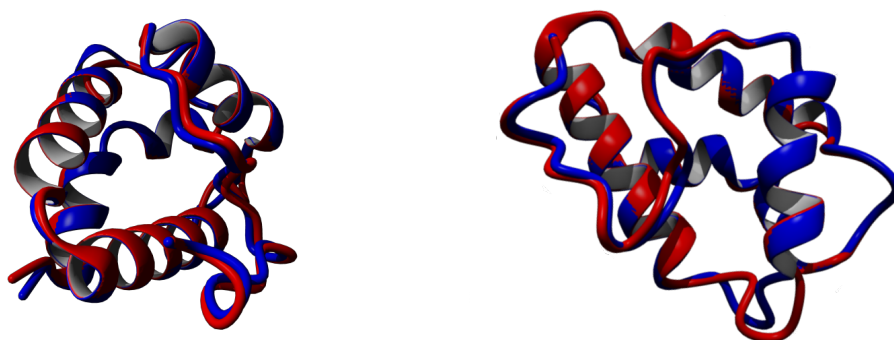


Figure 6.3: Optimal superimposition of the LTP5 model (red) and its template 1fk5.pdb (blue) as calculated by MUSTANG alignment in YASARA.

The alignment of the LTP8 model and 1bwo.pdb revealed that they have a backbone ($C\alpha$) RMSD of 0.413 Å, which is considered a good score. By visualizing the optimal superimposition of the LTP8 model and 1bwo.pdb (Fig. 6.4) deviations become apparent in the loop connecting H₁ and H₂ (Ser₂₀-Pro₂₆), and H₃ and H₄ (Val₆₀-Lys₆₄). In general, better agreements between the secondary structure elements than between the intermediate loops and C-terminal regions are observed for both 3D models.

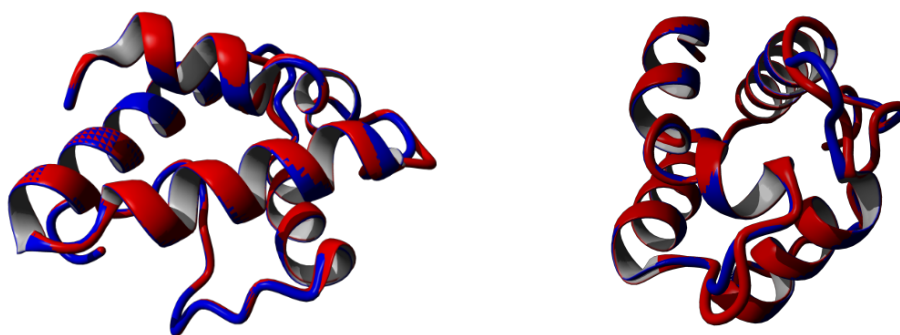


Figure 6.4: Optimal superimposition of the LTP8 model (red) and its template 1bwo.pdb (blue) as calculated by MUSTANG alignment in YASARA.

QMEAN scoring [114] is an absolute measure for the quality of protein models, which is independent of the size of the protein. The QMEAN scoring function provides an estimate of the degree of nativeness of the structural features observed in a model and describes the likelihood that a given model is of comparable quality to experimental structures. Model quality scores for individual models are expressed as Z-scores, and the absolute quality is estimated by relating the model's structural features to experimental structures of similar size. The Z-scores of the individual terms of the scoring function indicate which structural features of a model exhibit significant deviation from the expected native behavior. Higher Z-scores represents favorable states, that is, higher QMEAN Z-scores means better agreement with predicted features and lower mean force potential energy. [114]

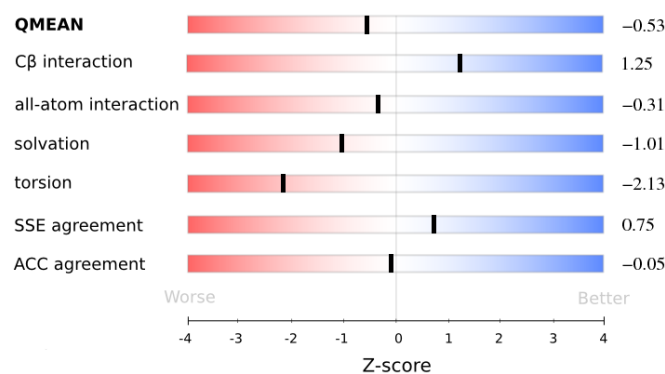


Figure 6.5: QMEAN6 plot for the LTP5 model. The Z-scores of the LTP5 model is estimated from pseudo-energies of the contributing terms with respect to scores obtained for high-resolution experimental structures of similar size. SSE is secondary structure agreement, and ACC is solvent accessibility agreement. A score of zero is average, negative scores are "worse" than average, and positive scores are "better" than average. Created by SWISS-MODEL.

The global QMEAN6 score consists of a linear combination of 6 terms, and reflects the predicted model reliability from 0-1. The six structural descriptors used in QMEAN6 can shortly be described as following. Long-range interactions are assessed by two distance-dependent interaction potentials of mean force based on C- α atoms and on all atom types (both are secondary structure dependent). Local backbone geometry of the structure is analyzed by applying a torsion angle potential over three consecutive amino acids. A solvation potential is applied to describe the burial status of the residues. Finally, two agreement terms take the agreement of

predicted and calculated secondary structure and solvent accessibility into account. [114] The QMEAN6 score of the LTP5 model was found to be 0.684. The QMEAN Z-score is a measure for the absolute quality of the model, and the average QMEAN Z-scores of high-resolution structures are 0. [114] The QMEAN Z-score of the LTP5 model was found to be -0.528, which is in the acceptable range. Assessment of the individual Z-scores for the LTP5 model (Fig. 6.5) reveals that especially the local backbone geometry has a low Z-score, while the score representing the burial status of the residues are also below average.

The QMEAN6 score of the LTP8 model is 0.612. The QMEAN Z-score of LTP8 model was found to be -1.10, which is in the lower end of acceptable. The individual Z-scores for the LTP8 model (Fig. 6.6) shows that especially the local backbone geometry has a low Z-score, but also the solvent accessibility agreement term scores relatively low.

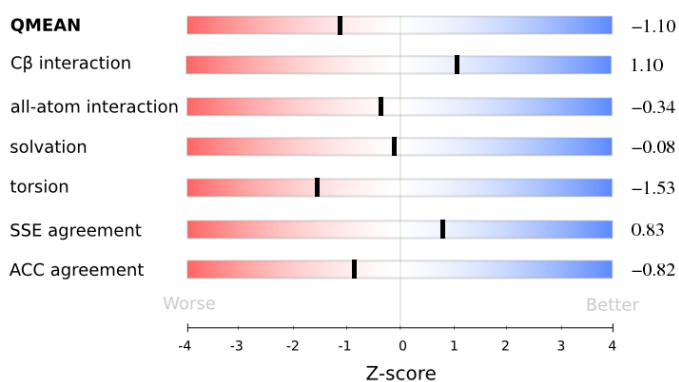


Figure 6.6: QMEAN6 plot for the LTP8 model. The Z-scores of the LTP8 model is estimated from pseudo-energies of the contributing terms with respect to scores obtained for high-resolution experimental structures of similar size. SSE is secondary structure agreement, and ACC is solvent accessibility agreement. A score of zero is average, negative scores are "worse" than average, and positive scores are "better" than average. Created by SWISS-MODEL.

PROCHECK [115] was used to determine the stereochemical quality of the models. This program assess how normal the geometry of the residues in a given protein structure is compared with stereochemical parameters derived from high-resolution structures. It has been found that as a protein structure is refined, the phi-psi angles migrate into allowed conformations, and therefore the distribution of phi-psi angles can provide a guide to the quality of the structure. [116] The PROCHECK Ramachandran plot of the LTP5 model (Fig. 6.7) showed that 90% of its residues are in most favored regions, 8% are in the additionally allowed regions, 3% (two residues) are in the generously allowed regions, while none are in the disallowed regions. Based on an analysis of 118 structures of resolution of at least 2.0 Å and R-factor no greater than 20%, a good quality model would be expected to have at least 90% of its residues in the most favored regions [115]. Thus, the LTP5 model result can be considered to be in the lower end of a good quality model score.

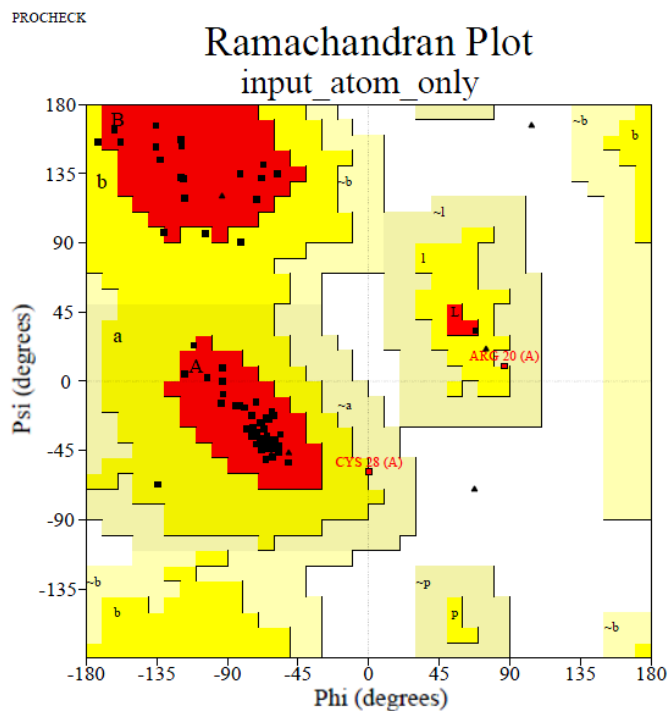


Figure 6.7: Ramachandran plot of the LTP5 model. Red areas [A, B, L] are the most favored regions (representing most favorable psi-phi combination), yellow areas [a, b, l, p] are additional allowed regions, pale orange areas [$\sim a$, $\sim b$, $\sim l$, $\sim p$] are generously allowed regions and white areas are the disallowed regions. Residues in generously allowed regions are labeled in red. Glycine residues are separately identified by triangles. Constructed by PROCHECK.

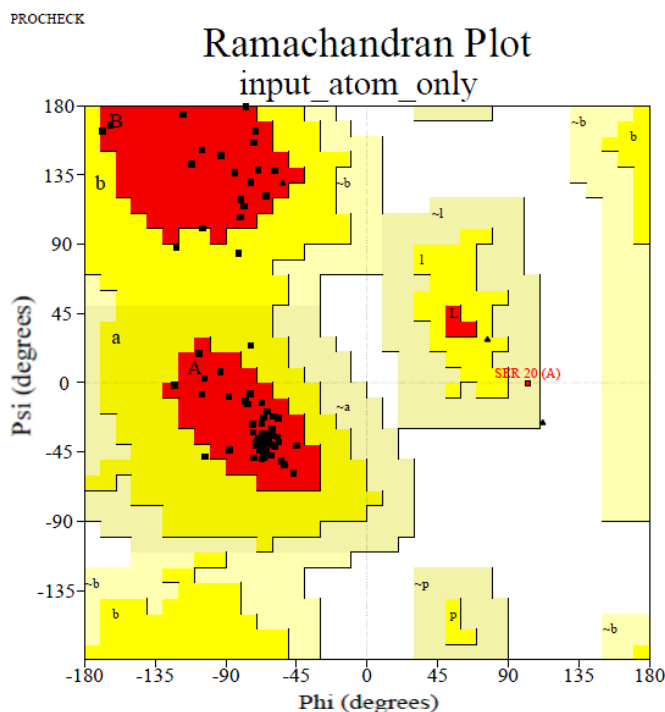


Figure 6.8: Ramachandran plot of the LTP8 model. Red areas [A, B, L] are the most favored regions (representing most favorable psi-phi combination), yellow areas [a, b, l, p] are additional allowed regions, pale orange areas [$\sim a$, $\sim b$, $\sim l$, $\sim p$] are generously allowed regions and white areas are the disallowed regions. Residues in generously allowed regions are labeled in red. Glycine residues are separately identified by triangles. Constructed by PROCHECK.

The PROCHECK Ramachandran plot of the LTP8 model (Fig. 6.8) showed that 95% of its residues are in most favored regions, 4% are in the additional allowed regions, 1% (1 residue) is in the generously allowed regions, while none are in the disallowed regions. Thus, the LTP8 model has a score equivalent to a good quality model.

6.1.3 Electrostatic Potentials

The electrostatic potentials of the LTP5 model, the LTP8 model and 1MZL.pdb were calculated by use of PyMol [102], PDB2PQR [103] and APBS [104]. Prior to the calculations, the 3D coordinates for the models and 1MZL.pdb were converted from PDB format to PQR format using PDB2PQR. The generated PQR files incorporate van der Waals radii and partial charges obtained from the PARSE forcefield [105]. The non-linearized Poisson–Boltzmann equation was solved at 298 K and pH 7, and an internal protein dielectric constant of 2 and a solvent dielectric constant of 80 were used.

The strength and spatial distribution of the electrostatic potential generated by the charges of the LTP5 model and their interactions with the solvent were visualized in PyMol (Fig. 6.9). The electrostatic potential has been mapped onto the solvent accessible surface in an interval from -5 to $5 k_B T/e$ (k_B is Boltzmann's constant, T is temperature, and e is the unit of charge, 1.6021×10^{-19} C), and visualized from different angles (Fig. 6.9, A2, B2, C2, and D2). It is noted that the LTP5 model generates a predominantly positive potential, and that only a few smaller negative areas can be detected.

Spatial distributions of the electrostatic potential are shown in the form of isopotential contours (Fig. 6.9, A3, B3, C3, and D3), plotted at $\pm 0.5 k_B T/e$ to be comparable with the previous described study of Ace-AMP1 by Gomar et al. [30]. The LTP5 model is found to be almost entirely wrapped in a positive electrostatic potential at these values. Only two negative areas can be found on the surface, which is located on the same side of the structure near H_3 (Fig. 6.9, D3). This finding is very similar to what was found for the spatial distribution of the electrostatic potential generated by the Ace-AMP1 model (Fig. 2.8, f).

The strength and spatial distribution of the electrostatic potential generated by the LTP8 model were visualized in PyMol (Fig. 6.10). The electrostatic potential has been mapped onto the solvent accessible surface in an interval from -5 to $5 k_B T/e$, and visualized from different angles (Fig. 6.10, A2, B2, C2, and D2). It is seen that the LTP8 model generate areas with positive and negative potentials, and that more solvent accessible areas have a neutral potential.

Spatial distributions of the electrostatic potential are shown in the form of isopotential contours (Fig. 6.10, A3, B3, C3, and D3), plotted at $\pm 0.5 k_B T/e$. The LTP8 model is almost equally divided into areas wrapped in either a positive or a negative valued contour. A positive potential is mainly found around H_3 and the N-terminus, while the negative potential dominates around H_2 , H_4 and the C-terminal tail. Clearly, the sign, shape and distribution of the contours differ significantly between the two models.

1MZL.pdb is a high-resolution crystal structure of a maize LTP (UniProtKB P19656), solved by Shin et al. in 1995 [21]. This maize LTP is 93 amino acids long in its mature form, contains LTP type 1 characteristic features, and has a pI of 9.1. Thus, it represents an LTP with an LTP-characteristic pI, and its electrostatic potential was therefore investigated for comparison purposes (Fig. C.1, Appendix). Its primary sequence contains 10 charged amino acids (six arginines, two lysines, and two aspartic acids), which is a typical amount for type 1 LTPs.

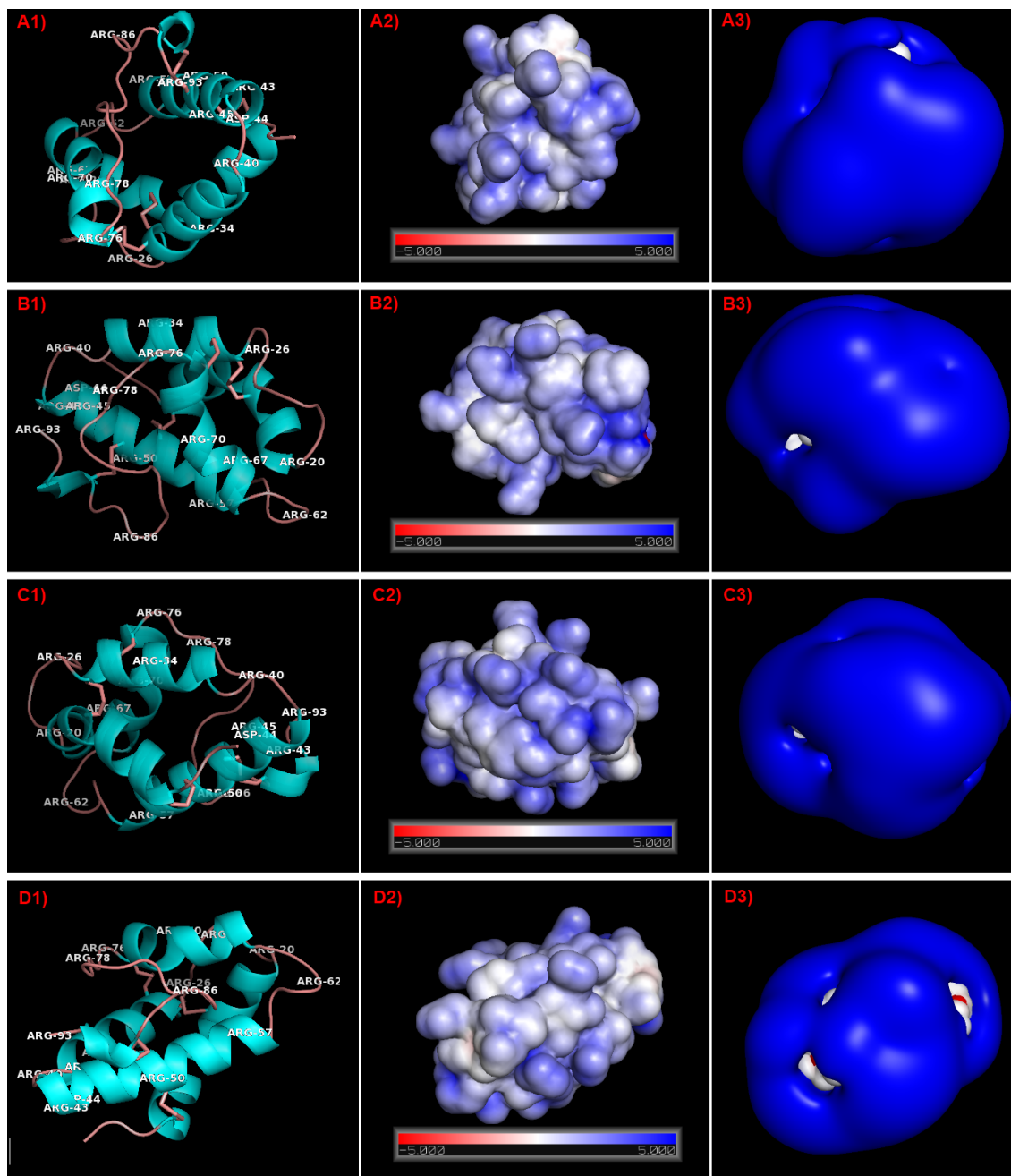


Figure 6.9: Strength and spatial distribution of the electrostatic potential generated by the LTP5 model, visualized from four different angles (A, B, C, and D). The color code is blue for positive electrostatic potential and red for negative electrostatic potential. **1)** 3D structures of the LTP5 model with labeling of charged residues. **2)** Electrostatic potential mapped onto the solvent accessible surface of the LTP5 model in an interval from -5 to $5 k_B T/e$. **3)** Isopotential contours plotted at $\pm 0.5 k_B T/e$. Calculated and visualized by use of PyMol, PDB2PQR and APBS.

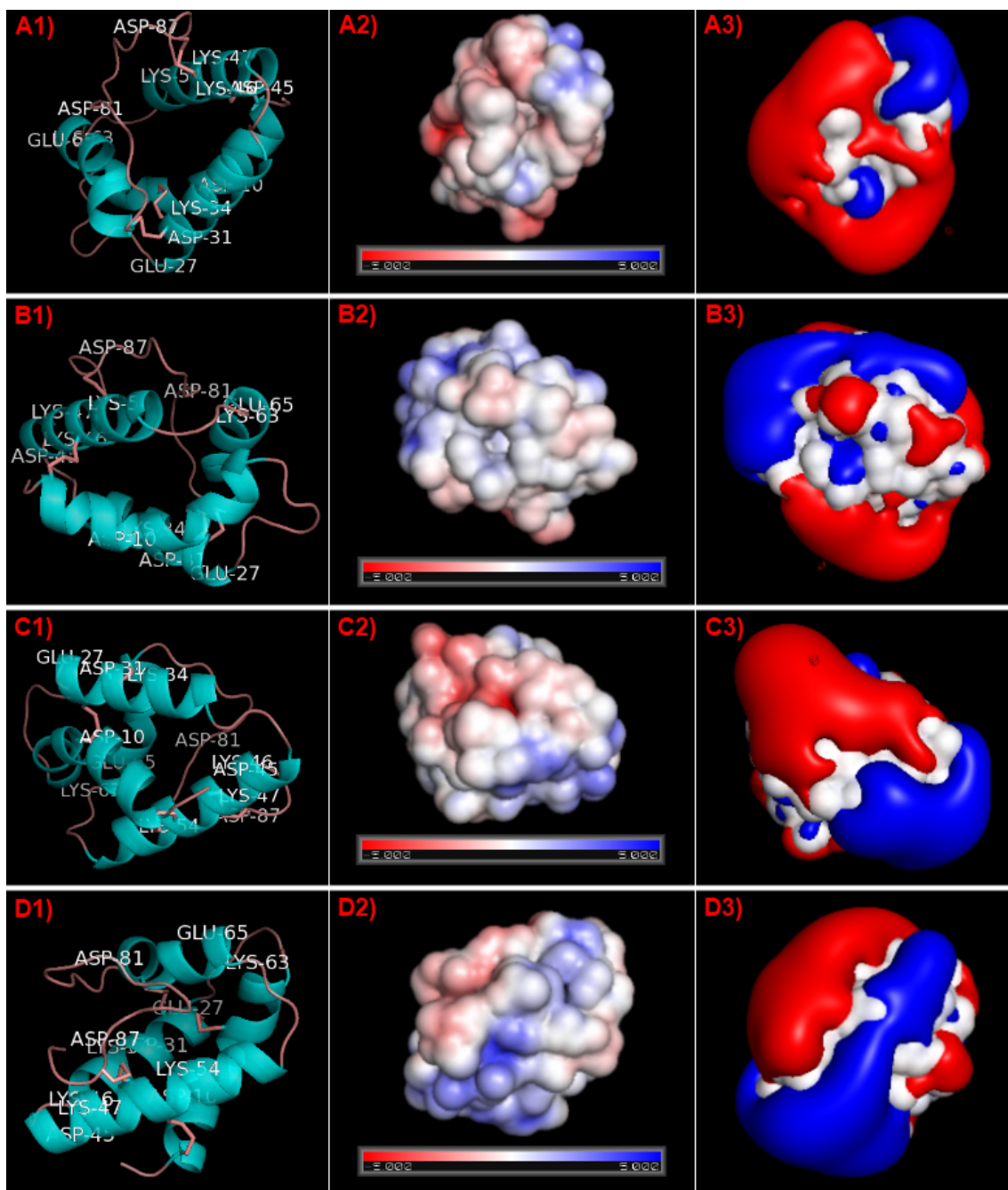


Figure 6.10: Strength and spatial distribution of the electrostatic potential generated by the LTP8 model, visualized from four different angles (A, B, C, and D). The color code is blue for positive electrostatic potential and red for negative electrostatic potential. **1)** 3D structures of the LTP8 model with labeling of charged residues. **2)** Electrostatic potential mapped onto the solvent accessible surface of the LTP8 model in an interval from -5 to $5 k_B T/e$. **3)** Isopotential contours plotted at $\pm 0.5 k_B T/e$. Calculated and visualized by use of PyMol, PDB2PQR and APBS.

When comparing the spatial distribution of the electrostatic potential generated by the LTP5 model, the LTP8 model, the Ace-AMP1 model and maize LTP (1MZL.pdb), a correlation between pI-value and the sign of the contours are not surprisingly found. The higher the pI, the more dominant the positive valued contour is, and vice versa. What is not trivial is however that in the two structures with unusual high pIs (LTP5 and Ace-AMP1), the positive potential seems

almost equally distributed throughout the solvent accessible surface of the structure, instead of clustering around a specific area. In LTPs with more LTP-characteristic pIs, the positive valued contours also dominate (Fig. 2.8, b, c, d, and e, and Fig. C.1, 3, Appendix), but is interrupted with areas of negative valued contours. In the LTP8 model on the other hand, almost equally distributed areas of positive and negative valued contours are found.

6.2 Recombinant Expression of LTPs in *P. pastoris*

6.2.1 DNA based Screening of *P. pastoris* X-33 Transformants

Four *P. pastoris* X-33 transformants harboring PIC-LTP5 or PIC-LTP8 was thawed from -80 °C on ice, and plated on YPD plates containing 300 µg/mL Zeocin. Chromosomal DNA was isolated and subjected to PCR screenings to verify that the constructs were still stably integrated.

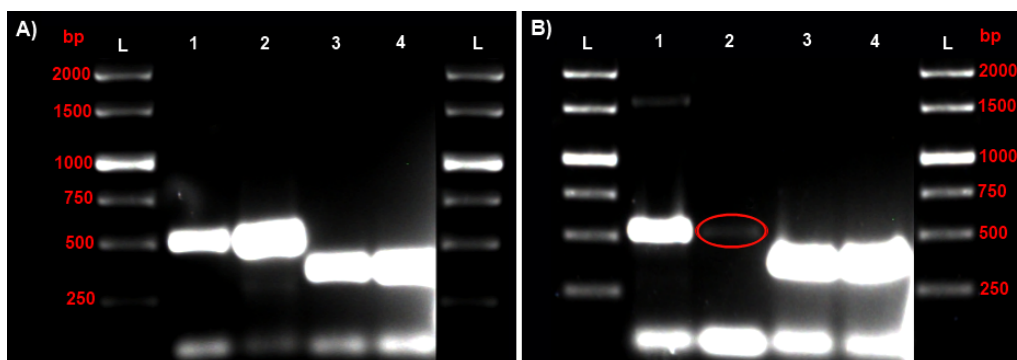


Figure 6.11: A) 1% agarose gel of products from PCRs with chromosomal DNA isolated from two PIC-LTP5 *P. pastoris* X-33 transformants as template. PCR 1 was performed with the primers α -factor and 3'AOX1, and PCR 2 was performed with the primers LTP53for and 3'AOX1. L) 6 µL 1 kb ladder (Fermentas). 1) 8 µL DNA sample from PCR 1 on DNA isolated from PIC-LTP5 *P. pastoris* X-33 transformant 1. 2) 8 µL DNA sample from PCR 1 on DNA isolated from pPIC-LTP5 *P. pastoris* X-33 transformant 2. 3) 8 µL DNA sample from PCR 2 on DNA isolated from PIC-LTP5 *P. pastoris* X-33 transformant 1. 4) 8 µL DNA sample from PCR 1 on DNA isolated from PIC-LTP5 *P. pastoris* X-33 transformant 2. B) 1% agarose gel of products from PCRs with chromosomal DNA isolated from two PIC-LTP8 *P. pastoris* X-33 transformants as template. PCR 1 was performed with the primers α -factor and 3'AOX1, and PCR 2 was performed with the primers LTP83for and 3'AOX1. L) 6 µL 1 kb ladder (Fermentas). 1) 8 µL DNA sample from PCR 1 on DNA isolated from pPIC-LTP8 *P. pastoris* X-33 transformant 1. 2) 8 µL DNA sample from PCR 1 on DNA isolated from PIC-LTP8 *P. pastoris* X-33 transformant 2. The DNA fragment is highlighted with a red circle. 3) 8 µL DNA sample from PCR 2 on DNA isolated from PIC-LTP8 *P. pastoris* X-33 transformants 1. 4) 8 µL DNA sample from PCR 1 on DNA isolated from PIC-LTP8 *P. pastoris* X-33 transformant 2.

The first PCRs on the two PIC-LTP5 *P. pastoris* X-33 transformants were performed with the primers α -factor and 3'AOX1. These PCRs should for PIC-LTP5 harboring transformants yield a single DNA fragment of 507 bp. The PCRs yielded a single DNA fragment just above 500 bp (Fig. 6.11, A, lane 1 and 2) for both transformants, as expected. The fragments below 50 bp presenting in all lanes are believed to be RNA originating from the DNA isolation [108].

The second PCR on the two PIC-LTP5 *P. pastoris* X-33 transformants was performed with

the primers LTP53for and 3'AOX1, which should yield a DNA fragment of 364 bp. A single fragment below 500 bp is observed as a result of this PCR on both of the transformants (Fig. 6.11, A, lane 3 and 4), which is consistent with the expected. On basis of these results, it was confirmed that the PIC-LTP5 constructs in both *P. pastoris* X-33 transformants were still integrated, and the transformants were used for to expression studies.

The primers α -factor and 3'AOX1 was used for the first PCRs on the two PIC-LTP8 *P. pastoris* X-33 transformants. These PCRs were expected to yield a single DNA fragment with a size of 504 bp for PIC-LTP8 harboring transformants. The PCRs yielded a single DNA fragment just above 500 bp (Fig. 6.11, B, lane 1 and 2) for both transformants, consistent with the expected. It is however observed that this first PCR with the second transformant resulted in a fragment with low concentration.

The second PCRs on the two PIC-LTP8 *P. pastoris* X-33 transformants were performed with the primers LTP83for and 3'AOX1, which was expected to yield a DNA fragment of 367 bp. As expected, a single fragment below 500 bp was observed as a result of these PCRs on both of the transformants (Fig. 6.11, B, lane 3 and 4). On basis of these results, it was concluded that the PIC-LTP8 constructs in both *P. pastoris* X-33 transformants was still intact, and the transformants were used for expression studies.

6.2.2 Transformation of *P. pastoris* SMD1168H

The pPIC-LTP5 and pPIC-LTP8 constructs were linearized with the restriction enzyme *Pme*I. The linearized plasmids were then introduced into *P. pastoris* SMD1168H host cells by electroporation. About 3 days after the transformation, only one colony from transformation with each construct appeared on YPDSZ plates. It seems that the efficiency of the transformation were very low, indicating that transformation of the SMD1168H strain by electroporation is more delicate than with the X-33 strain. No growth was observed on the control plates.

Chromosomal DNA was isolated from each of the colonies, and was following used to check for integration of the constructs into the chromosome. The first PCR on the putative PIC-LTP5 *P. pastoris* SMD1168H transformant was performed with the primers LTP53for and 3'AOX1, which for PIC-LTP5 harboring transformants was expected to yield a single DNA fragment of 364 bp. The PCR yielded a single DNA fragment below 400 bp (Fig. 6.12, A, lane 1), which is around the expected size. The fragments below 50 bp presenting in all lanes are RNA originating from the DNA isolation [108].

The second PCR was performed on the putative PIC-LTP5 *P. pastoris* SMD1168H transformant with the primers α -factor and 3'AOX1, which was expected to result in a single DNA fragment of 507 bp. A low concentration fragment just above 500 bp was observed as a result of this PCR (Fig. 6.12, A, lane 2). It was later realized that the annealing temperature used in this PCR was too high for the α -factor primer. A too high annealing temperature reduces the likelihood of annealing of the α -factor primer, and thereby lowered the product yield significantly.

A third PCR was performed as a negative control by using the primer 3'AOX1 in combination with LT83for, which should not be capable of annealing with the chromosomal DNA of PIC-LTP5 *P. pastoris* SMD1168H transformants. As expected, no DNA fragments were detected

as a result of this PCR (Fig. 6.12, A, lane 3). On basis of these DNA-based screenings, it seems likely that *P. pastoris* SMD1168H had been successfully transformed with PIC-LTP5, and this transformant was therefore subjected to expression studies.

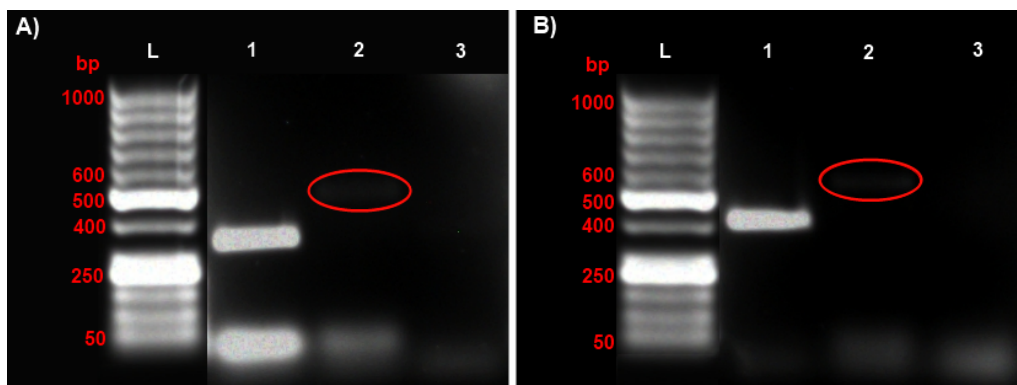


Figure 6.12: **A)** 1% agarose gel of products from PCRs with chromosomal DNA isolated from a putative PIC-LTP5 *P. pastoris* SMD1168H colony as template. PCR 1 was performed with the primers LTP53for and 3'AOX1, PCR 2 was performed with the primers α -factor and 3'AOX1, and PCR 3 was a negative control performed with the primers LTP83for and 3'AOX1. L) 6 μ L 50 bp ladder (Fermentas). 1) 10 μ L DNA sample from PCR 1. 2) 10 μ L DNA sample from PCR 2. The DNA fragment is highlighted with a red circle. 3) 10 μ L DNA sample from PCR 3. **B)** 1% agarose gel of products from PCRs with chromosomal DNA isolated from a putative PIC-LTP8 *P. pastoris* SMD1168H colony as template. PCR 1 was performed with the primers LTP83for and 3'AOX1, PCR 2 was performed with the primers α -factor and 3'AOX1, and PCR 3 was a negative control performed with the primers LTP53for and 3'AOX1. L) 6 μ L 50 bp ladder (Fermentas). 1) 10 μ L DNA sample from PCR 1. 2) 10 μ L DNA sample from PCR 2. The DNA fragment is highlighted with a red circle. 3) 10 μ L DNA sample from PCR 3.

The putative PIC-LTP8 *P. pastoris* SMD1168H transformant was subjected to a PCR with the primers LTP83for and 3'AOX1. This PCR should for PIC-LTP8 harboring transformants yield a single DNA fragment of 367 bp. The PCR of the putative PIC-LTP8 transformant yielded a single DNA fragment just above 400 bp (Fig. 6.12, B, lane 1). This does not seem to be consistent with the expected 367 bp. However, non-uniform migration of ladders placed in opposite sides of the gel was observed, indicating that size inaccuracies were significant. It is therefore believed that the discrepancy is due to experimental inaccuracies.

The second PCR was performed on the putative PIC-LTP8 *P. pastoris* SMD1168H transformant with the primers α -factor and 3'AOX1, which was expected to yield a single DNA fragment of 504 bp. A low concentration fragment above 500 bp is observed as a result of this PCR (Fig. 6.12, B, lane 2), as expected. A too high annealing temperature for the α -factor primer was also used in this PCR, probably responsible for the low fragment concentration.

A negative control PCR was also performed for the PIC-LTP8 *P. pastoris* SMD1168H transformant by using the primer 3'AOX1 in combination with LT53for. As expected, no DNA fragments were detectable as a result of this PCR (Fig. 6.12, B, lane 3). On basis of these PCRs it was found likely that the *P. pastoris* SMD1168H colony had been successfully transformed with PIC-LTP8, and this transformant was used for expression studies.

6.2.3 Expression Studies in Shake Flask Cultures

Expression Studies with Standard Conditions

The first expression study (E1) was performed with the *P. pastoris* X-33 transformants and standard conditions according to the protocol provided by Invitrogen [75]. The expression was performed at 28 °C for 96 hours while induction of the P_{AOX1} was maintained by addition of methanol to a final concentration of 0.5% every 24th hour. One deviation was made from the standard protocol. Due to an unexpected fast growth on glycerol, the start OD₆₀₀ of the expression cultures were 7 and not 1. An X-33 wild type *P. pastoris* reference culture was treated in the same way for determination of background expression. After ended expression study, the supernatants were isolated and lyophilized, and subjected to SDS-PAGEs.

10%, 12%, and 15% (w/v) acrylamide glycine SDS-PAGEs stained with Coomassie Brilliant Blue dye were used for screening of expressed protein (Fig. C.4, C.5, and C.6, respectively, Appendix, not all data shown). However, only one faint band at approximately 85 kDa is detected for all cultures and gel types. Because of the lack of distinctive bands, a Bradford protein assay was performed to test the protein concentration in the lyophilized culture supernatant (data not shown). This assay revealed that only approximately 0.2% of the lyophilized culture supernatant were protein. As no more than 5 mg of material is usually loaded in each well on the SDS-PAGEs, the total protein loading is only in the 10 µg range, and subsequently the amount of individual proteins are much lower. Individual protein bands containing a minimum of ~0.2 µg of protein can be detected with Coomassie staining [117], and it was therefore estimated that a more sensitive staining method was required. Silver staining was therefore used from this point on, which should be able to detect 100-folds lower protein concentrations [117].

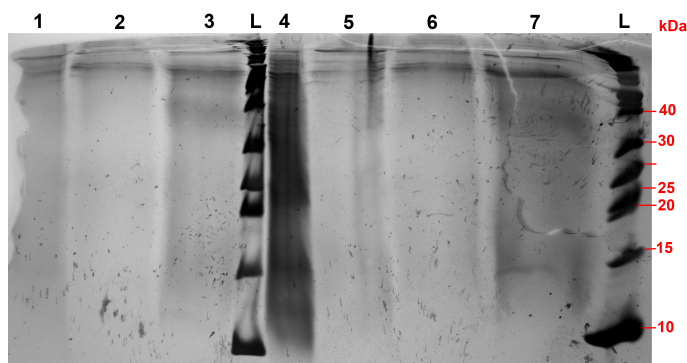


Figure 6.13: Silver stained 15% glycine SDS-PAGE of culture supernatant from expression studies of PIC-LTP5 *P. pastoris* X-33, PIC-LTP8 *P. pastoris* X-33, and wild type *P. pastoris* X-33. Expression 1 (E1) was performed at 28 °C for 96 hours, with methanol induction every 24th hour. Expression 2 (E2) was performed at 23 °C for 72 hours, with methanol induction every 24th hour. 1) 5 mg lyophilized supernatant from E1 with PIC-LTP5 *P. pastoris* X-33 culture 1. 2) 5 mg lyophilized supernatant from E1 with wild-type *P. pastoris* X-33 background culture 1. 3) 5 mg lyophilized supernatant from E1 with PIC-LTP8 *P. pastoris* X-33 culture 1. L) 3 µL PageRuler unstained protein ladder (Fermentas). 4) 10 µL supernatant from E2, time point 24 hours, with PIC-LTP5 *P. pastoris* X-33 culture 1. 5) 5 mg lyophilized supernatant from E1 with PIC-LTP5 *P. pastoris* X-33 culture 2. 6) 5 mg lyophilized supernatant from E1 with wild-type *P. pastoris* X-33 background culture 2. 7) 5 mg lyophilized supernatant from E1 with PIC-LTP8 *P. pastoris* X-33 culture 2.

15% (w/v) acrylamide glycine SDS-PAGEs on lyophilized culture supernatant from E1 were performed, followed by silver staining (Fig. 6.13, not all data shown). It seemed that the salt/protein ratio of the lyophilized supernatant were too high (seen by broadened lanes and lack of distinctive bands on Fig. 6.13, lane 1, 2, 3, 5, 6, and 7), resulting in distorted SDS-PAGEs. It was speculated that this was due to a high amount of proteolysis in the expression medium, and it was therefore attempted to lower the expression temperature and start OD.

Expression Studies with Lowered Temperature

The second expression study (E2) was performed with the PIC-LTP5 *P. pastoris* X-33 transformant. In an attempt to decrease protease release and activity, the temperature was lowered from 28 °C to 23 °C, and the start OD₆₀₀ was lowered to 1. The expression study was further shortened to 72 hours, as it was speculated that the protease activity increased over time. Induction of the P_{AOX1} was maintained by addition of methanol to a final concentration of 0.5% every 24th hour.

A silver stained, 15% glycine SDS-PAGE comparing E1 lyophilized supernatant at time point 96 hours (Fig. 6.13, lane 1, 2, 3, 5, 6, and 7) with E2 supernatant at time point 24 hours (Fig. 6.13, lane 4), indicated that the protein content of E2 is significantly higher than that of E1. At the same time, noticeable reduced growth rate was not observed as a consequence of the lowered temperature, and an expression temperature of 23 °C and start OD of 1 was therefore applied for all future expression studies.

It is well known that uniform high-acrylamide glycine SDS-PAGEs are not well suited for visualization of the small protein range, as the stacking limit in the Laemmli system is too high, and small proteins usually appear as smeared bands near the gel front [117]. In order to obtain a better resolution in the area of interest, precast, 10-20% gradient tricine SDS-PAGEs (BioRad) were tested for their applicability in analysis of the expression supernatant. When comparing Fig. 6.13 and Fig. 6.14, it became evident that the tricine gels resulted in a much better resolution below 100 kDa. It further became clear that the silver staining developed non-uniformly, as more intense staining were obtained at higher MW ranges. As the area of interest is around 10 kDa, the difference in developing intensity has resulted in overdeveloped areas above ~15 kDa throughout this study. This tendency also emphasizes that the concentration of non-adjacent proteins in the same lane cannot be compared when using this staining method.

To compare the expressed proteins resulting from E1 and E2, a tricine SDS-PAGE with culture supernatants from E1 (Fig. 6.14, lane 1, 2, 3, and 4) and E2 (Fig. 6.14, lane 5, 6, and 7) was made. A faint band was observed just below 10 kDa in all lanes, which is consistent with the expected size (LTP 5 should be 9.9 kDa, while LTP8 should be 9.1 kDa). Unfortunately, this band was also present in the background culture supernatants, indicating that *P. pastoris* X-33 secretes a natural protein with a similar size as that of the LTPs. The intensity of the >10 kDa band appears slightly lower in the background culture supernatant (Fig. 6.14, lane 3 and 6), however, this difference was almost undetectable. It however seemed clear, that a significant higher protein concentration had been obtained in E2, as a general higher intensity is observed in these lanes (Fig. 6.14, lane 5, 6, and 7, and Fig. 6.13, lane 4) in spite of the fact that the E2 culture super-

natant had not been concentrated through lyophilization.

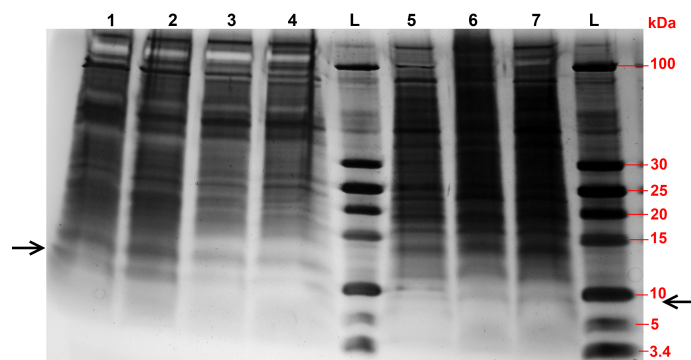


Figure 6.14: Silver stained, precast, 10-20% gradient tricine SDS-PAGE (BioRad) of culture supernatant from expression studies of PIC-LTP5 *P. pastoris* X-33, PIC-LTP8 *P. pastoris* X-33, and wild type *P. pastoris* X-33. Expression 1 (E1) was performed at 28 °C for 96 hours, with methanol induction every 24th hour. Expression 2 (E2) was performed at 23 °C for 72 hours, with methanol induction every 24th hour. Arrows indicate the areas of interest. 1) 5 mg lyophilized supernatant from E1 with PIC-LTP5 *P. pastoris* X-33 culture 1. 2) 5 mg lyophilized supernatant from E1 with PIC-LTP5 *P. pastoris* X-33 culture 2. 3) 5 mg lyophilized supernatant from E1 with wild-type *P. pastoris* X-33 background culture 1. 4) 5 mg lyophilized supernatant from E1 with PIC-LTP8 *P. pastoris* X-33 culture 1. L) 3 μ L PageRuler unstained Low Range protein ladder (Fermentas). 5) 25 μ L supernatant from E2 with PIC-LTP5 *P. pastoris* X-33 culture 2. 6) 25 μ L supernatant from E2 with wild-type *P. pastoris* X-33 background culture. 7) 25 μ L supernatant from E2 with PIC-LTP5 *P. pastoris* X-33 culture 1.

Expression Studies with protease-deficient Transformants

Proteolytic degradation is believed to be the most common problem encountered when foreign proteins are secreted in *P. pastoris*, as described in the introduction. Furthermore, the observation that lowering temperature, start OD and expression time resulted in a higher protein concentration indicated that proteolytic degradation may have been a significant issue in the performed expression studies. It was therefore tried to further reduce proteolytic degradation in the culture supernatant by different approaches, such as the use of the protease deficient strain SMD1168H.

An expression study with the *P. pastoris* SMD1168H transformants was performed at 23 °C for 96 hours while induction of the P_{AOX1} was maintained by addition of methanol to a final concentration of 0.5% every 24th hour. The tricine SDS-PAGE made on culture supernatant from the expression study on a PIC-LTP5 *P. pastoris* SMD1168H transformant at different time points again revealed a single band just below 10 kDa (Fig. 6.15, A, lane 1, 2, 3, and 4), which unfortunately was equally found in the *P. pastoris* SMD1168H background supernatant (Fig. 6.15, A, lane 5). It therefore seemed that the expression yield of LTP5 in this transformant was very low, if any expression occurred at all.

The tricine SDS-PAGE made on culture supernatant from the expression study on the PIC-LTP8 *P. pastoris* SMD1168H transformant at different time points, revealed a broader band just below 10 kDa (Fig. 6.15, B, lane 1, 2, 3, and 4). This could indicate the presence of two distinct proteins below 10 kDa, detectable because of the slightly smaller size of LTP8 (9.1 kDa compared to the 9.9 kDa of LTP5). Unfortunately, it could not be conclusively determined if both

of these proteins were also present in the *P. pastoris* SMD1168H background supernatant (Fig. 6.15, B, lane 5).

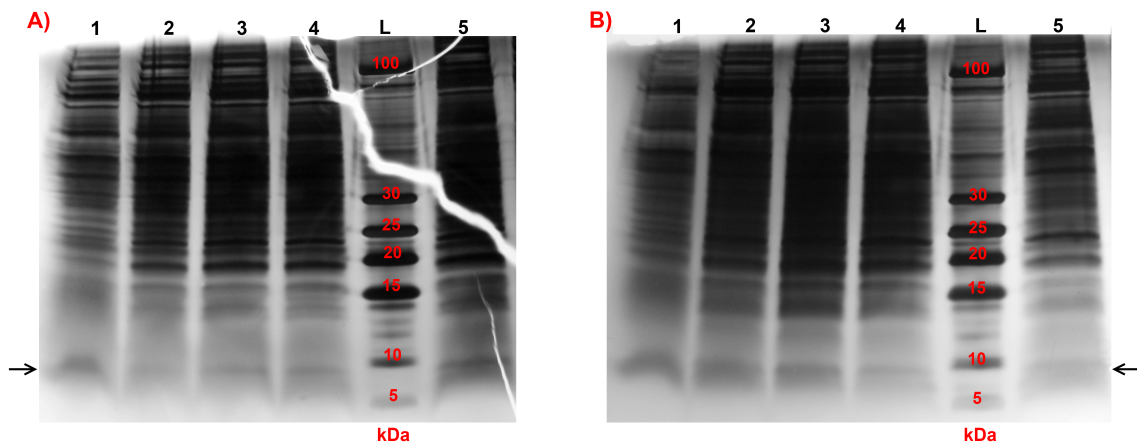


Figure 6.15: Silver stained, precast, 10-20% gradient tricine SDS-PAGE (BioRad) on culture supernatant from expression studies with *P. pastoris* SMD1168H transformants, performed at 23 °C for 96 hours, with methanol induction every 24th hour. Arrows indicate the areas of interest. **A)** Culture supernatant from expression study with PIC-LTP5 *P. pastoris* SMD1168H. 1) 30 μ L supernatant at time point 24 hours from PIC-LTP5 *P. pastoris* SMD1168H culture 1. 2) 30 μ L supernatant at time point 48 hours from PIC-LTP5 *P. pastoris* SMD1168H culture 1. 3) 30 μ L supernatant at time point 72 hours from PIC-LTP5 *P. pastoris* SMD1168H culture 1. 4) 30 μ L supernatant at time point 96 hours from PIC-LTP5 *P. pastoris* SMD1168H culture 1. L) 3 μ L PageRuler unstained Low Range protein ladder (Fermentas). 5) 30 μ L supernatant at time point 96 hours from *P. pastoris* SMD1168H background culture. **B)** Culture supernatant from expression study with PIC-LTP8 *P. pastoris* SMD1168H. 1) 30 μ L supernatant at time point 24 hours from PIC-LTP8 *P. pastoris* SMD1168H culture 2. 2) 30 μ L supernatant at time point 48 hours from PIC-LTP8 *P. pastoris* SMD1168H culture 2. 3) 30 μ L supernatant at time point 72 hours from PIC-LTP8 *P. pastoris* SMD1168H culture 2. 4) 30 μ L supernatant at time point 96 hours from PIC-LTP8 *P. pastoris* SMD1168H culture 2. L) 3 μ L PageRuler unstained Low Range protein ladder (Fermentas). 5) 30 μ L supernatant at time point 96 hours from *P. pastoris* SMD1168H background culture.

From a SDS-PAGE it seemed that a higher protein concentration in the culture supernatant had been obtained when using the protease deficient strain, compared to expression with the wild-type (Fig. C.8, Appendix). It was also in general noticed that the culture supernatant from *P. pastoris* SMD1168H expression cultures quickly acquired an orange glow, compared to the pale yellow of *P. pastoris* X-33 expression cultures. This suggests that there were changes in the culture supernatant, even though it appears from the SDS-PAGEs that the main protein components were conserved.

Expression Studies with addition of Protease Inhibitors

An additional approach to decrease proteolytic degradation in the culture supernatant is to add protease inhibitors. A combination of PMSF and EDTA has been found to be very efficient in preventing degradation of certain proteins in *P. pastoris* supernatant [86]. Usually these protease inhibitors are added to the supernatant after the cells have been harvested. In this study, the protease inhibitors were in addition added during the expression study to a final concentra-

tion of 1 mM every 12th hour. The continuous addition was especially a requirement for the effect of PMSF, as this compound is very unstable in aqueous solutions when unbound.

The protease inhibitor expression study of the *P. pastoris* X-33 transformants was performed at 23 °C for 96 hours, while also increasing the induction frequency of the P_{AOX1} by addition of methanol to a final concentration of 0.25% every 12th hour. A wild-type *P. pastoris* X-33 culture was treated in the same way for determination of background expression. A 10-20% gradient tricine SDS-PAGE (BioRad) of the culture supernatants from the PIC-LTP5 *P. pastoris* X-33 expression (Fig. 6.16, lane 1, 2, 3, and 4) and from the PIC-LTP8 *P. pastoris* X-33 expression (Fig. 6.16, lane 6, 7, 8, and 9) revealed bands just below 10 kDa, which was consistent with the expected. This band was however also present in the *P. pastoris* X-33 background culture (Fig. 6.16, lane 5) with a similar intensity. It therefore seems that the expression yields of LTP5 and LTP8 from these transformants were very low, if any expression occurred at all. Furthermore, it seemed that the silver staining was not uniform on this SDS-PAGE, making it impossible to conclude anything from band intensity.

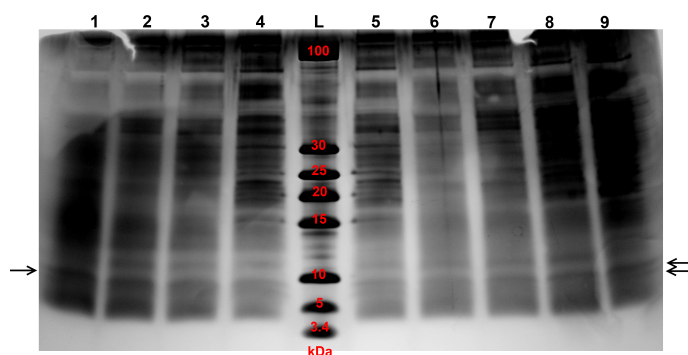


Figure 6.16: Silver stained, precast, 10-20% gradient tricine SDS-PAGE (BioRad) of culture supernatant from protease inhibitor expression studies of PIC-LTP5 *P. pastoris* X-33, PIC-LTP8 *P. pastoris* X-33, and wild type *P. pastoris* X-33. Expression was performed at 23 °C for 96 hours, with methanol induction every 12th hour. In addition, the protease inhibitors PMSF and EDTA was added to a final concentration of 1 mM and 1 mM, respectively, every 12th hour. Arrows indicate the areas of interest. 1) 30 μ L supernatant at time point 24 hours from PIC-LTP5 *P. pastoris* X-33 culture. 2) 30 μ L supernatant at time point 48 hours from PIC-LTP5 *P. pastoris* X-33 culture. 3) 30 μ L supernatant at time point 72 hours from PIC-LTP5 *P. pastoris* X-33 culture. 4) 30 μ L supernatant at time point 96 hours from PIC-LTP5 *P. pastoris* X-33 culture. L) 3 μ L PageRuler unstained Low Range protein ladder (Fermentas). 5) 30 μ L supernatant at time point 96 hours from *P. pastoris* X-33 background culture. 6) 30 μ L supernatant at time point 24 hours from PIC-LTP8 *P. pastoris* X-33 culture. 7) 30 μ L supernatant at time point 48 hours from PIC-LTP8 *P. pastoris* X-33 culture. 8) 30 μ L supernatant at time point 72 hours from PIC-LTP8 *P. pastoris* X-33 culture. 9) 30 μ L supernatant at time point 96 hours from PIC-LTP8 *P. pastoris* X-33 culture.

The protease inhibitor expression study of the *P. pastoris* SMD1168H transformants was performed at 23 °C for 96 hours, while also increasing the induction frequency of the P_{AOX1} by addition of methanol to a final concentration of 0.25% every 12th hour. A *P. pastoris* SMD1168H culture was treated in the same way for determination of background expression. A 10-20% gradient tricine SDS-PAGE (BioRad) of the culture supernatants from the PIC-LTP5 *P. pastoris* SMD1168H expression revealed the presence of a band just below 10 kDa (Fig. 6.17, A, lane 2, 3, 4, and 5), which was consistent with the expected. However, again a band with similar intensity

was found at the same position in the *P. pastoris* SMD1168H background culture supernatant (Fig. 6.17, A, lane 1). A similar result was obtained from the analysis of culture supernatants from the PIC-LTP8 *P. pastoris* SMD1168H expression study: a band could be detected just below 10 kDa (Fig. 6.17, B, lane 2, 3, 4, and 5), however a band of similar intensity was found at the same position in the *P. pastoris* SMD1168H background (Fig. 6.17, B, lane 1). It seemed that the expression yields of LTP5 and LTP8 from these transformants were very low, if any expression occurred at all.

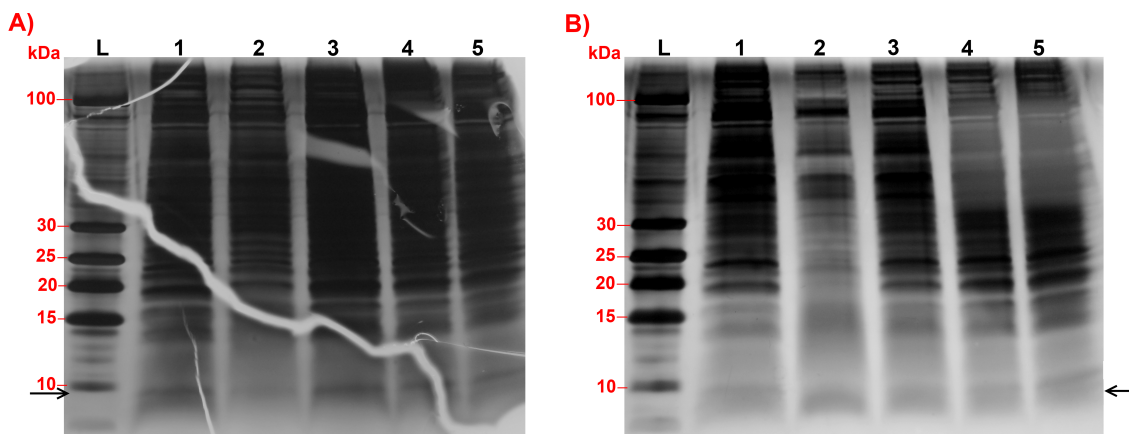


Figure 6.17: Silver stained, precast, 10-20% gradient tricine SDS-PAGE (BioRad) of culture supernatant from expression studies of PIC-LTP5 *P. pastoris* SMD1168H, PIC-LTP8 *P. pastoris* SMD1168H, and *P. pastoris* SMD1168H. Expression was performed at 23 °C for 96 hours, with methanol induction every 12th hour. In addition, the protease inhibitors PMSF and EDTA was added to a final concentration of 1 mM and 1 mM, respectively, every 12th hour. Arrows indicate the areas of interest. **A)** L) 3 μ L PageRuler unstained Low Range protein ladder (Fermentas). 1) 30 μ L supernatant at time point 96 hours from *P. pastoris* SMD1168H background culture. 2) 30 μ L supernatant at time point 24 hours from PIC-LTP5 *P. pastoris* SMD1168H culture. 3) 30 μ L supernatant at time point 48 hours from PIC-LTP5 *P. pastoris* SMD1168H culture. 4) 30 μ L supernatant at time point 72 hours from PIC-LTP5 *P. pastoris* SMD1168H culture. 5) 30 μ L supernatant at time point 96 hours from PIC-LTP5 *P. pastoris* SMD1168H culture. **B)** L) 3 μ L PageRuler unstained Low Range protein ladder (Fermentas). 1) 30 μ L supernatant at time point 96 hours from *P. pastoris* SMD1168H background culture. 2) 30 μ L supernatant at time point 24 hours from PIC-LTP8 *P. pastoris* SMD1168H culture. 3) 30 μ L supernatant at time point 48 hours from PIC-LTP8 *P. pastoris* SMD1168H culture. 4) 30 μ L supernatant at time point 72 hours from PIC-LTP8 *P. pastoris* SMD1168H culture. 5) 30 μ L supernatant at time point 96 hours from PIC-LTP8 *P. pastoris* SMD1168H culture.

In order to evaluate which transformant that could potentially be used for a fermentation study, a comparative 10-20% gradient tricine SDS-PAGE (BioRad) (Fig. 6.18) was made on concentrated culture supernatants from the expression studies with addition of protease inhibitors. Comparing the SMD1168H transformant expression supernatants (Fig. 6.18, lane 2 and 4) with the X-33 transformant expression supernatants ((Fig. 6.18, lane 3 and 5) it was clear that the supernatants from the SMD1168H transformant cultures had a higher protein concentration, which cannot be compensated for by the addition of protease inhibitors. When comparing the band just below 10 kDa from the supernatants of the SMD1168H transformant cultures (Fig. 6.18, lane 2 and 4) with the supernatant from the SMD1168H background culture (Fig. 6.18, lane 1) it appeared that two proteins with almost identical sizes were present in the transformant expression supernatants, while only one seemed to be present in the background. This

additional band may represent LTP5 or LTP8, respectively. These observations were supported by another comparative SDS-PAGE (Fig. C.8, Appendix). Based on these observations, PIC-LTP5 *P. pastoris* SMD1168H was selected for a fermentation study.

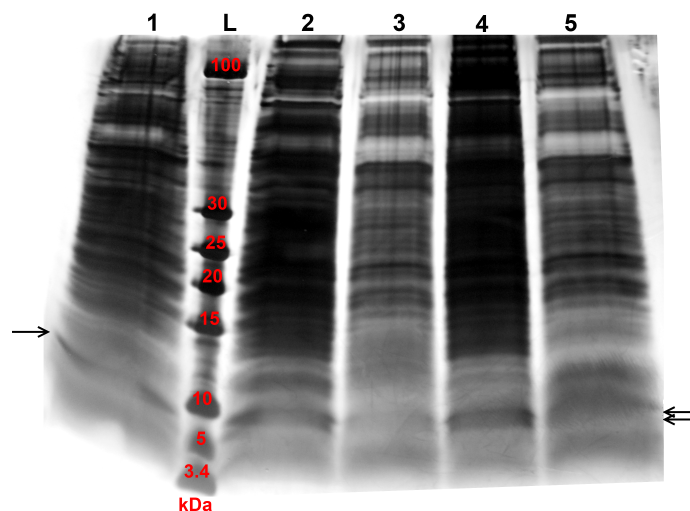


Figure 6.18: Silver stained, precast, 10-20% gradient tricine SDS-PAGE (BioRad), comparing lyophilized culture supernatant from expression studies with the protease deficient strain SMD1168H and X-33. All these expression studies was performed at 23 °C for 96 hours, with methanol induction every 12th hour. In addition, the protease inhibitors PMSF and EDTA was added to a final concentration of 1 mM and 1 mM, respectively, every 12th hour. Arrows indicate the areas of interest. 1) 6 mg lyophilized supernatant at time point 96 hours from *P. pastoris* SMD1168H background culture. L) 3 μ L PageRuler unstained Low Range protein ladder (Fermentas). 2) 6 mg lyophilized supernatant at time point 96 hours from PIC-LTP5 *P. pastoris* SMD1168H culture. 3) 6 mg lyophilized supernatant at time point 96 hours from PIC-LTP5 *P. pastoris* X-33 culture. 4) 6 mg lyophilized supernatant at time point 96 hours from PIC-LTP8 *P. pastoris* SMD1168H culture. 5) 6 mg lyophilized supernatant at time point 96 hours from PIC-LTP8 *P. pastoris* X-33 culture.

Growth of Expression Cultures

To investigate the influence on culture growth of the different expression conditions applied in the expression studies, OD_{600} were monitored periodically. To evaluate the effects of these different conditions, defined expression conditions needed to be maintained. Therefore the pH-development of the cultures were also followed, and it was found that the potassium phosphate buffer used were capable of maintaining the pH at 6-7 throughout the expression studies.

OD_{600} was measured every 24th hours and plotted against time (Fig. 6.19), to provide a rough estimate of the growth curve of each culture. It was expected that different strains and culture conditions would affect the growth rate. The load of expressing a foreign protein could for example affect the growth rate of transformants negatively. Furthermore, it was expected that the *P. pastoris* SMD1168H strain would have reduced growth rate compared to the *P. pastoris* X-33 strain because of the mutations performed in its genome. None of these expectations however seemed to be noticeably valid, as no significant difference in growth rate could be deduced from the relevant curves (Fig. 6.19, A, solid blue curve, solid red curve, dotted blue curve, and dotted red curve, and Fig. 6.19, B, solid blue curve, solid green curve, and solid red curve). One exception was though the growth rate of the PIC-LTP5 *P. pastoris* X-33 E1 expres-

sion cultures (Fig. 6.19, A, solid green curve), which appeared to be lower compared to the non-transformed wild type. This tendency was however not observed with the same transformants in E2 (Fig. 6.19, A, dotted red curve), and it was therefore believed to be due to inaccuracies rather than a true tendency.

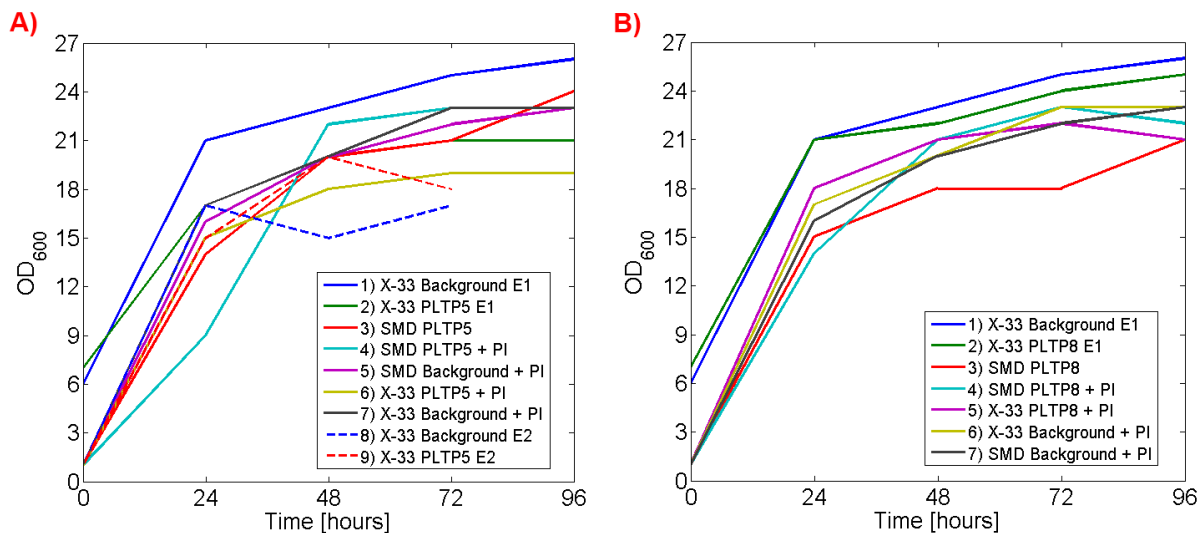


Figure 6.19: OD_{600} of expression cultures plotted against time, yielding a rough estimate of their growth curve. When several expression cultures had been conducted under the same conditions, the resulting OD_{600} profile is presented as an average. **A)** PIC-LTP5 transformants and background cultures. **B)** PIC-LTP8 transformants and background cultures.

Lowering of temperature and the addition of toxic protease inhibitors were expected to have a negative effect on the culture growth. A positive effect was on the other hand expected from a more frequent induction of the P_{AOX1} . Comparing the growth curves, the expected effects did however not seem to be noticeably present. One exception was the PIC-LTP5 *P. pastoris* SMD1168H culture from the expression study with addition of protease inhibitors, which seemed to have a delayed onset of growth (Fig. 6.19, A, light blue solid curve). However, as this tendency was not observed in any other cultures from the expression study with addition of protease inhibitors (Fig. 6.19, A, purple solid curve, yellow solid curve, and black solid curve, and Fig. 6.19, B, light blue solid curve, purple solid curve, yellow solid curve, and black solid curve), it was believed to be due to inaccuracies rather than being a true tendency.

From these rough estimated growth curves it appeared that growth was not significantly affected by the different experimentally applied expression conditions and the use of protease deficient strains.

Chromatographic Analysis

Lyophilized supernatant from the expression studies was subjected to chromatographic analysis with the purpose of investigating if any distinctive peaks could be detected in the transformant culture supernatants.

Analytical RP-HPLC scans with a linear gradient of acetonitrile were conducted with su-

pernatant of *P. pastoris* SMD1168H transformants and background (data not shown). Many peaks were detected in the chromatograms, but no distinctive peaks could be identified for PIC-LTP5 *P. pastoris* SMD1168H or PIC-LTP8 *P. pastoris* SMD1168H culture supernatant compared to the background.

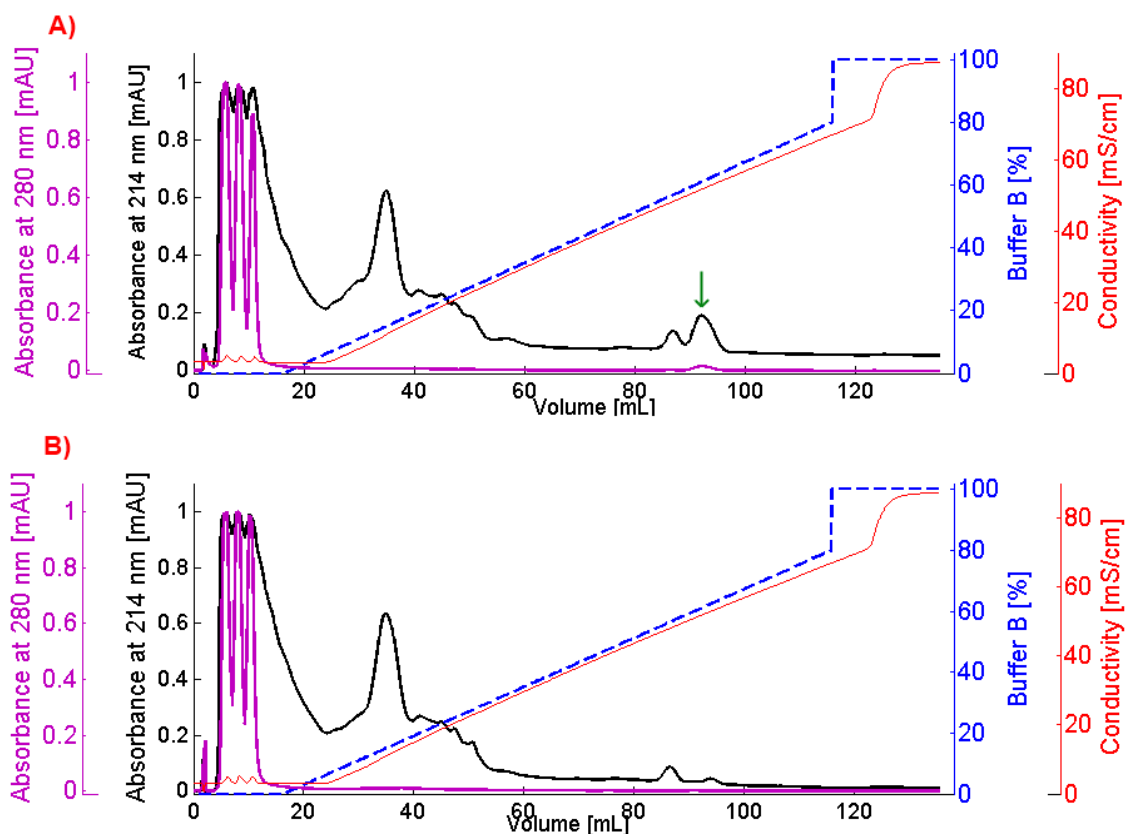


Figure 6.20: Cation-exchange chromatography with heat-treated, dialyzed, and lyophilized *P. pastoris* SMD1168 culture supernatants. The analysis was performed with a buffer containing 10 mM Tris-HCl and 10 mM NaCl (pH 4), and retained material was eluted with 1 M NaCl (buffer B) in the same buffer (4 mL/min). Percent of buffer B (blue dotted line), UV absorbance at 214 nm (black solid line), UV absorbance at 280 nm (purple solid line), and conductance (red solid line) is plotted against volume of eluent passed through the system. UV absorbance at 214 nm and 280 nm has been normalized to highest detection point. A concentrated sample derived from 25 mL untreated culture supernatant was applied through three injections in each run. **A)** Heat-treated, dialyzed, and lyophilized PIC-LTP5 *P. pastoris* SMD1168 culture supernatant. The green arrow highlights the peak of interest. **B)** Heat-treated, dialyzed, and lyophilized *P. pastoris* SMD1168 background supernatant.

LTP5 has a predicted pI of 11.4, and is therefore well-suited for purification with cation-exchange chromatography. The cation-exchange chromatography was performed on a FPLC system, with a buffer containing 10 mM Tris-HCl and 10 mM NaCl (pH 4), and elution of retained material with a 0-80% 1 M NaCl gradient in the same buffer. Dialyzed and lyophilized PIC-LTP5 *P. pastoris* X-33 culture supernatant (Fig. C.12, A, Appendix), and dialyzed and lyophilized *P. pastoris* X-33 background supernatant (Fig. C.12, B, Appendix) from the expression studies with addition of protease inhibitors were analyzed. No significant peak differences could be detected between the resulting chromatograms, indicating that no detectable level of LTP5 had

accumulated during the expression study of this transformant.

As described in the introduction, LTPs are known to be heat resistant due to their exceptionally stable fold. It was therefore attempted to up-concentrate the putatively expressed LTP5 by subjecting the supernatant to 80 °C for 15 min, and then removing all proteins that had precipitated. The resulting solution was dialyzed and concentrated by lyophilization, and powder corresponding to 25 mL of untreated culture supernatant was applied to the cation-exchange column through three injections in each run. A distinctive peak was detected in the chromatogram of PIC-LTP5 *P. pastoris* SMD1168 expression culture supernatant (Fig. 6.20, A, green arrow), which was not found in the chromatogram of *P. pastoris* SMD1168 background supernatant (Fig. 6.20, B). This peak may represent recombinantly expressed LTP5, and was collected for further analysis. Unfortunately, this identification and purification could not be reproduced (data not shown), which suggests that the peak could be the result of contamination or other experimental variations. Furthermore, no distinctive protein could be detected on a SDS-PAGE on the heat-treated, dialyzed and lyophilized culture supernatant from this expression study with the PIC-LTP5 *P. pastoris* SMD1168H transformant (Fig. C.7, Appendix).

Antimicrobial Activity Assays

Antimicrobial activity assays were performed on proteins collected from the cation-exchange chromatography. Studies have found that LTPs most often have activity against fungi and sometimes Gram positive bacteria as described in the introduction, and microbes fitting into these parameters were therefore chosen for the assays.

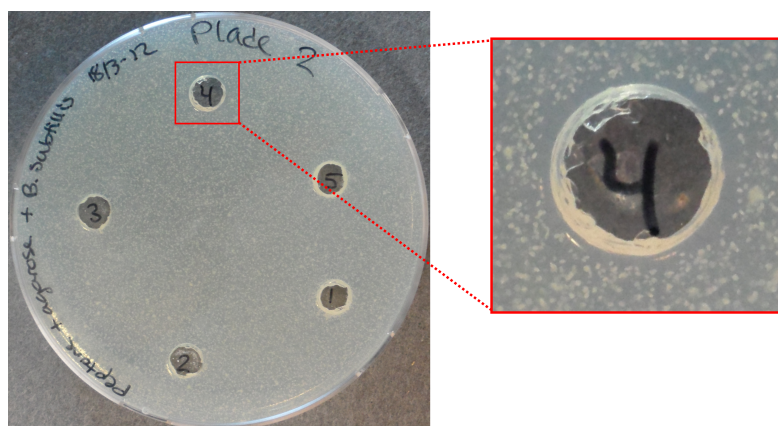


Figure 6.21: Radial diffusion antimicrobial activity assay with the Gram positive bacteria *B. subtilis*. 1) 100 μ L demineralized H_2O . 2) 100 μ L background reference with heat-treated, dialyzed, and lyophilized *P. pastoris* SMD1168H culture supernatant collected at 82 mL - 96 mL elution volume in the cation-exchange chromatography. 3) 100 μ L heat-treated, dialyzed, and lyophilized PIC-LTP5 *P. pastoris* SMD1168 culture supernatant collected at 82 mL - 90 mL elution volume in the cation-exchange chromatography. 4) 100 μ L heat-treated, dialyzed, and lyophilized PIC-LTP5 *P. pastoris* SMD1168 culture supernatant collected at 90-96 mL elution volume in the cation-exchange chromatography (green arrow). 5) 100 μ L demineralized H_2O .

Radial diffusion assays (RDAs) were performed on 0.8% agarose plates with two different Gram positive bacteria: *Micrococcus luteus* and *Bacillus subtilis*. The bacteria were moulded into plates, and wells were made for the placement of samples. Antifungal activity assay were made using the yeast *S. cerevisiae* and the plant pathogenic fungus *Fusarium graminearum*. The antifungal activity assay with *S. cerevisiae* were made according to the RDA protocol, while the hyphal growth of *F. graminearum* required a different approach. In this case, the sample was placed on top of a whatman no. 1 filter paper, while the fungal spores were placed in the center of the plate resulting in radial extension of hyphae after germination.

The proteins represented by the distinctive peak in the cation-exchange chromatography with heat-treated, dialyzed, and lyophilized PIC-LTP5 *P. pastoris* SMD1168 culture supernatant (Fig. 6.20, A, green arrow) was dialyzed, lyophilized and divided between the plates with the four microbes. As reference, proteins collected at the same elution point from cation-exchange chromatography with *P. pastoris* SMD1168H culture supernatant were used (Fig. 6.20, B). No antimicrobial activity could be detected on the assays with *M. luteus*, *S. cerevisiae*, and *F. graminearum* (data not shown). However, a compact clearing zone caused by the putative LTP5 containing fraction was found on *B. subtilis* (Fig. 6.21), while no clearing was caused by the reference. The small area of this clearing zone indicated that the inhibiting molecule had a low diffusivity.

6.2.4 Fermentation of PIC-LTP5 *P. pastoris* SMD1168H

Expression studies of wheat and fruit LTPs in *P. pastoris* have shown that the highest product accumulation was achieved after 96 hours of induction. [118], [51], [119] It was therefore speculated that a prolonged duration of the expression could result in a higher yield. Furthermore, fermentation often results in a significantly higher product yield because of the controlled conditions and higher cell densities obtained, as described in the introduction.

Fermentation of PIC-LTP5 *P. pastoris* SMD1168H was performed with an initial volume of 1 L, and consisted of both batch and fed-batch culture procedures. A seed culture was grown overnight in a shake flask, and used to inoculate the reactor containing 1 L BMGY medium (containing 2% glycerol). The fermentation was performed at 25 °C and pH 6, while stirring at 1093 rpm and addition of antifoam when foam-levels rose. OD₆₀₀ was measured approximately every 24th hour, to give a rough estimate of the growth. The first phase (batch culture on 2% glycerol) was designed for biomass accumulation, and the OD₆₀₀ rose from 2 to 16 within the first 24 hours (Fig. 6.22). A rapid oxygen increase was expected when the glycerol had been exhausted, but this did not occur. From 24 hours to 41 hours, the OD₆₀₀ development appeared nearly constant, while the oxygen level continued to decline. It was therefore believed that the glycerol had been exhausted in spite of the lacking dissolved oxygen response, and the induction phase was initiated. The induction phase was conducted as a methanol fed-batch procedure, with addition of 1.2 mL methanol pr. hour. The culture appeared to enter a lag phase after the carbon source starvation, as the OD₆₀₀ only increased slightly from 41 hours to 75 hours. The dissolved oxygen level declined from an initial level of 26.5% and converged towards ~4%. The methanol fed-batch culture was continued for 109 hours, after which the culture supernatant was harvested, added protease inhibitors and frozen.

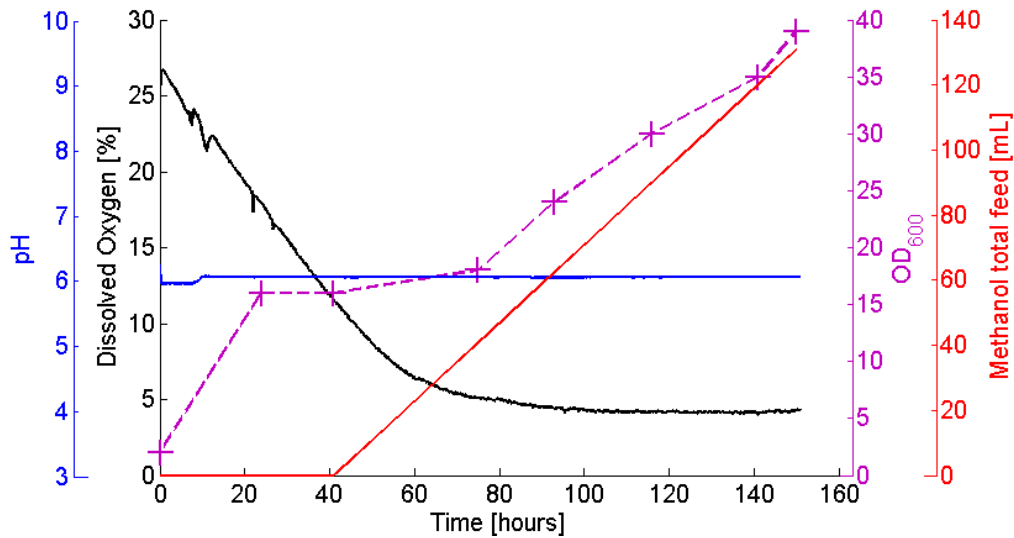


Figure 6.22: Fermentation of PIC-LTP5 *P. pastoris* SMD1168H. Dissolved oxygen (black line), OD_{600} (purple crosses), pH (blue line), and total methanol feed (red line) is plotted against batch time.

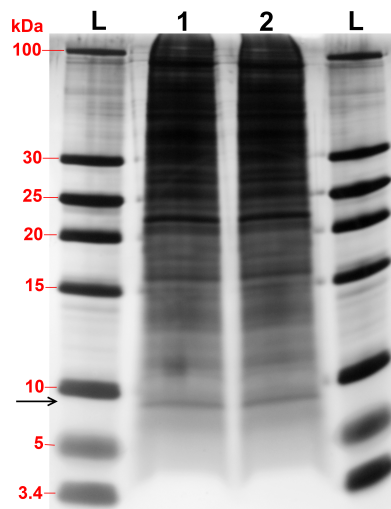


Figure 6.23: Silver stained, precast, 16.5% tricine SDS-PAGE (BioRad) of PIC-LTP5 *P. pastoris* SMD1168H fermentation supernatant. L) 3 μ L PageRuler unstained Low Range protein ladder (Fermentas). 1) 15 μ L fermentation supernatant. 2) 15 μ L fermentation supernatant.

A precast, 16.5% tricine SDS-PAGE (BioRad) (Fig. 6.23) was performed on the supernatant from the PIC-LTP5 *P. pastoris* SMD1168H fermentation study. No distinctive band, or a band of increased intensity, could be detected in the area of interest on this SDS-PAGE. It was however noted, that the use of the 16.5% tricine SDS-PAGE instead of the 10-20% gradient gel resulted in a better resolution of proteins below 15 kDa.

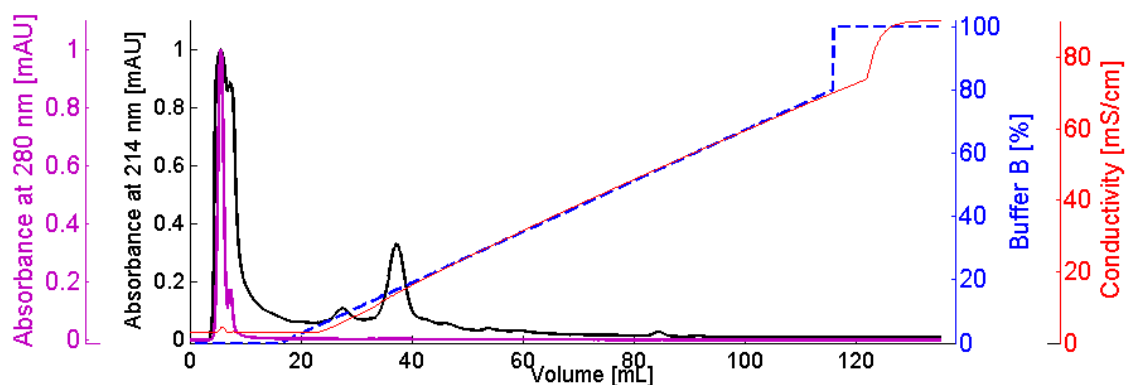


Figure 6.24: Cation-exchange chromatography of dialyzed and lyophilized supernatant from PIC-LTP5 *P. pastoris* SMD1168H fermentation study. Analysis was performed with a buffer containing 10 mM Tris-HCl and 10 mM NaCl (pH 4), and retained material was eluted with 1 M NaCl (buffer B) in the same buffer (4 mL/min). Percent of buffer B (blue dotted line), UV absorbance at 214 nm (black solid line), UV absorbance at 280 nm (purple solid line), and conductance (red solid line) is plotted against volume of eluent passed through the system. UV absorbance at 214 nm and 280 nm has been normalized to highest detection point. A sample derived from 25 mL untreated culture supernatant was applied to the column.

Supernatant from the PIC-LTP5 *P. pastoris* SMD1168H fermentation study was dialyzed, lyophilized, and subjected to cation-exchange chromatography (Fig. 6.24). The chromatography was performed with a buffer containing 10 mM Tris-HCl and 10 mM NaCl (pH 4), and retained material was eluted with a 0-80% 1 M NaCl gradient in the same buffer (4 mL/min). When comparing the elution profile to that of *P. pastoris* SMD1168H background culture supernatant (Fig. 6.20, B), no distinctive peak could be detected in the chromatogram of the fermentation supernatant. This, together with the SDS-PAGE, suggested that LTP5 had not accumulated during the fermentation process in detectable amounts.

Due to unavailability of the bioreactor, the fermentation study was not repeated in spite of obvious optimization possibilities.

6.3 Isolation and Characterization of Putative LTPs from *B. oleracea*

6.3.1 Wax Protein Extraction

Pyee et al. [32] have found that the major protein in surface wax of broccoli (*Brassica oleracea* var. *italica*) leaves was an LTP. They were capable of isolating 1.5 mg LTP from 1 kg of fresh leaves by using a modified version of the Folch lipid extraction protocol. It was therefore attempted in the present study to apply this simple LTP extraction protocol to leaves of *Brassica oleracea* var. *capitata* (cabbage). First, the protocol was performed with a mixture of young and old leaves. The isolated protein fraction was analyzed by SDS-PAGE (Fig. C.9, A, Appendix), which did not reveal any strong band around 10 kDa. LTPs usually have a pI around 9, and are therefore well-suited for purification with cation-exchange chromatography. Cation-exchange chromatography was performed on a FPLC system with dialyzed and lyophilized wax protein extraction material (data not shown). The chromatography was performed with a buffer con-

taining 10 mM Tris-HCl and 10 mM NaCl (pH 4), and retained material was eluted with a 0-80% 1 M NaCl gradient in the same buffer. No significant amount of protein was found to be retained by the cation column (data not shown).

Since Pyee et al. found that the LTP concentration was much higher in younger leaves of broccoli, it was tried to only use young leaves in the wax protein extraction. An SDS-PAGE of the extracted material (Fig. C.9, B, Appendix) showed similar results as the prior extraction. Furthermore, no significant amount of protein was retained in the cation-exchange chromatography (Fig. C.13, Appendix). It was therefore concluded that the wax extraction method for simple extraction of LTPs could not be transferred successfully from the *italica* cultivar to the *capitata* cultivar.

6.3.2 Protein Extraction from Plant Tissues

Extraction and purification protocols for isolation of putative LTPs from tissue of *Brassica oleracea* var. *capitata* (cabbage) was developed (Fig. 6.25). The protocols was based on protocols from literature, describing isolation methods of LTPs from various plants, fruits and seeds.

Since the LTP concentration may vary in different tissues, the components of the cabbage were divided into three groups; stem (S), younger leaves (YL), and older leaves (OL). The initial extraction steps were mainly derived from two studies by Palacin et al. ([50] and [106]). The obtained tissue powder was washed with acetone with the purpose of removing lipids and other undesired contaminants, followed by extractions with 0.5 M NaCl. The extraction supernatant was precipitated with 0-90% ammonium sulfate in order to concentrate the protein solutions (resulting in F0-90). The latter is believed to cause a significant yield decrease, as it was difficult to completely recover the pellet after centrifugation.

Most proteins are denatured by high temperature, and the process is usually irreversible and leads to insoluble aggregation. [120] LTPs are known to be quite heat resistant due to their fold, which has been used for isolation of these proteins by Terras et al. [61]. The F0-90 solution was therefore subjected to 80 °C for 15 min, followed by removal of all precipitated proteins, to enrich the solution in putative LTPs. Prior to further fractionation, the obtained heat-resistant fraction OL (FOL), fraction YL (FYL) and fraction S (FS) were dialyzed and lyophilized. An SDS-PAGE on these fractions (Fig. C.10, Appendix) revealed that the concentration of different proteins at this step was high, making it difficult to identify individual proteins. It however seemed that in the area of interest (around 9-10 kDa) a higher concentration of proteins were present in FYL and FS than in FOL.

Cabbage contains 1.28 g protein pr. 100 g of material, while other major weight contributors are carbohydrates (5.8 g), fat (0.1 g) and water. The protein, carbohydrate and fat content is approximately 20% lower than these numbers in the core/stem and outer leaves of the cabbage. [121] Approximately 54 mg of dry powder was obtained pr. 100 g of wet raw stem material. As the majority of lipids should be removed through acetone defatting and most molecules with a MW below 1000 Da should be removed through dialysis, this fraction should mainly contain proteins and large carbohydrate molecules. Through a rough estimation it is assessed that about 5% of the cabbage stem proteins were recovered after the extraction and heat denatura-

tion.

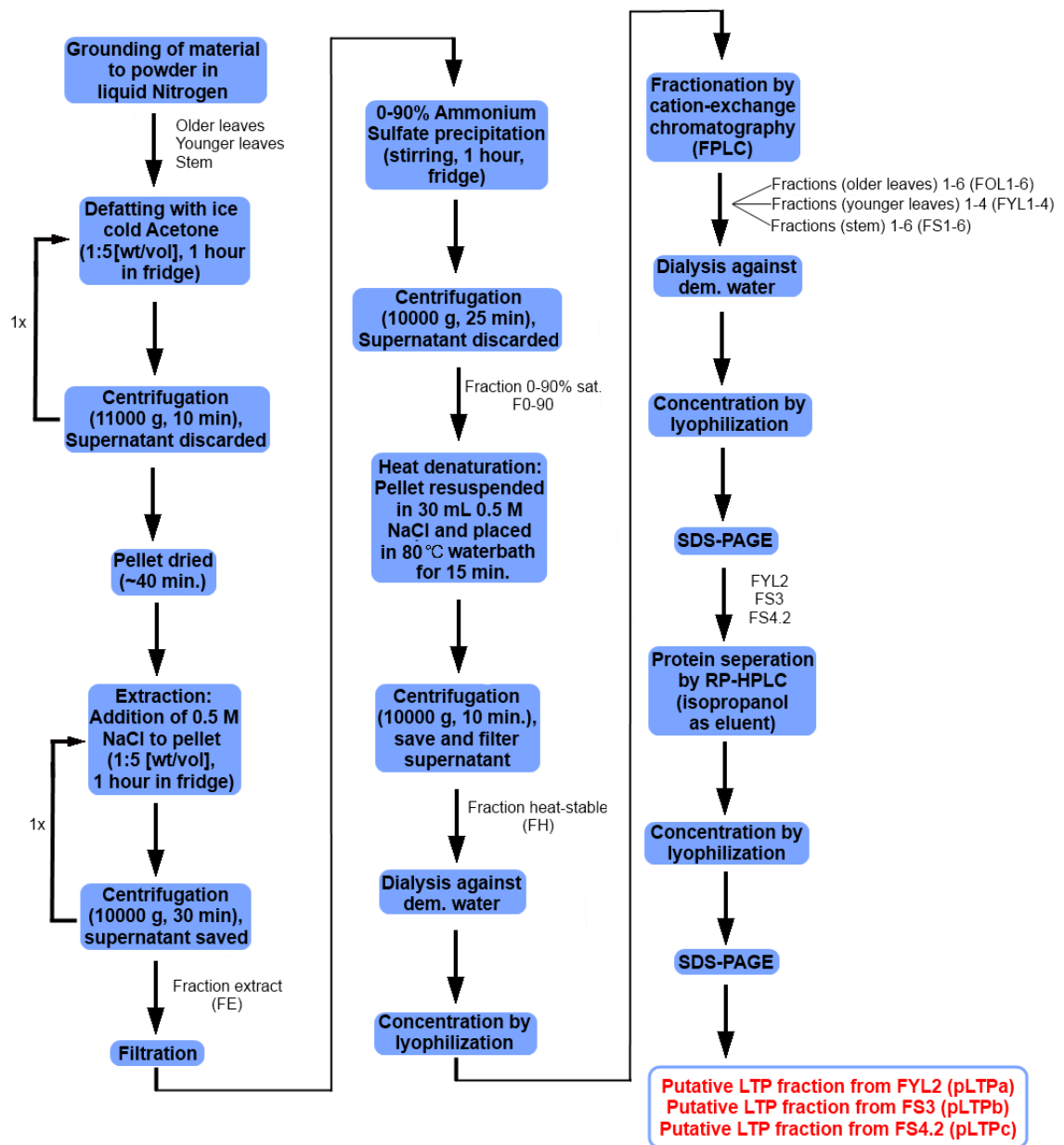


Figure 6.25: Flowchart of the developed extraction and purification protocols for isolation of putative LTPs from *Brassica oleracea* var. *capitata*.

6.3.3 Isolation of Putative LTPs

The extracted and heat-treated samples were fractionated by cation-exchange chromatography. Due to a high concentration of cationic proteins in the samples, elution was performed by applying a gradient over a broad range from 0-80% buffer B for the initial fractionation. Each fraction was subfractionated such that each subfraction contained proteins from a minimal number of peaks. The sample FOL was divided into seven subfractions; non-cationic flow through, substances eluting after 100% 1 M NaCl buffer, and FOL1-5 (Fig. 6.26, A). The sample FYL was also divided into seven subfractions; non-cationic flow through, substances eluting

after 100% 1 M NaCl buffer, and FYL1-5 (Fig. 6.26, B). Comparing the elution profiles of FOL and FYL it can be seen that the profiles appear very similar.

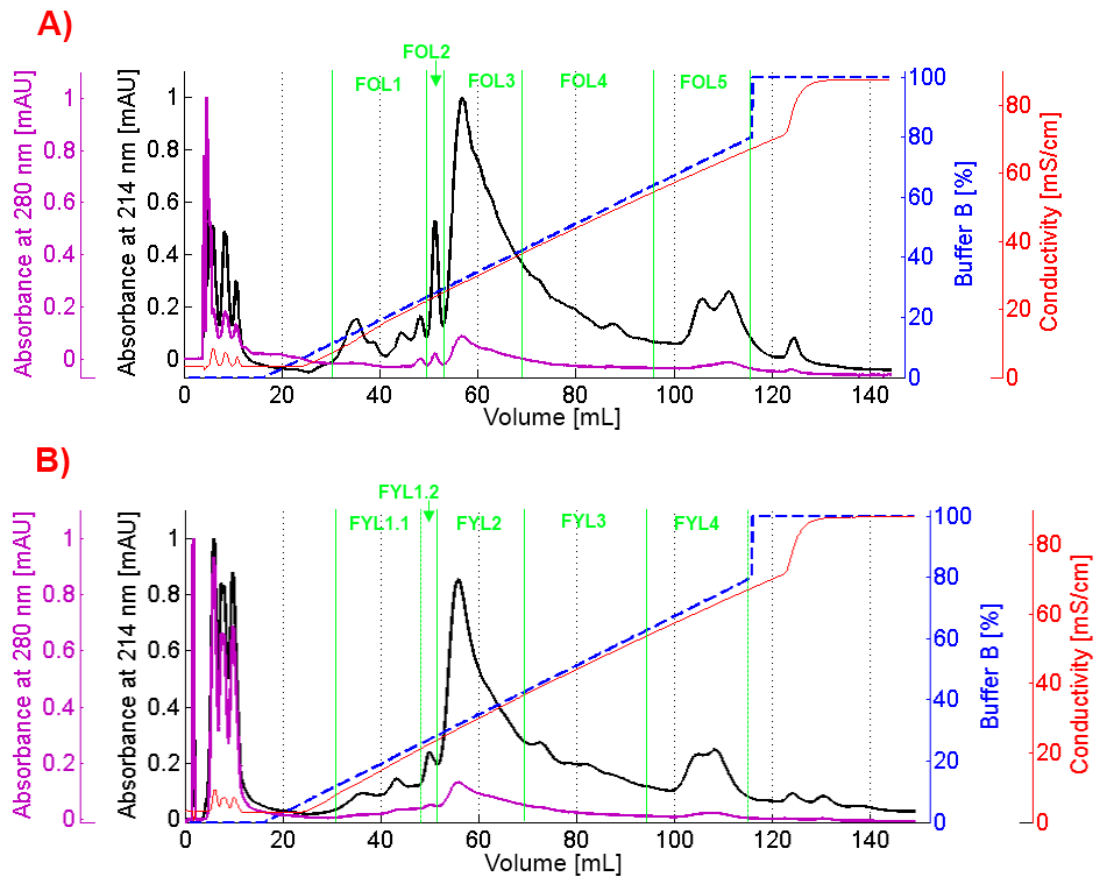


Figure 6.26: Cation-exchange chromatography of fraction older leaves (FOL) and fraction younger leaves (FYL). Fractionation was performed with a buffer containing 10 mM Tris-HCl and 10 mM NaCl (pH 4), and retained material was eluted with 1 M NaCl (buffer B) in the same buffer (4 mL/min). Percent of buffer B (blue dotted line), UV absorbance at 214 nm (black solid line), UV absorbance at 280 nm (purple solid line), and conductance (red solid line) is plotted against volume of eluent passed through the system. UV absorbance at 214 nm and 280 nm has been normalized to highest detection point. The green vertical lines indicates the division of subfractions. **A)** Cation-exchange chromatography of FOL with a linear gradient from 0-80% buffer B, and isocratic at 100% buffer B. **B)** Cation-exchange chromatography of FYL with a linear gradient from 0-80% buffer B, and isocratic mode at 100% buffer B.

The sample FS was divided into eight subfractions; non-cationic flow through, substances eluting after 100% 1 M NaCl buffer, and FS1-6 (Fig. 6.27, A). Some parts of the elution profiles of FOL, FYL and FS are quite similar. The overall profile for FS however seems to deviate from the other two. Because of the main focus on the FS fractions, a cation-exchange elution program with a more focused elution profile was in addition developed for this fraction (Fig. 6.27, B).

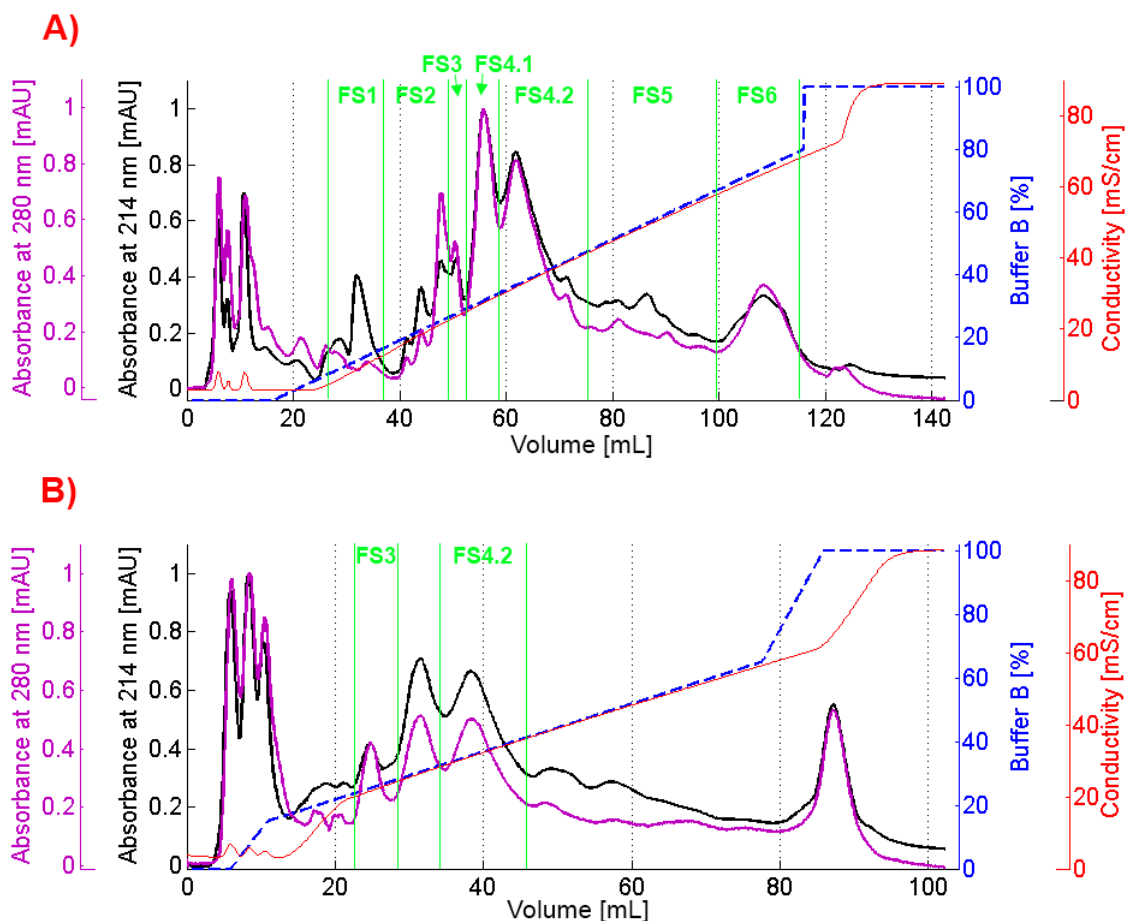


Figure 6.27: Cation-exchange chromatography of fraction stem (FS) with two different gradients. Fractionation was performed with a buffer containing 10 mM Tris-HCl and 10 mM NaCl (pH 4), and retained material was eluted with 1 M NaCl (buffer B) in the same buffer (4 mL/min). Percent of buffer B (blue dotted line), UV absorbance at 214 nm (black solid line), UV absorbance at 280 nm (purple solid line), and conductance (red solid line) is plotted against volume of eluent passed through the system. UV absorbance at 214 nm and 280 nm has been normalized to highest detection point. The green vertical lines indicates the division of subfractions. **A)** Cation-exchange chromatography of FS with a linear gradient from 0-80% buffer B, and isocratic mode at 100% buffer B. **B)** Cation-exchange chromatography of FS with a linear gradient from 0-20% buffer B, a shallower linear gradient from 20-60% buffer B, and a steep linear gradient from 60-100% buffer B.

To identify subfractions of interest, antimicrobial activity assays were initially used at this point. Radial diffusion assays (RDAs) were performed on all subfractions using *M. luteus* and *B. subtilis* (data not shown). No inhibition could be detected with these two Gram positive bacteria. It was assumed that the concentration of the target protein probably was too low, making antimicrobial assays a non-functional tool at this stage. Antifungal activity assays were also performed using *S. cerevisiae* and *F. graminearum* (not all data shown). In general, no inhibition could be detected for any of the proteins in the tested subfractions. However, one or more proteins present in the subfraction FS3 displayed inhibition of hyphal extension of *F. graminearum* (Fig. 6.28, 4), in spite of their low concentration. This result was one of the reasons for the subsequent general focus on FS.

As a result of these antimicrobial activity assays, it was realized that a different screening method was needed for selection of subfractions of interest. From this point on, subfractions were selected based on protein size by use of SDS-PAGEs. As it seemed that the cation-exchange chromatography elution profile of FOL and FYL were very similar, it was decided to continue only with one of these in order to reduce the work load. FYL was selected based on the following criteria: 1) According to literature, LTPs are found in higher concentrations in young tissue. 2) A SDS-PAGE revealed that a higher protein concentration was present in FYL within the area of interest (Fig. C.10, Appendix).

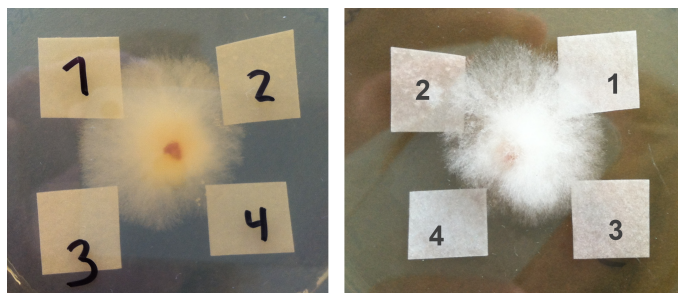


Figure 6.28: Hyphal extension inhibition assay with cation-exchange derived subfractions on the phytopathogen *Fusarium graminearum*, seen from the front and back. Less than 0.1 mg of the dialyzed and lyophilized subfractions were dissolved in 0.5 mL 10 mM Tris-HCl (pH 6). 1) 50 μ L 10 mM Tris-HCl (pH 6), 2) 50 μ L FS1, 3) 50 μ L FS2, 4) 50 μ L FS3.

SDS-PAGEs on the obtained FYL subfractions from two different extraction rounds (Fig. 6.29) revealed the presence of a protein a bit below 10 kDa in FYL2. This protein was named putative LTP a (pLTPa). Since high background and poor resolution disturbed the results obtained from a 10-20% gradient tricine SDS-PAGE (Fig. 6.29, B), a 16.5% tricine SDS-PAGE was used (Fig. 6.29, A). This 16.5% tricine SDS-PAGE revealed that at least eight other proteins were present in the FYL2 subfraction, with the most pronounced being a protein with a size of 12 kDa.

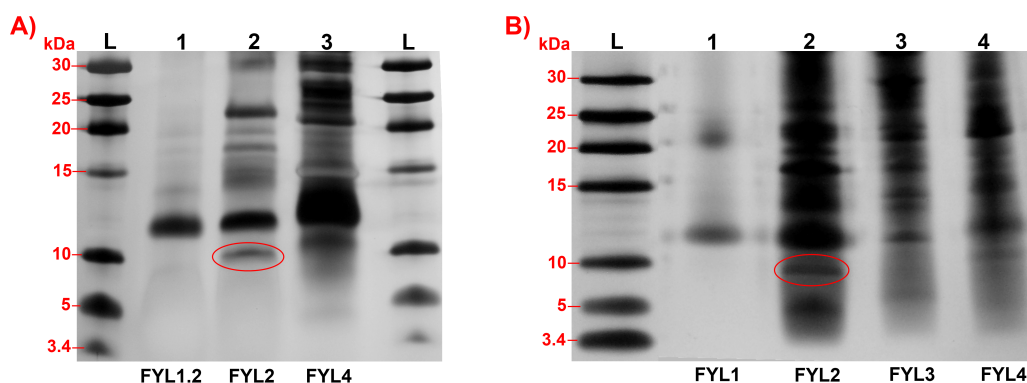


Figure 6.29: Silver stained, precast tricine SDS-PAGEs (BioRad) of the FYL subfractions obtained through cation-exchange chromatography, obtained through two separate extraction rounds. Less than 0.1 mg of dialyzed and lyophilized material were added to each well. The red circles highlight pLTPa. **A)** 16.5% tricine SDS-PAGE. L) 3 μ L PageRuler unstained Low Range protein ladder (Fermentas). 1) FYL1.2. 2) FYL2. 3) FYL4. **B)** 10-20% gradient tricine SDS-PAGE. L) 3 μ L PageRuler unstained Low Range protein ladder (Fermentas). 1) FYL1. 2) FYL2. 3) FYL3. 4) FYL4.

SDS-PAGEs on FS subfractions (Fig. 6.30, not all data shown) revealed that proteins with a size just below 10 kDa were present in FS3 and FS4.2. The protein with an approximate size of 10 kDa present in FS3 was named putative LTP b (pLTPb), while the protein with an approximate size of 10 kDa present in FS4.2 was named putative LTP c (pLTPc). Aside from the proteins of interest, a relatively high number of other proteins were also present, especially in FS4.2.

It was at this point assumed that pLTPa and pLTPc were equivalents, as they have a similar size and pI, deduced from the similar conductivity of their elution points in the cation-exchange chromatography. Furthermore it does not seem unlikely that the stem and leaf tissue contains the same protein. Because of this, the work performed after this assumption was mainly reduced to FS.

Approximately 1 mg of purified FS3 and 6 mg of purified FS4.2 (dialyzed and lyophilized) were obtained pr. 100 g of raw stem material. That is, FS3 accounts for approximately 2% of the heat-stable fraction from cabbage stem extraction, while FS4.2 accounts for approximately 11%. It is however uncertain to what extent protein was lost during the experimental procedures.

As it was observed that each of the subfractions contained around 10-30 relatively small proteins, it became clear that further purification was required.

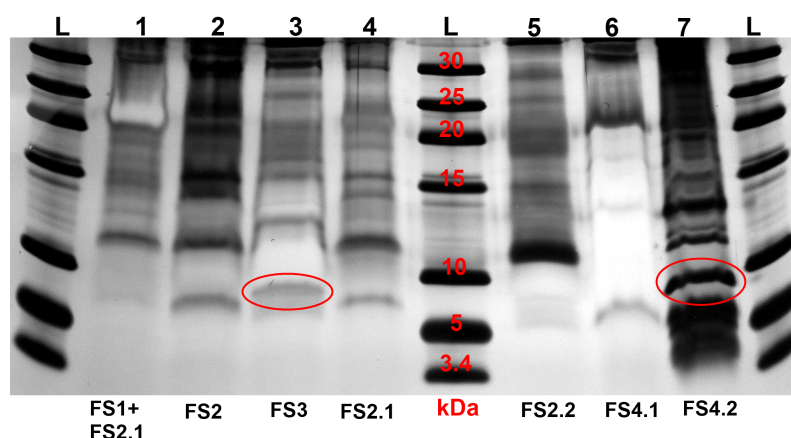


Figure 6.30: Silver stained, precast, 16.5% tricine SDS-PAGE (BioRad) of the FS subfractions obtained through cation-exchange chromatography. Less than 0.1 mg of dialyzed and lyophilized material were added to each well. The red circles highlight pLTPb and pLTPc. L) 3 μ L PageRuler unstained Low Range protein ladder (Fermentas). 1) FS1+FS2.1. 2) FS2. 3) FS3. 4) FS2.1. 5) FS2.2. 6) FS4.1. 7) FS4.2.

Aiming at purification of pLTPa, pLTPb, and pLTPc, RP-HPLC with isopropanol as eluent was performed on FYL2, FS3, and FS4.2. It is well-known that RP-HPLC may result in protein denaturation and loss of activity due to harsh conditions. However, studies have shown that LTPs are capable of maintaining their 3D structure during RP-HPLC because of their compact fold. According to literature, replacement of acetonitrile with isopropanol is beneficial for conservation of the biological activity of LTPs. Isopropanol however has six times higher viscosity than acetonitrile, resulting in a higher back pressure. To prevent a too high back pressure, a reduced flowrate of 1.25 mL/min was used with the preparative RP-HPLC column. Furthermore, isopropanol has its maximum absorbance at 204 nm, resulting in a higher background noise and

a drifting baseline for the absorbance measured at 214 nm. [122] A high and sharp peak could be detected at the gradient initiation (appearing at a retention time of 10-20 min), which was found to be caused by the applied method, since the same peak was detected without applying the sample (data not shown).

Initial RP-HPLC runs were performed using a wide gradient from 1-55% isopropanol, performed over a period of 40 min (data not shown). After identification of the peaks of interest, a focused gradient was developed. It consisted of a steep gradient from 1-16% isopropanol over 15 min, a more shallow gradient from 16-40% over 40 min, another steep gradient from 40-55% over 15 min, and finally the isopropanol level was kept at 55% over 10 min. This gradient profile was applied for all RP-HPLC runs displayed in this section. The displayed chromatograms have been corrected for the column-volume induced delay to enhance transparency, as this was approximately 15 min.

The resulting chromatogram from the focused RP-HPLC run on FYL2 (Fig. 6.31) displayed several peaks, with the majority of the proteins eluting between 23-33% isopropanol. After lyophilization, an SDS-PAGE revealed which fraction contained pLTPa (Fig. 6.33, A and B). pLTPa eluted at approximately 32% isopropanol (Fig. 6.31, F9), and the proteins present in the collected pLTPa fraction was displayed as one peak.

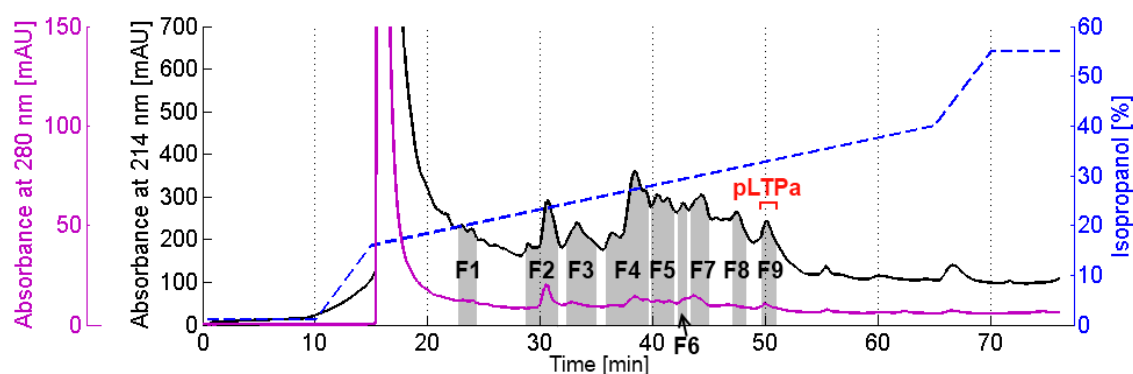


Figure 6.31: Reversed-phase high-performance liquid chromatography (RP-HPLC) with FYL2. The chromatogram was performed with 0.1% TFA and 1% isopropanol, and retained material was eluted with a isopropanol gradient with a flowrate of 1.25 mL/min. A steep gradient from 1-16% isopropanol was applied over 15 min, a more shallow gradient from 16-40% was applied over 40 min, a steep gradient from 40-55% was applied over 15 min, and isocratic mode at 55% over 10 min ended the run. Percent of isopropanol (blue dotted line), UV absorbance at 214 nm (black solid line), and UV absorbance at 280 nm (purple solid line) is plotted against retention time. The chromatogram has been corrected for the column-volume induced delay, and a zoom-in has been performed, as the high peak appearing at the gradient offset is due to background effects. The gray shading indicates the collected fractions.

RP-HPLC purification of the proteins in FS3 (Fig. 6.32) resulted in detection of several peaks, and that the majority of proteins eluted between 19-29% isopropanol. After lyophilization, SDS-PAGEs revealed the fraction containing pLTPb (Fig. 6.33, C and Fig. C.11 in Appendix). pLTPb eluted at approximately 23% isopropanol (Fig. 6.32, F2), and the proteins present in the collected pLTPb fraction was displayed as one peak.

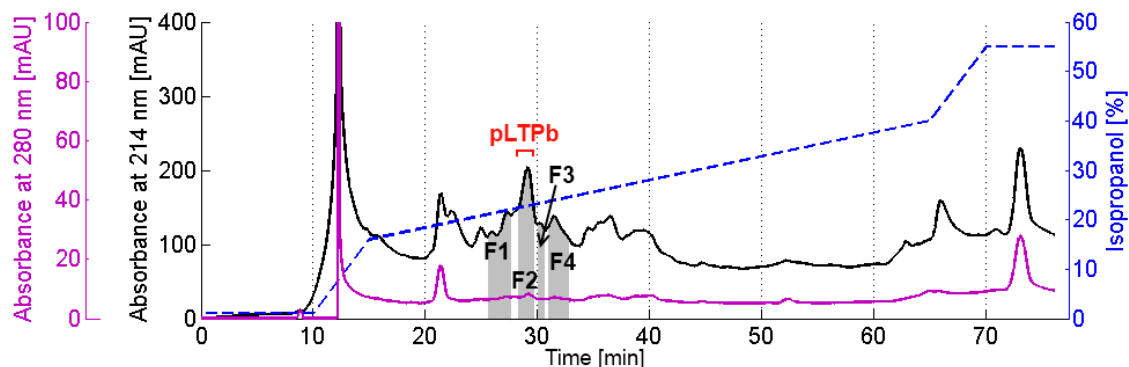


Figure 6.32: Reversed-phase high-performance liquid chromatography (RP-HPLC) with FS3. The chromatography was performed with 0.1% TFA and 1% isopropanol, and retained material was eluted with a isopropanol gradient with a flowrate of 1.25 mL/min. A steep gradient from 1-16% isopropanol was applied over 15 min, a more shallow gradient from 16-40% was applied over 40 min, a steep gradient from 40-55% was applied over 15 min, and isocratic mode at 55% over 10 min ended the run. Percent of isopropanol (blue dotted line), UV absorbance at 214 nm (black solid line), and UV absorbance at 280 nm (purple solid line) is plotted against retention time. The chromatogram has been corrected for the column-volume induced delay, and a zoom-in has been performed, as the high peak appearing at the gradient offset is due to background effects. The gray shading indicates the collected fractions.

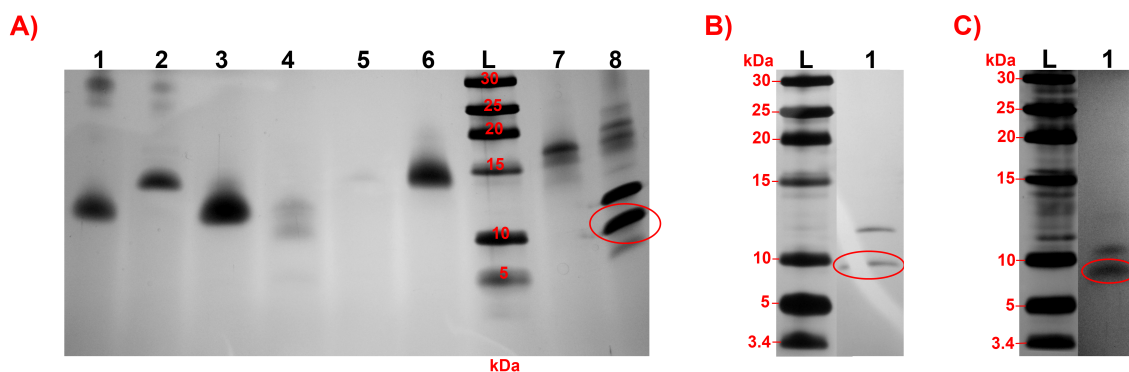


Figure 6.33: Silver stained, precast, 16.5% tricine SDS-PAGEs (BioRad) of lyophilized fractions collected from reversed-phase high-performance liquid chromatography (RP-HPLC). Less than 0.1 mg of dialyzed and lyophilized material were added to each well. The red circles highlight pLTPa and pLTPb. **A)** Fractions collected from RP-HPLC on the FYL2 subfraction. Fraction numbers are equivalent to those found on Fig. 6.31. 1) F2, 2) F3, 3) F4, 4) F5, 5) F6, 6) F7, L) 3 μ L PageRuler unstained Low Range protein ladder (Fermentas), 7) F8, 8) F9. **B)** Fraction collected from RP-HPLC on the FYL2 subfraction. L) 3 μ L PageRuler unstained Low Range protein ladder (Fermentas), 1) Fraction harboring pLTPa. **C)** Fraction collected from RP-HPLC on the FS3 subfraction. L) 3 μ L PageRuler unstained Low Range protein ladder (Fermentas), 1) Fraction harboring pLTPb. The other collected fractions from this RP-HPLC on FS3 did not reveal any visible bands after silver staining.

RP-HPLC purification of the proteins in FS4.2 (Fig. 6.34) resulted in detection of several peaks, and that the majority of proteins eluted between 19-29% isopropanol. After lyophilization, an SDS-PAGE revealed the fraction containing pLTPc (Fig. 6.35, Fig. C.11 in Appendix, not all data shown). pLTPc eluted at approximately 28% isopropanol (Fig. 6.34, F2), and the proteins present in the collected pLTPc fraction was displayed as two very close peaks.

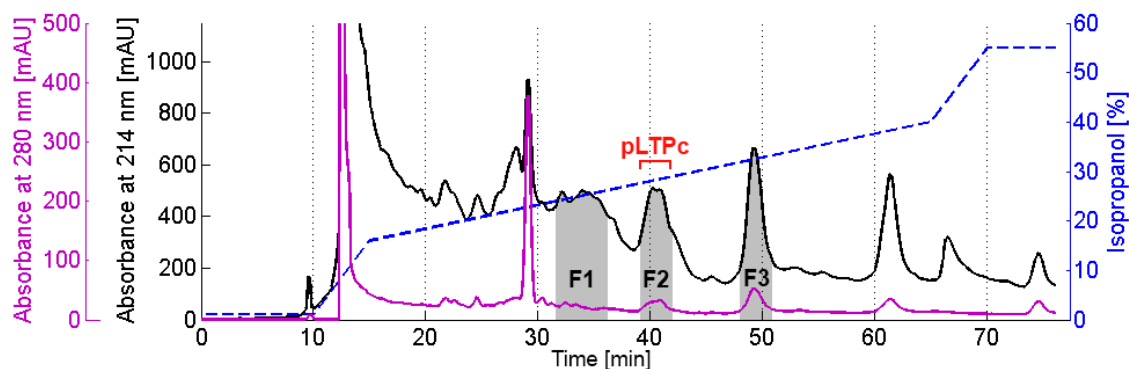


Figure 6.34: Reversed-phase high-performance liquid chromatography (RP-HPLC) with FS4.2. The chromatography was performed with 0.1% TFA and 1% isopropanol, and retained material was eluted with a isopropanol gradient with a flowrate of 1.25 mL/min. A steep gradient from 1-16% isopropanol was applied over 15 min, a more shallow gradient from 16-40% was applied over 40 min, a steep gradient from 40-55% was applied over 15 min, and isocratic mode at 55% over 10 min ended the run. Percent of isopropanol (blue dotted line), UV absorbance at 214 nm (black solid line), and UV absorbance at 280 nm (purple solid line) is plotted against retention time. The chromatogram has been corrected for the column-volume induced delay, and a zoom-in has been performed, as the high peak appearing at the gradient offset is due to background effects. The gray shading indicates the collected fractions.

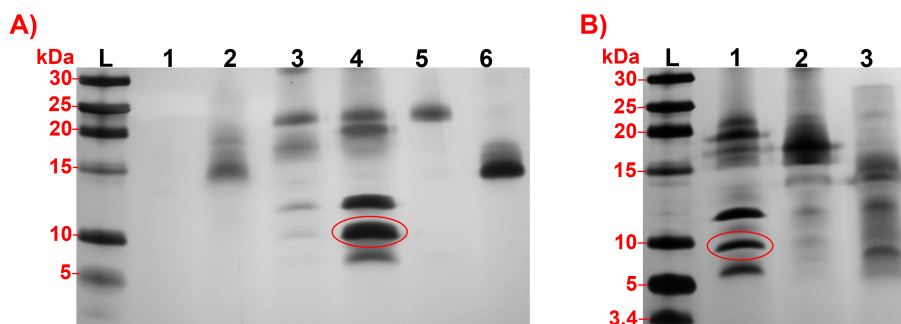


Figure 6.35: Silver stained, precast, 16.5% tricine SDS-PAGEs (BioRad) of lyophilized fractions collected from reversed-phase high-performance liquid chromatography (RP-HPLC) on FS4. Less than 0.1 mg of dialyzed and lyophilized material were added to each well. The red circles highlight pLTPc. **A)** Fractions collected from RP-HPLC on the FS4.2 subfraction. Fraction numbers are equivalent to those found in Fig. C.14 found in Appendix. L) 3 μ L PageRuler unstained Low Range protein ladder (Fermentas), 1) F1, 2) F2, 3) F3, 4) F4, 5) F5, 6) F6. **B)** Fractions collected from RP-HPLC on the FS4 subfraction. The chromatogram to match fraction numbers are not shown. L) 3 μ L PageRuler unstained Low Range protein ladder (Fermentas), 1) F1, 2) F2, 3) F3.

The shallow gradient applied in the RP-HPLC runs did not result in a resolution good enough to obtain a complete separation of individual proteins. It was initially assumed that pLTPa and pLTPc were the same protein present in both stem and leaf tissue, as both eluted at similar salt concentrations in the cation-exchange chromatography. However, as the three putative LTPs were all eluted at different isopropanol concentrations, it seems unlikely that they are identical. It is further noticed that in all of the pLTP fractions obtained from the RP-HPLCs, a protein with a size of \sim 12 kDa was present (Fig. 6.33 and Fig. 6.35). This protein was also found in the FYL2 and FS4.2 subfractions (Fig. 6.29 and Fig. 6.30). Moreover, it appeared that the FS3 subfraction also contained a high concentration of a protein around 12 kDa, as it is known that protein

overloading may result in negative staining (white bands, e.g. in the lane containing FS1+FS2.1 below 25 kDa in Fig. 6.30) when using silver staining (Fig. 6.30). In the pLTPc fraction, a protein with a size of ~6 kDa was also present. This was supported by the additional peak presenting in RP-HPLC purifications of the pLTPc fraction.

It was observed that the majority of the other proteins collected from the RP-HPLCs appeared as smeared bands on the SDS-PAGEs, or did not appear in detectable amounts at all. Many proteins are denatured when subjected to RP-HPLC due to the harsh conditions, which leaves proteins vulnerable to degradation. The small size differences resulting from such degradations could be the explanation for the smeared bands. The sharp bands representing pLTPs (and the ~6 kDa and ~12 kDa bands) indicates that these proteins have maintained their size, and possibly also their structure and activity.

The applied extraction and isolation protocols has resulted in partial isolation of three heat-stable, cationic proteins with a size just below 10 kDa from tissue of *Brassica oleracea* var. *capitata*. The amount of protein obtained from purification with RP-HPLC were too low to be quantified, illustrating the very low yield obtained from up to 260 g of raw stem material. It further appeared from the SDS-PAGEs that the pLTP-containing fractions needed further polishing to completely remove the ~6 kDa and ~12 kDa proteins, and small amounts of other proteins. Typically, remaining contaminants after two separation steps share many properties with the target protein. In this case, these proteins have similar pIs, stability, and hydrophobic characteristics. However, adding an additional purification step to the protocol comes at the cost of yield due to experimental losses. As the yield at this point was already very low, and the time frame for completion of this study was almost present, characterizations of the three fractions were performed without additional polishing.

6.3.4 Lipid Transfer Activity Assays

Lipid transfer activity assays were performed to confirm that pLTPb and pLTPc are true members of the LTP family. The conducted assay has been built on the principle of donor and acceptor membranes combined with a reporter system. Donor membranes should contain a high concentration of fluorescent C₁₂-NBD PC lipids, which is self-quenched such that fluorescence is low at the beginning of an experiment. When labeled lipid molecules are transferred into acceptor membranes, self-quenching is released and fluorescence emission from NBD is increased. This way lipid transfer activity should be detectable as a rapid increase in fluorescence intensity.

The lipid transfer activity assay was attempted several times. Initially, it was discovered that the background fluorescence were too high, as the background fluorescence counts were in the order of 10⁵⁻⁶ and no increase could be detected following addition of SDS (data not shown). It was speculated that the concentration of C₁₂-NBD PC lipids were too low in the donor membranes, causing insufficient quenching. Therefore a new vesicle batch was made using a higher amount of lipids, to make a more precise lipid composition in the vesicles. However, a similar result was obtained from this batch of prepared vesicles. Both pLTP fractions and SDS were added, but no fluorescence intensity changes could be observed (data not shown).

At this point it was assumed that too many non-quenched NBD-lipids were present in the donor vesicle solution. It was therefore attempted to get rid of these by applying the donor vesicle solution to a desalting column. This column is packed with a matrix that excludes solutes greater than 6 kDa, allowing them to elute in the void volume. Seven fractions were collected, with the latter three having a bright yellow color. The fractions were subjected to fluorescence spectroscopy, with excitation at 475 nm and emission measured by two channels at 530 nm. Background fluorescence was monitored, and 100 μL 10% SDS was added to measure the fluorescence intensity when all fluorophores were de-quenched (not all data shown). Donor vesicle fraction 3 and 4 showed satisfyingly low background fluorescence, with a high fluorescence increase upon addition of SDS (Fig. C.15, Appendix, not all data shown). In general, the fluorescence intensity of fraction 4 was higher than that of fraction 3. After addition of acceptor vesicles, the fluorescence intensity of fraction 4 became significantly higher (data not shown), and fraction 3 was therefore chosen for the subsequent assays.

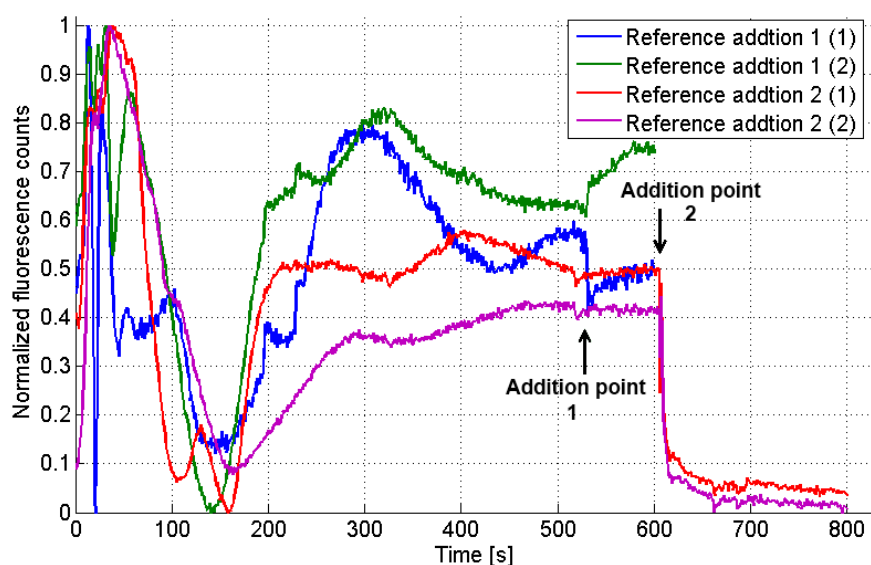


Figure 6.36: Time resolved fluorescence plot of emission measured for 2 mL 10 mM HEPES buffer (pH 7.3), 20 μL acceptor vesicles and 30 μL diluted donor vesicles, without addition of pLTP fractions. As a reference, addition of 15 μL HEPES buffer was performed (black arrows). Fluorescence was excited at 475 nm and emission measured by two channels at 530 nm. The fluorescence intensity has been normalized to the highest detection point of the individual measurements.

Time resolved fluorescence plots with excitation at 475 nm and emission measurement by two channels at 530 nm were made with 2 mL 10 mM HEPES buffer (pH 7.3), 20 μL acceptor vesicles and 30 μL diluted donor vesicles. These amounts were estimated to ensure an over-representation of acceptor vesicles, which is necessary to decrease self-quenching of transferred C_{12} -NBD PC lipids. Reference measurements were performed with addition of 15 μL HEPES buffer instead of pLTP fractions (Fig. 6.36, addition at black arrows, not all data shown). A relatively stable and similar baseline was expected for the emission plots. This is however not observed. In all the experiments performed almost the same fluctuation pattern was observed, with characteristic peaks and valleys. Furthermore, the two channels measuring emission at 530 nm did not always agree. The origin of this behavior is unknown, and such fluctuations do not provide a solid base for the assay. The problem could not be resolved within the time

frame of the present study, and it was therefore attempted to perform the assay in spite of these issues. Ideally, curves should be normalized to the fluorescence intensity obtained when the total amount of fluorophores incubated with the acceptor membranes were de-quenched (addition of SDS). However, as the fluorescence intensity varied significantly between different measurements, this approach was not feasible. The fluorescence intensity has therefore been normalized to the highest detection point of the individual measurements.

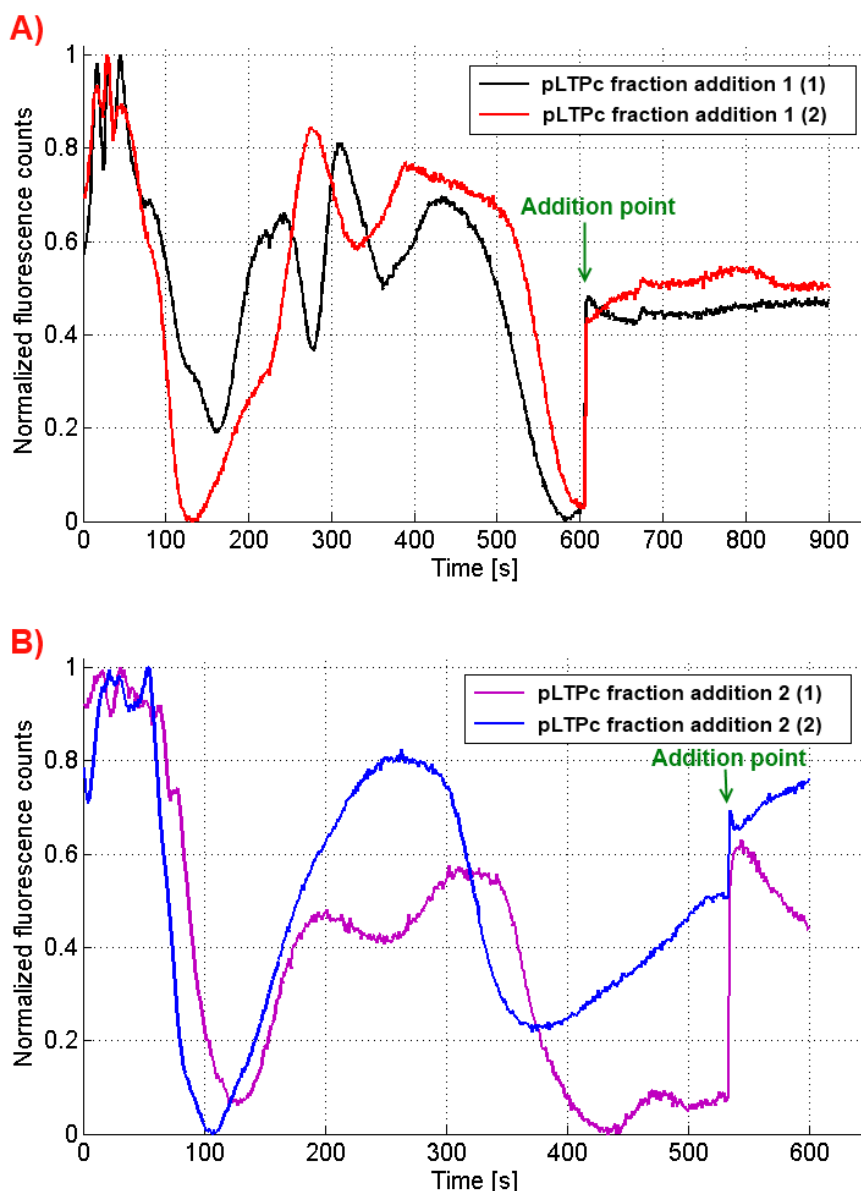


Figure 6.37: Time resolved fluorescence plot of emission measured for 2 mL 10 mM HEPES buffer (pH 7.3), 20 μ L acceptor vesicles and 30 μ L diluted donor vesicles, with the addition of pLTPc fractions (green arrows). Fluorescence was excited at 475 nm and emission measured by two channels at 530 nm. The fluorescence intensity has been normalized to the highest detection point of the individual measurements. **A)** Measurement with addition of pLTPc fraction, conducted over a period of 900 s. **B)** Measurement with addition of pLTPc fraction, conducted over a period of 600 s.

The general behavior observed after addition of the 15 μL HEPES buffer (reference) is a decline in fluorescence intensity (Fig. 6.36, addition at black arrows), which is consistent with a dilution of the fluorophores. However, reference addition 1, channel 2 (green line) does not agree with the other measurements. Strangely, this channel measures a slight increase in emission, while channel 1 measures a slight decrease. This could however be a result of insufficient mixing. Furthermore, the decline in fluorescence intensity observed for reference addition 2 seems excessive.

Time resolved fluorescence plots of the 2 mL 10 mM HEPES buffer (pH 7.3), 20 μL acceptor vesicles and 30 μL diluted donor vesicles were measured with addition of 15 μL pLTPc fraction (Fig. 6.37, A and B, addition at green arrows). Additions were performed when the curves became somewhat stable, and the two separate addition points were a bit shifted to limit the influence of the overall fluctuations. In both experiments the addition of the pLTPc fraction resulted in a rapid increase in fluorescence. It should be kept in mind that a ~ 10 -15 s break in the measurements were applied during the addition of the pLTPc fractions, which means that the curves in reality should be shifted a bit to the right, making this increase less sharp. The observed increase in fluorescence was the expected result of the addition of an active LTP to the mixture. However, due to the general strange behavior of the emission measurements, these results seemed uncertain at best. Furthermore, a strange disagreement between the emission measurements from the two channels was again observed following the fluorescence increase from one of the measurements (Fig. 6.37, B).

Additional measurements to confirm the observed tendency after addition of the pLTPc fraction were desirable, but unfortunately not durable within the time frame because of unavailability of pLTPc fractions.

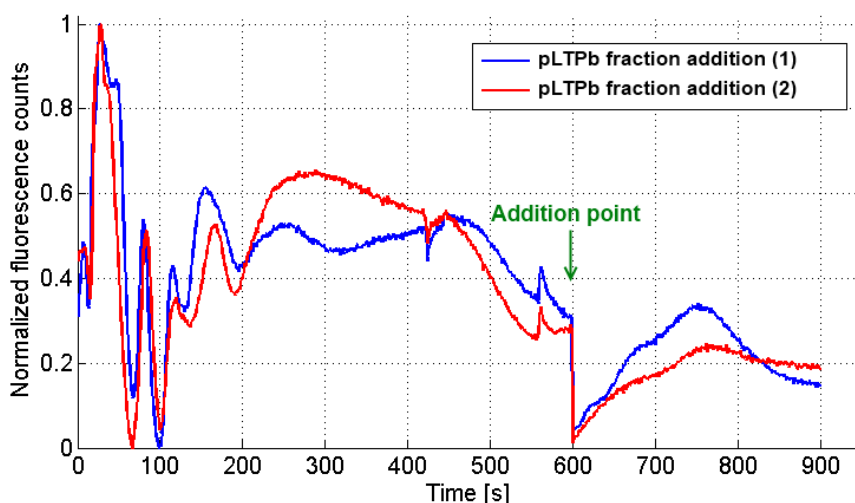


Figure 6.38: Time resolved fluorescence plot of emission measured for 2 mL 10 mM HEPES buffer (pH 7.3), 20 μL acceptor vesicles and 30 μL diluted donor vesicles, with the addition of pLTPb fraction (green arrow). Fluorescence was excited at 475 nm and emission measured by two channels at 530 nm. The fluorescence intensity has been normalized to the highest detection point of the individual measurements.

Time resolved fluorescence plots of 2 mL 10 mM HEPES buffer (pH 7.3), 20 μ L acceptor vesicles and 30 μ L diluted donor vesicles were measured with addition of 15 μ L pLTPb fraction (Fig. 6.38, addition at green arrow). Strangely, the addition of the pLTPc fraction resulted in a rapid decrease in fluorescence, followed by a slow increase. This pattern was inconsistent with the one observed for pLTPc, and the decrease seemed too excessive to be explained by dilution. These inconsistencies further underline the uncertainties of the performed assay, and the presence of lipid transfer activity has therefore not been conclusively confirmed or disproved by the conducted assays.

6.3.5 Antimicrobial Activity Assays

Antimicrobial activity assays were conducted to investigate if any antimicrobial activity could be detected in the pLTP fractions. As earlier described, LTPs mainly have activity against fungi and sometimes Gram positive bacteria, and microbes fitting into these parameters were therefore chosen for the assays. RDAs were performed on 0.8% agarose plates with two different Gram positive bacteria: *M. luteus* and *B. subtilis*. The bacteria were molded into plates, and wells were made for the placement of samples. Antifungal activity assay were made with the yeast *S. cerevisiae* and the plant pathogenic fungi *Fusarium graminearum*. The antifungal activity assay with *S. cerevisiae* were made according to the RDA protocol, while the hyphal growth of *F. graminearum* required a different approach. In this case, the sample was placed on top of a Whatman no. 1 filter paper, while the fungal spores were placed in the center of the plate resulting in radial extension of hyphae after germination.

Antimicrobial assays were performed on selected fractions collected from RP-HPLC. Unfortunately, the yield of proteins in individual fractions was too low to be quantified, indicating an amount below 0.1 mg pr. fraction was obtained. 7% of this yield dissolved in 40 μ L Tris-HCl (pH 6) were used for each of the RDAs, while 40% dissolved in 60 μ L Tris-HCl (pH 6) were used for each antifungal assay with *F. graminearum*.

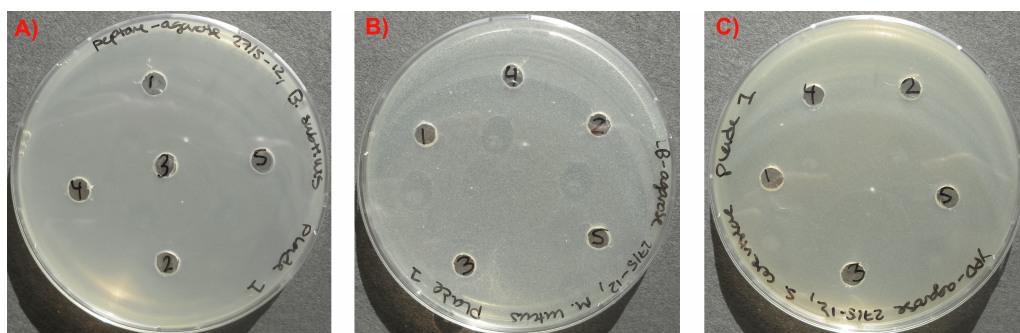


Figure 6.39: Radial diffusion antimicrobial activity assays on collected lyophilized fractions from RP-HPLC with FS4.2. Numbering of FS4.2 fractions is equivalent to Fig. 6.34 and Fig. C.11. **A)** RDA with the Gram positive bacteria *B. subtilis*. 1) 40 μ L Tris-HCl (pH 6). 2) 40 μ L 0.1% TFA. 3) 40 μ L FS4.2 F1. 4) 40 μ L FS4.2 F2 (pLTPc). 5) 40 μ L FS4.2 F3. **B)** RDA with the Gram positive bacteria *M. luteus*. 1) 40 μ L Tris-HCl (pH 6). 2) 40 μ L 0.1% TFA. 3) 40 μ L FS4.2 F1. 4) 40 μ L FS4.2 F2 (pLTPc). 5) 40 μ L FS4.2 F3. **C)** RDA with the yeast *S. cerevisiae*. 1) 40 μ L Tris-HCl (pH 6). 2) 40 μ L 0.1% TFA. 3) 40 μ L FS4.2 F1. 4) 40 μ L FS4.2 F2 (pLTPc). 5) 40 μ L FS4.2 F3.

The RDAs were performed with F1, F2 (pLTPb), F3, and F4 collected from the RP-HPLC with FS3 (numbering relative to Fig. 6.32). No antimicrobial activity for any of these fractions could be detected against these microbes (data not shown). RDAs were also performed with F1, F2 (pLTPc), and F3 collected from the RP-HPLC with FS4.2 (numbering relative to Fig. 6.34). No antimicrobial activity for any of these fractions could be detected against these microbes (Fig. 6.39).

Antifungal activity assays were performed with *F. graminearum* on F1 and F2 (pLTPb) collected from the RP-HPLC with FS3 (numbering relative to Fig. 6.32). No true hyphal extension inhibition could be detected after the hyphae had extended to the filters (Fig. 6.40, A, not all data shown). The antifungal activity assay performed similarly on F2 (pLTPc) and F3 collected from the RP-HPLC with FS4.2 (numbering relative to Fig. 6.34), did not either reveal any true activity (Fig. 6.40, B, not all data shown). In these antifungal assays, the fractions were not added to the plates until after spore germination. The plates were then left to grow for three additional days.

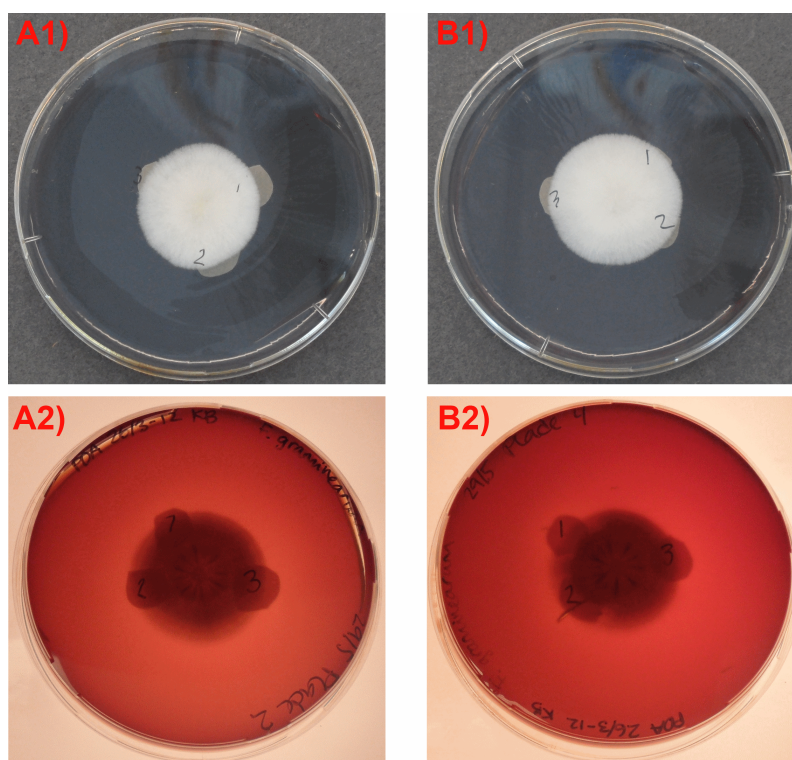


Figure 6.40: Hyphael extension inhibition assay with the pLTPb and pLTPc fractions with the phytopathogen *Fusarium graminearum*. Front pictures are taken from an angle to avoid reflections. **A1)** Front of antifungal activity assay with pLTPb. **A2)** Backside of antifungal activity assay with pLTPb with numbering relative to Fig. 6.32. 1) 60 μ L Tris-HCl (pH 6), 2) 60 μ L 0.1% TFA, 3) 60 μ L pLTPb fraction (FS3 F2). **B1)** Front of antifungal activity assay with pLTPc. **A2)** Backside of antifungal activity assay with pLTPc with numbering relative to Fig. 6.34. 1) 60 μ L Tris-HCl (pH 6), 2) 60 μ L 0.1% TFA, 3) 60 μ L pLTPc fraction (FS4.2 F2).

No antimicrobial activity against the four microbes tested could be detected for neither the pLTPb fraction nor the pLTPc fraction. This finding was done in spite of antifungal activity being present in the FS3 fraction.

7.1 Theoretical Characterizations of LTP5 and LTP8

Tertiary structure models of LTP5 and LTP8 were created by use of the automated protein homology modeling server "SWISS-MODEL", with the assumption that they both are members of the LTP family 1. The LTP5 model was build with the LTP structure 1fk5.pdb as template, while LTP8 was build with the LTP structure 1bwo.pdb as template.

LTP5 shares 49% sequence identity with the amino acid sequence of its template LTP, while LTP8 only shares 34% sequence identity with its template. Due to the construction principle used in homology modeling, the quality of models is critically dependent on the target-template sequence alignment. The 49% sequence identity of LTP5 and its template is barely within the range recommended for simple homology modeling, while the 34% sequence identity of LTP8 and its template is usually considered too low. However, as all members of the LTP family 1 that has been characterized so far have been found in a strictly conserved all- α -type fold, it seems fair to model the 3D structure of LTP5 and LTP8 with these templates. Furthermore, the conserved LTP type 1 cysteine motif has been found to function as a crucial underlying scaffold for the LTP 3D structure, and therefore provides a reliable frame for the sequence alignment. In general, the overall fold is moreover often conserved between evolutionary related proteins, even when they have diverged significantly in their primary sequence. The relatively low sequence identities between the targets and their templates should however be kept in mind when considering the reliability of the LTP5 and LTP8 model.

"SWISS-MODEL" rank suggested model templates by sequence identity, and favor high resolution template structures with reasonable stereochemical properties as assessed by ANOLEA mean force potential and Gromos96 force field energy. In case of the LTP5 model, the template suggestion with the highest sequence identity was used as template. However, in the case of LTP8, a template with a lower sequence identity to LTP8 was chosen, as it resulted in significantly better validation scores. An important limitation of the LTP8-template alignment was that the template sequence is two amino acids shorter than LTP8. The optimal alignment resulted in that the first and last amino acid (alanine and glycine, respectively) of LTP8 was not included in the 3D model. None of these amino acids are charged or usually conserved among members of the LTP 1 family, and it was therefore assessed that their absence did not significantly limit the validity of the 3D model for the objective at hand.

Both of the tertiary structure models displayed LTP type 1 characteristic features. They consisted of a single compact domain, through which a tunnel ran. The tunnel was delineated with conserved hydrophobic amino acids, providing it with a hydrophobic environment suitable for binding of lipids. The conserved disulfide bonding pattern was observed in both models, along with the characteristic all- α -type secondary structure with a C-terminal tail. Moreover, a conserved tyrosine (position 82) was found at the larger entrance of the LTP5 model, which is believed to be involved in stabilizing the lipid binding. These LTP structure consisten-

cies support that these two proteins belong to the LTP type 1 family, and that they are capable of binding lipids *in vitro*. It was noticed that the amino acid composition of the tunnel was largely conserved, while the non-conserved amino acids were mainly located at the surface of the structure. For example, all charged residues were found in solvent-accessible positions, even though the content of these varied significantly between LTP5 and LTP8. These observations seem consistent with the conservation of the ability to bind lipids of all characterized LTPs (except Ace-AMP1), while these LTPs at the same time often display different additional biological activities and are expected to fulfill different biological roles. It therefore may be that the functionality of different types of LTPs are encoded by the amino acid composition at the surface of the protein, while the specific fold provides a convenient, exceptionally stable carrier for the different activities. The different activities of diverse LTPs could be imagined to be secondary functions acquired through evolution of proteins having some kind of role in lipid transport.

The validation scores of the LTP8 model were in general poorer than those of LTP5. This is not surprising when taking the significantly lower target-template sequence identity into account. In the MUSTANG alignment, low backbone ($C\alpha$) RMSD scores were obtained for both models, indicating that the model structures have a very similar composition to that of their templates. In general, a better agreement between the secondary structure elements than between the intermediate loops and C-terminal regions were observed. This is not surprising, but it should be kept in mind that these regions represent areas of less confidence.

The Ramachandran plots of both models resulted in scores equivalent with good quality models. Surprisingly, the LTP8 model scored better than the LTP5 model. Only one amino acid (Ser₂₀) was found in the generously allowed region in the Ramachandran plot of LTP8. This amino acid was located in the loop connecting H₁ and H₂, which was also found to deviate from the template in the MUSTANG alignment because of an additional amino acid in LTP8 compared to the template in this loop. The validity of the conformation of Ser₂₀ in the LTP8 models was therefore questionable. Arg₂₀ and Cys₂₈ was found in generously allowed regions in the Ramachandran plot of LTP5. That is, position 20 in the loop connecting H₁ and H₂ was a problematic position in both models.

The QMEAN6 scores of the LTP5 model mainly revealed issues with the burial status of the residues and the local backbone geometry. Especially the latter resulted in a relatively low Z-score, which was surprising compared to the result of the Ramachandran plot. However, all of the six individual terms were found within an acceptable range, and the global QMEAN6 score was a little below the average obtained for high-resolution structures. The QMEAN6 scores of the LTP8 model also mainly revealed issues with local backbone geometry, and some issues with solvent accessibility agreement. The global QMEAN6 score of the LTP8 model was poorer than that of the LTP5 model, but still within an acceptable range.

The 3D structure models of LTP5 and LTP8 were created with the objective of investigating the strength and spatial distribution of their electrostatic potential. Overall, both models were believed to have a high enough reliability for the objective at hand; however, minor reservations should be kept in mind. Circumstantial evidence for the notion that the antimicrobial activity of some LTPs may be mediated by electrostatic interactions with anionic membrane phospholipids have been presented in several studies [42], [44], [46], [4], [10]. Furthermore, it has been suggested that the ability of LTPs to discriminate between cell types may be connected to the

diverse composition and distribution of phospholipids with varying charge characteristics in different cell type membranes [42]. With these findings in mind, it seems likely that the electrostatic properties of LTPs are a crucial determinant when it comes to antimicrobial activity. It should however be kept in mind that since LTPs have the ability to transfer lipids between model membranes, the evidence of interactions with lipid membranes may not be related to a possible antimicrobial activity. It is however remarkable, that the most potent LTP discovered till now (Ace-AMP1) have an unusual high pI above 11, while not being capable of binding lipids. This indicates that high pI may be correlated with high antimicrobial potency.

The calculation and visualization of the electrostatic potentials of the LTP5 and LTP8 models revealed significant differences. The LTP5 model generated a predominantly positive potential, and was almost completely wrapped in this positive potential with only a few negative areas near H₃. The spatial distribution of the electrostatic potential appeared very similar to the one found for Ace-AMP1 in the study by Gomar et al. [30]. The model of Ace-AMP1 was in this study found to be wrapped in a positive potential, with two negative areas found in the area close to H₃. LTP5 and Ace-AMP1 furthermore share related characteristics such as pIs above 11 and an arginine rich primary structure. The potent antimicrobial activity of Ace-AMP1 may be related to strong electrostatic interactions with microbe membranes. It has been speculated that this arginine-rich protein may be interacting electrostatically with negatively charged headgroups of phospholipid membranes, and this way perhaps initiate some kind of membrane permeabilization. The shared spatial distribution of the electrostatic potential and arginine-rich structure of Ace-AMP1 and LTP5 may indicate that LTP5 interacts with membranes in a similar way to Ace-AMP1. A major difference between the two proteins is however that Ace-AMP1 has a C-terminal extension of 12 amino acids. It is unknown what kind of influence this LTP abnormality has on the activity of Ace-AMP1. Furthermore, Ace-AMP1 possess several additional charged amino acids besides the arginines, which may also influence its activity.

Gomar et al. questions whether Ace-AMP1 should be classified as an LTP. They do this partly because of the missing lipid transfer ability and the C-terminal extension, but also because of the dissimilar spatial distribution of the electrostatic potential. However, it has in the present study been shown that another LTP with a more LTP-characteristic structure has a very similar electrostatic potential distribution. Experimental studies are however crucial to determine the 3D structure of both Ace-AMP1 and LTP5, whether LTP5 are capable of transporting lipids *in vitro* (and thereby are a true LTP), and if LTP5 have a similar antimicrobial activity as that of Ace-AMP1.

The LTP8 model was in the present study found to generate both a negative potential area and a positive potential area, fitted together in a similar way to the patches of a tennis ball. A slight domination of the negative potential was overall observed for the LTP8 model, consistent with its slightly anionic pI of 4.9. To the knowledge of the author, no tertiary structures or electrostatic calculations of anionic LTPs have been published in literature, making present study the first structural investigation of this LTP type. Compared to LTP5, LTP8 had a spatial electrostatic potential distribution that was more similar to that of the maize LTP, however with a much more dominating negative potential. It was expected that a positive potential would be found at the larger entrance of the hydrophobic tunnel to facilitate the initial interaction with negatively charged lipids. However, a mainly negative potential was found around this entrance, with only a few positive patches (Fig. 6.10, A). It remains unresolved from these data if interactions with negatively charged lipids are possible with this potential distribution at the entrance. In

the study by Gomar et al. [30] it was however found that one or two positive potential areas between the second loop and the C-terminal tail was the sole conserved electrostatic potential area between three LTPs capable of transporting lipids *in vitro*. The placement of these positive areas was consistent, however more widely distributed, with the ones observed at the tunnel entrance of the LTP8 model. The conservation of the placement of these positive potential patches indicates their involvement in the lipid binding process, and therefore suggests that LTP8 are capable of binding lipids. This speculation however needs to be investigated further with molecular dynamics simulations, or by experimental studies. Likewise, it is unknown if LTP8 or other anionic LTPs displays antimicrobial activity, or what their putative biological role may be.

The spatial distributions of the electrostatic potential were clearly different for the LTP5 and LTP8 model. The LTP5 model generated a mainly positive electrostatic potential with an almost equal distribution throughout its solvent accessible surface, while LTP8 had a solvent accessible surface divided in potentials with opposite signs. The only similarity observed was that the least dominating potential was most present around H₃, meaning that a potential of opposite sign was found at this position in the two models. The electrostatic potential is important in charge interactions between two closely positioned molecules. It therefore seemed unlikely that two proteins with such different electrostatic properties exhibit a similar mode of action. The obtained results indicated that LTP5 may interact with lipids in a similar way to that of Ace-AMP1, and perhaps therefore have antimicrobial activity comparable with that of Ace-AMP1. The activity and mode of action of LTP8 is unknown, but expected to be different. Experimental studies are however crucial for characterizing these proteins. It seems highly interesting to investigate the differences in properties between these two proteins which appear to have a similar global fold, but with different surface characteristics. Following experimental characterizations, comparisons with the obtained theoretical characterizations could perhaps lead to the inferring of a structure-function relationship.

7.2 Recombinant Expression of LTPs in *P. pastoris*

Based on screenings at DNA level it was believed that the PIC-LTP5 or PIC-LTP8 constructs had been correctly integrated into the chromosomes of both *P. pastoris* strains. It could however not be excluded that mutations had occurred in the constructs, however, the construct sequences were validated by DNA sequencing prior to transformations into *P. pastoris*. Only one PIC-LTP5 and one PIC-LTP8 *P. pastoris* SMD1168H transformant was obtained when using the same protocol as applied for the wild-type X-33 strain. This indicates that transformation by use of electroporation is more delicate when dealing with the protease deficient strain, which is also supported in literature [123], [124]. It is recommendable to test the expression level of several transformants, which was not possible due to this low transformant yield.

Expression studies in shake flask cultures with all transformant types were conducted, applying different conditions. The initial expression studies with *P. pastoris* X-33 transformants employing standard conditions and a relatively high start OD, appeared to result in a low protein concentration, a high salt/protein ratio, and no detectable LTP5 or LTP8 accumulation. Low-

ering of temperature, start OD and expression time resulted in a higher protein concentration in the supernatant. Proteolytic activity as well as the general yeast machinery is slowed down at temperatures below the optimal [79], and a lower amount of dead (and subsequent lysed) cells is expected from a decreased start OD and expression time. That these changes resulted in a higher protein concentration therefore points at proteolytic degradation as a major player in the culture supernatant of the *P. pastoris* X-33 transformants. In support of this, current literature states that the most common problem encountered with secreted expression in *P. pastoris* is proteolytic degradation [80], [79]. As a consequence of these findings, several different measures were taken to further address this putative problem. One of these were the transformation of the PIC-LTP5 and PIC-LTP8 constructs into the protease-deficient *P. pastoris* SMD1168H strain. A higher protein concentration in the supernatant was obtained with these transformants, supporting significant proteolytic activity in the X-33 supernatant. However, a clear prove of accumulation of LTP5 or LTP8 was still not present.

In a final attempt to eliminate the putative proteolytic degradation of the proteins of interest, two protease inhibitors were added during and after expression studies with both types of strains. PMSF inhibits cysteine and serine proteases [125], such as trypsin-like serine proteases that cleaves peptide bonds following a positively charged amino acid, which especially can be found at the surface of LTP5. EDTA inactivates metalloproteases [125], which may both be endo- and exopeptidases. The combination of these two protease inhibitors has in a study by Sinha et al. [86] been found to reduce the total protease activity on a specific substrate by 94%. Addition of these protease inhibitors was however potentially problematic, since PMSF is extremely unstable when unbound in aqueous solutions and toxic to cells [89]. This meant that frequent additions of this compound were necessary, with the potential risk of high toxicity. It therefore may be that the addition of PMSF increased cell death (and lysing) and/or induced cell stress, resulting in an up-regulation of protease expression, and possibly a higher protease release to the culture medium through lysing or leakage. Addition of PMSF during the expression may therefore potentially lead to an opposite effect than the intended. It was however found that the overall growth of the cultures was not noticeably affected by PMSF in the present study. In the expression studies with addition of protease inhibitors, the induction frequency was also increased while the total amount of methanol added was kept constant. It was expected that this resulted in less methanol toxicity from the media, while the induction level was conserved. No direct positive effect of this was however observed on the overall growth curves. It is though unknown if the opposite effects of PMSF and less methanol in the media could have balanced each other out, especially when considering the coarseness of these curves. In addition to the above issues, protease inhibitors may inhibit specific amino acids found in active sites of proteins in general, such as a putative active site of the produced proteins of interest.

In general, proteases in *P. pastoris* is not well characterized [126], however, the major vacuolar proteases in *P. pastrois* are believed to be proteinase A (PrA, aspartic protease), proteinase B (PrB), carboxypeptidases, and aminopeptidases. [86], [126] Of these it has been found that PMSF inhibits PrB and carboxypeptidases, while EDTA inhibits aminopeptidases [86]. Aspartic proteases are often most active in the cleavage of peptide bonds between two hydrophobic residues [127]. This protease is encoded by *pep4*, which has been knocked out in the SMD strain [71], resulting in that all of these major proteases should be targeted in the expression studies of SMD1168H transformants with addition of PMSF and EDTA. However, it is unknown if the inhibited proteases are capable of attacking LTP5 or LTP8, or if other uncharacterized *P. pa-*

storis proteases in reality should have been targeted instead. In spite of a seemingly increased protein concentration in the supernatant, a clear conformation of the presence of LTP5 or LTP8 could not immediately be identified following the above shake flask expression studies. It is impossible to predict with certainty if these two LTPs are vulnerable to (a) certain *P. pastoris* protease(s). However, when considering the general characteristics of LTPs, it seems improbable that correctly folded versions of LTP5 and LTP8 would be subjected to proteolytic degradation, as LTPs are known to be exceptionally stable and resistant to proteolytic degradation by some proteases. Furthermore, none of the literature reporting expression of LTPs in *P. pastoris* describe problems with proteolytic degradation. Because of this and the lacking effectiveness of lowering the protease activity in the supernatant, it is believed that the missing accumulation of LTP5 and LTP8 was not mainly caused by proteolytic degradation.

Fermentation of *P. pastoris* may result in a significantly higher product yield, because of the controlled environment, high cell densities, and utilization of different batch techniques. Furthermore, studies with expression of wheat and fruit LTPs in *P. pastoris* have shown that the highest product accumulation was achieved after 96 hours of induction. [118], [51], [119] It was therefore assumed that a prolonged duration of the expression study could result in a higher yield. The PIC-LTP5 *P. pastoris* SMD1168H transformant was chosen for the fermentation study because of SDS-PAGEs indicating that the highest protein concentration in the area of interest was obtained with this transformant, and because of easy detection of LTP5 with cation-exchange chromatography. Furthermore, the protease deficiency of this transformant seemed to be an advantage in high cell density fermentation studies. The overall higher protein level in the expression supernatant may however be considered a disadvantage in downstream purification. If correctly folded versions of LTP5 and LTP8 could be obtained, their resistance to proteases released to the *P. pastoris* supernatant could be tested, and used to minimize the downstream purification load. However, because of the above stated advantages, the PIC-LTP5 *P. pastoris* SMD1168H transformant was chosen for the fermentation study in the present work.

The fermentation study was hampered by different problematic issues. A rapid increase in the dissolved oxygen level was expected when the glycerol had been exhausted, because the depletion of carbon sources should result in ceasing of culture growth. This oxygen response should therefore serve as an indication for a suitable methanol induction start. The rapid increase in oxygen level was however not detected, even though it was observed that the culture had ceased to rise in density. Overall, an inconsistency between the course of the dissolved oxygen level and the growth curve of the culture were obtained after the initial growth. It was besides the rapid increase in oxygen level expected that periods with high growth rate would result in a decline in the dissolved oxygen level, whereas static periods would result in constant or increasing levels of dissolved oxygen. However, it was observed that in the static growth period the dissolved oxygen level continued to decrease linearly, whereas a constant dissolved oxygen level was maintained while the culture was growing rapidly. These observations may suggest that the oxygen sensor were incorrectly calibrated or malfunctioning. It is speculated that the convergence of the dissolved oxygen level towards 4% may in reality be towards 0%. If this is the case, it would explain the inconsistency with the occurrence of the exponential growth phase, as the dissolved oxygen level then simply could not decrease further.

The suspected malfunction of the oxygen sensor had several consequences. It resulted in culture starvation somewhere between 10 and 40 hours into the fermentation, because glycerol exhaustion was not properly detected. This starvation resulted in a lower biomass accumula-

tion, possibly a higher number of dead cells, and caused the culture to enter a new lag phase. Moreover, it was not realized that the cells most likely were subjected to severe oxygen limitation. Oxygen starvation has however been found in literature not to have as many negative effects as initially thought [70]. However, biomass accumulation was probably lowered as a consequence of this, as it has been found that oxygen starvation causes an increased maintenance demand, resulting in a lower biomass yield per methanol quantity added [70].

Basal salt medium is most often used for fermentation studies with *P. pastoris* because of its low costs. In this study BMGY/BMMY media were used, which might have effect on fermentation. It may be that the cause for the lacking oxygen response to glycerol exhaustion was due to the yeast utilizing some sort of alternative carbon source from this rich media, however, this remains to be investigated. It was also not known if the methanol feeding rate resulted in methanol being the growth limiting factor or if excess methanol was added, as the methanol concentration in the fermentation media was not measured and oxygen limitation probably occurred. At low methanol concentrations, the specific growth rate exhibits Monod kinetics, whereas higher concentrations result in methanol-inhibiting effects on growth [70].

Overall, the problems with this fermentation study resulted in non-optimal conditions for the LTP5 production. Even though the methanol induction phase was performed for 109 hours, the appearance of a new lag phase probably means that the production period was reduced significantly. One major reason why expression in fermentor cultures often results in higher yields is the significantly higher number of cells. In this study, the biomass accumulation was found unsatisfactory. Summarizing, it might be that the PIC-LTP5 *P. pastoris* SMD1168H transformant are capable of producing a satisfying amount of LTP5 through fermentation, as the missing LTP5 accumulation in the conducted fermentation study may be caused by the non-optimal conditions.

No definitive evidence of production of LTP5 or LTP8 in the expression studies has been obtained. However, some SDS-PAGE results (Fig. 6.18 and Fig. C.8) indicated the presence of two proteins with a size just below 10 kDa. Only one of these proteins seemed to be present in the reference. Furthermore, the presence of LTP8, which is a bit smaller than LTP5, may be additionally confirmed by the presence of two proteins just below 10 kDa on the SDS-PAGE in Fig. 6.15, B. Based on screenings at DNA level it has also been concluded that the constructs had been correctly integrated into the *P. pastoris* genome of at least three PIC-LTP5 and three PIC-LTP8 transformants, supporting that expression should be possible. In addition, a distinctive peak was identified in the cation-exchange chromatogram of heat-treated, dialyzed and lyophilized culture supernatant from shake flask expression studies of the PIC-LTP5 *P. pastoris* SMD1168H transformant. The elution of this protein at approximately 60% buffer B (1 M NaCl) seemed consistent with a protein with a relatively high pI above 11. The apparent up-concentration of the protein after heat-treatment also supported the assumption that this protein is LTP5, as LTPs are known to be heat-resistant. Only a very low amount of protein was obtained from this isolation, which was used for antimicrobial assays. A compact clearing zone were obtained on the RDA with *B. subtilis*, consistent with the inhibiting molecule having a relatively low diffusivity. These observations indicate that LTP5 was expressed by the *P. pastoris* SMD1168H transformant in its correctly folded version. Even though the heat-treatment had up-concentrated the supernatant at least 5-fold, the distinctive peak in the cation-exchange chromatogram was barely detectable, which could be the reason that this protein had not been

detected with other methods.

Other observations however indicate that LTP5 and LTP8 did not accumulate in detectable levels in any of the expression studies. The appearance of two bands on some of the SDS-PAGEs may be considered to subtle to be conclusive, and most chromatographic analysis did not reveal any distinctive peaks. In spite of a similar up-concentration of harvested supernatant, the detection of the distinctive peak could not be reproduced, which indicates that it might be caused by contamination. When the heat-treated, dialyzed and lyophilized supernatant was analyzed by SDS-PAGE, no distinctive proteins within the area of interest could be detected. In general, the protein content appeared to be the same after the heat-treatment, but this was believed to be due to that not all denatured protein had been removed by centrifugation. The non-reproducibility of the putative LTP5 purification could however also be caused by a non-uniform distribution of LTP5 in the expression supernatant. It is speculated that LTP5 were e.g. enriched in the foam of the expression supernatant, and thereby were transferred to a single portion of the supernatant. An LTP from barley has for instance been found to be the main protein of beer foam [128], which supports this theory. If this is in fact the case, LTP5 has been expressed and correctly folded, but in extremely low amounts. This putative LTP5 seems to display antimicrobial activity against *B. subtilis* even at this low concentration. That no antimicrobial activity was detected against the other microbes could be caused by a too low concentration, and these assays therefore does not allow for any reliable conclusions, other than *B. subtilis* was more easily inhibited by the compound. It therefore may be that LTP5 holds potent antimicrobial activity as predicted theoretically, but this requires extensive characterizations to be confirmed.

Several factors should be considered when trying to explain the cause for the missing or low expression of LTP5 and LTP8. First of all, the most common problem of protease degradation has already been found unlikely, even though it cannot be entirely excluded. At DNA level, several studies have found that the AT content of a gene influences the protein expression level in *P. pastoris* [91], [82], [92]. These studies report that the presence of AT-rich stretches in the gene correlates with low or missing expression, possibly caused by inefficient transcription due to premature termination. The DNA sequence of the LTP5 gene does not contain unusual AT-stretches, whereas that of LTP8 possesses some regions which could be problematic. This putative problem could be circumvented by designing synthetic genes with optimized AT content, utilizing the degeneracy of codons.

Boettner et al. [92] found in their previously described study that three factors proved to have statistically significant association with the expression level: rare occurrence of AT-clusters in the cDNA was associated with a high expression level, a high pI was associated with no detectable protein expression, and the presence of a protein in yeast closely related to the heterologous protein was associated with general success of the expression. Of these factors, the influence of high pI seems very relevant for the expression of LTP5. Five out of five proteins with a predicted pI above 10 were in the study found to have no detectable expression in *P. pastoris* [92]. It therefore may be that *P. pastoris* in its current form is an unsuitable expression system for production of LTP5. This issue however does not explain the equally missing accumulation of LTP8.

Another issue that may cause problems is the secretion of the produced proteins. If LTP5 and/or LTP8 for some reason are not secreted properly, this could account for their undetectability in the expression supernatant. Studies have shown that the secretion efficiency is

not only dependent on the used signal sequence, but also on the structure of the foreign protein and is interplay with the used signal sequence. Unfortunately there is currently no way of predicting which signal sequence will be most successful for secretion of a particular protein in *P. pastoris*. [80] Switching to other signal sequences is therefore the only way of determining if this will resolve the problems.

Numerous factors are as described in the introduction speculated to influence the success of foreign protein expression in *P. pastoris*, and in the above only those found most likely are discussed. If the cause for the low or absent expression should be found and resolved experimentally, it is recommendable to initiate by determining if the problem is located at transcriptional or post-transcriptional level. This is commonly done by determining the mRNA levels of the gene of interest. Other LTPs have been successfully produced in *P. pastoris* [118], [119], [95], [51], however with varying yields. It therefore seems reasonable to assume that the low or missing expression of LTP5 and LTP8 was not caused by LTP characteristic features, but by specific features of LTP5 and LTP8 in combination with the applied conditions. LTP5 and LTP8 both posses traits that are not typical features of LTPs, such as e.g. the high pI of LTP5, which may influence expression negatively. It is stated in literature that the initial expression level of a heterologous protein expressed in *P. pastoris* typically is too low to be detected with SDS-PAGEs [124]. It is therefore believed that a study with an extended time frame is necessary to achieve expression of LTP5 and LTP8 at reasonable levels in *P. pastoris*, as empirical approaches are required to resolve the problems. This is supported by the comparative study by Boettner et al., in which 44 of 79 proteins had no detectable expression levels in *P. pastoris* when no expression optimizations had been performed. [92]

7.3 Isolation and Characterization of LTPs from Cabbage

Two different approaches to protein extraction from cabbage were applied in the present study. A relatively simple wax protein extraction protocol applied on the leaves of the *B. oleracea* cultivar broccoli by Pyee et al. [32] was adopted to leaves of cabbage. In the study by Pyee et al. it was found that an LTP was the main protein in the surface wax of young leaves, which could be detected on SDS-PAGEs as the major band. In the present work, the general protein yield resulting from this procedure was very low, and no strong band around 10 kDa could be identified with subsequent SDS-PAGEs. Furthermore no significant amount of protein could be detected in the eluent from cation-exchange chromatography. Applying the wax protein extraction protocol to cabbage was therefore considered unsuccessful. It is not known if this method cannot be used with cabbage, or if the adaption of the protocol was not performed well enough. To exclude experimental errors it could be useful to apply the protocol to broccoli leaves. It may however be that the failure of the extraction could be caused by differences in the wax thickness between the two cultivars, perhaps necessitating prolonged exposure to the chloroform-methanol mixture with cabbage leaves.

Since the use of the wax protein extraction protocol was not successful, total cabbage protein extraction was performed. Total protein extraction was less advantageous, as a significantly higher amount of isolation steps were required following this approach. In present study, a

specific protocol for protein extraction from cabbage was developed based on methods found in literature. Through rough estimations it was assessed that about 5% of the cabbage stem proteins were recovered after the extraction and heat denaturation steps of this protocol had been performed. Even though proteins were excluded on purpose in the heat-denaturation step, it is still clear that the yield of the total heat-stable protein fraction from cabbage is rather low. Adding to this, our laboratory facilities only allowed for small-scale production, which resulted in that it was very time consuming to obtain the appropriate amount of material. It would therefore be advantageous to be able to up-scale the production as well as improve the yield. The initial grounding of the material in liquid nitrogen has great influence on the yield, as the extraction efficiency is believed to be increased with the surface/volume ratio of the material. The utilization of an instrument with higher through-put and efficiency for this purpose therefore has the potential to be rewarding in terms of yield. It is possible that less volume of acetone and extraction buffer per mass of raw material could be beneficial, but due to time limitations the effect on yield of this could not be investigated. A more successful extraction could also make the ammonium sulfate precipitation step unnecessary, which was suspected to significantly reduce yield. Another bottleneck of the isolation procedure both in terms of the production scale and time, was the dialysis and lyophilization. It would be an advantage if this step could be performed on a larger scale. The sorting of proteins after the heat-denaturation step is also considered to have optimization potential, both in terms of improving yield of the proteins of interest as well as in removing contaminant proteins.

Overall, it was concluded that the developed extraction protocol was capable of fulfilling its purpose, but needs further improvements in terms of yield and through-put.

As LTPs are often cationic, cation-exchange chromatography was applied for the initial fractionation of the extracted, heat-stable cabbage protein samples. The elution profiles obtained from the cation-exchange chromatography were in general observed to be similar between the extracted material from stem, younger leaf and older leaf, indicating that the majority of cationic proteins were conserved between these tissue types. The stem protein elution profile however deviated slightly from the other two. Due to the elution profile similarities obtained for young and old leaf material and evidence in literature for higher presence of LTPs in younger tissue, focus was reduced to the stem and younger leaf material.

The fractionation step utilizing cation-exchange chromatography is in general considered successful. The yield of the individual fractions of interest seems reasonable and the elution profiles were very reproducible. By developing an even more tailored elution program the separation and processing time may easily be improved. The bottleneck imposed by the subsequent dialysis and lyophilization step can be ignored when confidence in fraction collection has been obtained, as the ionic strength of the collected fractions does not influence the following RP-HPLC purification. The disadvantage of this isolation step was however the necessity of an additional purification dimension, which inevitably will result in loss of target proteins. The insufficiency of the cation-exchange purification was caused by a combination of too low resolution and a high amount of cationic proteins in the extracted material.

Following the cation-exchange chromatography, a screening method for identifying fractions of interest was necessary as a relatively high amount of different fractions had been collected. Initially antimicrobial activity was conceived for this purpose. It was however concluded that the concentration of putative antimicrobial proteins were too low in the fractions. Further-

more, not all LTPs display antimicrobial activity, which further makes this screening approach questionable, even though antimicrobial LTPs were the main target. Antifungal activity however seemed to be displayed by one or more components of FS3 against the fungus *E. gramin-earum*. Often antimicrobial activity towards bacteria requires a lower concentration of antimicrobial proteins. However, no antibacterial activity of FS3 could be detected. This might indicate a high specificity of the protein(s) present in FS3 towards fungi, which is typically found for LTPs. Based on these results, FS3 was considered highly interesting.

Size discrimination by use of SDS-PAGEs was applied as replacement of the antimicrobial assays. This was a suitable method because type 1 LTPs have a well-defined size, typically ranging between 9 and 10 kDa. The advantage of this approach is that it is straight forward and easy applicable, whereas the disadvantage is that potentially interesting antimicrobial proteins of a different size might not be detected. Based on these SDS-PAGEs, fractions containing pLTPa, pLTPb, and pLTPc were identified.

With the objective of purifying pLTPa, pLTPb, and pLTPc completely, RP-HPLC was performed as a second isolation step. A peak of high intensity was observed at the onset of the isopropanol gradient for all chromatograms. This peak was found to be caused by background effects, and was believed to be a result of the change in dielectric constant as the solvent environment goes from aqueous to non-aqueous. This transition of the environment affects π - π electron interactions, which affects the adsorption spectrum in the 190-250 nm region [129].

In the RP-HPLC runs, the three putative LTPs were found to elute at different isopropanol concentrations, which suggests that they represent three distinct proteins. It was initially speculated that pLTPa and pLTPc were the same protein present in both stem and leaf tissue, as both eluted at similar conductivity in the cation-exchange chromatography. This does however not seem to be the case since they differ in the modifier concentration required for their desorption in RP-HPLC. It appeared that pLTPa were only present in leaf tissue, while pLTPb and pLTPc were only found in stem tissue. pLTPa seemed to be the most hydrophobic of the three, followed by pLTPc, while pLTPb was the least hydrophobic.

From the subsequent SDS-PAGEs on the protein fractions collected from the RP-HPLC, it was observed that the pLTPs were not completely purified. In all of the pLTP fractions, a protein with a size of ~12 kDa was also present. This was surprising, as this indicated that for each of the three different pLTPs, a slightly bigger protein with a very similar electrostatic and hydrophobic profile was present. However, another explanation could be that the reducing conditions of the SDS-PAGEs were not strong enough to reduce the disulfide bridges completely. Studies have shown that LTPs are highly stable proteins, which sometimes do not denature at temperatures up to 100 °C [130]. This stability is however partially caused by the disulfide bridges, which should be reduced by mercaptoethanol. However, if insufficient amounts or batches with compromised functionality of mercaptoethanol have been used, the LTPs may not be adequately denatured prior to the SDS-PAGEs. In a study by Zoccatelli et al. [131], LTPs appeared around 12 kDa on SDS-PAGEs conducted under non-reducing conditions. It therefore may be that the ~12 kDa band represents insufficiently reduced LTPs. This was supported by detection of only one peak for both putative proteins in the RP-HPLC. Another possible explanation could be that pLTPs in the process of making their way through the secretion system of the plant cells have been isolated with their signal sequences still intact. The similar characteristics and slightly bigger size of the protein is consistent with this theory. However, this

theory also implies that a similar amount of secreted and non-secreted LTPs are found in the plant, which seems unlikely. The 12 kDa band could however also simply represent another protein. The characteristics of this protein is consistent with that of the ubiquitous distributed cytochrome c. Isoforms of this protein have sizes around 12 kDa, pIs ranging from 10.0-10.5, and are believed to be responsible for the heat-stability of photosynthesis in plants [132]. These characteristics are consistent with the selection criteria employed for isolation of putative LTPs in this study, and it therefore may be that cytochrome c was the protein represented by the ~12 kDa band. Each of these theories could be turned into evidence by mass spectrometry analysis. However, the result from this experiment was not obtained prior to the deadline of the present work.

In the pLTPc fraction, a protein with a size of ~6 kDa was also present. This protein could be responsible for the additional peak present in the chromatograms of the pLTPc fraction. It is speculated that this heat-resistant, cationic peptide may be a type 2 LTP or a member of the plant defensin family.

It was observed that the majority of other proteins collected from the RP-HPLCs appeared as smeared bands on the SDS-PAGEs, or did not appear in detectable amounts at all. Most proteins are denatured when subjected to RP-HPLC due to the harsh conditions (organic solvent, low pH, and not biocompatible material used for tubings), which leaves proteins vulnerable to degradation. The small size differences resulting from such degradations could be the explanation for the smeared bands. If this is the case, the sharp bands representing pLTPs (and the ~6 kDa and ~12 kDa proteins) indicates that these proteins are still intact. It is however unknown if the pLTPs could overall maintain their structure and activity following the RP-HPLC, and too what extend their structure may have been lost. In general, the yield after this final step was extremely low, and it was not possible to quantify the lyophilized fractions. The presence of resulting material could however be verified by visible powder presenting after the lyophilization.

Several possibilities for optimization are present for this second purification step. To increase the retainment of activity, a biocompatible RP-HPLC system could be employed, possibly with features allowing elevation of temperature to reduce the back pressure caused by isopropanol. Furthermore, optimized elution gradients could be developed. These should especially be tailored to have an even shallower gradient in the area between 20-33% isopropanol, to enhance resolution in this area.

The developed extraction and isolation protocols resulted in partial isolation of three heat-stable, cationic proteins with a size just below 10 kDa from tissue of *Brassica oleracea* var. *capitata*. In other studies, proteins isolated from plants with these characteristics have been found to be members of the LTP type 1 family [133], [134], [37], [61]. The characteristics of the isolated pLTPs combined with these observations, makes it likely that the three proteins are members of the LTP family. This assumption however needs to be verified by protein sequencing or *in vitro* lipid transfer activity assays. The pLTP-containing fractions needs further polishing to completely remove the ~6 kDa and ~12 kDa proteins, and small amounts of other proteins. However, an additional purification step comes at the cost of yield. As the yield at this point was already very low, and the time frame for completion of the present study was short, further characterizations of the three fractions were performed without this additional polishing. In general the present work has been hampered by low yields. Every approach has been extremely time consuming, since it required a new round of material production each time. The low yields

have furthermore resulted in problems with determination of the pLTP concentrations for the subsequent assays. The idea was initially that the developed selective isolation protocol should only be applied for identification, and initial characterizations of new LTPs, whereas exhaustive characterization would probably require either large-scale isolation or recombinant expression of the proteins. It however seems that even for these initial characterizations, extensive yield improvements or scale-ups of the protocol are necessary to obtain meaningful results.

Even though the obtained fractions had a low protein concentration, two properties were partially characterized: lipid transfer activity and antimicrobial activity. The lipid transfer activity assay was designed on the principle of donor and acceptor membranes combined with a reporter system. Donor membranes contained a high proportion of fluorescent C₁₂-NBD PC lipids, which is self-quenched such that fluorescence is low at the beginning of the experiment. The self-quenching is released and fluorescence emission from NBD is increased when labeled lipid molecules are transferred into acceptor membranes. This way lipid transfer activity should be detectable as a rapid increase in fluorescence intensity after addition of the protein.

Despite of several attempts, an assay with a satisfying fluorescence intensity baseline was not obtained in this study. Either a too high background fluorescence or a fluctuating emission were observed. A decrease in background fluorescence was obtained by sorting out fluorescent monomeric lipids from the donor vesicles. However, the decrease in background could also be due to some degree of dilution. The fluctuations of the emission in the time-resolved plots could be caused by some kind of structural instability of the vesicles. Furthermore, it may be that a high amount of spontaneous lipid exchanges occur, even though the rate of these in theory should be low when operating below the T_m [135]. It was further noticed that the fluorescence intensity increased significantly when acceptor vesicles were added to a solution containing donor vesicles. That this occurred in spite of a low background fluorescence of isolated acceptor membranes, indicated that a high amount of spontaneous lipid exchanges occurred. Additionally, the two channels measuring emission at 530 nm did not always agree, which points towards instrumental inaccuracies. Adding up, these issues do not provide a solid base for the assay. Optimization of the assay was however hampered by the limited time frame, and the lack of testing material and a positive control.

In a study by Geldwerth et al. [135], similar lipid transfer activity assays were performed on plant LTPs. Lipid transfer activity was in this study detected as a rapid increase in fluorescence intensity, with the establishment of a plateau level with constant fluorescence intensity often within one minute after addition. The fluorescence spectroscopy experiments with additions of pLTPc fractions performed in present work did yield similar results, if the lack of a stable baseline is disregarded. This indicates that an active LTP was present in the pLTPc fraction, capable of transferring lipids *in vitro*. However, due to the general strange behavior of the emission measurements, these results seemed unreliable to some extent, and no true conclusions could be drawn from these experiments. This was supported by the strange behavior observed in the fluorescence spectroscopy with addition of the pLTPb fraction. After addition, the fluorescence intensity in this experiment decreased rapidly, followed by a steady increase. In the study by Geldwerth et al. [135] it was found that lowering the LTP concentration resulted in decreased lipid transfer rates. This tendency could be the explanation for the less steep fluorescence intensity increase observed after addition of the pLTPb fraction, especially when adding that the yield of the pLTPb fraction in general was lower. However, this explanation still

does not account for the initial rapid fluorescence decrease, which seemed too intense to be explained by dilution alone.

Based on the obtained results, it was concluded that an improved lipid transfer activity assays were necessary to confirm that pLTPa, pLTPb, and LTPc are true LTPs.

Antibacterial activity assays were performed with the two Gram positive bacteria *M. luteus* and *B. subtilis*, whereas antifungal activity assays were performed with the yeast *S. cerevisiae* and the plant pathogenic fungi *F. graminearum*. No antimicrobial activity was displayed by any of the three pLTP fractions against the tested microbes. Antifungal activity was detected for the FS3 fraction at low concentrations of individual proteins. Therefore it seems that the antifungal protein(s) present in FS3 either was not pLTPb, or that the pLTPb had been inactivated during the subsequent RP-HPLC or handling.

When evaluating these antimicrobial assays, it should be considered that the pLTP concentrations could not be determined due to low yields. It may therefore be that the applied concentration was too low to result in detectable activity. Furthermore, 70 hours passed between the addition of the pLTP fractions and the hyphae reaching the addition points in the antifungal activity assays with *F. graminearum*. It is unknown if this caused a diffusion-based dilution of the pLTPs, resulting in a too low concentration for the putative activity to be present. Furthermore, LTP antimicrobial activity is often very selective, and therefore the missing activity on four microbes does not exclude activity on other microbes. As not all LTPs have been found to display antimicrobial activity, the results of these assays do not support nor reject that these pLTPs are true LTPs.

Summarizing, it is believed that the developed extraction and isolation protocols lead to identification and partial isolation of three distinctive LTPs from cabbage. These LTPs appear to be tissue-specific, with one originating from young leaf tissue and two originating from stem tissue. Characterizations of these LTPs were hampered by low yields and a short time frame, and it was concluded that significant yield and production scale optimizations are required before the developed protocols become truly functional. If this is achieved, the protocols could be used for similar LTP identification in other plants, with subsequent screening for antimicrobial activity as the objective. No antimicrobial activity could be detected for any of the pLTP-containing fractions on four different microbes in this work. These characterizations however cannot conclusively eliminate that these pLTPs have antimicrobial activity because of the low concentration used, and the high specificity of this activity for LTPs in general.

Outlining the complete work of this study, it is in spite of the problems encountered still believed that LTPs hold great potential as antimicrobial agents. It was indicated through theoretical investigations that certain electrostatic characteristics may be correlated with a potent antimicrobial activity of LTPs. Further it is speculated that the stable characteristic LTP fold is utilized in nature as a robust carrier of different activities. This high stability may also be utilized when applying their antimicrobial activity for different purposes, as these proteins can be maintained in harsh environments and still be active. The mode of action and structure-function relationship of this activity however needs further characterization studies to be elucidated, which was not durable within the time frame of this study.

Conclusion



3D structure models of LTP5 and LTP8 has been created by use of homology modeling. Both models displayed characteristic LTP type 1 features, such as an all- α -type structure, a long C-terminal tail, a hydrophobic cavity in their core and the expected disulfide bonding pattern, which supported that these two proteins belongs to the LTP type 1 family. The amino acid compositions in the tunnels of LTP5 and LTP8 were found to be largely conserved, while the non-conserved amino acids were located mainly at the surface of the structures. This observation is consistent with the conservation of the ability to bind lipids of all characterized LTPs (except Ace-AMP1), while these LTPs often display different biological activities and are expected to fulfill different biological roles.

The calculation and visualization of the electrostatic potentials of the two models revealed significant differences. The LTP5 model generated a predominantly positive potential, and was almost completely wrapped in this positive potential with only a few small negative areas. The spatial distribution of the electrostatic potential of LTP5 was found to be very similar to the one found for Ace-AMP1. This observation combined with the one of a shared arginine-rich structure may indicate that LTP5 interacts with membranes in a similar way to Ace-AMP1, which displays exceptionally potent antimicrobial activity. The LTP8 model was found to generate both negative and positive potential areas, with a slight domination of the negative potential areas. The finding of conserved positive potential patches between the second loop and the C-terminal tail suggested that LTP8 are capable of interacting with lipids at the main entrance of its hydrophobic tunnel.

With the observed differences in electrostatic characteristics in mind, it seemed unlikely that LTP5 and LTP8 exhibit similar modes of action. LTP5 may have antimicrobial activity comparable with that of Ace-AMP1, while the activity and mode of action of LTP8 are unknown, but expected to be different. Experimental studies are however necessary to support or disprove these speculations.

Confirmation of correct integrations into the chromosome of the *P. pastoris* strains X-33 and SMD1168H of both the PIC-LTP5 and PIC-LTP8 constructs were obtained by DNA-based screenings. Shake flask expression studies with different transformants and expression yield optimization strategies were conducted, especially with focus on reducing protease activity. Moreover, a fermentation study with the PIC-LTP5 *P. pastoris* SMD1168H transformant was performed. The protein content of the culture supernatants was evaluated by SDS-PAGEs, RP-HPLC and cation-exchange chromatography. However, no clear indication of accumulation of LTP5 or LTP8 in the expression studies could be detected. A protein with characteristics similar to the expected for LTP5 was however detected in very small amounts in heat-treated, dialyzed and lyophilized culture supernatant from shake flask expression studies with the PIC-LTP5 *P. pastoris* SMD1168H transformant. This putative LTP5 was found to have antimicrobial activity against *B. subtilis* at very low concentration, but its detection and isolation could not be reproduced. It is however believed that LTP5 has been expressed and correctly folded in *P. pastoris*, but in extremely low amounts.

Several issues could be the cause for the low or absent expression of LTP5 and LTP8 in *P.*

pastoris. Empirical approaches are however required to find the specific cause, and it is therefore concluded that a study with an extended time frame is necessary to achieve expression of LTP5 and LTP8 at reasonable levels in *P. pastoris*. Due to the missing accumulation of LTP5 and LTP8 in the expression studies, experimental characterizations of these proteins were not conducted.

In the last part of the study, protocols for extraction and isolation of putative LTPs from cabbage were developed. The applied protocol resulted in partial isolation of three heat stable, cationic proteins with a size just below 10 kDa. These three proteins were believed to be three distinct members of the LTP family 1, but this needs to be further verified. The pLTPs appeared to be tissue-specific, with one originating from young leaf tissue and two originating from stem tissue. The pLTP-containing fractions was found to be in need of further polishing to completely remove other proteins, but due to the short time frame and low yields, further characterizations of the three fractions were performed without this additional polishing. Lipid transfer activity assays did indicate lipid transfer activity in the pLTP-fractions. Because of different problematic issues with the execution of these assays, the obtained results however seemed uncertain at best, and no true conclusions could be drawn from these experiments. No antimicrobial activity on four microbes could be detected for the pLTP-fractions. Characterizations of the obtained pLTPs were hampered by low yields and a short time frame, and it was concluded that significant yield and production scale optimizations are required before the developed extraction and isolation protocol becomes truly functional. If this is achieved, it is believed that the protocol can be used for similar LTP identification in other plants, with subsequent screening for antimicrobial activity as objective.

8.1 Perspectives

The 3D models of LTP5 and LTP8 could in further studies be subjected to molecular dynamics simulations to obtain clues of their interactions with lipid bilayers. It is indicated through the theoretical investigations that certain electrostatic characteristics may be correlated with a potent antimicrobial activity of LTPs. The theoretical characterization performed on LTP5 and LTP8 could be extended to other LTPs, possibly with the purpose of making large scale comparisons of the spatial distribution of the electrostatic potential generated by different LTPs. By holding the results obtained against experimentally derived data, a correlation between electrostatic characteristics and specific functionalities could perhaps be derived or excluded.

It was in present study hoped that the theoretical characterizations of LTP5 and LTP8 could be compared with experimental characterizations of these. Unfortunately, expression in *P. pastoris* of LTP5 and LTP8 was not obtained at reasonable levels. As mentioned in the discussion, it is believed that the next step should be an investigation of the mRNA level of the integrated genes, to determine if the problems occur at transcriptional or post-transcriptional level. Following, it is believed that expression of these two proteins may be possible by applying an extended time frame and empirical approaches to expression optimization. Because of the high stability of these proteins, protocols with a fast down-stream processing could be developed for their subsequent purification. It is believed that a characterization of the antimicrobial properties of these two LTPs with unusual electrostatic characteristics may reveal clues

about the LTP antimicrobial mode of action, and possibly a high potency of LTP5.

Several optimization possibilities for the developed extraction and isolation protocols for acquisition of LTPs directly from plants have already been suggested in the discussion. If a yield-optimized protocol is successfully developed it may be applied to other plants, with subsequent large-scale screening for LTPs with potent antimicrobial activity. A dedicated screening for LTPs with antimicrobial activity may lead to discovery of potent variants and an elucidation of their mode of action, selectivity and structure/function relationship, which is required for their full potential to be utilized. It is believed that LTPs hold great potential as antimicrobial agents, especially because of the stable characteristic LTP fold. This high stability could e.g. be advantageous when utilizing their antimicrobial activity for different purposes, as these proteins can be maintained in harsh environments and still be active.

Bibliography

- [1] A. Gust, F. Brunner, and T. Nürnberger, "Biotechnological concepts for improving plant innate immunity," *Current opinion in biotechnology*, vol. 21, no. 2, pp. 204–210, 2010.
- [2] M. Castro and W. Fontes, "Plant defense and antimicrobial peptides," *Protein and Peptide Letters*, vol. 12, no. 1, pp. 11–16, 2005.
- [3] K. Keymanesh, S. Soltani, and S. Sardari, "Application of antimicrobial peptides in agriculture and food industry," *World Journal of Microbiology and Biotechnology*, vol. 25, no. 6, pp. 933–944, 2009.
- [4] J. Wong, T. Ng, R. Cheung, X. Ye, H. Wang, S. Lam, P. Lin, Y. Chan, E. Fang, P. Ngai, *et al.*, "Proteins with antifungal properties and other medicinal applications from plants and mushrooms," *Applied microbiology and biotechnology*, pp. 1–15, 2010.
- [5] J. Dangl and J. Jones, "Plant pathogens and integrated defence responses to infection," *Nature*, vol. 411.
- [6] J. Jones and J. Dangl, "The plant immune system," *Nature*, vol. 444, no. 7117, pp. 323–329, 2006.
- [7] L. Padovan, M. Scocchi, and A. Tossi, "Structural aspects of plant antimicrobial peptides," *Current Protein and Peptide Science*, vol. 11, no. 3, pp. 210–219, 2010.
- [8] Y. Gordon, E. Romanowski, and A. McDermott, "A review of antimicrobial peptides and their therapeutic potential as anti-infective drugs," *Current eye research*, vol. 30, no. 7, pp. 505–515, 2005.
- [9] K. Elmorjani, V. Lurquin, A. Lelion, H. Rogniaux, and D. Marion, "A bacterial expression system revisited for the recombinant production of cystine-rich plant lipid transfer proteins," *Biochemical and biophysical research communications*, vol. 316, no. 4, pp. 1202–1209, 2004.
- [10] F. García-Olmedo, A. Molina, A. Segura, and M. Moreno, "The defensive role of nonspecific lipid-transfer proteins in plants," *Trends in Microbiology*, vol. 3, no. 2, pp. 72–74, 1995.
- [11] J. KADER, M. JULIENNE, and C. VERGNOLLE, "Purification and characterization of a spinach-leaf protein capable of transferring phospholipids from liposomes to mitochondria or chloroplasts," *European Journal of Biochemistry*, vol. 139, no. 2, pp. 411–416, 1984.
- [12] J. Kader, "Lipid-transfer proteins: a puzzling family of plant proteins," *Trends in plant science*, vol. 2, no. 2, pp. 66–70, 1997.
- [13] J. Kader, "LIPID-TRANSFER PROTEINS IN PLANTS," *Trends in plant science*, vol. 47, no. 47, pp. 627–654, 1996.
- [14] A. Carvalho and V. Gomes, "Role of plant lipid transfer proteins in plant cell physiology—A concise review," *Peptides*, vol. 28, no. 5, pp. 1144–1153, 2007.
- [15] J. Douliez, C. Pato, H. Rabesona, D. Mollé, and D. Marion, "Disulfide bond assignment, lipid transfer activity and secondary structure of a 7-kDa plant lipid transfer protein, LTP2," *European Journal of Biochemistry*, vol. 268, no. 5, pp. 1400–1403, 2001.
- [16] E. Yubero-Serrano, E. Moyano, N. Medina-Escobar, J. Muñoz-Blanco, and J. Caballero, "Identification of a strawberry gene encoding a non-specific lipid transfer protein that responds to ABA, wounding and cold stress*," *Journal of experimental botany*, vol. 54, no. 389, p. 1865, 2003.
- [17] G. Salcedo, R. Sanchez-Monge, A. Diaz-Perales, G. Garcia-Casado, and D. Barber, "Plant non-specific lipid transfer proteins as food and pollen allergens," *Clinical & Experimental Allergy*, vol. 34, no. 9, pp. 1336–1341, 2004.
- [18] E. Vassilopoulou, N. Rigby, F. Moreno, L. Zuidmeer, J. Akkerdaas, I. Tassios, N. Papadopoulos, P. Saxoni-Papageorgiou, R. van Ree, and C. Mills, "Effect of in vitro gastric and duodenal digestion on the allergenicity of grape lipid transfer protein," *Journal of allergy and clinical immunology*, vol. 118, no. 2, pp. 473–480, 2006.

- [19] J. Douliez, T. Michon, K. Elmorjani, and D. Marion, "Mini review: Structure, biological and technological functions of lipid transfer proteins and indolines, the major lipid binding proteins from cereal kernels," *Journal of Cereal Science*, vol. 32, no. 1, pp. 1–20, 2000.
- [20] T. Yeats and J. Rose, "The biochemistry and biology of extracellular plant lipid-transfer proteins (ltps)," *Protein Science*, vol. 17, no. 2, pp. 191–198, 2008.
- [21] D. Shin, J. Lee, K. Hwang, K. Kyu Kim, and S. Suh, "High-resolution crystal structure of the non-specific lipid-transfer protein from maize seedlings," *Structure*, vol. 3, no. 2, pp. 189–199, 1995.
- [22] F. Hoh, J. Pons, M. Gautier, F. de Lamotte, and C. Dumas, "Structure of a liganded type 2 non-specific lipid-transfer protein from wheat and the molecular basis of lipid binding," *Acta Crystallographica Section D: Biological Crystallography*, vol. 61, no. 4, pp. 397–406, 2005.
- [23] J. Gomar, M. Petit, P. Sodano, D. Sy, D. Marion, J. Kader, F. Vovelle, and M. Ptak, "Solution structure and lipid binding of a nonspecific lipid transfer protein extracted from maize seeds," *Protein science*, vol. 5, no. 4, pp. 565–577, 1996.
- [24] B. Heinemann, K. Andersen, P. Nielsen, L. Bech, and F. Poulsen, "Structure in solution of a four-helix lipid binding protein," *Protein science*, vol. 5, no. 1, pp. 13–23, 1996.
- [25] J. Lee, K. Min, H. Cha, D. Shin, K. Hwang, and S. Suh, "Rice non-specific lipid transfer protein: the 1.6 Å crystal structure in the unliganded state reveals a small hydrophobic cavity1," *Journal of molecular biology*, vol. 276, no. 2, pp. 437–448, 1998.
- [26] D. Samuel, Y. Liu, C. Cheng, and P. Lyu, "Solution structure of plant nonspecific lipid transfer protein-2 from rice (*oryza sativa*)," *Journal of Biological Chemistry*, vol. 277, no. 38, p. 35267, 2002.
- [27] D. Charvolin, J. Douliez, D. Marion, C. Cohen-Addad, and E. Pebay-Peyroula, "The crystal structure of a wheat nonspecific lipid transfer protein (ns-ltp1) complexed with two molecules of phospholipid at 2.1 Å resolution," *European Journal of Biochemistry*, vol. 264, no. 2, pp. 562–568, 1999.
- [28] P. Sodano, A. Caille, D. Sy, G. de Person, D. Marion, and M. Ptak, "1H NMR and fluorescence studies of the complexation of DMPG by wheat non-specific lipid transfer protein. Global fold of the complex," *FEBS letters*, vol. 416, no. 2, pp. 130–134, 1997.
- [29] D. Hinch, B. Neukamm, H. Srör, F. Sieg, W. Weckwarth, M. Rückels, V. Lullien-Pellerin, W. Schröder, and J. Schmitt, "Cabbage cryoprotectin is a member of the nonspecific plant lipid transfer protein gene family," *Plant physiology*, vol. 125, no. 2, pp. 835–846, 2001.
- [30] J. Gomar, P. Sodano, M. Ptak, F. Vovelle, *et al.*, "Homology modelling of an antimicrobial protein, ace-amp1, from lipid transfer protein structures," *Folding and Design*, vol. 2, no. 3, pp. 183–192, 1997.
- [31] S. Thoma, U. Hecht, A. Kippers, J. Botella, S. De Vries, and C. Somerville, "Tissue-specific expression of a gene encoding a cell wall-localized lipid transfer protein from Arabidopsis," *Plant Physiology*, vol. 105, no. 1, p. 35, 1994.
- [32] J. Pyee, H. Yu, and P. Kolattukudy, "Identification of a lipid transfer protein as the major protein in the surface wax of broccoli (*Brassica oleracea*) leaves," *Archives of Biochemistry and Biophysics*, vol. 311, no. 2, pp. 460–468, 1994.
- [33] T. Gaffney, L. Friedrich, B. Vernooij, D. Negrotto, G. Nye, S. Uknes, E. Ward, H. Kessmann, and J. Ryals, "Requirement of salicylic acid for the induction of systemic acquired resistance," *Science*, vol. 261, no. 5122, pp. 754–756, 1993.
- [34] A. Maldonado, P. Doerner, R. Dixon, C. Lamb, and R. Cameron, "A putative lipid transfer protein involved in systemic resistance signalling in Arabidopsis," *Nature*, vol. 419, no. 6905, pp. 399–403, 2002.
- [35] N. Buhot, J. Douliez, A. Jacquemard, D. Marion, V. Tran, B. Maume, M. Milat, M. Ponchet, V. Mikes, J. Kader, *et al.*, "A lipid transfer protein binds to a receptor involved in the control of plant defence responses," *FEBS letters*, vol. 509, no. 1, pp. 27–30, 2001.
- [36] A. Molina, A. Segura, and F. Garcia-Olmedo, "Lipid transfer proteins (nsLTPs) from barley and maize leaves are potent inhibitors of bacterial and fungal plant pathogens," *FEBS letters*, vol. 316, no. 2, pp. 119–122, 1993.
- [37] A. Segura, M. Moreno, and F. Garcia-Olmedo, "Purification and antipathogenic activity of lipid transfer proteins (LTPs) from the leaves of Arabidopsis and spinach," *FEBS letters*, vol. 332, no. 3, pp. 243–246, 1993.
- [38] A. Carvalho, O. Machado, M. Da Cunha, I. Santos, and V. Gomes, "Antimicrobial peptides and immunolocalization of a LTP in *Vigna unguiculata* seeds," *Plant Physiology and Biochemistry*, vol. 39, no. 2, pp. 137–146, 2001.

- [39] S. Wang, J. Wu, T. Ng, X. Ye, and P. Rao, "A non-specific lipid transfer protein with antifungal and antibacterial activities from the mung bean," *Peptides*, vol. 25, no. 8, pp. 1235–1242, 2004.
- [40] I. Blilou, J. Ocampo, and J. García-Garrido, "Induction of Ltp (lipid transfer protein) and Pal (phenylalanine ammonia-lyase) gene expression in rice roots colonized by the arbuscular mycorrhizal fungus *Glomus mosseae*," *Journal of experimental botany*, vol. 51, no. 353, p. 1969, 2000.
- [41] R. Velazhahan, R. Radhajeyalakshmi, R. Thangavelu, and S. Muthukrishnan, "An antifungal protein purified from pearl millet seeds shows sequence homology to lipid transfer proteins," *Biologia plantarum*, vol. 44, no. 3, pp. 417–421, 2001.
- [42] M. Regente, A. Giudici, J. Villalain, and L. Canal, "The cytotoxic properties of a plant lipid transfer protein involve membrane permeabilization of target cells," *Letters in applied microbiology*, vol. 40, no. 3, pp. 183–189, 2005.
- [43] M. Diz, A. Carvalho, R. Rodrigues, A. Neves-Ferreira, M. Da Cunha, E. Alves, A. Okorokova-Façanha, M. Oliveira, J. Perales, O. Machado, *et al.*, "Antimicrobial peptides from chili pepper seeds causes yeast plasma membrane permeabilization and inhibits the acidification of the medium by yeast cells," *Biochimica et Biophysica Acta (BBA)-General Subjects*, vol. 1760, no. 9, pp. 1323–1332, 2006.
- [44] J. Caaveiro, A. Molina, J. González-Mañas, P. Rodríguez-Palenzuela, F. García-Olmedo, and F. Goñi, "Differential effects of five types of antipathogenic plant peptides on model membranes," *FEBS letters*, vol. 410, no. 2-3, pp. 338–342, 1997.
- [45] M. Regente and L. De La Canal, "Purification, characterization and antifungal properties of a lipid-transfer protein from sunflower (*helianthus annuus*) seeds," *Physiologia Plantarum*, vol. 110, no. 2, pp. 158–163, 2000.
- [46] B. Cammue, K. Thevissen, M. Hendriks, K. Eggermont, I. Goderis, P. Proost, J. Van Damme, R. Osborn, F. Gurbette, J. Kader, *et al.*, "A potent antimicrobial protein from onion seeds showing sequence homology to plant lipid transfer proteins," *Plant physiology*, vol. 109, no. 2, p. 445, 1995.
- [47] S. Roy-Barman, C. Sautter, and B. Chattoo, "Expression of the lipid transfer protein ace-amp1 in transgenic wheat enhances antifungal activity and defense responses," *Transgenic research*, vol. 15, no. 4, pp. 435–446, 2006.
- [48] X. Li, K. Gasic, B. Cammue, W. Broekaert, and S. Korban, "Transgenic rose lines harboring an antimicrobial protein gene, ace-amp1, demonstrate enhanced resistance to powdery mildew (*sphaerotheca pannosa*)," *Planta*, vol. 218, no. 2, pp. 226–232, 2003.
- [49] J. Sun, D. Gaudet, Z. Lu, M. Frick, B. Puchalski, and A. Laroche, "Characterization and antifungal properties of wheat nonspecific lipid transfer proteins," *Molecular plant-microbe interactions*, vol. 21, no. 3, pp. 346–360, 2008.
- [50] A. Palacin, S. Quirce, A. Armentia, M. Fernández-Nieto, L. Pacios, T. Asensio, J. Sastre, A. Diaz-Perales, and G. Salcedo, "Wheat lipid transfer protein is a major allergen associated with baker's asthma," *Journal of Allergy and Clinical Immunology*, vol. 120, no. 5, pp. 1132–1138, 2007.
- [51] C. Klein, F. de Lamotte-Guéry, F. Gautier, G. Moulin, H. Boze, P. Joudrier, and M. Gautier, "High-level secretion of a wheat lipid transfer protein in *pichia pastoris*," *Protein expression and purification*, vol. 13, no. 1, pp. 73–82, 1998.
- [52] O. Duffort, F. Polo, M. Lombardero, A. Díaz-Perales, R. Sánchez-Monge, G. García-Casado, G. Salcedo, and D. Barber, "Immunoassay to quantify the major peach allergen pru p 3 in foodstuffs. differential allergen release and stability under physiological conditions," *Journal of agricultural and food chemistry*, vol. 50, no. 26, pp. 7738–7741, 2002.
- [53] M. Dunn, A. White, S. Vural, and M. Hughes, "Identification of promoter elements in a low-temperature-responsive gene (blt4. 9) from barley (*hordeum vulgare* l.)," *Plant molecular biology*, vol. 38, no. 4, pp. 551–564, 1998.
- [54] B. Jones and L. Marinac, "Purification and partial characterization of a second cysteine proteinase inhibitor from ungerminated barley (*hordeum vulgare* l.)," *Journal of agricultural and food chemistry*, vol. 48, no. 2, pp. 257–264, 2000.
- [55] F. Vignols, M. Wigger, J. Garci'a-Garrido, F. Grellet, J. Kader, and M. Delseny, "Rice lipid transfer protein (ltp) genes belong to a complex multigene family and are differentially regulated," *Gene*, vol. 195, no. 2, pp. 177–186, 1997.

- [56] L. Sossountzov, L. Ruiz-Avila, F. Vignols, A. Jolliot, V. Arondel, F. Tchang, M. Grosbois, F. Guerbette, E. Miginiac, M. Delseny, *et al.*, "Spatial and temporal expression of a maize lipid transfer protein gene," *The Plant Cell Online*, vol. 3, no. 9, pp. 923–933, 1991.
- [57] S. Sarowar, Y. Kim, K. Kim, B. Hwang, S. Ok, and J. Shin, "Overexpression of lipid transfer protein (ltp) genes enhances resistance to plant pathogens and ltp functions in long-distance systemic signaling in tobacco," *Plant cell reports*, vol. 28, no. 3, pp. 419–427, 2009.
- [58] A. Fleming, T. Mandel, S. Hofmann, P. Sterk, S. Vries, and C. Kuhlemeier, "Expression pattern of a tobacco lipid transfer protein gene within the shoot apex," *The Plant Journal*, vol. 2, no. 6, pp. 855–862, 1992.
- [59] K. Takishima, S. Watanabe, M. Yamada, and G. Mamiya, "The amino-acid sequence of the nonspecific lipid transfer protein from germinated castor bean endosperms," *Biochimica et Biophysica Acta (BBA)-Protein Structure and Molecular Enzymology*, vol. 870, no. 2, pp. 248–255, 1986.
- [60] V. Arondel, C. Vergnolle, C. Cantrel, and J. Kader, "Lipid transfer proteins are encoded by a small multigene family in *Arabidopsis thaliana*," *Plant Science*, vol. 157, no. 1, pp. 1–12, 2000.
- [61] F. Terras, I. Goderis, F. Van Leuven, J. Vanderleyden, B. Cammue, and W. Broekaert, "In vitro antifungal activity of a radish (*Raphanus sativus* L.) seed protein homologous to nonspecific lipid transfer proteins," *Plant physiology*, vol. 100, no. 2, p. 1055, 1992.
- [62] I. Soufleri, C. Vergnolle, E. Miginiac, and J. Kader, "Germination-specific lipid transfer protein cDNAs in *Brassica napus* L.," *Planta*, vol. 199, no. 2, pp. 229–237, 1996.
- [63] M. Koch and K. Mummenhoff, "Editorial: Evolution and phylogeny of the brassicaceae," *Plant Systematics and Evolution*, vol. 259, no. 2, pp. 81–83, 2006.
- [64] C. Bailey, M. Koch, M. Mayer, K. Mummenhoff, S. O'Kane Jr, S. Warwick, M. Windham, and I. Al-Shehbaz, "Toward a global phylogeny of the brassicaceae," *Molecular Biology and Evolution*, vol. 23, no. 11, pp. 2142–2160, 2006.
- [65] S. Warwick and C. Sauder, "Phylogeny of tribe brassicaceae (brassicaceae) based on chloroplast restriction site polymorphisms and nuclear ribosomal internal transcribed spacer and chloroplast trnI intron sequences," *Canadian Journal of Botany*, vol. 83, no. 5, pp. 467–483, 2005.
- [66] S. Berot, J. Compoin, C. Larre, C. Malabat, and J. Gueguen, "Large scale purification of rapeseed proteins (< i> Brassica napus</i> L.)," *Journal of Chromatography B*, vol. 818, no. 1, pp. 35–42, 2005.
- [67] U. Consortium *et al.*, "Reorganizing the protein space at the universal protein resource (uniprot)," *Nucleic Acids Res*, vol. 40, pp. D71–D75, 2012.
- [68] G. Gellissen, *Production of Recombinant Protein. Novel Microbial and Eukaryotic Expression Systems*. WILEY-VCH, 2005, ISBN: 3-527-31036-3, p: 143-157.
- [69] M. R. Dyson and Y. Durocher, *Expression Systems*. Scion Publishing Limited, 2007, ISBN: 978-1-904842-43-9, p: 123-144.
- [70] T. Charoenrat, M. Ketudat-Cairns, H. Stendahl-Andersen, M. Jahic, and S. Enfors, "Oxygen-limited fed-batch process: an alternative control for *Pichia pastoris* recombinant protein processes," *Bioprocess and biosystems engineering*, vol. 27, no. 6, pp. 399–406, 2005.
- [71] J. M. Cregg, *Pichia Protocols*. Hunana Press, second edition ed., 2007, ISBN: 978-1-59745-456-8.
- [72] J. M. Fernandez and J. P. Hoeffler, *Gene Expression Systems. Using nature for the art of expression*. Academic Press, 1999, ISBN: 0-12-253840-4.
- [73] J. Cregg, J. Cereghino, J. Shi, and D. Higgins, "Recombinant protein expression in *Pichia pastoris*," *Molecular biotechnology*, vol. 16, no. 1, pp. 23–52, 2000.
- [74] S. Macauley-Patrick, M. Fazenda, B. McNeil, and L. Harvey, "Heterologous protein production using the *Pichia pastoris* expression system," *Yeast*, vol. 22, no. 4, pp. 249–270, 2005.
- [75] K.-. Invitrogen, *EasySelect Pichia Expression Kit. A Manual of Methods for Expression of Recombinant Proteins Using pPICZ and pPICZα in Pichia pastoris*.
- [76] M. Jahic, A. Veide, T. Charoenrat, T. Teeri, and S. Enfors, "Process technology for production and recovery of heterologous proteins with *Pichia pastoris*," *Biotechnology progress*, vol. 22, no. 6, pp. 1465–1473, 2006.
- [77] H. Lodish, A. Berk, C. A. Kaiser, M. Krieger, M. P. Scott, A. Bretscher, H. Ploegh, and P. Matsudaira, *Molecular Cell Biology*. W. H Freeman and Company, sixth edition ed., 2008, ISBN: 978-0-7167-7601-7, p: 533-536.
-

- [78] S. Wildt and T. U. Gerngross, "The humanization of N-glycosylation pathways in yeast," *Nature Reviews Microbiology*, vol. 3, no. 2, pp. 119–128, 2005.
- [79] M. Jahic, F. Wallberg, M. Bollok, P. Garcia, and S. Enfors, "Temperature limited fed-batch technique for control of proteolysis in pichia pastoris bioreactor cultures," *Microbial Cell Factories*, vol. 2, no. 1, p. 6, 2003.
- [80] M. Romanos, "Advances in the use of pichia pastoris for high-level gene expression," *Current Opinion in biotechnology*, vol. 6, no. 5, pp. 527–533, 1995.
- [81] M. Romanos, C. Scorer, and J. Clare, "Foreign gene expression in yeast: a review," *Yeast*, vol. 8, no. 6, pp. 423–488, 1992.
- [82] K. Sreekrishna, R. Brankamp, K. Kropp, D. Blankenship, J. Tsay, P. Smith, J. Wierschke, A. Subramaniam, and L. Birkenberger, "Strategies for optimal synthesis and secretion of heterologous proteins in the methylotrophic yeast pichia pastoris," *Gene*, vol. 190, no. 1, pp. 55–62, 1997.
- [83] O. Burrowes, G. Diamond, T. Lee, *et al.*, "Recombinant expression of pleurocidin cdna using the pichia pastoris expression system," *Journal of Biomedicine and Biotechnology*, vol. 2005, no. 4, pp. 374–384, 2005.
- [84] K. Kobayashi, S. Kuwae, T. Ohya, T. Ohda, M. Ohyama, H. Ohi, K. Tomomitsu, and T. Ohmura, "High-level expression of recombinant human serum albumin from the methylotrophic yeast pichia pastoris with minimal protease production and activation," *Journal of bioscience and bioengineering*, vol. 89, no. 1, pp. 55–61, 2000.
- [85] X. Zhou and Y. Zhang, "Decrease of proteolytic degradation of recombinant hirudin produced by pichia pastoris by controlling the specific growth rate," *Biotechnology letters*, vol. 24, no. 17, pp. 1449–1453, 2002.
- [86] J. Sinha, B. Plantz, M. Inan, and M. Meagher, "Causes of proteolytic degradation of secreted recombinant proteins produced in methylotrophic yeast pichia pastoris: Case study with recombinant ovine interferon- τ ," *Biotechnology and bioengineering*, vol. 89, no. 1, pp. 102–112, 2005.
- [87] W. Zhang, M. Inan, and M. Meagher, "Fermentation strategies for recombinant protein expression in the methylotrophic yeast pichia pastoris," *Biotechnology and Bioprocess Engineering*, vol. 5, no. 4, pp. 275–287, 2000.
- [88] Invitrogen, *PichiaPink™ Expression System For High-level and Large-scale Expression and Secretion of Bioactive Recombinant Proteins in Pichia pastoris*.
- [89] G. James, "Inactivation of the protease inhibitor phenylmethylsulfonyl fluoride in buffers.," *Analytical biochemistry*, vol. 86, no. 2, pp. 574–579, 1978.
- [90] K. Sreekrishna, J. Tschopp, G. Thill, R. Brierley, and K. Barr, "Expression of human serum albumin in pichia pastoris," Jan. 13 1998. US Patent 5,707,828.
- [91] C. Scorer, R. Buckholz, J. Clare, and M. Romanes, "The intracellular production and secretion of hiv-1 envelope protein in the methylotrophic yeast pichia pastoris," *Gene*, vol. 136, no. 1-2, pp. 111–119, 1993.
- [92] M. Boettner, C. Steffens, C. von Mering, P. Bork, U. Stahl, and C. Lang, "Sequence-based factors influencing the expression of heterologous genes in the yeast pichia pastoris—a comparative view on 79 human genes," *Journal of biotechnology*, vol. 130, no. 1, pp. 1–10, 2007.
- [93] K. Bugge, "Cloning, expression and characterization of two lipid transport proteins from *Arabidopsis thaliana*," *AAU Nanobiotechnology*, vol. 8th semester, 2011.
- [94] J. Borges, R. Culerrier, D. Aldon, A. Barre, H. Benoist, O. Saurel, A. Milon, A. Didier, and P. Rougé, "GATEWAY (TM) technology and E. coli recombinant system produce a properly folded and functional recombinant allergen of the lipid transfer protein of apple (Mal d 3)," *Protein expression and purification*, vol. 70, no. 2, pp. 277–282, 2010.
- [95] S. Pokoj, I. Lauer, K. Fotisch, M. Himly, A. Mari, E. Enrique, M. Miguel-Moncin, J. Lidholm, S. Vieths, and S. Scheurer, "Pichia pastoris is superior to e. coli for the production of recombinant allergenic non-specific lipid-transfer proteins," *Protein expression and purification*, vol. 69, no. 1, pp. 68–75, 2010.
- [96] K. Arnold, L. Bordoli, J. Kopp, and T. Schwede, "The swiss-model workspace: a web-based environment for protein structure homology modelling," *Bioinformatics*, vol. 22, no. 2, pp. 195–201, 2006.
- [97] F. Kiefer, K. Arnold, M. Künzli, L. Bordoli, and T. Schwede, "The swiss-model repository and associated resources," *Nucleic acids research*, vol. 37, no. suppl 1, pp. D387–D392, 2009.
- [98] T. Schwede, J. Kopp, N. Guex, and M. Peitsch, "Swiss-model: an automated protein homology-modeling server," *Nucleic acids research*, vol. 31, no. 13, pp. 3381–3385, 2003.

- [99] N. Guex and M. Peitsch, "Swiss-model and the swiss-pdb viewer: an environment for comparative protein modeling," *Electrophoresis*, vol. 18, no. 15, pp. 2714–2723, 1997.
- [100] M. Peitsch, "Protein modeling by e-mail," *Bio/technology*, vol. 13, pp. 658–660, 1995.
- [101] J. Andaloro, K. Rose, A. Shelton, C. Hoy, and R. Becker, "Cabbage growth stages," 1983.
- [102] W. DeLano, "The pymol molecular graphics system," 2002.
- [103] T. Dolinsky, J. Nielsen, J. McCammon, and N. Baker, "Pdb2pqr: an automated pipeline for the setup of poisson–boltzmann electrostatics calculations," *Nucleic acids research*, vol. 32, no. suppl 2, pp. W665–W667, 2004.
- [104] N. Baker, D. Sept, S. Joseph, M. Holst, and J. McCammon, "Electrostatics of nanosystems: application to microtubules and the ribosome," *Proceedings of the National Academy of Sciences*, vol. 98, no. 18, p. 10037, 2001.
- [105] D. Sitkoff, K. Sharp, and B. Honig, "Accurate calculation of hydration free energies using macroscopic solvent models," *The Journal of Physical Chemistry*, vol. 98, no. 7, pp. 1978–1988, 1994.
- [106] A. Palacín, J. Cumplido, J. Figueroa, O. Ahrazem, R. Sánchez-Monge, T. Carrillo, G. Salcedo, and C. Blanco, "Cabbage lipid transfer protein bra o 3 is a major allergen responsible for cross-reactivity between plant foods and pollens," *Journal of allergy and clinical immunology*, vol. 117, no. 6, pp. 1423–1429, 2006.
- [107] F. Bourgis and J. Kader, "Lipid-transfer proteins: Tools for manipulating membrane lipids," *Physiologia Plantarum*, vol. 100, no. 1, pp. 78–84, 1997.
- [108] M. Lööke, K. Kristjuhan, and A. Kristjuhan, "Extraction of genomic dna from yeasts for pcr-based applications," *BioTechniques*, vol. 50, no. 5, p. 325, 2011.
- [109] U. Laemmli, "Most commonly used discontinuous buffer system for sds electrophoresis," *Nature*, vol. 227, pp. 680–685, 1970.
- [110] G. Han, J. Lee, H. Song, C. Chang, K. Min, J. Moon, D. Shin, M. Kopka, M. Sawaya, H. Yuan, *et al.*, "Structural basis of non-specific lipid binding in maize lipid-transfer protein complexes revealed by high-resolution x-ray crystallography1," *Journal of molecular biology*, vol. 308, no. 2, pp. 263–278, 2001.
- [111] E. Hutchinson and J. Thornton, "Promotif—a program to identify and analyze structural motifs in proteins.," *Protein science: a publication of the Protein Society*, vol. 5, no. 2, p. 212, 1996.
- [112] A. Konagurthu, J. Whisstock, P. Stuckey, and A. Lesk, "Mustang: a multiple structural alignment algorithm," *Proteins: Structure, Function, and Bioinformatics*, vol. 64, no. 3, pp. 559–574, 2006.
- [113] H. Rangwala and G. Karypis, "frmsdpred: Predicting local rmsd between structural fragments using sequence information," tech. rep., DTIC Document, 2007.
- [114] P. Benkert, M. Biasini, and T. Schwede, "Toward the estimation of the absolute quality of individual protein structure models," *Bioinformatics*, vol. 27, no. 3, pp. 343–350, 2011.
- [115] R. Laskowski, M. MacArthur, D. Moss, and J. Thornton, "Procheck: a program to check the stereochemical quality of protein structures," *Journal of Applied Crystallography*, vol. 26, no. 2, pp. 283–291, 1993.
- [116] A. Morris, M. MacArthur, E. Hutchinson, and J. Thornton, "Stereochemical quality of protein structure coordinates," *Proteins: Structure, Function, and Bioinformatics*, vol. 12, no. 4, pp. 345–364, 1992.
- [117] H. Schägger, "Tricine–sds–page," *Nature protocols*, vol. 1, no. 1, pp. 16–22, 2006.
- [118] O. Ahrazem, M. Ibáñez, G. López-Torrejón, R. Sánchez-Monge, J. Sastre, M. Lombardero, D. Barber, and G. Salcedo, "Lipid transfer proteins and allergy to oranges," *International archives of allergy and immunology*, vol. 137, no. 3, pp. 201–210, 2005.
- [119] A. Diaz-Perales, G. Garcia-Casado, R. Sanchez-Monge, F. Garcia-Selles, D. Barber, and G. Salcedo, "cdna cloning and heterologous expression of the major allergens from peach and apple belonging to the lipid-transfer protein family," *Clinical & Experimental Allergy*, vol. 32, no. 1, pp. 87–92, 2002.
- [120] T. Kim, H. Ryu, H. Cho, C. Yang, and J. Kim, "Thermal behavior of proteins: heat-resistant proteins and their heat-induced secondary structural changes," *Biochemistry*, vol. 39, no. 48, pp. 14839–14846, 2000.
- [121] U. N. A. Library, *National Nutrient Database*. URL: <http://ndb.nal.usda.gov/ndb/foods/show/2956>.
- [122] S. Ball, K. Mapp, and L. Lloyd, *Investigation into the Alternatives to Acetonitrile for the Analysis of Peptides on a VariTide RPC, Application Note*. Agilent Technologies, 2011.

- [123] J. Cereghino and J. Cregg, "Heterologous protein expression in the methylotrophic yeast *pichia pastoris*," *FEMS microbiology reviews*, vol. 24, no. 1, pp. 45–66, 2000.
- [124] J. Cregg, I. Tolstorukov, A. Kusari, J. Sunga, K. Madden, and T. Chappell, "Expression in the yeast *pichia pastoris*," *Methods in enzymology*, vol. 463, pp. 169–189, 2009.
- [125] R. A. Science, *The Complete Guide for Protease Inhibition*. URL: http://www.roche-applied-science.com/ProteaseInhibitor/pdf/proteaseinhibition_guide.pdf.
- [126] Y. Zhang, R. Liu, and X. Wu, "The proteolytic systems and heterologous proteins degradation in the methylotrophic yeast *pichia pastoris*," *Annals of microbiology*, vol. 57, no. 4, pp. 553–560, 2007.
- [127] U. of Virginia, *Chapter 16: Mechanisms of Enzyme Action*. URL: <http://web.virginia.edu/Heidi/chapter16/chp16.htm>.
- [128] S. Gorjanović, E. Spillner, M. Beljanski, R. Gorjanović, M. Pavlović, and G. Gojgić-Cvijanović, "Malting barley grain non-specific lipid-transfer protein (ns-ltp): importance for grain protection," *J. Inst. Brew*, vol. 111, no. 2, pp. 99–104, 2005.
- [129] D. Carr, "The handbook of analysis and purification of peptides and proteins by reversed-phase hplc," *Vydac Trade Materials, USA (California)*, 2002.
- [130] K. Lindorff-Larsen and J. Winther, "Surprisingly high stability of barley lipid transfer protein, ltp1, towards denaturant, heat and proteases," *FEBS letters*, vol. 488, no. 3, pp. 145–148, 2001.
- [131] G. Zoccatelli, C. Dalla Pellegrina, M. Consolini, M. Fusi, S. Sforza, G. Aquino, A. Dossena, R. Chignola, A. Peruffo, M. Olivieri, *et al.*, "Isolation and identification of two lipid transfer proteins in pomegranate (*punica granatum*)," *Journal of agricultural and food chemistry*, vol. 55, no. 26, pp. 11057–11062, 2007.
- [132] Y. Nishiyama, H. Hayashi, T. Watanabe, and N. Murata, "Photosynthetic oxygen evolution is stabilized by cytochrome c550 against heat inactivation in *synechococcus* sp. pcc 7002," *Plant physiology*, vol. 105, no. 4, pp. 1313–1319, 1994.
- [133] U. Zottich, M. Da Cunha, A. Carvalho, G. Dias, N. Silva, I. Santos, V. do Nascimento, E. Miguel, O. Machado, and V. Gomes, "Purification, biochemical characterization and antifungal activity of a new lipid transfer protein (ltp) from *coffea canephora* seeds with α -amylase inhibitor properties," *Biochimica et Biophysica Acta (BBA)-General Subjects*, vol. 1810, no. 4, pp. 375–383, 2011.
- [134] R. Asero, G. Mistrello, D. Roncarolo, S. de Vries, M. Gautier, C. Ciurana, E. Verbeek, T. Mohammadi, V. Knul-Brettlova, J. Akkerdaas, *et al.*, "Lipid transfer protein: a pan-allergen in plant-derived foods that is highly resistant to pepsin digestion," *International archives of allergy and immunology*, vol. 122, no. 1, pp. 20–32, 2000.
- [135] D. Geldwerth, A. De Kermel, A. Zachowski, F. Guerbet, J. Kader, J. Henry, and P. Devaux, "Use of spin-labeled and fluorescent lipids to study the activity of the phospholipid transfer protein from maize seedlings," *Biochimica et Biophysica Acta (BBA)-Lipids and Lipid Metabolism*, vol. 1082, no. 3, pp. 255–264, 1991.
- [136] S. Zumdahl and Z. S., *Chemistry*. Houghton Mifflin, New York, 2007.
- [137] A. James and A. Martin, "Gas-liquid partition chromatography: the separation and micro-estimation of volatile fatty acids from formic acid to dodecanoic acid," *Biochemical Journal*, vol. 50, no. 5, p. 679, 1952.
- [138] amersham pharmacia biotech, *Reversed Phase Chromatography: Principles and Methods*. 1999.
- [139] T. N. Drenthe College, *High Performance Liquid Chromatography*. URL: <http://www.standardbase.com/tech/HPLC.pdf>.
- [140] I. Molnar and C. Horváth, "Reverse-phase chromatography of polar biological substances: separation of catechol compounds by high-performance liquid chromatography," *Clinical chemistry*, vol. 22, no. 9, pp. 1497–1502, 1976.
- [141] D. Sheehan and S. O Sullivan, "Fast protein liquid chromatography," *METHODS IN MOLECULAR BIOLOGY-CLIFTON THEN TOTOWA-*, vol. 244, pp. 253–258, 2004.
- [142] A. Madadlou, S. O'Sullivan, and D. Sheehan, "Fast protein liquid chromatography," *Methods Mol Biol*, vol. 681, pp. 439–447, 2011.
- [143] T. Scientific, *Tech Tip 62: Ion exchange chromatography (TR0062.0)*. URL: <http://www.piercenet.com/files/TR0062-Ion-exchange-chrom.pdf>.
- [144] P. Benkert, T. Schwede, and S. Tosatto, "Qmeanclust: estimation of protein model quality by combining a composite scoring function with structural density information," *BMC structural biology*, vol. 9, no. 1, p. 35, 2009.

Appendix



A.1 Chromatography

Chromatography is the general name applied for a series of separation methods that employ a system with two phases of matter: a mobile phase (a liquid or gas) and a stationary phase (a solid or gel). The separation occurs because the components of the sample have different affinities for the two phases, which results in movement through the system at different rates. Components with high affinity for the mobile phase moves relatively fast through the chromatographic system, while components with high affinity for the solid phase move more slowly. [136]

Chromatography may be analytical or preparative (or both). Analytical chromatography is used for analyzing the relative proportions of analytes in a mixture, and is usually performed on smaller quantities than preparative chromatography. Preparative chromatography has the purpose of separating components for downstream use, and can be described as a purification method. [129]

The chromatographic column can be described by the plate model, which James et al. [137] introduced in 1951. In this model, the column is approximated as if it contained a large number of separate layers, called theoretical plates. An analyte can be described as being in equilibrium between the solid and liquid phase. In each of the theoretical plates, separate equilibrations of the analyte between the stationary and mobile phase occur, and the analyte moves down the column by transfer of equilibrated mobile phase from one plate to the next. [137] The concept of theoretical plates are used for treating the concept of column efficiency (peak width). Usually, the term used to describe the separation efficiency of a column is the number of theoretical plates 'N'. The higher the value of N, the better efficiency the column has, and the higher resolution can be achieved. N is dimensionless and defined as the column length 'L' divided by the height 'H' of an individual plate. This relationship tells that N can be increased by using longer columns, or using columns with smaller plate height. The efficiency is also affected by flow rate. [137], [138]

The time it takes for a compound to travel through a column (from injection to detector) is known as the retention time t . The time it takes for an unretained compound to travel through the column is known as the dead time t_0 . From these two definitions, the retention factor of a compound can be deduced. Resolution is defined as the distance between the centers of two eluting peaks as measured by retention time or volume, divided by the average width of the respective peaks. The resolution of a column is a function of retention factor, selectivity, and efficiency. Selectivity of a column is equivalent to relative retention of the solute peaks, and depends strongly on the chemical surface chemistry of the chromatography medium, the mobile phase, and the gradient shape. [138]

A number of different chromatography techniques can be used for protein purification. These include size-exclusion chromatography (separation according to size), ion-exchange chroma-

tography (separation according to charge), and reverse-phase and hydrophobic interaction chromatography (separation based on hydrophobic interactions between sample and stationary phase). Crude extracts often require several chromatography steps before the desired substance is purified. [138]

A.1.1 Reverse-Phase High-Performance Liquid Chromatography

The term reversed-phase high-performance liquid chromatography (RP-HPLC) is used for any chromatographic method involving a hydrophobic stationary phase. Initially, HPLC was an abbreviation for "high pressure liquid performance". This was however an unfortunate term because it indicates that the improved performance of the HPLC system is primarily due to the high pressure. This is not true, as the high performance is the result of many factors, such as very small particles and uniform pore size and distribution, column packing techniques, accurate low volume sample injectors, sensitive low volume detectors, and good pumping systems. [139] In normal phase HPLC, a polar stationary phase and a less polar eluent are used, resulting in hydrophobic molecules being eluted first. The term "reversed-phase" is used to describe RP-HPLC because the eluent in this method is more polar than the stationary phase. This means that hydrophobic molecules are more retained than hydrophilic in this type of chromatography. [140]

RP-HPLC has become a widely used tool for analysis and purification of biomolecules. The popularity of RP-HPLC is mainly due to its high resolution, but also its simplicity and reproducibility are popular traits. Today, polypeptides that only differ by a single amino acid in their sequences can be separated using RP-HPLC. [140], [129]

RP-HPLC operates on the principle of hydrophobic interactions, and is in general a dynamic adsorption process, which involves mass transfer between the stationary and mobile phase. The analyte mixture is dissolved in the mobile phase and then forced through a column under high pressure. In the column, the mobile and stationary phase separates the analyte molecules depending on both the choice of mobile and stationary phase. Because the mobile phase is more polar than the stationary phase, the more nonpolar the analyte is, the longer it will be retained in the stationary phase. [140], [139], [129]

Columns often consist of stainless steel tubes filled with small diameter, spherical adsorbent silica particles, whose surfaces have obtained a hydrophobic character by addition of hydrophobic alkyl chains. The alkyl chains are usually linear aliphatic hydrocarbons of either eighteen (C18), eight (C8) or four (C4) carbons. Often, shorter hydrocarbons are recommended for more hydrophobic proteins (often bigger proteins), while longer chains are recommended for more hydrophilic proteins (often peptides). [140], [139], [129]

The mechanism by which polypeptides interact with reversed-phase surfaces differs from that of small molecules. Separation of small molecules involves continuous partitioning of the molecules between the mobile phase and the hydrophobic stationary phase. Polypeptides are however too big to partition into the hydrophobic phase. Instead they adsorb to the hydrophobic surface after entering the column (Fig. A.1). Here, they remain adsorbed until the concentration of organic modifier reaches the critical concentration necessary to cause des-

orption. After desorption the polypeptides only interact slightly with the surface as they elute down the column. Polypeptides may be thought of as having a "hydrophobic foot" which is in contact with the reversed-phase surface, while most of the protein remains exposed to the mobile phase. The separation of polypeptides is in RP-HPLC based on subtle differences in this hydrophobic foot, such as differences in amino acid sequence or conformation. [129]

A practical consequence of the adsorption/desorption mechanism of polypeptide-RP surface interactions is the sudden desorption of polypeptides when the critical organic concentration is reached. The sensitivity of polypeptide desorption to precise concentrations of organic modifier accounts for the selectivity of RP-HPLC in the separation of polypeptides. Due to the high sensitivity of the polypeptide interaction to organic modifier concentration, gradient elution is preferable to isocratic elution for the separation of polypeptides. The adsorption/desorption mechanism also results in that protein resolution is almost indifferent to mobile phase flow rate. [129]

Adsorption/desorption of proteins takes almost exclusively place near the top of the column. For this reason, column length does not significantly affect separation and resolution of protein separations. However, longer columns maximize sample capacity and lowers back-pressure when using viscous solvents. Broader peaks are obtained with polypeptides compared to small molecules, because large polypeptides diffuse slowly. [129]

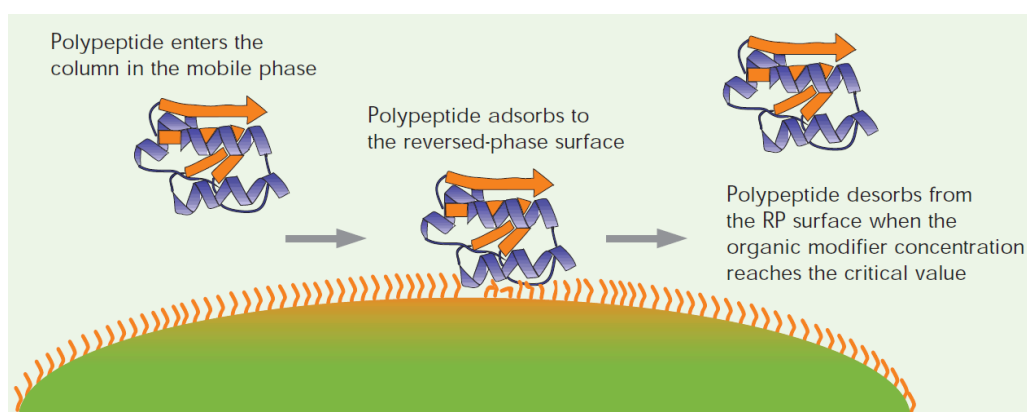


Figure A.1: The polypeptide enters the reversed-phase high performance liquid chromatography column in the mobile phase. The "hydrophobic foot" of the polypeptide adsorbs to the hydrophobic surface of the reversed-phase material. It remains here until the organic modifier concentration rises to the critical concentration and desorbs the polypeptide. Adapted from [129].

The elution of polypeptides from RP-HPLC columns is accomplished with aqueous solvents containing an organic modifier and an ion-pair reagent. The ion-pair reagent is often trifluoroacetic acid (TFA) or ortho-phosphoric acid. The ion-pair reagent is necessary to suppress the ionization of the acidic groups in the solute molecules and to maintain a low pH environment. By using this ion suppression in RP-HPLC, mixed mode retention effects is eliminated. Mixed mode retention will result in increased retention times and significant peak broadening, which is caused by ionizable silanol groups remaining on the silica gel surface performing a ion exchange with the positively charged amino groups on the solute molecules. Furthermore, ion pairing agents is sometimes required for binding of the solute to the reversed phase medium. TFA is widely used as ion-pairing agent because it is volatile and easily removed from collected fractions, and has little UV absorption. The concentration of the acid is generally in the 0.1-0.3% range. [138], [129]

The organic solvent (modifier) is added to lower the polarity of the aqueous mobile phase, which results in desorption of the polypeptide from the hydrophobic surface. In reversed phase chromatography, the eluting strength of the mobile phase increases when the polarity of the mobile phase is lowered. A large variety of organic solvents can be used, however, only a few are routinely employed. The most popular modifier is acetonitrile. Isopropanol is also used due to its strong eluting properties, but has the disadvantage of high viscosity, resulting in lower efficiency and high back pressure. Both of these solvents are essentially UV transparent, but acetonitrile offers lower background absorbance at low wavelengths. [138], [129]

Preparative RP-HPLC is generally performed with gradient elution. The gradient always proceeds from a condition of high polarity (low concentration of organic modifier) to low polarity (higher concentration of organic modifier). Gradient shape, slope and volume are all important factors, and often a broad gradient is used for initial screening of a complex sample. After initial screening, the gradient slope may be adjusted to optimize separation of desired components. This is done by decreasing the gradient slope where the desired component elutes, and increasing it before and after. In general, decreasing the gradient slope increases resolution. [138]

Biological activity of proteins depends on their tertiary structure, and a permanent disruption of this therefore eliminates biological activity. The hydrophobic solvents and the interaction of the protein with the hydrophobic surface may disrupt the 3D structure of proteins in RP-HPLC. The amount of biological activity that is lost depends on the protein stability and the conditions applied. Denaturation of proteins on hydrophobic surfaces is kinetically slow, and loss of activity can therefore be minimized by reducing residence time. Furthermore, isopropanol can be used as modifier, as it has been found to be most effective in retaining the biological activity of proteins. [129]

Height and width of individual peaks seen from HPLC data can be used for quantification of the analyte mixture, and resolution is decreased by sample overload (resulting in peak broadening). [129]

A.1.2 Fast Protein Liquid Chromatography

Pharmacia (now known as Amersham Biosciences) developed fast protein liquid chromatography (FPLC) in 1982 as a biocompatible alternative to HPLC for high-resolution separation of biopolymers. FPLC has features such as fast flow, high loading capacity compared to HPLC, and small-diameter stationary phases that makes high resolution possible. The FPLC technique gives the possibility of a variety of chromatography modes, such as ion exchange, gel filtration, hydrophobic interaction and reverse phase, based on particles with average diameter sizes in the same range as those used with HPLC. [141], [142]

The cost per run with FPLC can be nearly 30 times cheaper than a run with HPLC, and the cost of a FPLC column is approximately ten times less than that of a corresponding HPLC column. ÄKTA FPLC is the most recent system produced by Amersham Pharmacia Biotech, and this system is designed for research-scale protein purification, with the possibility of flow rates

up to 20 mL/min and pressures up to 5 MPa. [142]

The first step in FPLC is binding of soluble proteins onto the chromatography medium. Following, unbound proteins are washed out with buffer A. The protein separation is often done by gradient elution, which in case of ion-exchange mode involves a gradual increase in counterion concentration by increasing the percentage of eluent buffer B. FPLC can however also be run with an isocratic gradient (constant %B). The FPLC typically consists of a program controller, up to four P-900 pumps (two each for buffers A and B), a mixer, a prefilter, a seven-port M-7 valve, an autosampler or loading loops, a column, a UV-900 UV monitor, a flow restrictor, and a fraction collector. Buffer A and B are separate buffers, which are mixed to yield the gradient throughout the chromatographic run. [142]

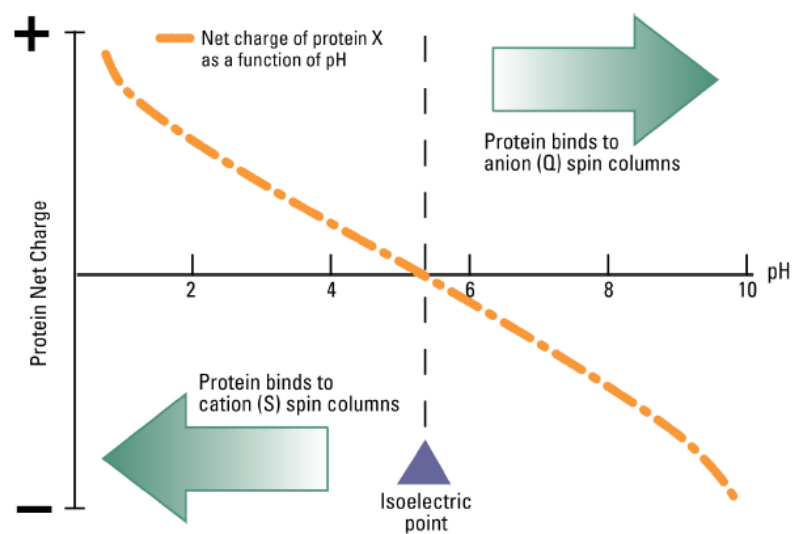


Figure A.2: Pierce Ion Exchange Spin Column purification example. Effect of buffer pH on protein X with a pI of 5.2. Adapted from [143].

One of the most popular FPLC modes is ion-exchange, which can be performed with either a cat- or anion-exchange column. In this mode, the elution time of various proteins depends on their relative charge differences. The less charged proteins are eluted at low salt concentrations, while highly charged proteins require higher salt concentrations to elute. After ion-exchange separation, it is often necessary to desalt the fractions. Negatively charged molecules bind to anion-exchange columns (positively charged solid supports), whereas positively charged molecules bind to cation-exchange columns (negatively charged solid supports). To ensure that the protein of interest has a particular net charge, it should be dissolved in a buffer that is either below or above its pI (Fig. A.2). A protein with e.g. a pI of 5 will possess a net negative charge in a buffer at pH 7, while it will possess a net positive charge in a buffer at pH 3. [141], [142], [143]

Sodium chloride is in both cation- and anion-exchange chromatography often used to elute the bound protein. In an anion application chloride is the counter ion, and in a cation application sodium is the counter ion. The strength of the electrostatic interaction between a target and the solid support is a function of the difference in the pI of the target and the buffer that contains the target. A protein with e.g. a pI of 7 will bind more tightly to a cation column if

its buffer has a pH of 3 rather than 4. Because of this fact, alteration of pH of the buffer can be used as an alternative to elution by increase in salt concentration. [143]

Appendix

B

B.1 Chemicals

Chemicals	Description	Manufacturer
Acetic acid (CH ₃ COOH)	Lot: K39595863-903	Merck
Acetone, pure	Pr. no. 20065.470	VWR
Acetonitrile, HPLC grade	Lot: 0000184378	Hiperpur Panreac
Acrylamide/Bis solution (30 %) (N,N'-methylene-Bis-acrylamide), 29:1	Cat. no: 161-0156	Bio-Rad Laboratories
Agar-agar	Lot: BCBC2317	Sigma-Aldrich
Agarose	CAS: 9012-36-6	Sigma-Aldrich
Ammonium hydroxide (NH ₄ OH) 28-30%	Lot: SZBB1390V	Sigma-Aldrich
Ammonium sulfate	Lot: SZBB0180V	Sigma-Aldrich
Bovine serum albumin (BSA)	CAS: 9048-46-8	Sigma
Chloroform	Lot: SHBB3233V	Sigma-Aldrich
Citric acid monohydrate, 99-102%	Lot: 5949-29-1	Sigma-Aldrich
dATP	Lot: 100-846	Fermentas
d-Biotin app. 99% (TLC)	Lot: 034k1338	Sigma-Aldrich
dCTP	Lot: 9701	Fermentas
D-(+)-Dextrose	CAS: 50-99-7	Sigma
dGTP	Lot: 8603	Fermentas
DNA water	Lot: 50K8414	Sigma
D-Sorbitol	Lot: BCBD5878V	Sigma
dTTP	Lot: 00020452	Fermentas
Dye Reagent Concentrate	Catalog no. 500-0006	BioRad
Ethylenediaminetetraacetic acid disodium salt hydrate (EDTA), 99+%	CAS: 6381-92-6	Sigma
Ethanol 96 % vol.	UN-no: 1170	Kemetyl
Ethidium bromide (EtBr)	10 mg/mL	Roche Diagnostics Corporation
Formaldehyde (CH ₂ O) solution 36.5-38%	Lot: SZBB2800V	Sigma
Generuler TM 1 kb DNA ladder	Lot: 00032587	Fermentas
Generuler TM 50 bp DNA ladder	Lot: 00028112	Fermentas
Glycerol min. 99%	CAS: 56-81-5	Sigma-Aldrich
HEPES (4-(2-hydroxyethyl)-1-piperazineethanesulfonic acid) sodium salt	CAS: 75277-39-3	Sigma
Isopropanol (2-propanol), HPLC grade	Lot: 81955	Sigma-Aldrich
Lithium acetate dihydrate (LiOAc)	Lot: 011M00051V	Sigma-Aldrich
Low Molecular Weight ladder	Lot: 374351	GE Healthcare

Chemicals	Description	Manufacturer
Methanol 99.6%	Lot: 58844-469	Sigma-Aldrich
Methanol, HPLC grade	Lot: SZBB006DV	Sigma-Aldrich
NEBuffer 4 10x concentrate	Lot: 0041009	NEB
PageRuler unstained Low Range Protein ladder, SM0661	Lot: 00063008	Fermentas
Peptone enzymatic digest from Casein	Lot: BCBD0141V	Fluka Analytical
PhastGel BlueR, Coomassie Brilliant Blue R-350	Lot: 0289363	Amersham Pharmacia Biotech
Phenyl methyl sulfonyl fluoride (PMSF)	CAS: 329-98-6	Sigma
Phosphoric acid (H ₃ PO ₄), 85%	CAS: 7664-38-2	Sigma-Aldrich
Potassium phosphate dibasic, ACS reagent (98%)	CAS: 7758-11-4	Sigma-Aldrich
Potato Extract	Lot: BCBG0934V	Fluka Analytical
Sample Buffer, Laemmli 2× Concentrate	S3401	Sigma-Aldrich
Select agar, ultra pure	080M1575V	Sigma-Aldrich
Silver nitrate (AgNO ₃), >99% titration	CAS: 7761-88-8	Sigma
Sodium Acetate (NaAc)	Lot: 112K1373	Sigma
Sodium chloride (NaCl)	Table salt	
Sodium dodecyl sulfate (SDS) 99%	CAS: 151-21-3	Sigma-Aldrich Chemie GmbH
Sodiumhydroxide (NaOH)	BBB23110	Bie and Berntsen A-S
Spectra Multicolor Low Range Protein Ladder	26628	Thermo Scientific
Trifluoroacetic acid (TFA), peptide grade	CAS: 76-05-1	Iris Biotech GmbH
Tris-acetate-EDTA, TAE-buffer (1x)	Tris base 40 mM, 0.5M EDTA (pH 8) 2 mM, glacial acetic acid 20 mM, pH 8.5	
Tris/Tricine/SDS Buffer (10x)	Cat. no.: 161-0744	Bio-Rad
Trizma base, Biotech. performance certified	CAS: 77-81-1	Sigma
Tryptone	Lot: 0F007962	AppliChem
UltraPure TM Temed	Lot: 0905028	Invitrogen
Yeast Nitrogen Base (YNB)	Lot: 0001420470	Fluka Analytical
Yeast Extract	Lot: BCBD0078V	Fluka Analytical
Zeocin TM	Lot: 849072	Invitrogen
6x DNA loading dye	Lot: 00034551	Fermentas
10x DreamTaq TM Buffer	Lot: 00058293	Fermentas
10x Tris/Glycine/SDS (TGS) buffer	Cat. no.: 161-0772	Bio-Rad Laboratories

Table B.1: Chemicals used in this project.

Appendix

C

C.1 Supplementary Figures for Theoretical Characterizations

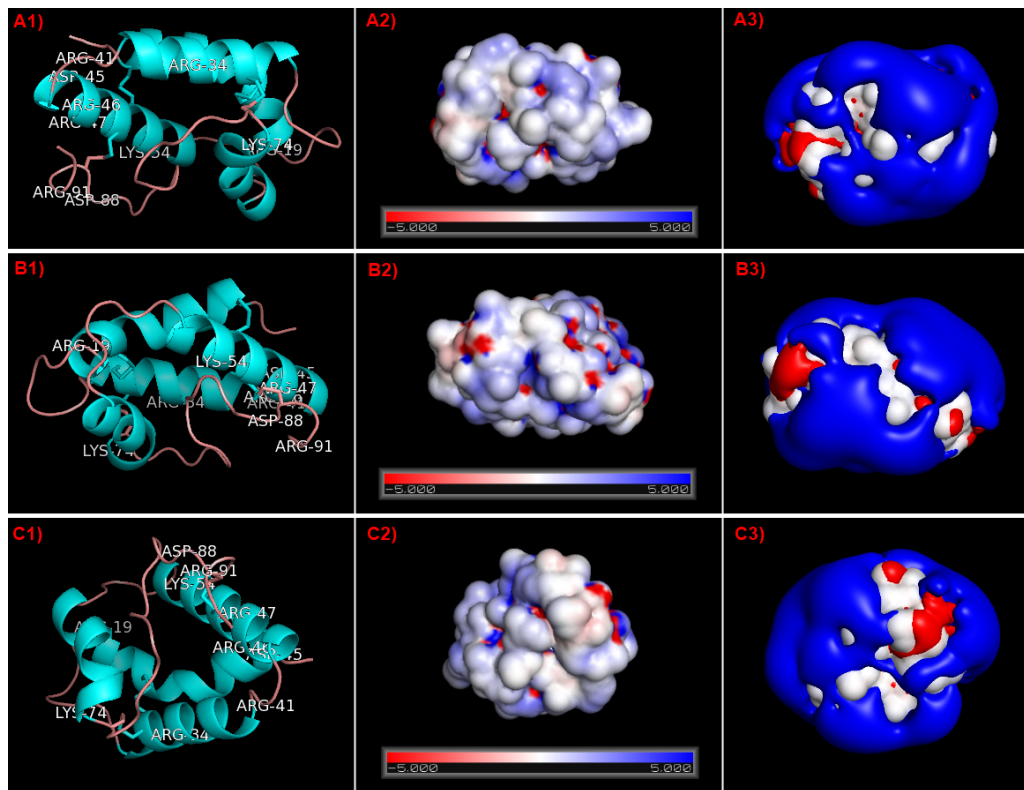


Figure C.1: Strength and spatial distribution at pH 7 of the electrostatic potential generated by 1MZL.pdb, visualized from three different angles (A, B, and C). The color code is blue for positive electrostatic potential and red for negative electrostatic potential. **1)** 3D structure of 1MZL.pdb with labeling of charged residues. **2)** Electrostatic potential mapped onto the solvent accessible surface of 1MZL.pdb in an interval from -5 to 5 $k_B T/e$. **3)** Isopotential contours plotted at $\pm 0.5 k_B T/e$. Calculated and visualized by use of PyMol, PDB2PQR and APBS.

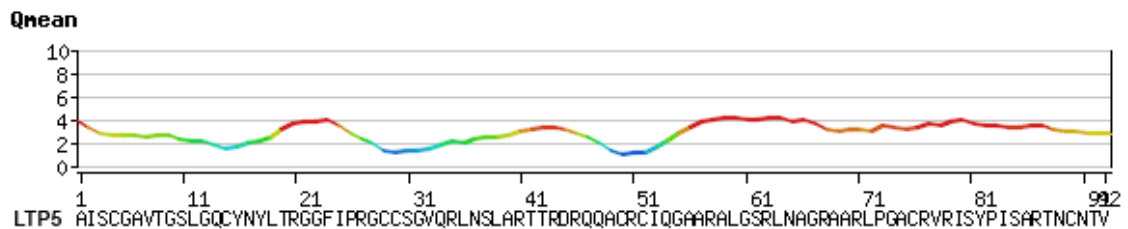


Figure C.2: Residue error plot of the LTP5 model, which shows the local QMEAN score for each position in the model. The local score is an estimate of the expected structural inaccuracy at a given position, with small values corresponding to regions in the model being potentially more reliable. [144]. Constructed by SWISS-MODEL.

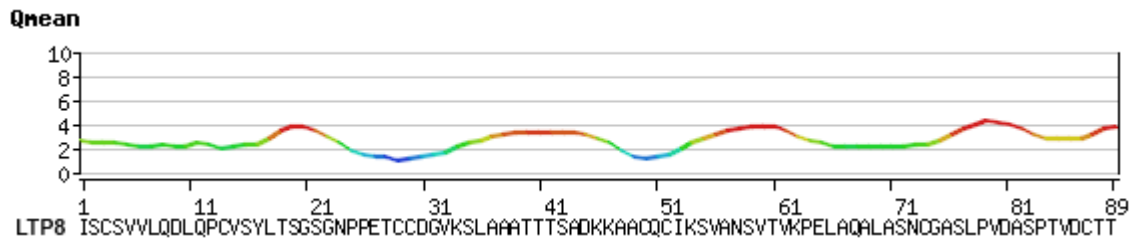


Figure C.3: Residue error plot of the LTP8 model, which shows the local QMEAN score for each position in the model. The local score is an estimate of the expected structural inaccuracy at a given position, with small values corresponding to regions in the model being potentially more reliable. [144]. Constructed by SWISS-MODEL.

C.2 Supplementary SDS-PAGES

C.2.1 SDS-PAGES from Expression Studies

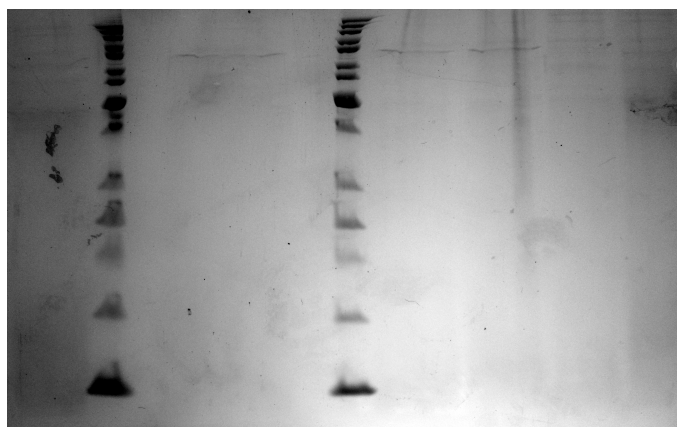


Figure C.4: Coomassie stained, 10% glycine SDS-PAGE of lyophilized culture supernatant from expression studies of PIC-LTP5 *P. pastoris* X-33, PIC-LTP8 *P. pastoris* X-33, and wild type *P. pastoris* X-33. This expression 1 (E1) was performed at 28 °C for 96 hours, with methanol induction every 24th hour. 5 mg lyophilized supernatant was loaded in each well, which has not been labeled due to lack of visibility. The ladder used is PageRuler unstained protein ladder (Fermantas).

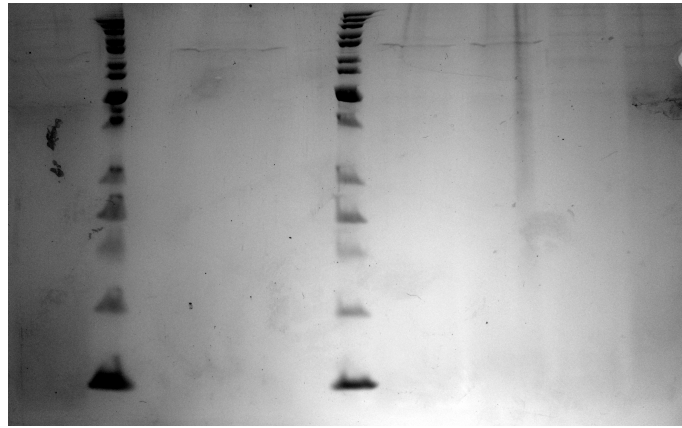


Figure C.5: Coomassie stained, 12% glycine SDS-PAGE of lyophilized culture supernatant from expression studies of PIC-LTP5 *P. pastoris* X-33, PIC-LTP8 *P. pastoris* X-33, and wild type *P. pastoris* X-33. This expression 1 (E1) was performed at 28 °C for 96 hours, with methanol induction every 24th hour. 5 mg lyophilized supernatant was loaded in each well, which has not been labeled due to lack of visibility. The ladder used is PageRuler unstained protein ladder (Fermentas).

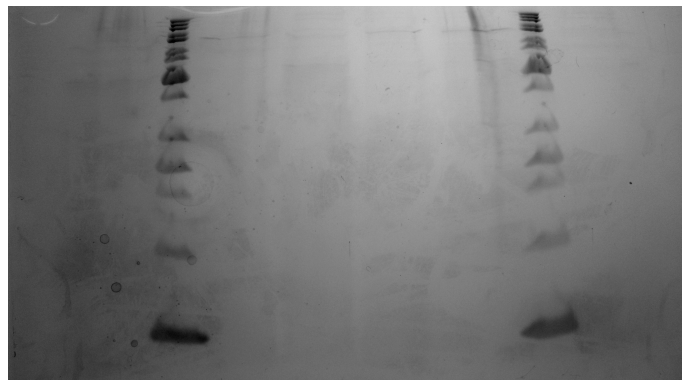


Figure C.6: Coomassie stained, 15% glycine SDS-PAGE of lyophilized culture supernatant from expression studies of PIC-LTP5 *P. pastoris* X-33, PIC-LTP8 *P. pastoris* X-33, and wild type *P. pastoris* X-33. This expression 1 (E1) was performed at 28 °C for 96 hours, with methanol induction every 24th hour. 5 mg lyophilized supernatant was loaded in each well, which has not been labeled due to lack of visibility. The ladder used is PageRuler unstained protein ladder (Fermentas).

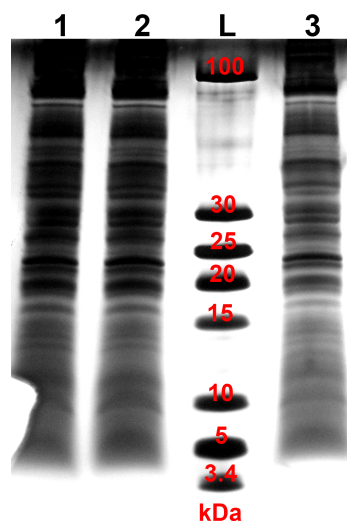


Figure C.7: Silver stained, precast, 10-20% gradient tricine SDS-PAGE (BioRad) of heat-treated, dialyzed and lyophilized culture supernatant from expression studies with *P. pastoris* SMD1168H transformants, performed at 23°C for 96 hours, with methanol induction every 24th hour. 1) 1 mg heat-treated, dialyzed and lyophilized culture supernatant from expression study with PIC-LTP5 *P. pastoris* SMD1168H. 2) 1 mg heat-treated, dialyzed and lyophilized culture supernatant from expression study with PIC-LTP8 *P. pastoris* SMD1168H. L) 3 µL PageRuler unstained Low Range protein ladder (Fermentas). 3) 1 mg heat-treated, dialyzed and lyophilized culture supernatant from expression study with *P. pastoris* SMD1168H background.

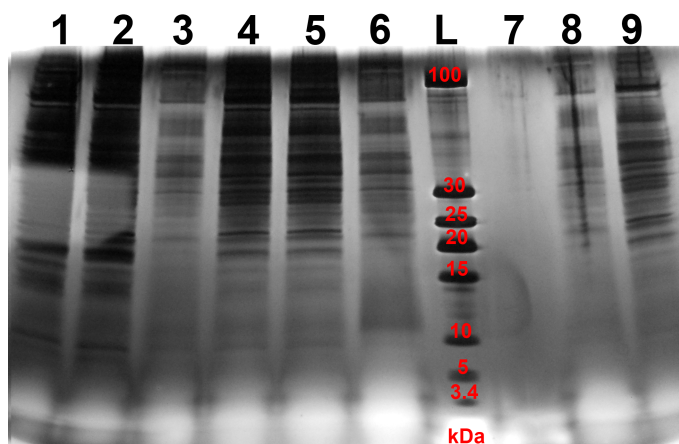


Figure C.8: Silver stained, precast, 10-20% gradient tricine SDS-PAGE (BioRad), comparing culture supernatant from expression studies with the transformants of the protease deficient strain SMD1168H, and protease inhibitor expression studies of the transformants of the protease deficient strain SMD1168H and X-33. 1) 20 µL expression supernatant from PIC-LTP5 *P. pastoris* SMD1168H expression study. 2) 20 µL expression supernatant from the protease inhibitor expression study with PIC-LTP5 *P. pastoris* SMD1168H. 3) 20 µL expression supernatant from the protease inhibitor expression study with PIC-LTP5 *P. pastoris* X-33. 4) 20 µL expression supernatant from PIC-LTP8 *P. pastoris* SMD1168H expression study. 5) 20 µL expression supernatant from the protease inhibitor expression study with PIC-LTP8 *P. pastoris* SMD1168H. 6) 20 µL expression supernatant from the protease inhibitor expression study with PIC-LTP8 *P. pastoris* X-33. L) 3 µL PageRuler unstained Low Range protein ladder (Fermentas). 7) Empty. 8) 20 µL expression supernatant from the protease inhibitor expression study with *P. pastoris* X-33 background. 9) 20 µL expression supernatant from the protease inhibitor expression study with *P. pastoris* SMD1168H background.

C.2.2 SDS-PAGES from Isolation of LTPs from Cabbage

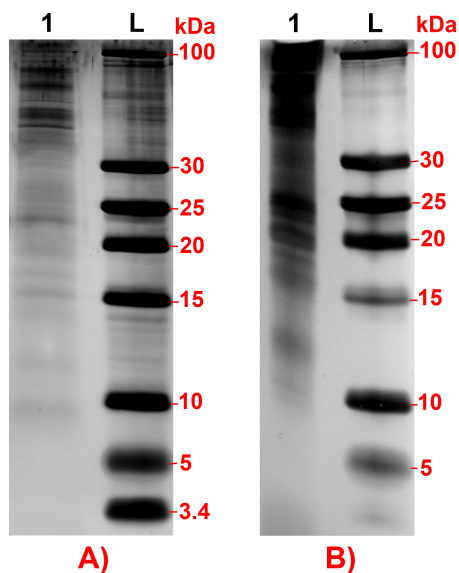


Figure C.9: Silver stained, precast, 16.5% tricine SDS-PAGEs (BioRad) of the two wax protein extractions. **A)** L) 3 μ L PageRuler unstained Low Range protein ladder (Fermentas). 1) Approximately 0.5 mg dialyzed and lyophilized aqueous phase from wax extraction of a mixture of leaves from cabbage. **B)** L) 3 μ L PageRuler unstained Low Range protein ladder (Fermentas). 1) Approximately 0.5 mg dialyzed and lyophilized aqueous phase from wax extraction of young leaves from cabbage.

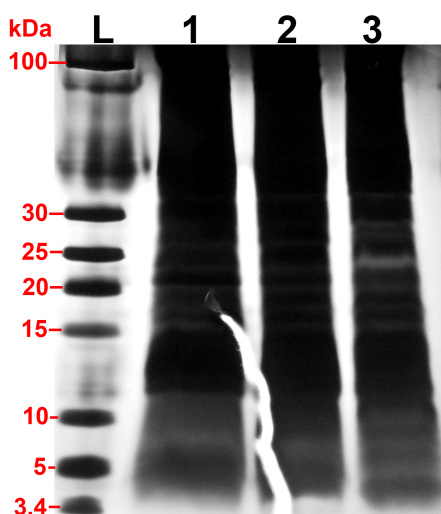


Figure C.10: Silver stained, precast, 10-20% gradient tricine SDS-PAGE (BioRad) of lyophilized samples recovered from extraction and heat-treatment of cabbage material. L) 3 μ L PageRuler unstained Low Range protein ladder (Fermentas). 1) 0.4 mg FOL. 2) 0.4 mg FYL. 3) 0.4 mg FS.

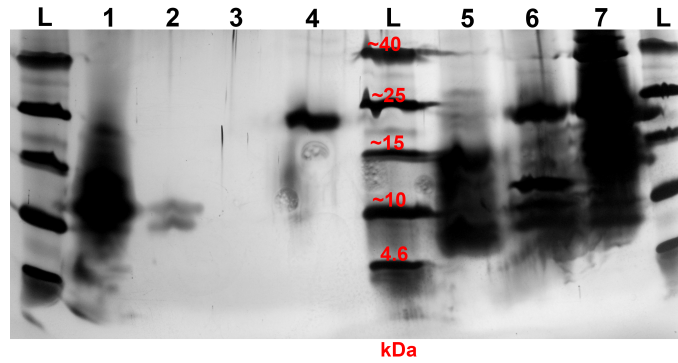


Figure C.11: Silver stained, precast, 10-20% gradient tricine SDS-PAGE (BioRad) of lyophilized fractions collected from reversed-phase high performance liquid chromatography (RP-HPLC). The SDS-PAGE is distorted because it has passed its expiry date. Fraction numbers for FS3 are equivalent to those found on Fig. 6.32, and fractions numbers for FS4.2 are equivalent to those found on Fig. 6.34. L) 3 μ L Spectra Multicolor Low Range protein ladder (Thermo Scientific). 1) 15 μ L FS3 F1. 2) 15 μ L FS3 F2. 3) 15 μ L FS3 F3. 4) 15 μ L FS3 F4. 5) 15 μ L FS4.2 F1. 6) 15 μ L FS4.2 F2. 7) 15 μ L FS4.2 F3.

C.3 Supplementary Chromatograms

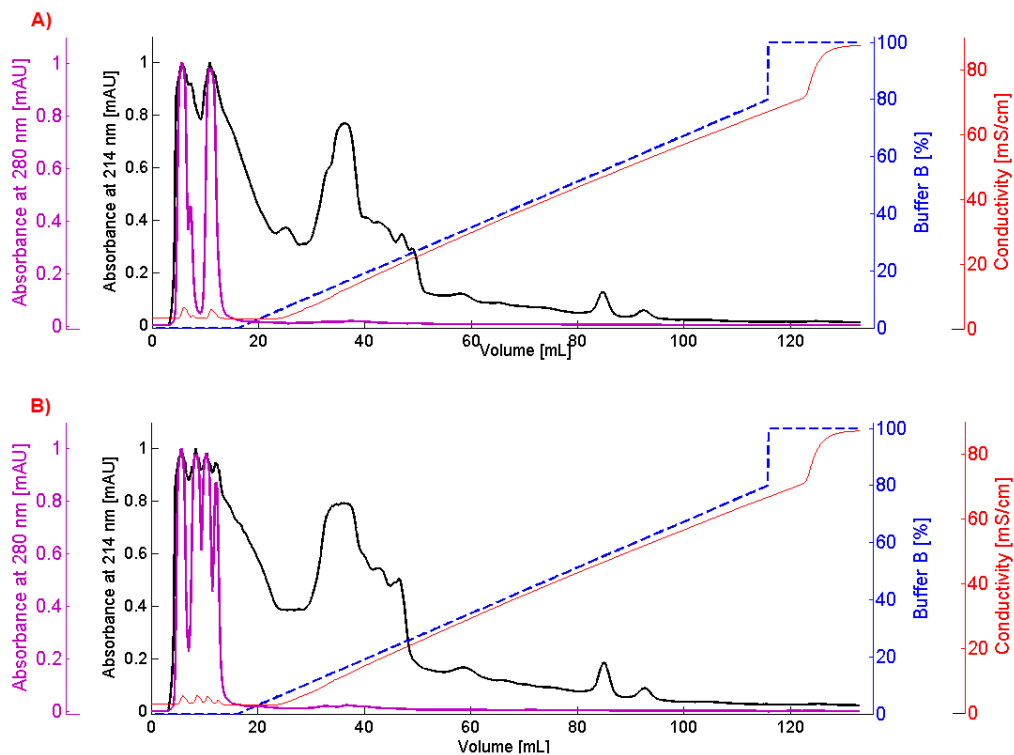


Figure C.12: Cation-exchange chromatography on dialyzed and lyophilized *P. pastoris* X-33 culture supernatants. Elution was performed with a buffer containing 10 mM Tris-HCl and 10 mM NaCl (pH 4), and retained material was eluted with 1 M NaCl (buffer B) in the same buffer (4 mL/min). Percent of buffer B (blue dotted line), UV absorbance at 214 nm (black solid line), UV absorbance at 280 nm (purple solid line), and conductance (red solid line) is plotted against volume of eluent passed through the system. UV absorbance at 214 nm and 280 nm has been normalized to highest detection point. **A)** Dialyzed and lyophilized PIC-LTP5 *P. pastoris* X-33 culture supernatant. **B)** Dialyzed and lyophilized *P. pastoris* X-33 background culture supernatant.

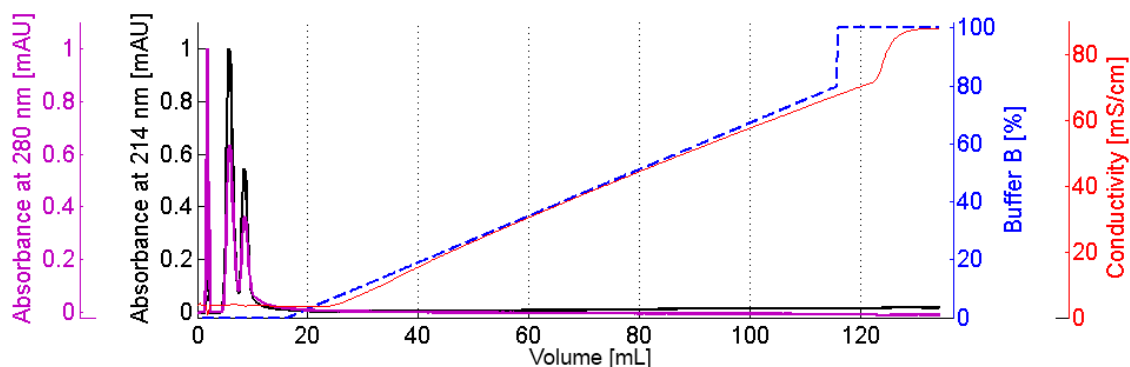


Figure C.13: Cation-exchange chromatography of dialyzed and lyophilized sample from wax protein extraction of younger leaves. Elution was performed with a buffer containing 10 mM Tris-HCl and 10 mM NaCl (pH 4), and retained material was eluted with 1 M NaCl (buffer B) in the same buffer (4 mL/min). Percent of buffer B (blue dotted line), UV absorbance at 214 nm (black solid line), UV absorbance at 280 nm (purple solid line), and conductance (red solid line) is plotted against volume of eluent passed through the system. UV absorbance at 214 nm and 280 nm has been normalized to highest detection point.

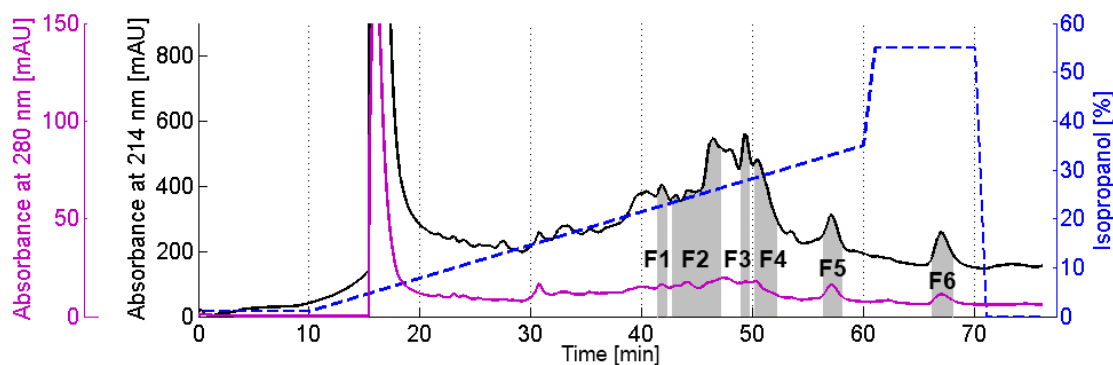


Figure C.14: Reversed-phase high performance liquid chromatography with FS4.2. Purification was performed with 0.1% TFA and 1% isopropanol, and retained material was eluted with a isopropanol gradient with a flowrate of 1.25 mL/min. A gradient from 1-35% isopropanol was applied over 50 min, followed by isocratic mode at 55% over 10 min. Percent of isopropanol (blue dotted line), UV absorbance at 214 nm (black solid line), and UV absorbance at 280 nm (purple solid line) is plotted against retention time. The chromatogram has been corrected for the column-volume induced delay, and a zoom-in has been performed, as the high peak appearing at the gradient offset is due to background effects. The gray shading indicates the collected fractions.

C.4 Supplementary Time Resolved Fluorescence Plot

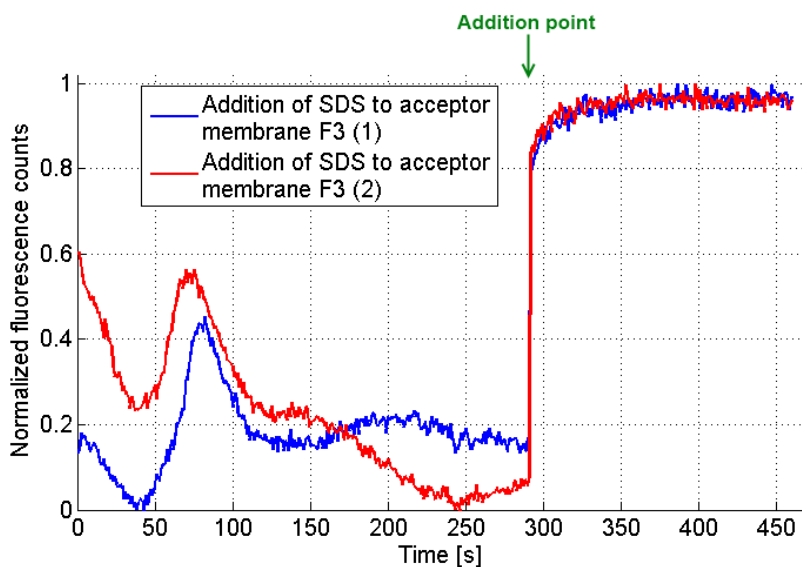


Figure C.15: Time resolved fluorescence plot of fluorescence spectroscopy performed on 2 mL 10 mM HEPES buffer (pH 7.3) and 30 μ L diluted donor vesicles fraction 3, without addition of pLTP fractions. To measure fluorescence when all fluorophores were de-quenched, 100 μ L 10% SDS were added (green arrow). Fluorescence was excited at 475 nm and emission measured at 530 nm by two channels. The fluorescence intensity has been normalized to the highest detection point of the individual measurements.

Appendix

D

D.1 Expression Constructs

Primer	DNA Sequence	T _m	GC%
LTP51for	5'-CTACT CGAG AAAAGAGCAATCTCGTGCG-3'	66.6 °C	50%
LTP52rev	5'-ACGT CTAGAT CATCACCTGACGGTGTTAC-3'	66.7 °C	48%
LTP53for	5'-GTT CAGAGGCTCAACACTTGG -3'	62.1 °C	54.5%
LTP81for	5'-TACT CGAG AAAAGAGCTATATCTTGCAGTGTTG-3'	65.8 °C	40%
LTP82rev	5'-CTGCGGT CTAGAT CATCAACCAACAG-3'	64.8 °C	50%
LTP83for	5'-TGCGACGGAGTTAAGAGTTTAGC-3'	60.6 °C	48%
α -factor	5'-TACTATTGCCAGCATTGCTGC-3'	57.9°C	48%
α -factor2	5'-ACAACAGAAGATGAAACGGCAC-3'	53.0°C	46%
3'AOX1	5'-GCAAATGGCATTCTGACATCC-3'	57.9°C	48%

Table D.1: Primers used to construct, sequence and screen for the LTP5 and LTP8 expression construct in Fig. D.1 and D.2. Restriction sites are marked in bold face and the Kex2 recognition sequence is marked in italic.

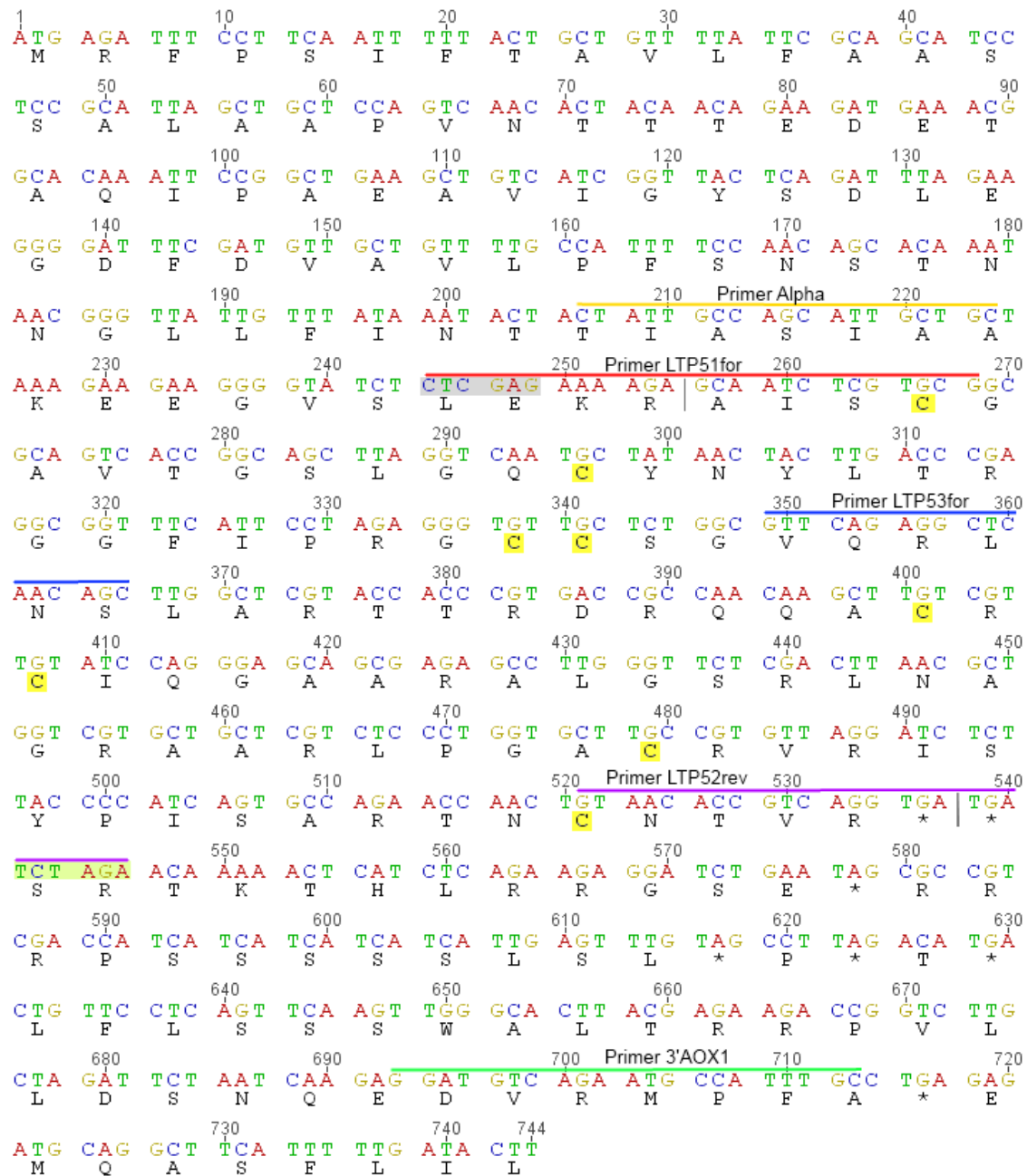


Figure D.1: Nucleotide and deduced amino acid sequence of LTP5 inserted in the pPICZα A vector. Only the sequence of the pPICZα A vector surrounding the used cloning site are showed, and the gray vertical lines indicates the fusion site of the vector and the LTP5 sequence. The annealing sites of the different primers are highlighted with different colored lines above the nucleotide sequence. The XhoI restriction site is highlighted with a gray box, and the XbaI restriction site is highlighted with a light green box. The eight conserved cysteine residues are highlighted with a yellow box. The α-factor signal sequence is not highlighted but runs from nucleotide 1 to 255. The stars indicate the stop codons. Created with Bioedit.

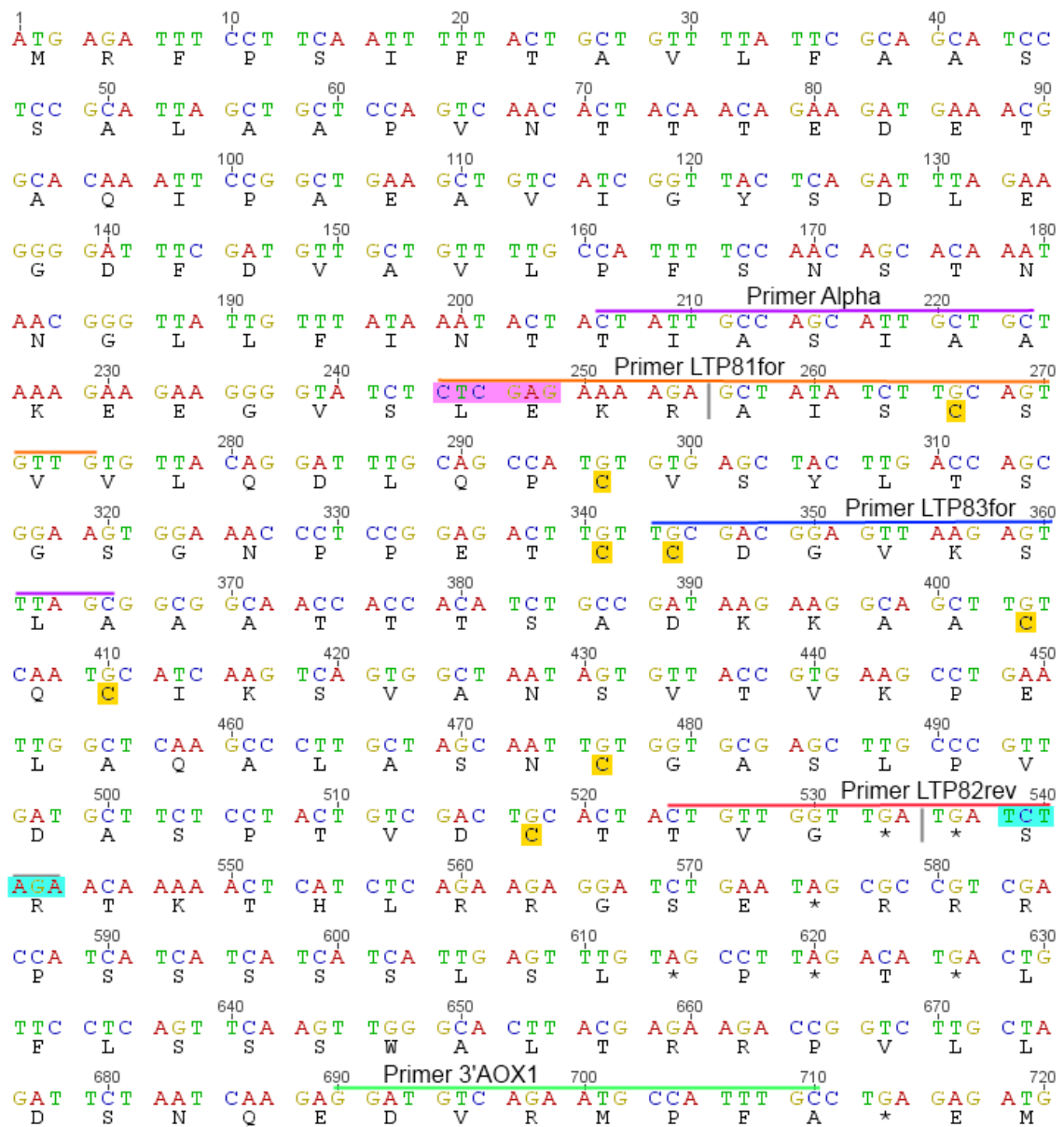


Figure D.2: Nucleotide and deduced amino acid sequence of LTP8 inserted in the pPICZ α A vector. Only the sequence of the pPICZ α A vector surrounding the used cloning site are showed, and the gray vertical lines indicates the fusion site of the vector and the LTP8 sequence. The annealing sites of the different primers are highlighted with different colored lines above the nucleotide sequence. The XhoI restriction site is highlighted with a pink box, and the XbaI restriction site is highlighted with a light blue box. The eight conserved cysteine residues are highlighted with a yellow box. The α -factor signal sequence is not highlighted but runs from nucleotide 1 to 255. The stars indicate the stop codons. Created with Bioedit.